

**THERMODYNAMICS OF
CHEMICALLY RECUPERATED GAS TURBINES**

Alistair Lloyd

CEES Report No 256

January 1991

Center for Energy and Environmental Studies

Engineering Quadrangle

Princeton University

Princeton NJ 08544

THERMODYNAMICS OF CHEMICALLY RECUPERATED GAS TURBINES

by

Alistair Lloyd

January 1991

Princeton University

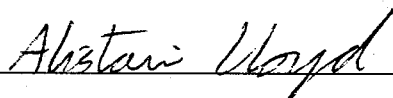
School of Engineering and Applied Sciences

Department of Mechanical and Aerospace Engineering

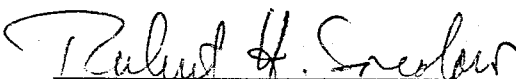
Center for Energy and Environmental Studies

Submitted in partial fulfillment of the requirements for the degree of Master of Science in Engineering from Princeton University, 1990

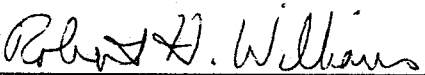
Prepared by:



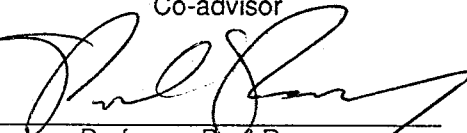
Approved by:



Professor Robert Socolow
Thesis Advisor



Dr Robert Williams
Co-advisor



Professor Paul Ronney
Thesis Reader



ACKNOWLEDGMENTS

The author wishes to thank a number of colleagues for their advice and suggestions. Special thanks are due to Stefano Consonni for being a dependable source of wisdom on gas turbines and for allowing use of his gas turbine model for cycle calculations. Eric Larson, George Sidebotham, and thesis supervisor Robert Williams contributed valuable ideas and comments. Thanks go also to academic advisor Robert Socolow and thesis reader Paul Ronney. Clint Ashworth of Pacific Gas and Electric Company provided helpful comments on an early draft.

This thesis carries the identification 1905-T in the records of the Department of Mechanical and Aerospace Engineering.

CONTENTS

CHAPTER ONE: INTRODUCTION

1.1 Introduction	1.1
1.2 Evolution of Stationary Gas Turbines	1.3
1.3 The Chemically Recuperated Gas Turbine	1.10
References	1.12
Figures	1.15

CHAPTER TWO: THERMODYNAMIC FUNDAMENTALS

2.1 Introduction	2.1
2.2 Thermodynamics of STIG Cycles	2.2
2.3 Regeneration and Chemical Recuperation	2.6
2.4 Exergy Analysis	2.8
2.5 CRGT with Supplementary Firing	2.11
2.6 CRGT with Reheat	2.13
2.7 Review	2.14
References	2.15
Notation	2.15
Appendix 2A	2.16
Figures	2.20

CHAPTER THREE: CHEMICAL FUNDAMENTALS

3.1 Introduction	3.1
3.2 Steam Reforming of Methane	3.2
3.3 Steam Reforming of Methanol	3.4
References	3.5
Figures	3.6

CHAPTER FOUR: PRACTICAL CONSIDERATIONS

4.1 Introduction	4.1
4.2 Existing Gas Turbine Emissions Control Technologies	4.1

4.3 Chemically Recuperated Gas Turbine Emissions	4.7
4.4 Combustion of Low Heating Value Fuels	4.9
4.5 Gas Turbine Design Issues	4.11
4.6 Heat Recovery Steam Reformer	4.15
4.7 Operational Issues	4.19
4.8 Economics	4.20
References	4.23
Figures	4.26

CHAPTER FIVE: CHEMICALLY RECUPERATED GAS TURBINE COMPUTER MODEL

5.1 Introduction	5.1
5.2 The Consonni Gas Turbine Model	5.1
5.3 Modelling Chemical Recuperation	5.4
5.4 General Approach for Cycle Calculations	5.5
References	5.7
Appendix 5A	5.7
Notation	5.12
Figures	5.14

CHAPTER SIX: SIMPLE CRGT CYCLES

6.1 Cycle Description	6.1
6.2 Example Comparison of CRGT with STIG and Combined Cycles	6.4
6.3 Parametric Analysis	6.12
6.4 Discussion	6.15
References	6.19
Appendix 6A	6.20
Figures	6.26

CHAPTER SEVEN: ADVANCED CRGT CYCLES

7.1 Introduction	7.1
7.2 CRGT with Back Pressure Steam Turbine	7.2
7.3 CRGT with Supplementary Firing	7.6

SYNOPSIS

The chemically recuperated gas turbine (CRGT) is a variant of the steam-injected gas turbine (STIG) in which gas turbine exhaust heat drives an endothermic chemical reaction between the natural gas fuel and steam. The product is a low heating value fuel gas rich in hydrogen. Interest in CRGT stems from very low projected NO_x levels. Thermal efficiency for a cycle employing intercooling and reheat is expected to be well over 50% (lower heating value basis), making CRGT a possible candidate for central station power generation.

The thermodynamics of CRGT cycles are not yet well understood. This thesis uses First and Second Law methods to investigate the fundamental thermodynamics of CRGT cycles. A detailed computer model is used to generate performance predictions for various CRGT configurations, ranging from the most simple cycle to cycles with intercooling, reheat, and steam cooling.

The thesis finds that a simple CRGT cycle is generally more efficient than a STIG cycle owing to lower irreversibilities associated with heat recovery. For a given turbine inlet temperature the maximum efficiency of the CRGT is around half a percentage point greater than that of the STIG, and occurs at a lower pressure ratio. The efficiency gain is achieved only at the expense of a reduction in power output of approximately 20%.

A CRGT is less efficient than a combined cycle because, like the STIG, it suffers from irreversibilities associated with mixing steam into the gas cycle. For this reason the combined cycle is likely to remain the preferred option for base-load power generation. A CRGT with intercooling and reheat is estimated to have an efficiency around 53%, but this value is strongly dependent on the assumed cooling flows.

The presence of hydrogen in the reformed fuel gas enables combustion at lower flame temperatures, and hence lower thermal NO_x emissions than are possible with dry low NO_x combustors or steam or water injection. A CRGT cycle can meet the strictest NO_x limits in operation today without the need for selective catalytic reduction. Estimates of NO_x emissions are as low as 1ppm. Good environmental characteristics are the primary reason fuelling interest in CRGT.

7.4 CRGT with Intercooling and Reheat	7.10
7.5 Summary	7.20
References	7.22
Figures	7.23

CHAPTER EIGHT: CONCLUSIONS

8.1 Review of Results	8.1
8.2 Prospects for Chemically Recuperated Gas Turbines	8.5
8.3 Suggestions for Future Work	8.13
References	8.15

CHAPTER ONE: INTRODUCTION

1.1 Introduction

1.2 Evolution of Stationary Gas Turbines

1.3 The Chemically Recuperated Gas Turbine

References

Figures

1.1 INTRODUCTION

As we approach the end of the Twentieth Century, energy is once again becoming a major issue. Whereas worries about security of oil supply fueled the energy crisis of the 1970s, the new energy debate will center on the environmental consequences of energy use¹. Mankind's thirst for energy is at the heart of environmental problems such as acid rain, local air pollution, and global warming.

Electricity production accounts for a growing fraction of primary energy use². Electricity has traditionally been generated in large steam-electric power stations, mostly coal-fired and nuclear. In recent years construction costs for these have escalated substantially. Environmental regulations and public opinion have increased the difficulty of siting large new power plants. Consequently utilities have looked for new power generation technologies that can be installed in small increments of power capacity and at low cost. This search has led them to the gas turbine.

The gas turbine is not new to the electricity industry, but until recently has not been competitive with steam-electric plants, except for peaking service, in terms of life-cycle cost and reliability. Section 1.2 explains how recent technical and institutional innovations have reversed this situation. Gas turbines are now the most popular choice for new generating capacity³.

¹ At the time of writing, Iraq's invasion of Kuwait has rekindled concerns about energy security.

² In 1988 US electric utilities accounted for 36% of total primary energy consumption. This compares with 32% in 1980 and 25% in 1970 (Annual Energy Review, 1988).

³ US utilities plan to order 40,000MW of new gas turbine-based generating capacity by 1995. Of all new capacity built in the 1990s, around 60% is expected to be gas turbine-based (Smock, 1989).

Although cleaner than coal-fired power stations, natural gas- or oil-fired gas turbines do give rise to undesirable emissions. The main pollutant of concern is oxides of nitrogen (NO_x), which plays a role in both local ozone pollution and acid rain formation. Technological solutions such as steam or water injection, dry low NO_x combustors, and selective catalytic reduction (SCR) have been introduced to reduce NO_x emissions, but these are either costly or might restrict operational flexibility or both⁴. Modern gas turbines typically have guaranteed NO_x levels of 25 parts per million (ppm) without SCR.

California's South Coast Air Quality Management District (SCAQMD) has recently proposed tough new regulations to combat the acute air pollution problem in Southern California. These call for very low NO_x levels for new gas turbine power plants⁵. SCR can achieve these levels, but is unpopular with utilities because of its complexity and inflexibility of operation. The search is on for other methods of obtaining ultra-low NO_x levels.

Mr Jack Janes of the California Energy Commission has proposed a new gas turbine cycle which promises NO_x levels as low as 1ppm (Janes, January 1990). This is the chemically recuperated gas turbine (CRGT). While further research is needed to validate these claims, the prospect of ultra-low NO_x levels is a major factor fueling interest in CRGT.

Besides excellent emissions characteristics, CRGT promises the additional benefits of very high efficiency and low capital costs. Further research is needed to validate these claims, as uncertainty surrounds both the emissions issue and the expected thermodynamic performance. A definitive economic analysis cannot be carried out until these technical issues are better understood.

⁴ Chapter Four contains a detailed description of NO_x control technologies.

⁵ The SCAQMD plan calls for installation of SCR to obtain 9ppm NO_x on all gas turbines larger than 0.3MW (SCAQMD, 1989, Appendix IV-A). Gas Turbine World (September-October 1989), reports that SCAQMD has agreed to modify the plan to allow steam injection as an alternative control technology. For steam-injected systems the limits would be 12ppm for machines in the range 10-60MW, and 15ppm for 60+MW and 3-10MW. Any system using SCR would still have to comply with the 9ppm limit.

The objective of this thesis is to gain an understanding of the thermodynamics of CRGT cycles. The remainder of this chapter summarizes the history of gas turbine development, and reviews CRGT research to date. Chapter Two explores the thermodynamic theory behind the expected high efficiency, while Chapter Three considers the chemical reaction central to the CRGT concept. While the thesis focuses mainly on thermodynamic issues, Chapter Four looks at some of the practical problems, which must be addressed if CRGT is to be developed. Chapter Four also addresses the NO_x issue in detail. Chapter Five describes the computer model used to perform cycle calculations. Chapters Six and Seven present the results of these calculations for simple and complex CRGT cycle configurations, and compare the predicted performances with those for other gas turbine cycles. Chapter Eight draws conclusions and suggests opportunities for future work.

1.2 EVOLUTION OF STATIONARY GAS TURBINES

This section briefly relates the history of gas turbine development for power generation. Further descriptions can be found in Williams and Larson (1989), Janes (January 1990), and Cohen et al (1987).

1.2.1 Simple Cycles

Figure 1.1 shows a gas turbine in diagrammatic form. While gas turbines were originally developed for aircraft propulsion, they are now used in many ground-based applications. Gas turbines have traditionally been used in the electricity supply industry to supply peaking power. Despite low capital cost, they have not been considered for base-load use because they run on oil or natural gas, which are more expensive than coal. Gas turbine performances have improved over the years, but simple cycle efficiencies are still below those of the large condensing steam turbines traditionally used in power stations. A modern steam-electric plant may be up to 44% efficient⁶, but most have a more conservative efficiency in the range 38-40% for improved reliability (Macchi, 1990). The most efficient commercially available gas turbine has an efficiency

⁶ Unless stated otherwise, all efficiencies are quoted on a lower heating value basis throughout this thesis.

of 38% (Gas Turbine World 1990 Handbook). The forthcoming General Electric LM6000, available in 1992, will have a simple cycle efficiency of 41.5% (de Biasi, 1990).

The improvement in gas turbine performance results from a steady increase in turbine inlet temperature and cycle pressure ratio. The turbine inlet temperature, the most important parameter determining overall thermal efficiency, is constrained by metallurgical limits of the turbine blades. Improvements in metallurgy and blade cooling techniques have led to an increase in turbine inlet temperature from around 900C in 1960 to over 1200C today⁷.

Stationary gas turbines can be divided into two categories: heavy-duty industrial and aeroderivative. Heavy-duty industrial gas turbines are designed specifically for ground-based operation, where weight and size are not a constraint. They are available in a range of sizes up to 150MW. Pressure ratio is typically in the range 10-16. The compressor, turbine, and generator are usually mounted on a single shaft. Aeroderivatives are stationary versions of specific aircraft engines and so have a high power-to-weight ratio. They tend to operate at higher pressure ratios (up to 30) than heavy-duty, but come in sizes only up to 40MW. The generator is driven by a power turbine not physically coupled to the "core" of the gas turbine, known as the gas generator. The gas generator provides a gas flow to drive the power turbine, and might have two or three concentric shafts, each with a turbine driving a compressor. The choice of aeroderivative or heavy-duty gas turbine depends on the application.

1.2.2 Regeneration

Gas turbine cycle efficiency can be improved by modifying the simple cycle to recover heat from the gas turbine exhaust (which ranges in temperature from around 600C in heavy-duty to below 500C in aeroderivatives). An early modification was the addition of a regenerator (Figure 1.2). This is a simple heat exchanger where the exhaust flow preheats the compressor discharge air

⁷ The General Electric Frame F, introduced in 1987, has a turbine inlet temperature of 1260C (2300F).

Stationary gas turbines operate at turbine inlet temperatures over 100C lower than in aircraft engine gas turbines. One reason for this is the time delay in transferring innovations in the aircraft sector to stationary applications. Another is that the use of advanced aero-engine materials might not be economically justifiable for ground-based turbines. Even if the same materials are used, a stationary turbine will have a lower turbine inlet temperature than the aero-engine in order to extend its working life.

prior to combustion. The resulting fuel savings lead to an increase in efficiency. The main disadvantage is the cost of the large heat exchanger. As cycle pressure ratios have increased, turbine exhaust temperatures have decreased while compressor discharge temperatures have increased. Consequently the advantage from a regenerator has diminished to a point where they rarely economically justifiable⁸.

1.2.3 Combined Cycles

Another cycle variation is the combined cycle (Figure 1.3). The gas turbine exhaust produces steam in a heat recovery steam generator (HRSG). The resulting steam drives a steam turbine in a conventional Rankine cycle. Heavy-duty gas turbines are well suited for use in combined cycles because of their relatively high turbine outlet temperatures. Combined cycles are the most efficient thermal power plants operating today. Jeffs (1990) reports a net plant efficiency of 52% for a plant in the Netherlands. Many utilities are choosing combined cycle technology for new base-load and load-following generating capacity.

The steam produced in a HRSG can be increased by installing a duct burner in the gas turbine exhaust. Because gas turbine combustors operate at very lean fuel-to-air ratios, the exhaust contains sufficient oxygen to allow this further combustion step. Duct burning, or supplementary firing, increases power output at the expense of efficiency⁹. It is often used in cogeneration applications where the process steam demand is greater than that obtainable from an unfired HRSG.

1.2.4 Steam-Injected Gas Turbines

An alternative to the combined cycle is the steam-injected gas turbine (STIG). Instead of being expanded in a separate steam turbine, steam from the HRSG is injected into the gas turbine combustor (Figure 1.4). Because only a negligibly small amount of work is required to pump the

⁸ The US Navy is currently developing a regenerative gas turbine for marine propulsion. The need for a dry cycle means that regeneration is the only available method of improving efficiency over the simple cycle value.

⁹ Duct burning in this application is analogous to afterburning in aircraft engines.

feedwater up to combustor pressure, extra turbine work is obtained without the penalty of extra compression work. The resulting power output and efficiency are higher than for the simple cycle. For example, a steam-injected General Electric LM5000 gas turbine has a power rating and efficiency of 47-52MW¹⁰ and 43% respectively, compared to simple cycle values of 34MW and 36%.

The amount of steam injection is limited either by the amount of heat in the exhaust or by constraints on the mass flow in the turbine. If an existing "dry" turbine is to be modified for steam injection, the mass flow of steam which can be injected might be limited to maintain a sufficient compressor surge margin or by the extent of shaft strengthening feasible. Design modifications can relax these limits, but are costly. Aeroderivatives are better suited to steam injection than heavy-duty gas turbines because of their greater ability to accommodate increased mass flow¹¹.

Injection of small amounts of steam into the gas turbine combustor for NO_x reduction is a well-established practice. However large-scale steam injection for power augmentation is a more recent development. Up to now STIGs have been used mainly in cogeneration applications, where steam injection offers the flexibility to provide a wide range of electrical and steam outputs with good performance (Larson and Williams, 1987)¹². The 1980s saw a boom in the use of gas turbines for cogeneration, brought about by the Public Utilities Regulatory Policies Act (PURPA) of 1978, which requires utilities to buy electricity from independent power producers at fair prices.

STIGs are not competitive with combined cycles for central station power applications. For large plant sizes, combined cycles have a higher efficiency than STIGs. However STIGs avoid the cost of the steam turbine, condenser, and possible cooling tower of combined cycles, and are attractive for small plant sizes (up to about 50MW) as they do not suffer from the poor scale economies associated with the steam cycle of combined cycles. This advantage is partially offset by the fact that commercially available STIG cycles are based on aeroderivative gas turbines, which are usually more expensive than the heavy-duty gas turbines used in large combined

¹⁰ Depending on the amount of steam injection.

¹¹ To allow for a range of operating conditions, aircraft engines are designed to accommodate air flows considerably in excess of their nominal ratings. For example, a large compressor surge margin is chosen.

¹² When process steam demand is low, excess steam can be injected into the gas turbine to boost electricity production. Electricity not needed on site can then be sold to the grid.

cycles¹³. Although a STIG plant might have a lower water consumption than a combined cycle, the purification burden is greater¹⁴.

A proposed development of the STIG cycle which might make it suitable for central station applications is the addition of intercooling (Figure 1.5). This is expected to increase greatly both power output and efficiency. For example the General Electric LM8000 intercooled STIG (ISTIG) is predicted to produce around 110MW at 52% efficiency (PG&E, 1984). The use of intercooling reduces the compressor work¹⁵, and because the air bled for turbine blade cooling is colder a higher turbine inlet temperature is possible than in the STIG case. ISTIG is still on the drawing board with no immediate plans for development. The cost of development has been estimated at \$100m to \$150m (Gas Turbine World, December 1988).

1.2.5 Evaporative-Regenerative Cycles

A recently proposed cycle modification has renewed interest in cycles involving a regenerator. The basic idea is to re-establish the temperature difference between the two flows in a regenerator by spray-cooling the compressor discharge (aftercooling), thus allowing heat recovery down to a much lower exhaust temperature. This is the so-called evaporative-regenerative or humid air turbine (HAT) cycle (Figure 1.6). As well as a higher efficiency, this cycle offers an improved power output compared to the simple regenerative cycle because water introduced for cooling evaporates to steam and performs work in the turbine. Efficiency is expected to be higher than for a STIG cycle, and close to that of combined cycles. While the evaporative-regenerative cycle suffers from high losses associated with mixing water into the gas cycle, as does the STIG, the temperature profiles in a regenerator are better matched than the profiles in a HRSG in a STIG or combined cycle.

¹³ See Chapter Four for a more detailed discussion of gas turbine economics.

¹⁴ Water quality requirements are set by the HRSG and, for steam-injected cycles, by the need to protect turbine blades from corrosion. In a combined cycle plant most make-up water is used to replace evaporation losses from the cooling tower, and this does not require extensive treatment. In a STIG, all make-up feedwater travels through the HRSG and gas turbine, and so must be of high purity. However the cost of clean water is small compared to the total gas turbine cost (see for example Soroka and Kamali, 1987).

¹⁵ This is particularly advantageous in aeroderivatives where high pressure ratios lead to high compressor work.

Annerval and Svedberg (1990) add evaporative regeneration to a simple cycle and obtain a power increase of around 40% while efficiency improves from 32% to 46%. Addition of intercooling leads to a further efficiency improvement of 4 percentage points to 50%. El-Masri (1988) presents calculations for a cycle incorporating intercooling, aftercooling, and a water-injected regenerator (which allows close matching of hot- and cold-side temperature profiles in the regenerator). He reports efficiencies of 45% for a cycle with conservative component assumptions and 50% for one with advanced component assumptions.

1.2.6 Reheat

Reheat is the further addition of heat to the working fluid part way through its expansion. Reheat is routinely used in steam turbines to increase cycle power output and efficiency, but has not often been applied to gas turbines. Providing a low stack temperature can be maintained, then a reheat cycle is theoretically more efficient than one without reheat because it has a higher mean temperature of heat addition¹⁶. However the need to provide additional cooling with reheat complicates this simplistic argument. Adding reheat to a gas turbine increases the turbine outlet temperature, and this leads to greater amounts of steam available for steam injection (Figure 1.7) or use in a combined cycle. A reheat ISTIG based on the LM8000 has been estimated to produce 185MW at 54% efficiency (PG&E, 1989). Rice (1980) predicts that adding reheat to a (non-intercooled) combined cycle based on the LM5000 improves efficiency by approximately 5 percentage points.

A few reheat gas turbines were built in the early years of gas turbine development, particularly in Europe and the USSR. These were not particularly successful, partly because the relatively low turbine inlet temperatures and pressure ratios of that era are far from optimal for reheat cycles. Rice (1980; 1982b) argues that the high turbine inlet temperatures and pressure ratios of modern aeroderivative engines are well suited for reheat cycles, and sees the development of reheat gas turbines as inevitable.

¹⁶ The need to provide additional cooling with reheat complicates the effect of reheat on performance.

Introduction of reheat requires the development of a reheat combustor and a high temperature, cooled, power turbine. This represents a major development effort and is likely to be very expensive. Chapter Four includes a discussion of design issues surrounding reheat.

1.2.7 Steam Cooling

The high turbine inlet temperatures used by modern gas turbines demand cooling of the combustor and the leading stages of turbine blading. This is usually implemented by bleeding some of the compressor air flow, typically around 20-25%. Cooling flows much greater than this have a significant adverse effect on performance, meaning that there are diminishing returns to increasing turbine inlet temperature by increasing bleed-air flow. Introduction of reheat would more than double the amount of metal to be cooled, and would heighten the need to find ways of reducing the amount of bleed-air¹⁷.

Steam has been advanced as an alternative to bleed-air (Rice 1982a). This would be produced using the gas turbine exhaust in a heat recovery steam generator. Steam is a more effective coolant than bleed-air because of its higher specific heat capacity, and is likely to be available at a lower temperature. An additional advantage is that steam coolant, unlike bleed-air, requires no compressor work. Steam cooling is conceptually similar to steam injection, because after passing through the blade cooling passages the steam mixes with the main flow and performs work¹⁸. Takeya and Yasui (1988) estimate that a steam-injected gas turbine with intercooling, reheat, and steam cooling will be 54% efficient. A major uncertainty surrounding steam cooling concerns how much steam is required and whether an unfired HRSG will be able to supply it all. Further investigation is required in this area.

¹⁷ One method already used by some manufacturers is to pre-cool the bleed-air before using it for cooling.

¹⁸ However some potential work is lost because the steam enters the main flow part-way down the turbine rather than in the combustor.

1.3 THE CHEMICALLY RECUPERATED GAS TURBINE

1.3.1 Basic Description

The chemically recuperated gas turbine (CRGT) is a development of the STIG cycle. The basic concept is that while some of the exhaust heat generates steam, some drives an endothermic chemical reaction between that steam and the natural gas fuel. This reaction is often referred to as "steam reforming". The result is a low heating value fuel gas containing combustibles such as hydrogen and carbon monoxide, and non-combustibles such as carbon dioxide and steam. The fuel gas is then burned in the gas turbine combustor. This is expected to lead to NO_x and carbon monoxide emissions low enough to meet existing regulations without exhaust gas clean-up.

The endothermic reaction is an efficient means of recovering energy from the gas turbine exhaust and returning it to the gas turbine to produce work. Chapter Two shows how substituting chemical recuperation for some steam production in a STIG cycle leads to enhanced thermal efficiency. In a CRGT cycle the HRSG is replaced by a heat recovery steam reformer (HRSR) which serves both as a steam generator and as a chemical reactor. Figure 1.8 shows a schematic for a typical CRGT cycle.

CRGT cycles may employ either aeroderivative or heavy-duty gas turbines. If an existing gas turbine design is to be used, then an aeroderivative will be the easier to modify to accommodate the extra mass flow in the turbine. However it will be shown in Chapter Three that the low pressure ratio and high turbine outlet temperature of heavy-duty turbines are favorable for chemical recuperation. A reheat CRGT cycle appears promising because the high turbine outlet temperature associated with reheat facilitates steam reforming.

1.3.2 Review of Research to Date

The idea of improving heat engine performance by using a chemical reaction to recover waste heat has been around at least since 1972 (Olmsted and Grimes, 1972).

The idea was first applied to gas turbines in the late 1970s. In this period concern about energy security arising from the Arab oil crisis led to increased interest in synthetic fuels. One such fuel was methanol, which can be manufactured from coal. The reaction between methanol and steam, previously of interest only in methanol fuel cells (Kurpit, 1975), was found to be well suited for chemical recuperation of gas turbine exhaust heat (Janes, 1979). A Westinghouse study (Davies et al, 1983) showed that adding chemical recuperation to a methanol-fired 501D gas turbine improved power output by 10% over the simple cycle value, while efficiency rose from 34% to 42%. While interest in methanol as a gas turbine fuel faded in the 1980s, several further studies pointed to the favorable performance of methanol-fired CRGTs (Klaeyle et al, 1987; Tsuruno and Fujimoto, 1987; Granquist et al, 1990).

Although steam reforming of natural gas has been considered for heat recovery from industrial furnaces in the Soviet Union (Pereletov et al, 1978), the application of this reaction to gas turbines is only recent. The California Energy Commission (CEC) is interested in CRGT as a means of meeting new NO_x emission standards recently proposed by the South Coast Air Quality Management District. A draft report, authored by Mr Jack Janes of the Commission, points to a triple benefit of excellent emissions characteristics, high efficiency, and low capital cost (Janes, January 1990). The report incorporates performance estimates, based on gas turbine data supplied by General Electric, which predict that a CRGT derived from the CF6-80C2 aircraft engine with intercooling and reheat could have an efficiency as high as 59%. A study conducted by the Pacific Gas and Electric Company, based on the same GE data, puts this value at 56% (De Candia, 1989).

At a recent workshop held to discuss the CEC report¹⁹, a panel of industry experts broadly agreed with its findings. However they emphasized the need for further research. The required first follow-on step is experimental verification of the predicted emissions levels. The Gas Research Institute is planning to sponsor appropriate tests at General Electric in 1991 (Puzson, 1990). It was agreed also that the advanced technology proposed will take many years and many dollars to develop. One way of achieving the full CRGT concept might be to prove it in stages²⁰.

¹⁹ Chemically Recuperated Gas Turbines Workshop organized by the California Energy Commission at the California Museum of Science and Industry, Los Angeles, 1 February 1990.

The first step could be to retrofit an existing STIG plant. Some of these plants will have to install SCR to meet the new Southern California NO_x regulations, and it might prove cost-effective to add chemical recuperation instead. The University of California at Davis proposes to investigate this option (Kesser, 1989). The Sunlaw Energy Corporation, a California-based cogenerator, is showing an interest in placing a launch-order for a number of full CRGTs (Janes, May 1990).

Also at the workshop, participants expressed concern about the predicted thermodynamic performance of CRGT. The General Electric calculation contains some uncertainty, particularly about the amount of cooling air and steam required. The GE calculation is for one specific machine (the LM8000). There is a need for a more general study to gain a better understanding of the thermodynamics of CRGT cycles. That is the objective of this thesis. The aim is to discover the fundamental merits and drawbacks of CRGT cycles compared to other cycles, especially STIG and combined cycles. Particular attention is given to the suitability of CRGTs for base-load power generation, as the projected high efficiency suggests their use in this application.

REFERENCES

K Annerval and G Svedberg, A Study on Modified Gas Turbine Systems with Steam Injection or Evaporative Regeneration, Royal Institute of Technology Department of Heat Technology, Stockholm Sweden, April 1990

Annual Energy Review, Department of Energy DOE/EIA-0384(88), 1988

V de Biasi, "LM6000 dubbed the 40/40 machine due for full-load tests in late 1991", Gas Turbine World, May-June 1990

J B Burnham, M H Giuliani, and D J Moeller, "Development, Installation, and Operating Results of a Steam Injection System (STIG) in a General Electric LM5000 Gas Generator", ASME Journal of Engineering for Gas Turbines and Power, July 1987

F De Candia, ISTIG Enhancement Evaluation, Volume I, Pacific Gas and Electric Company report 007.4-89.1, September 1989

H Cohen, G F C Rogers, and H I H Saravanamuttoo, Gas Turbine Theory, Longman, 1987

D G Davies, N H Woodley, R W Foster-Pegg, and M E Karpuk, Improved Combustion Turbine Efficiency with Reformed Alcohol Fuels, ASME 83-GT-60

M A El-Masri, "A Modified, High-Efficiency, Recuperated Gas Turbine Cycle", ASME Journal of Engineering for Gas Turbines and Power, April 1988

Gas Turbine World, pp40, December 1988

²⁰ In a similar fashion the LM5000 STIG was demonstrated in stages, firstly by retrofitting an existing LM5000 for partial steam injection, then building a full steam injection machine (Burnham et al, 1987)

Gas Turbine World, pp30, September-October 1989

Gas Turbine World 1990 Handbook, Pequot Publishing, Southport CT, February 1990

A Granquist, I Grunden, F Houllis, T Schmidt, and C Tarnstrom, Foradlad Metanol Som Bransle For Gasturbin, Department of Heat Technology, Kungl Tekniska Hogskolan (Royal Institute of Technology), Stockholm Sweden, March 1990

J Janes, "Increasing Gas Turbine Efficiency through the use of a Waste Heat Methanol Reactor", Proceedings of the 14th Intersocietal Energy Conversion Engineering Conference, 1979

J Janes, Chemically Recuperated Gas Turbine, California Energy Commission Draft Staff Report, January 1990

J Janes of the California Energy Commission, personal communication, May 1990

E Jeffs, "Utrect 225MW Combined Cycle Certified at 52% Efficiency", Gas Turbine World, January/February 1990

K Kesser of University of California at Davis, personal communication, February 1989

D A Kolp and D J Moeller, "World's First Full STIG LM5000 Installed at Simpson Paper Company", ASME Journal of Engineering for Gas Turbines and Power, April 1989

S Klaeyle, R Laurent, and F Nandjee, New Cycles for Methanol-Fuelled Gas Turbines, ASME 87-GT-175

S S Kurpit, "1.5 and 3kW Indirect Methanol-Air Fuel Cell Power", Proceedings of the 10th Intersocietal Energy Conversion Engineering Conference, 1975

E D Larson and R H Williams, "Steam-Injected Gas Turbines", ASME Journal of Engineering for Gas Turbines and Power, January 1987

E Macchi, "Power Generation (Including Cogeneration)", Department of Energetics, Politecnico di Milano, Milan, Italy, 1990

J H Olmsted and P G Grimes, "Heat Engine Efficiency Enhancement - through Chemical Recovery of Waste Heat", Proceedings of the 7th Intersocietal Energy Conversion Engineering Conference, 1972

PG&E: Scoping Study: LM5000 Steam-Injected Gas Turbine, Pacific Gas and Electric Company, San Francisco, July 1984

I I Pereletov, E A Chulanov, V N Novoseltsev, M F Shopsin, A I Tyurin, V A Volkov, Y V Lashenkov, and V I Chugunkov, "Catalytic Reforming of the Natural Gas in the Industrial Furnace Heat Recovery System", translated from the book Catalytic Reforming of the Hydrocarbons (1978) by the Institute of Gas Technology

J Puzson of the Gas Research Institute, Chicago IL, personal communication, November 1990.

I G Rice, "The Combined Reheat Gas Turbine/Steam Turbine Cycle", ASME Journal of Engineering for Gas Turbines and Power, January 1980

I G Rice, 1982a, "The Reheat Gas Turbine with Steam-Blade Cooling - a Means of Increasing Reheat Pressure, Output, and Combined Cycle Efficiency", ASME Journal of Engineering for Gas Turbines and Power, January 1982

I G Rice, 1982b, "The Reheat-Gas-Turbine Combined Cycle", Mechanical Engineering, April 1982

SCAQMD, Air Quality Management Plan, South Coast Air Quality Management District, 1989 Revision, March 1989

R Smock, "Gas Turbines Dominate New Capacity Ordering", Power Engineering, August 1989

G Soroka and K Kamali, "Modular Remotely Operated, Fully Steam-Injected Plant for Utility Application", Proceedings of the 1987 ASME Cogen-Turbo Conference, Montreux Switzerland, September 1987

K Takeya and H Yasui, "Performance of the Integrated Gas and Steam Cycle (IGSC) for Reheat Gas Turbines", ASME Journal of Engineering for Gas Turbines and Power, April 1988

S Tsuruno and S Fujimoto, Gas Turbine Cycle with Steam Reforming of Methanol, presented at 1987 Tokyo International Gas Turbine Congress

R H Williams and E D Larson, "Expanding Roles for Gas Turbines in Power Generation", in T B Johansson, B Bodlund, and R H Williams, editors, Electricity: Efficient End-Use and New Generation Technologies, and Their Planning Implications, Lund University Press, 1989

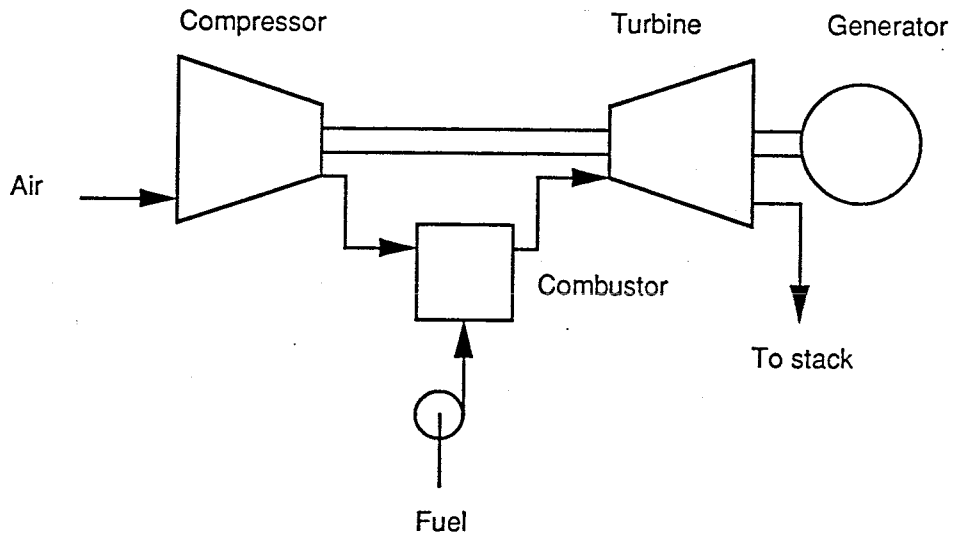


Figure 1.1: Simple Cycle Gas Turbine

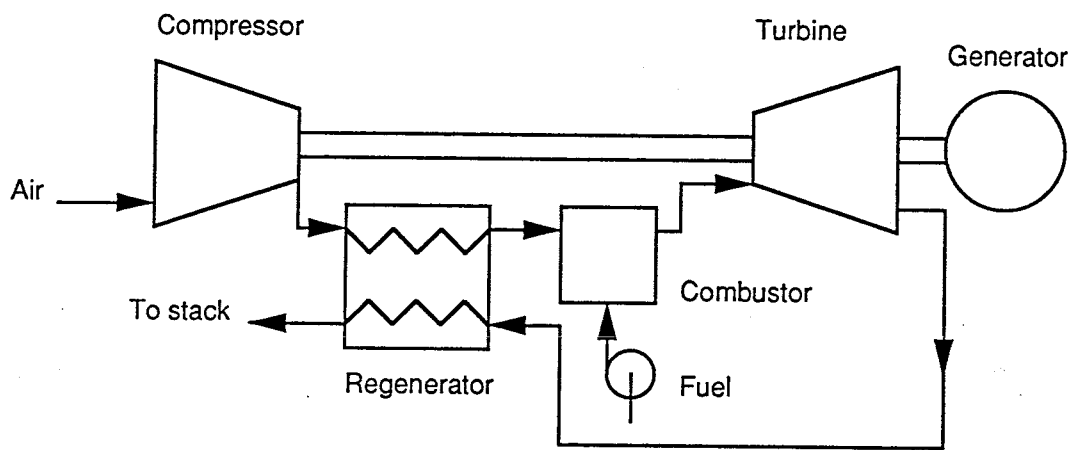


Figure 1.2: Simple Cycle with Regeneration

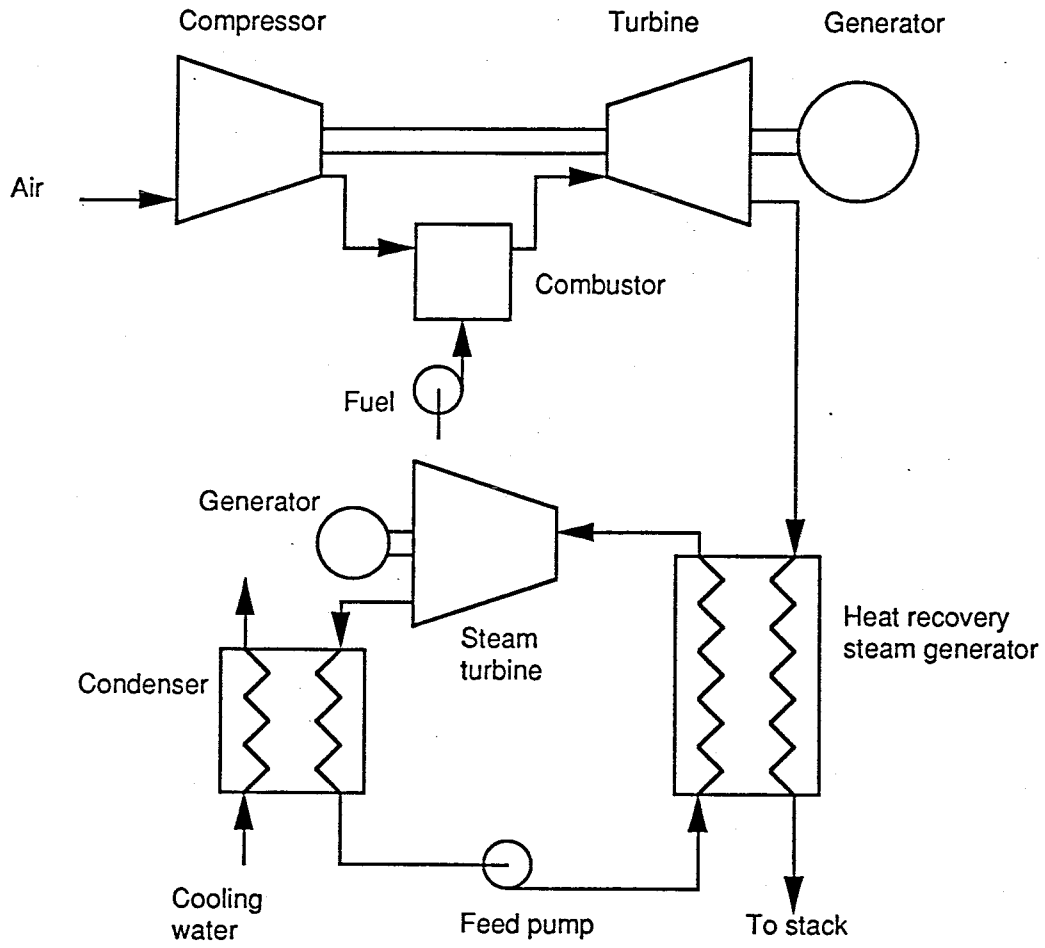


Figure 1.3: Combined Cycle

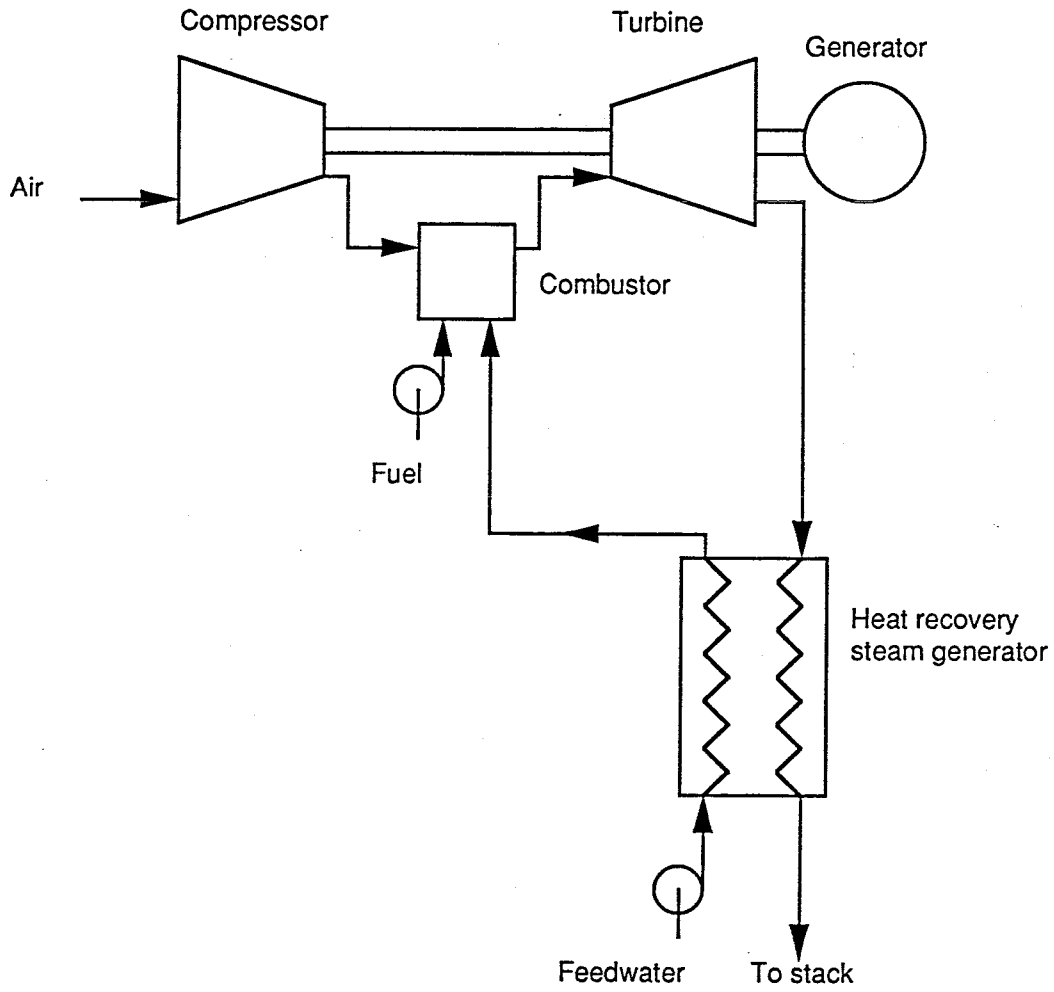


Figure 1.4: Steam-Injected Gas Turbine (STIG) Cycle

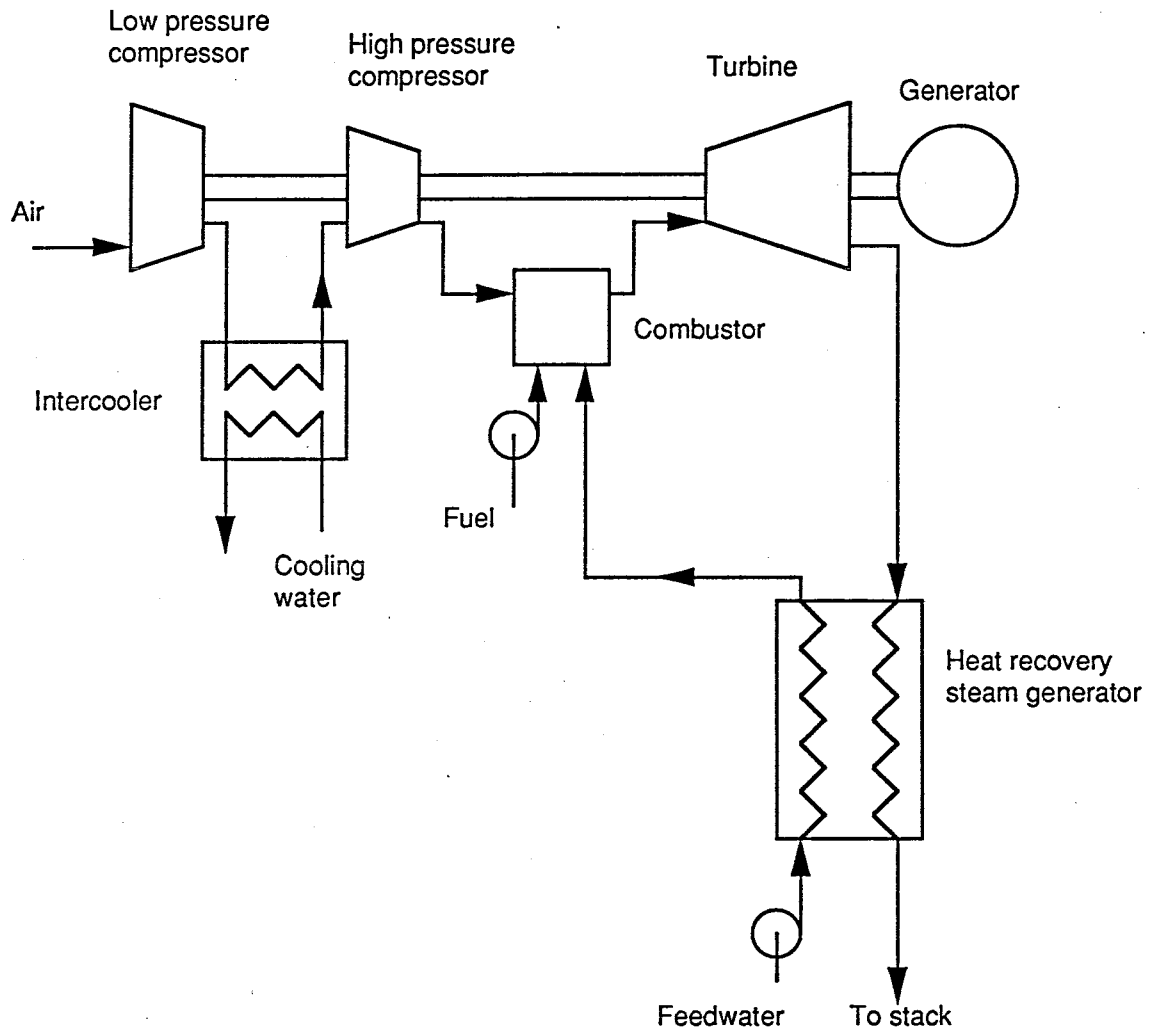


Figure 1.5: Intercooled Steam-Injected Gas Turbine (ISTIG) Cycle

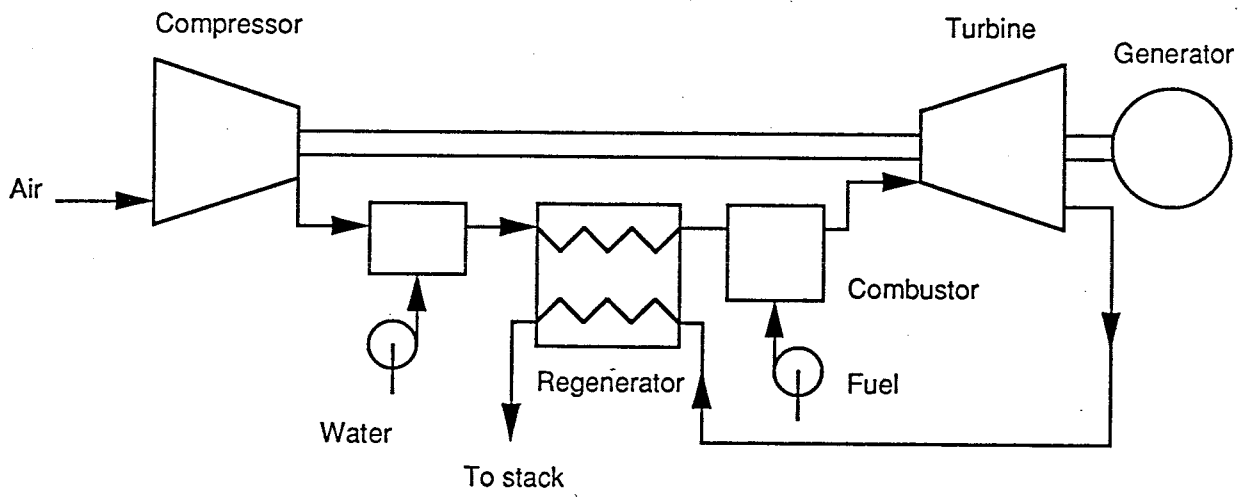


Figure 1.6: Evaporative-Regenerative Cycle

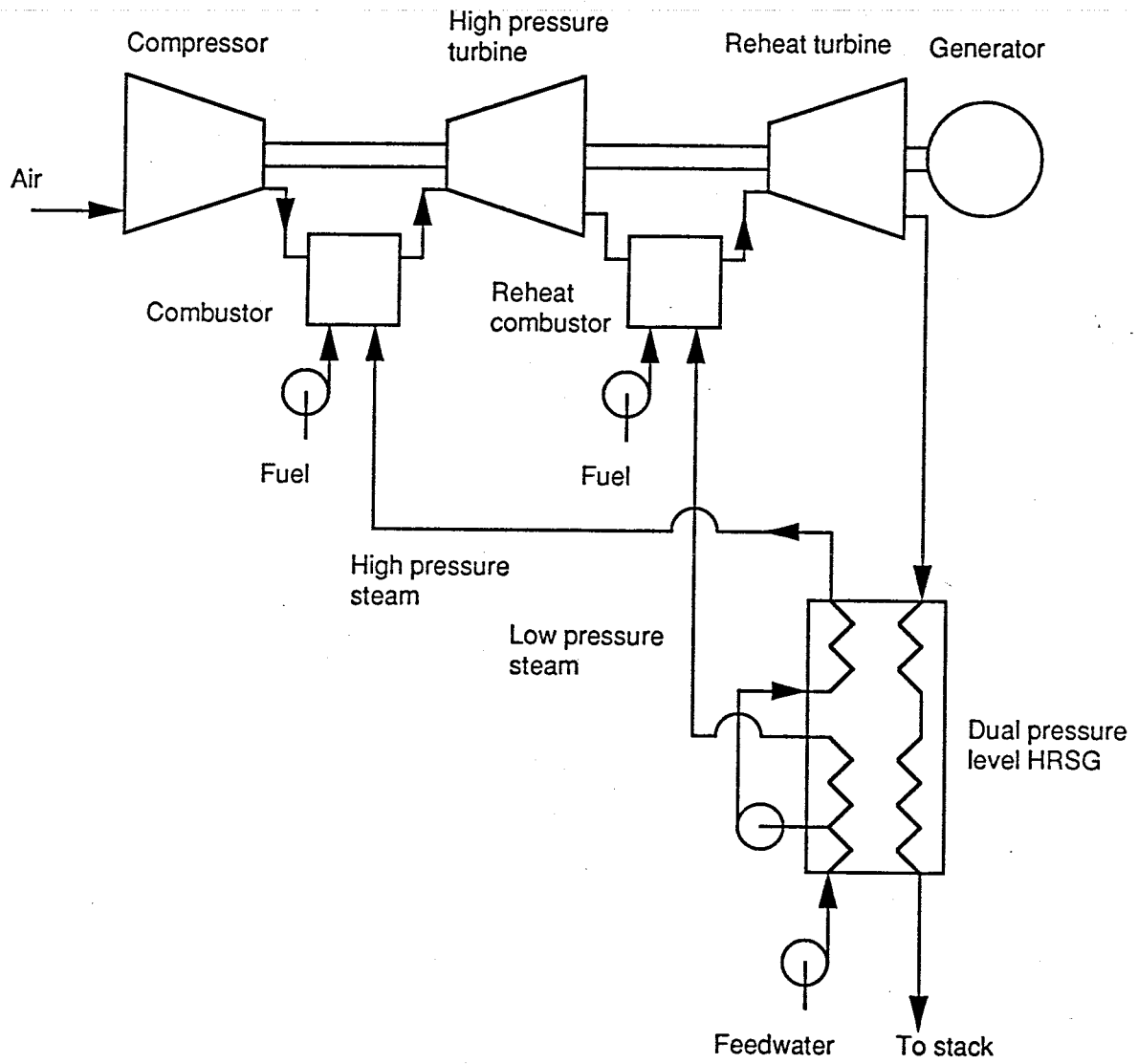


Figure 1.7: Reheat ISTIG Cycle

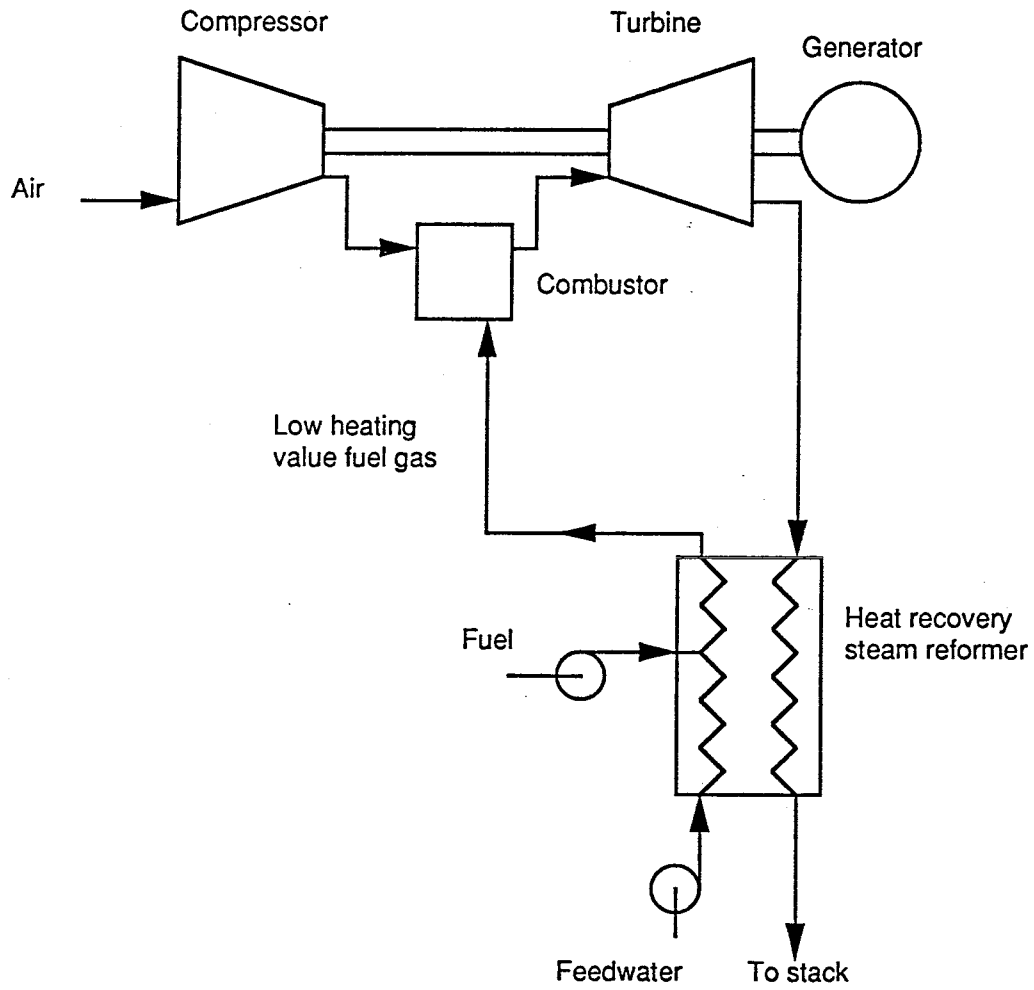


Figure 1.8: Chemically Recuperated Gas Turbine Cycle

CHAPTER TWO: THERMODYNAMIC FUNDAMENTALS

2.1 Introduction

2.2 Thermodynamics of STIG Cycles

2.3 Regeneration and Chemical Recuperation

2.4 Exergy Analysis

2.5 CRGT with Supplementary Firing

2.6 CRGT with Reheat

2.7 Review

References

Notation

Appendix 2A

Figures

2.1 INTRODUCTION

This chapter presents a thermodynamic exploration of how chemical recuperation might affect overall cycle performance. Simplified arguments are developed to enable comparison of CRGT with other cycles. The resulting predictions are tested in Chapters Six and Seven using a detailed cycle calculation model.

As the CRGT cycle is a development of the STIG cycle, familiarity with the thermodynamics of STIG cycles is a prerequisite for understanding the effect of chemical recuperation. Section 2.2 looks at STIG cycles in detail, and develops simplified expressions describing cycle performance. Section 2.3 investigate the effects of adding chemical recuperation or simple regeneration to a STIG cycle. These two cycle modifications turn out to be very similar thermodynamically. The amount of steam production emerges as an important parameter determining cycle performance.

Sections 2.2 and 2.3 use simple mass, heat, and enthalpy balances to describe STIG and CRGT cycles. While easy to understand, this "First Law" approach has the limitation that it does not take into account the quality of heat or work. Section 2.4 uses the more powerful tool of exergy

analysis (Second Law analysis) to achieve a more rigorous thermodynamic comparison of the two cycles.

Sections 2.5 and 2.6 introduce supplementary firing and reheat.

2.2 THERMODYNAMICS OF THE STIG CYCLE

In the steam-injected gas turbine (STIG) cycle, the hot gas turbine exhaust gases raise steam in a heat recovery steam generator (HRSG). The steam is then injected back into the gas turbine (Figure 2.1). The recovery of exhaust heat raises efficiency over the simple cycle value, while the additional mass flow in the turbine boosts the power output.

The analysis of this chapter assumes that the gas turbine can accommodate all of the steam that can be generated by the heat available in the exhaust¹. For simplicity a single evaporation pressure HRSG is considered.

2.2.1 HRSG Operation

The HRSG consists of three sections: an economizer, a boiler, and a superheater. The incoming feedwater is preheated to saturation temperature in the economizer, evaporates at constant pressure and temperature in the boiler, and the resulting steam is heated above saturation temperature in the superheater. The turbine exhaust gases, which flow in a counter-current direction, provide the heat required for these processes. Figure 2.2 shows the water- and gas-side temperature profiles as a function of the amount of heat exchanged. The gas-side profile is

¹ The use of a "rubber turbine", where the gas turbine is assumed to be optimally designed for the cycle under consideration, is justified in a fundamental thermodynamic analysis such as this. However it should be remembered that because of the high cost of developing a gas turbine, a practical cycle will to some extent be designed around an existing gas turbine.

If an existing gas turbine is modified for steam injection, then the amount of steam which can be injected into the combustor might be limited by gas turbine design constraints. See Section 1.2.4.

The performance penalty imposed by this restriction could be partially overcome by generating additional steam at a lower pressure (or pressures) and injecting this part-way down the turbine, thus enabling further heat recovery. Multi-pressure evaporation is thermodynamically attractive in that it reduces exergy losses in the HRSG by allowing the water-side temperature profile to more closely follow the gas-side profile.

essentially linear, with a slope determined by the mass flow rate and specific heat (assumed constant in this expression for pedagogic purposes only)²:

$$Q = m_g c_{p,g} \Delta T$$

The water-side profile consists of three linear sections. The boiler section has zero slope as boiling takes place at constant temperature. The slopes of the economizer and superheater sections depend on the specific heats of water and steam, and on the ratio between the water- and gas-side mass flow rates³.

A number of design constraints affect HRSG operation. The temperature difference between the water- and gas-side flows at any point must exceed a certain finite minimum. The size of this approach temperature is determined by an economic trade-off between the large heat exchanger size required for a small approach and the resulting improved cycle performance. This limit typically applies at the boiler water inlet (known as the "pinch-point") and maybe at the superheater steam outlet (the "hot-end")⁴. Another limit is that the stack gas temperature must exceed a certain minimum, usually around 100C, in order to prevent condensation and subsequent corrosion in the stack (the "dew-point limit") and to maintain buoyancy of the stack gases⁵. Metallurgical considerations usually limit the temperature of steam exiting the superheater (typically to around 550C).

Figure 2.3 shows how the HRSG profiles change as the steam-to-air ratio S varies. At low S , steam exits the superheater at a high temperature. This temperature is limited either by the maximum allowable metal temperature or by the requirement that it is lower than the temperature

² A list of notation appears at the end of the chapter.

³ For convenience, the analysis of this chapter will measure the amount of steam (or water) in a cycle using the variable S , defined as the mass flow rate of steam (or water) divided by the mass flow rate of air entering the compressor.

⁴ Typical values are 20C for the hot-end approach and 10C for the pinch-point. At the pinch-point one of the fluids is a liquid, while at the hot-end both are gases. This leads to higher heat transfer coefficients at the pinch-point, and hence the pinch-point temperature difference is generally smaller than the hot-end approach.

⁵ The stack limit could be lowered by using a condensing HRSG, which has non-corrosive materials, together with a fan to maintain buoyancy. This option is rarely considered owing to the extra expense involved, but might be justifiable in certain situations. For example, in regions of limited water availability, a condensing HRSG can recover water from the exhaust for reuse. Another potential application is in low temperature district heating networks (see Annerwall and Svedberg, 1988).

of the incoming gas turbine exhaust flow by at least the minimum hot-end approach. As S increases, the pinch-point temperature difference decreases until it also is at its limit. At higher S still, the superheater exit temperature falls while the pinch-point limit still applies. When the pinch-point limit is in effect, stack temperature falls as S increases. This follows from the increased heating load in the economizer. If the stack temperature reaches its lower limit, then further increasing S causes the pinch-point approach to move back above its minimum, while total heat transfer stays constant. Eventually S reaches a point where the steam exits the HRSG saturated (zero superheat).

The value of S at which these various regimes start and end depends on the temperatures of the incoming water and gas flows, on the evaporation pressure (which sets the evaporation temperature), and on the values specified for the various limits. For a specified steam temperature at the superheater outlet, the maximum available steam production is fixed by either the pinch-point or the stack limit. This maximum is higher with a lower degree of superheat. Hence the amount of steam available from recovering the heat in a gas turbine exhaust is greatest when the steam is saturated rather than superheated.

Simple "back-of-the-envelope" calculations can illustrate these various operating regimes. Case A in Figure 2.4 assumes an evaporation pressure and inlet gas temperature representative of a STIG cycle based on a heavy-duty gas turbine, while Case B corresponds to an aeroderivative. In Case A the high inlet gas temperature and low evaporation pressure lead to relatively high steam production. The lower exhaust gas temperature and higher evaporation pressure of the aeroderivative lead to a lower steam availability⁶.

2.2.2 Effect of Steam Flow on Efficiency

Armed with this understanding of HRSG operation, we can proceed to investigate overall cycle performance. Consider the cycle shown in Figure 2.1. One way of understanding the cycle is to consider it as a thermodynamic "black box" into which flow air and feedwater at ambient temperature and out of which flows a mixture of steam and air at elevated temperature T_5 ⁷. Heat

⁶ Note that this discussion is for a "rubber" HRSG. The assumption is that at a given steam production S the HRSG is optimally designed for that value of S .

q_{in} is added (per kg of compressor inlet air), and the resulting work w_x is given by the difference between the turbine and compressor works:

$$w_x = (1+S)(h_3-h_4) - (h_2-h_1)$$

Heat rejection occurs in the form of a net enthalpy gain of the water and air flows:

$$q_{out} = (1+S)h_5 - h_1 - S.h_6$$

Efficiency is given by

$$\eta = w_x/q_{in} = w_x/(w_x+q_{out}) = 1/(1+q_{out}/w_x)$$

Substituting for w_x and q_{out} leads to an expression for thermal efficiency in terms of enthalpies around the cycle and the steam-to-air ratio S (Appendix 2A presents an alternative derivation of this expression)⁸:

$$\eta = \frac{[(1+S)(h_3-h_4)-(h_2-h_1)]}{[(1+S)(h_3-h_4)-(h_2-h_1)] + [(1+S)h_5-h_1-S.h_6]}$$

For high efficiency, the quantity (q_{out}/w_x) must be as close to one as possible, where

$$q_{out}/w_x = \frac{(1+S)h_5-h_1-S.h_6}{(1+S)(h_3-h_4)-(h_2-h_1)}$$

Consider a cycle where the turbine inlet temperature, pressure ratio, and inlet air and water temperatures are fixed. The sole independent variable is then the steam flow S , while h_5 , η , and (q_{out}/w_x) are dependent variables⁹. As S increases from zero, the work obtained increases monotonically. Meanwhile the stack temperature initially falls as more and more exhaust heat is recovered, and so the stack enthalpy h_5 declines. Hence q_{out} increases more slowly with S than does w_x , or might even decline. The ratio q_{out}/w_x decreases, and so efficiency increases. Eventually the stack temperature reaches and remains at its lower limit, and h_5 remains constant

⁷ The mass flow rate of fuel is neglected for simplicity. Instead it is assumed that heat is added in the combustor without addition of extra mass or change of chemical composition.

⁸ Section 2.2.1 showed that, for a given steam exit temperature, steam production in the HRSG is constrained either by the minimum acceptable pinch-point temperature difference or the minimum stack temperature. In deriving expressions for efficiency, it is assumed that the stack limit is in operation. The analysis of this chapter is essentially the same when the pinch-point limit is in operation.

⁹ Actually h_3 and h_4 will change slightly with the amount of steam injection. The simplified argument of this chapter assumes these remain constant.

as S increases further. In this regime q_{out} generally increases with S at a faster rate than does w_x , and efficiency declines.

Hence the efficiency of a STIG cycle peaks at an optimal value of S (Case A of Figure 2.5). At this point the stack temperature limit (or the minimum pinch-point) is in operation, while the steam outlet temperature is at its upper limit. The conclusion is that a STIG cycle is at its most efficient when as much steam is generated as is possible at maximum superheat. The existence of this optimum is the key to understanding the potential benefits of chemical recuperation. Note that the work output is at a maximum when S is as large as possible, that is when steam leaves the HRSG saturated. Hence STIG cycle efficiency and power output optimize at different steam flows.

This argument about the variation of efficiency with S depends on the enthalpy values around the cycle. Case A of Figure 2.5 is derived from simplified calculations for a STIG cycle with a pressure ratio of 12 and a turbine inlet temperature of 1100C. However at a pressure ratio of 35 efficiency is greatest when the steam is saturated (Case B of Figure 2.5). At high evaporation pressure and low turbine outlet temperature, the amount of steam available at maximum superheat is small. The pinch-point limit constrains steam production, while stack temperature remains well above its limiting value. Reducing the stack temperature becomes important, and the higher steam flow obtainable with saturated steam enables a lower stack temperature¹⁰. Since the combination of low TIT and high pressure ratio is far from optimal (high pressure ratio cycles optimize at high TIT), most practical STIG cycles will show the trend of Case A of Figure 2.5.

2.3 REGENERATION AND CHEMICAL RECUPERATION

Suppose now that some amount of heat q_r is recovered from the gas turbine exhaust by some means other than steam generation (Figure 2.6). For the moment the nature of this heat recovery is not specified, except to say that the heat recovered somehow returns to the combustor.

¹⁰ Section 2.4 discovers that efficiency is greatest at zero superheat if the penalty of generating saturated steam in the HRSG is more than offset by the gain from recovering exhaust heat down to a lower temperature.

The expression for the cycle efficiency, derived in Appendix 2A, is exactly the same as that for the STIG cycle:

$$\eta = \frac{[(1+S)(h_3-h_4)-(h_2-h_1)]}{[(1+S)(h_3-h_4)-(h_2-h_1)] + [(1+S)h_5-h_1-S.h_6]}$$

This is unsurprising since the two cycles are the same from the "black box" perspective. The difference between the two cycles lies in the dependence of the stack temperature on S . At zero steam production the modified cycle has a lower stack temperature T_5 than the STIG cycle, as heat is recovered from the exhaust by some other means, and so efficiency is higher. As steam production increases, stack temperature falls and efficiency rises further just as in the STIG case. However, the limiting stack temperature is reached at a lower value of S . Increasing S beyond this value leads to a fall-off in efficiency as before.

The expression for efficiency can be used to trace out the modified curve of efficiency against steam production (Figure 2.7). At high S , h_5 is constant at a value set by the stack limit, and so the curve is the same as for the STIG case. At low S , h_5 at a given S is lower than for the STIG, and so efficiency is higher. The meeting point between these two regimes is at lower S and higher efficiency. The modified cycle is more efficient because heat is recovered to the same low temperature as in the STIG cycle, but with a lower steam flow. Section 2.4 discovers that steam production has its drawbacks as a means of heat recovery, and that other means of heat recovery are generally preferable.

An exception to this is the special case, mentioned in Section 2.2, where efficiency is greatest with saturated steam. In this case the modified cycle would have an optimized efficiency less than that of the STIG cycle.

The additional heat recovery q_r can be achieved in various ways. One is by regeneration, where the compressor discharge air is preheated prior to combustion (Figure 2.8). The regenerator, a large heat exchanger, is located in the exhaust stream between the turbine and the HRSG. An expression for efficiency can be derived and is exactly as before. Regeneration is feasible only if the turbine outlet temperature is greater than the compressor discharge temperature. Even then,

the difference between these temperatures limits the amount of heat recoverable. Regeneration is rarely economically feasible owing to the expense of the large heat exchanger required for effective heat transfer between two gas flows.

An alternative means of heat recovery is chemical recuperation. Heat from the exhaust transfers back to the combustor by driving an endothermic chemical reaction between steam and fuel (Figure 2.9). The recovered heat is carried in the form of enhanced chemical energy of the fuel. Again the same expression for efficiency can be derived. Chemical recuperation does not suffer from the temperature constraints that apply to regeneration. Instead, the amount of chemical heat recovery is determined by the chemistry of the reaction¹¹.

There are still others means of heat recovery without extra steam production. One example is to use the gas turbine exhaust to preheat the fuel before it enters the combustor. The amount of heat involved is likely to be small, especially for gaseous fuels. Another way would be to further superheat any existing steam if the degree of superheat is not already at its upper limit.

Figure 2.7 also shows the variation of work output with S . The curve is the same for the modified and STIG cycles, but the upper limit on steam production is lower for the modified cycle because some exhaust heat is recovered by means other than steam generation. Both the maximum achievable work and the work at the optimal efficiency are lower for the modified cycle. This trade-off between work and efficiency is a major drawback of chemical recuperation.

2.4 EXERGY ANALYSIS

Second Law or exergy analysis is a useful tool for pinpointing thermodynamic losses in a cycle. The fuel input to the cycle has an associated availability, or exergy, which is the work obtained if fuel produces work in a fully reversible process. This exergy must be equal to the sum of the actual work obtained, the exergy of all output streams, and the component irreversibilities. Exergy analysis is an accounting procedure which allows identification and comparison of the various sources of loss in a cycle.

¹¹ Chapter Three discusses the heat recovery potential of the steam-fuel reaction.

This section comprises a qualitative description of where these losses occur in a STIG cycle. A simplified calculation shows how the loss distribution changes when the cycle is modified as in Section 2.3. In this example, heat is recovered by regeneration rather than chemical recuperation, as the presence of chemical reaction slightly complicates matters. These two methods of heat recovery affect STIG cycle performance in a similar manner. Chapter Six presents a quantitative exergy analysis of a CRGT cycle.

In a STIG cycle, exergy is lost in the four components (compressor, combustor, turbine, and HRSG) and up the stack. The stack flow represents a loss because it is above ambient temperature and could theoretically drive a reversible heat engine. The component losses stem from a variety of sources such as irreversible heat transfer and pressure loss. The compressor and turbine irreversibilities arise mainly from aerodynamic losses, and are quantified as the adiabatic or polytropic efficiency. The main irreversibility in the combustor is the chemical reaction between fuel and air, while injection of steam leads to further loss through irreversible mixing. Irreversible heat transfer is the major source of loss in the HRSG.

The combustor loss is by far the largest, typically 20-30% of the fuel exergy, but the other four loss sources are all significant. The difference between the exergy of the fuel and the sum of the losses is the actual work obtained. The ratio of actual work to the reversible work available from the fuel is the cycle efficiency¹².

Because the loss associated with the combustion reaction loss is so large, it is important to understand the factors which influence this. The exergy loss arises because combustion is a highly irreversible reaction (the only reversible chemical reaction is one that is at equilibrium). Its magnitude depends on thermodynamic properties of the reactants and products, which in turn are influenced primarily by the combustor exit temperature, the incoming air temperature, and the chemical composition of the fuel. For typical gas turbine fuels, the thermodynamic properties of the fuel and combustion products are such that combustion exergy loss declines with higher combustor exit temperature. A high incoming air temperature favors a low combustion loss

¹² This definition leads to a slightly different value from the more usual definition of efficiency as the work obtained divided by the heat added by the fuel. The exergy of a fuel is different from its heating value because, in addition to the enthalpy of combustion, it also includes the work available from reversibly mixing the products of combustion with the environment.

because the irreversibility associated with internal heat transfer from the primary air to the dilution air is reduced¹³.

Figure 2.10 shows the exergy analyses for the simplified STIG and modified STIG cycles of Figure 2.7. Both cycles are analyzed at the steam-to-air ratio S which leads to the greatest efficiency. The major difference between the two cycles is that the modified cycle has substantially lower HRSG losses than does the STIG cycle. The reduction in HRSG losses more than outweighs the extra losses arising from the introduction of the regenerator. As a result the modified cycle recovers more of the fuel exergy as work, and so it is more efficient¹⁴.

The reason for the reduced HRSG losses can be seen by comparing the heat recovery temperature profiles for the two cycles (Figure 2.11). Losses in the HRSG and regenerator arise from irreversible heat transfer across finite temperature differences between the hot- and cold-side flows. These temperature differences can be substantial in a HRSG, where evaporation occurs at constant temperature. This represents a fundamental drawback for steam generation as a means of heat recovery. A regenerator does not suffer from this problem, and a good matching of temperature profiles is possible. Hence substituting regeneration for some steam generation in a STIG cycle leads to reduced heat recovery losses and increased efficiency.

Chemical recuperation is similar to regeneration in its effect on the heat recovery profiles. The cold-side flow in the recuperator is a reacting mixture of methane and steam. Heat transferred to this flow sustains the endothermic reaction in addition to raising the temperature. Hence the cold-side profile has a gentle slope, similar to that of the hot-side. Figure 2.12 is a schematic diagram showing how introducing chemical recuperation leads to a better matching of heat recovery profiles¹⁵.

¹³ In a gas turbine combustor, an approximately stoichiometric amount of air reacts with the fuel in the primary zone, leading to peak temperatures equal to the adiabatic flame temperature. Dilution air is added downstream to reduce the temperature to the desired combustor exit temperature. Chapter Four contains a detailed description of gas turbine combustors.

¹⁴ Since losses are expressed as percentages of input fuel exergy, small differences in the values of the other component losses arise from the fact that the two cycles operate at different air-to-fuel and steam-to-fuel ratios. For example, the modified cycle has greater compressor losses than the STIG cycle, even though the air flow is identical, because the fuel flow rate is lower.

There might be cases when regeneration or chemical recuperation does not lead to an efficiency improvement, for example the very high pressure ratio cycle of Case B of Figure 2.5. In this case a combination of low turbine outlet temperature and high evaporation pressure leads to a low steam production and a high stack temperature. STIG cycle efficiency is greatest when the steam flow is maximized by producing saturated steam. The reduced stack temperature more than offsets the penalty of poorly matched HRSG profiles. Adding regeneration or chemical recuperation will lead to improved profile matching but the lower steam production and higher stack temperature might outweigh this.

It is believed that such cases are uncommon, and that for most practical cycles the addition of chemical recuperation improves efficiency. The quantitative analysis of Chapter Six seeks to confirm this. Until then, the findings of this section can be summarized by saying that addition of chemical recuperation to a STIG cycle is likely to lead to improved efficiency through reductions in the heat transfer irreversibilities associated with heat recovery.

2.5 CRGT WITH SUPPLEMENTARY FIRING

The efficiency gain achievable with chemical recuperation depends on the amount of chemical heat recovery q_r . Chapter Three shows that this is strongly dependent on the reforming temperature, which in turn depends on the temperature of the exhaust-side flow entering the reformer. This section considers whether employing supplementary firing (also known as duct-burning) to raise these temperatures will lead to an efficiency improvement over the unfired cycle.

Figure 2.13 shows the cycle. Steam is produced at two pressures in the HRSG, and two separate chemical recuperation processes occur in parallel but at different pressures in the reformer. The low pressure steam mass flow is a fraction F of the total steam production S .

¹⁵ Neither regeneration nor chemical recuperation can be substituted entirely for steam production. Regeneration can recover heat only down to a temperature determined by the compressor discharge temperature, and so steam generation is needed to recover down to a lower temperature. Chapter Three shows that the heat absorbed by the steam reforming reaction declines with temperature. Moreover, a CRGT cycle requires steam for the steam reforming reaction. However, both modifications replace some steam production with a more effective method of heat recovery.

The intuitive response as to the effect of supplementary firing is that it is more likely to lead to a loss rather than a gain of efficiency. From the argument developed so far, it is clear that efficiency will rise only if optimized total steam production falls. This optimum occurs when the stack temperature is at the lower limit and the steam superheat at its upper limit. Supplementary firing adds heat to the exhaust, and so, for a given amount of chemical heat recovery q_r , more steam production is necessary to maintain the stack temperature at its lower limit. Supplementary firing will be more efficient only if the resulting increase in q_r is greater than the heat added by supplementary firing. Whether this is the case will depend on the chemistry of the recuperation reaction.

A further drawback is that the steam used in the low pressure reformer by-passes the turbine, and this represents a loss of work and a penalty on efficiency if the exhaust heat used to generate this steam could otherwise be used to produce high pressure injection steam. The increase in q_r must compensate for this also.

An expression for efficiency can be derived in the same manner as before (see Appendix 2A), but this time the equation includes the extra variable F:

$$\eta = \frac{[1+(1-F)S](h_3-h_4)-(h_2-h_1)}{[1+(1-F)S](h_3-h_4)-(h_2-h_1)+(1+S)h_5-h_1-S.h_6}$$

If F is equal to zero, the expression is as before. This represents an unfired CRGT cycle or one in which unreformed fuel fires the supplementary firer. If the fuel for the supplementary firer is reformed, then F is some fraction between zero and one, the value of which increases with the supplementary firing temperature. F influences the work output but not the heat rejection:

$$w_x = [1+(1-F)S](h_3-h_4) - (h_2-h_1)$$

$$q_{out} = (1+S)h_5 - h_1 - S.h_6$$

Hence as F increases there is a reduction in work due to the diversion of some steam through the reformer, but the heat rejection is unchanged. The implication of this is that efficiency is greatest when unreformed fuel fires the supplementary firer. Otherwise, the supplementary fired cycle will be less efficient even if the optimum value of S is the same as for the unfired cycle¹⁶.

A Second Law perspective is inconclusive. A supplementary-fired STIG cycle has a higher fuel-to-air ratio than an unfired cycle, and this tends to reduce the importance of turbomachinery losses and stack losses. However the high steam flow required to achieve a low stack temperature leads to large heat transfer irreversibilities in the HRSG. Adding chemical recuperation will alleviate this by reducing steam flow and enabling a better matching of temperature profiles, but it is unclear whether this will be enough to improve efficiency above the unfired STIG value.

To summarize, supplementary firing will lead to an efficiency gain only if the increase in chemical heat recovery outweighs the heat added by the supplementary fuel. Chapter Seven performs detailed cycle calculations to see if this is actually the case.

2.6 REHEAT

The drawbacks of supplementary firing might potentially be overcome with reheat. To evaluate the reheat CRGT cycle, it is first necessary to look at the reheat STIG cycle (Figure 2.14). The second combustion stage is located part way down the turbine rather than in the exhaust. Some of the heat added in the reheat combustor is converted directly into work in the reheat turbine, while the remainder contributes to an elevated turbine outlet temperature. The HRSG produces steam at two pressures. High pressure steam is injected into the main combustor, and low pressure steam into the reheat combustor.

The presence of reheat leads to an enhanced work output compared to the non-reheat STIG. However the fuel flow is higher too, and of course efficiency increases only if the work obtained per unit of fuel increases. This depends on how reheat changes the exergy losses around the cycle. The high turbine outlet temperature associated with reheat requires high steam production

¹⁶ The situation is actually more subtle than this. Using steam to reform the supplementary fuel penalizes efficiency only if the steam is generated at the expense of high pressure steam for injection or HP fuel reforming. Even if as much high pressure steam as possible is produced, it is usually possible to take advantage of a lower evaporation pressure to produce a small amount of low pressure steam.

to recover the exhaust heat, and this leads to high HRSG irreversibilities. The net result is that while addition of reheat improves the power output of a cycle, the effect on efficiency is unclear.

Figure 2.15 shows a reheat CRGT cycle. The effect of adding chemical recuperation to a reheat STIG cycle is similar to the non-reheat case. Chemically recovering some of the exhaust heat allows achievement of a low stack temperature with a lower steam production. This leads to a better matching of heat recovery temperature profiles, and makes for an improved efficiency. The hot turbine exhaust leads to a high chemical heat recovery, pointing to a large efficiency gain. However, if the reheat combustor fuel is steam-reformed, then the steam used for steam-reforming by-passes the high pressure turbine, representing a loss of work compared to the reheat STIG. The loss-of-work effect is not as severe as for the supplementary-fired CRGT, but nonetheless means that it is unclear whether a reheat CRGT will be more efficient than a reheat STIG. Detailed calculations are needed to clarify this point.

2.7 REVIEW

The simple analyses developed in this chapter have indicated that a CRGT cycle is generally more efficient than an equivalent STIG cycle. Chemical heat recovery is advantageous in that it allows a reduction in steam production while maintaining a low stack temperature. High heat transfer irreversibilities in the HRSG represent a fundamental drawback of steam production as a means of heat recovery. Chemical recuperation alleviates this by enabling a better match of heat recovery temperature profiles. The efficiency gain is achieved only at the expense of a loss of work output resulting from the reduced steam flow.

Cycles with a very high pressure ratio are possible exceptions to this finding. Addition of chemical recuperation will lead to a reduction in efficiency if the effect of a rise in stack temperature resulting from the reduced steam flow outweighs the benefit of improved heat recovery profiles.

Adding supplementary firing to a CRGT cycle will further increase efficiency only if the extra chemical heat recovery outweighs the heat added in the supplementary firer. The high turbine outlet temperature of a reheat gas turbine enables more chemical heat recovery in a reheat CRGT cycle than in the non-reheat case. This suggests that the efficiency gain from adding

chemical recuperation will be greater for a reheat STIG than for a STIG without reheat. However the work loss from diverting steam through the low pressure reformer will counteract this.

Detailed cycle calculations are required to gauge the precise effect of these various cycle modifications. Chapters Six and Seven present such calculations. An important factor affecting CRGT performance is the amount of chemical heat recovery achievable, which in turn depends on the chemistry of the steam reforming reaction. Chapter Three addresses this subject.

REFERENCES

K Annerwall and G Svedberg, Analysis of Steam-Injected Gas Turbine Cogeneration with Condensing Heat Recovery, Royal Institute of Technology Department of Heat Technology, Stockholm Sweden, April 1988

NOTATION

Units are given in parentheses. Note that most heat and work quantities are expressed per unit mass of air entering the compressor.

$c_{p,g}$ - specific heat of gas turbine exhaust stream (kJ/kgK)

F - fraction of total steam used for reforming fuel for supplementary firer

h_n - enthalpy of working fluid at point n (kJ/kg)

m_g - mass flow of gas turbine exhaust stream (kg)

Q - heat transfer (kJ)

q_c - heat added by combustion by fuel (kJ/kg of air)

q_{in} - total heat added to cycle by fuel combustion (kJ/kg of air)

q_{out} - heat rejection from cycle to environment (kJ/kg of air)

q_r - heat recovered from exhaust by regeneration or chemical recuperation (kJ/kg of air)

q_{sup} - heat added by supplementary firing (kJ/kg of air)

S - total steam production (kg/kg of air)

T_n - temperature at point n (K)

w_x - specific work (kJ/kg of air)

η - efficiency

ΔT_{he} - hot end approach temperature (C or K)

ΔT_{pp} - pinch-point temperature difference (C or K)

APPENDIX 2A: EXPRESSIONS FOR EFFICIENCY

In this appendix expressions are derived for the work output and thermal efficiency of the various cycles considered in Chapter Two. All expressions are normalized with respect to the mass flow rate of compressor inlet air. Notation is as given above. As the aim is to promote an understanding of the basic concepts involved, a number of simplifying assumptions are made:

- 1) No heat loss from any component.
- 2) No cooling air bleed flows, nor any other mass leakages.
- 3) The fuel adds heat in the combustor without addition of mass.

STIG Cycle

Figure 2.1 shows the cycle. The net specific work is obtained by subtracting the compressor work from the turbine work:

$$w_x = (1+S)(h_3-h_4) - (h_2-h_1)$$

The heat input to the combustor is

$$q_{in} = (1+S)h_3 - h_2 - S.h_7$$

An enthalpy balance across the HRSG yields

$$S(h_7-h_6) = (1+S)(h_4-h_5)$$

Eliminating h_7 from the preceding two equations gives

$$q_{in} = (1+S)h_3 - h_2 - S.h_6 - (1+S)(h_4-h_5)$$

which rearranges to

$$q_{in} = (1+S)(h_3-h_4) - (h_2-h_1) + (1+S)h_5-h_1-S.h_6$$

The cycle thermal efficiency is the net work divided by the heat input:

$$\eta = w_x/q_{in}$$

$$\eta = \frac{(1+S)(h_3-h_4)-(h_2-h_1)}{(1+S)(h_3-h_4)-(h_2-h_1)+(1+S)h_5-h_1-S.h_6}$$

Because the heat input to the cycle is related to the work output and the heat rejection by the First Law

$$q_{in} = w_x + q_{out}$$

the efficiency can be written as

$$\eta = w_x / (w_x + q_{out})$$

where

$$q_{out} = (1+S)h_5 - h_1 - S.h_6$$

STIG Cycle with Regeneration or Chemical Recuperation

In this cycle, shown in Figure 2.6, some heat q_r is recovered from the gas turbine exhaust by some means other than steam generation and is returned directly to the combustor. This might be by regeneration or by chemical recuperation. The following analysis does not specify a particular method but can easily be adapted so that it does. Equations can be written in the same manner as before:

Work:

$$w_x = (1+S)(h_3-h_4) - (h_2-h_1)$$

There are now two heat inputs to the combustor; the recovered heat and the external heat input provided by the fuel:

$$q_{in} + q_r = (1+S)h_3 - h_2 - S.h_7$$

The heat balance for the HRSG is as before except that the incoming exhaust stream is at a lower temperature:

$$S(h_7-h_6) = (1+S)(h_8-h_5)$$

The heat recovered by regeneration or chemical recuperation is:

$$q_r = (1+S)(h_4-h_8)$$

Eliminating h_8 , h_7 , and q_r yields

$$q_{in} = (1+S)(h_3-h_4) - (h_2-h_1) + (1+S)h_5 - h_1 - S.h_6$$

The expressions for w_x and q_{in} are the same as for the STIG cycle, and so the expression for efficiency is also unchanged:

$$\eta = \frac{(1+S)(h_3-h_4)-(h_2-h_1)}{(1+S)(h_3-h_4)-(h_2-h_1)+(1+S)h_5-h_1-S.h_6}$$

CRGT with Supplementary Firing

Figure 2.13 shows the cycle. F is the fraction of total steam S which is sent to the low pressure reformer to produce fuel gas for the supplementary firer. The total external heat added to the cycle is the sum of the combustor heat q_c and the supplementary firer heat q_{sup} . The chemical heat recovery q_r does not appear explicitly in the equations, but is embedded in the enthalpies of the fuel gas streams leaving the reformer.

Work:

$$w_x = [1+(1-F)S](h_3-h_4) - (h_2-h_1)$$

Combustor:

$$q_c = [1+(1-F)S]h_3 - h_2 - (1-F)S.h_{12}$$

Supplementary Firer:

$$q_{sup} = (1+S)h_{10} - [1+(1-F)S]h_4 - F.S.h_{11}$$

HRSG:

$$(1-F)S(h_8-h_6) + F.S(h_9-h_6) = (1+S)(h_7-h_5)$$

Reformer:

$$(1+S)(h_{10}-h_7) = (1-F)S(h_{12}-h_8) + F.S(h_{11}-h_9)$$

The above four equations combine to yield:

$$\begin{aligned} q_{in} &= q_c + q_{sup} \\ &= [1+(1-F)S](h_3-h_4) - (h_2-h_1) + (1+S)h_5 - h_1 - S.h_6 \end{aligned}$$

Hence the expression for efficiency is:

$$\eta = \frac{[1+(1-F)S](h_3-h_4)-(h_2-h_1)}{[1+(1-F)S](h_3-h_4)-(h_2-h_1) + (1+S)h_5-h_1-S.h_6}$$

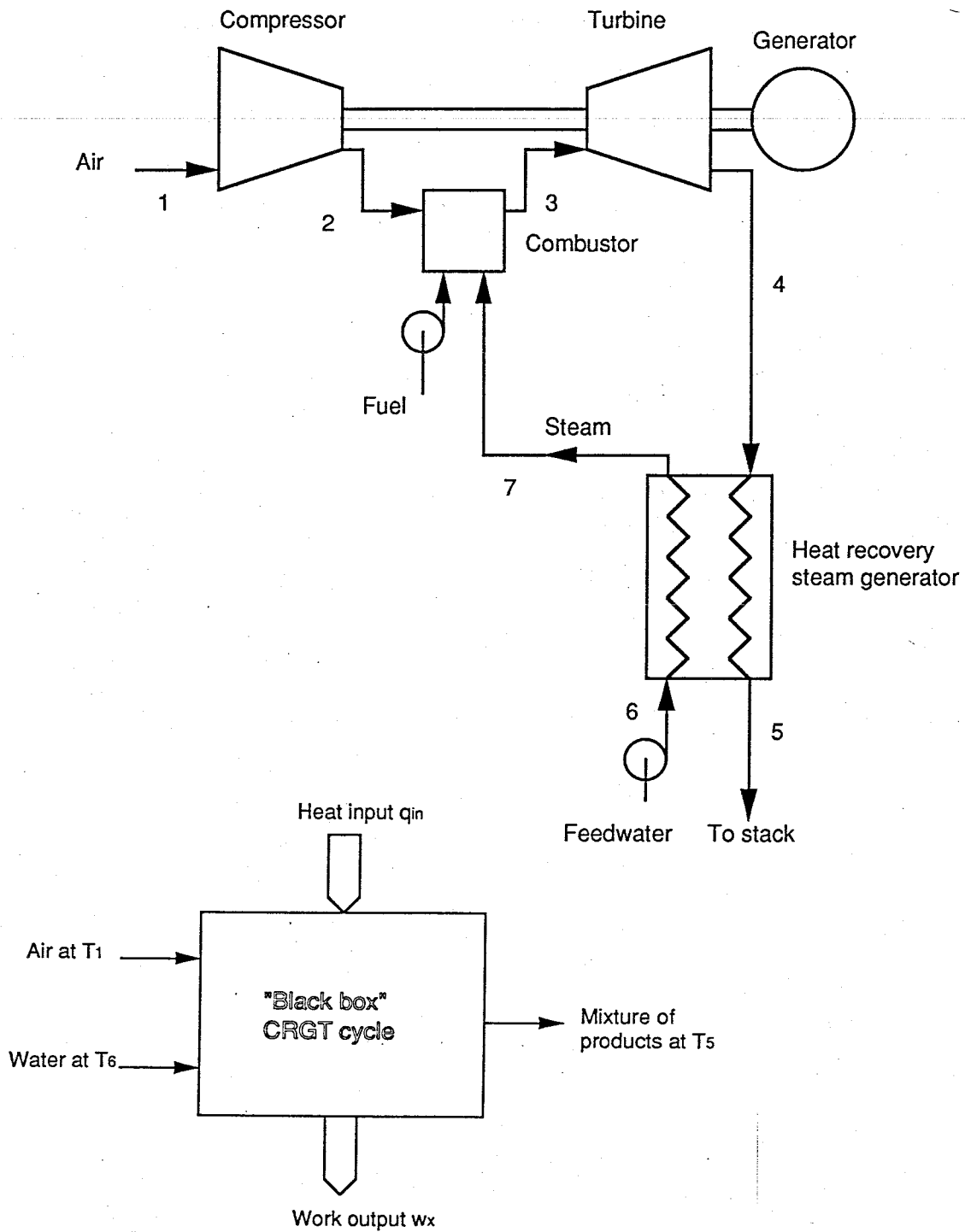


Figure 2.1: Steam-Injected Gas Turbine Cycle

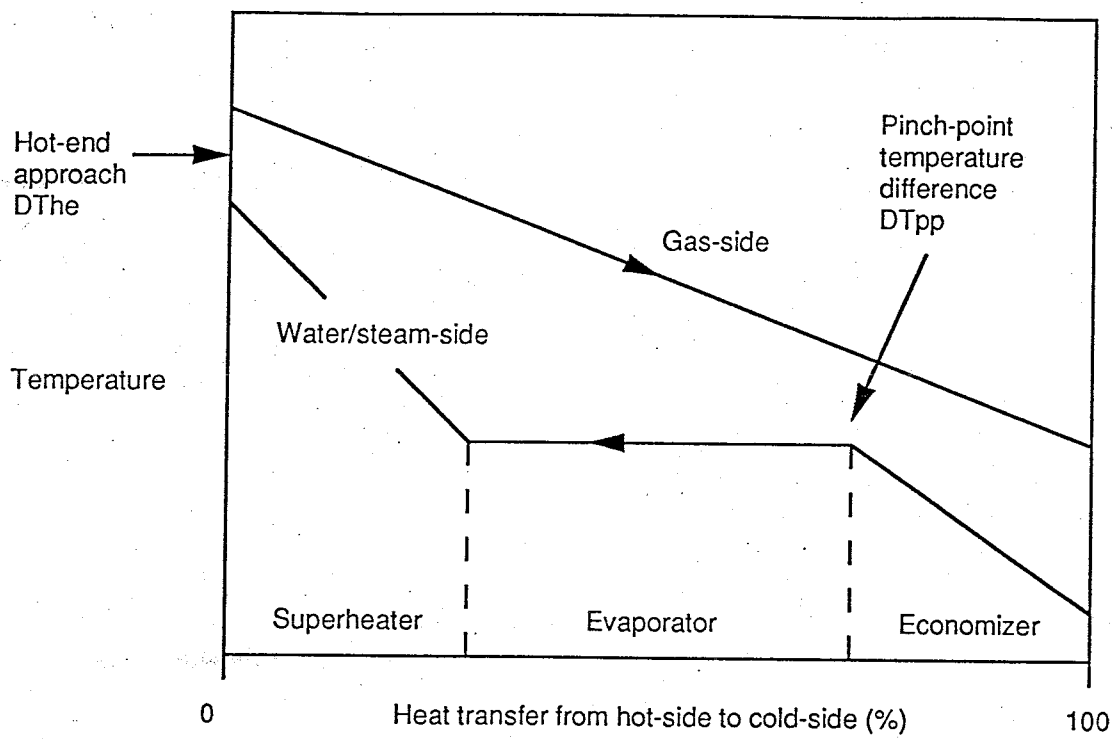
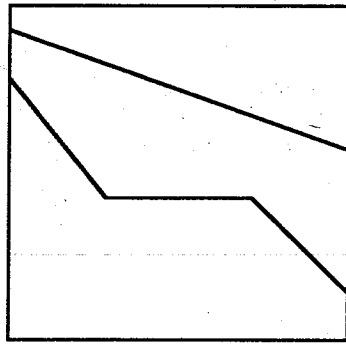
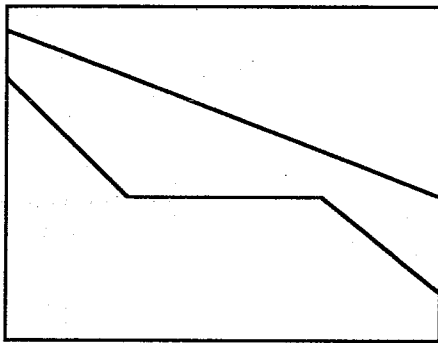


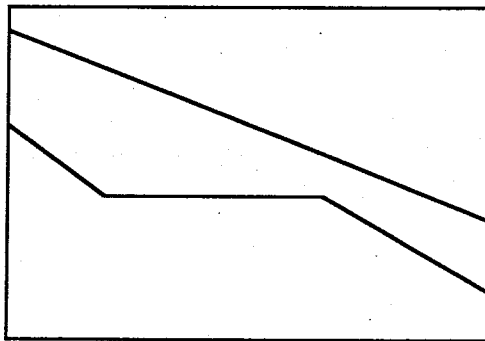
Figure 2.2: HRS Temperature Profiles



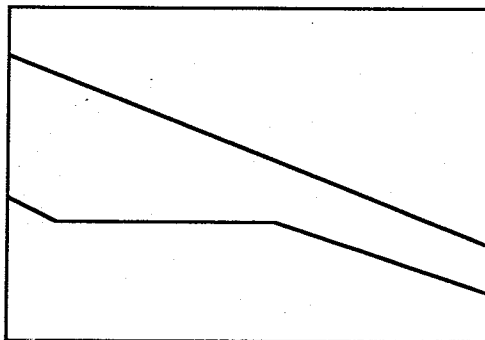
(a) At low S , steam exits HRSG at maximum allowable temperature, set by minimum hot end approach or by metallurgical limits. The pinch point temperature difference DT_{pp} is above its minimum limit.



(b) As S increases, a point is reached where steam exit temperature is at its upper limit and DT_{pp} is at its lower limit. Total heat transfer is greater than above. Efficiency is maximized at this steam flow.



(c) As S continues to increase, heat transfer between hot end and pinch-point remains constant, so steam exit temperature decreases. Heat transfer in economizer increases, so stack temperature falls. DT_{pp} still at limit, but steam exit temperature no longer at limit.



(d) Stack temperature now at lower limit, and so total heat transfer remains constant. Pinch-point moves off limit. Steam exit temperature continues to decrease as S increases until there is no superheat at all. Then S is at its maximum possible value.

Figure 2.3: Variation of HRSG Profiles with Steam Flow Rate

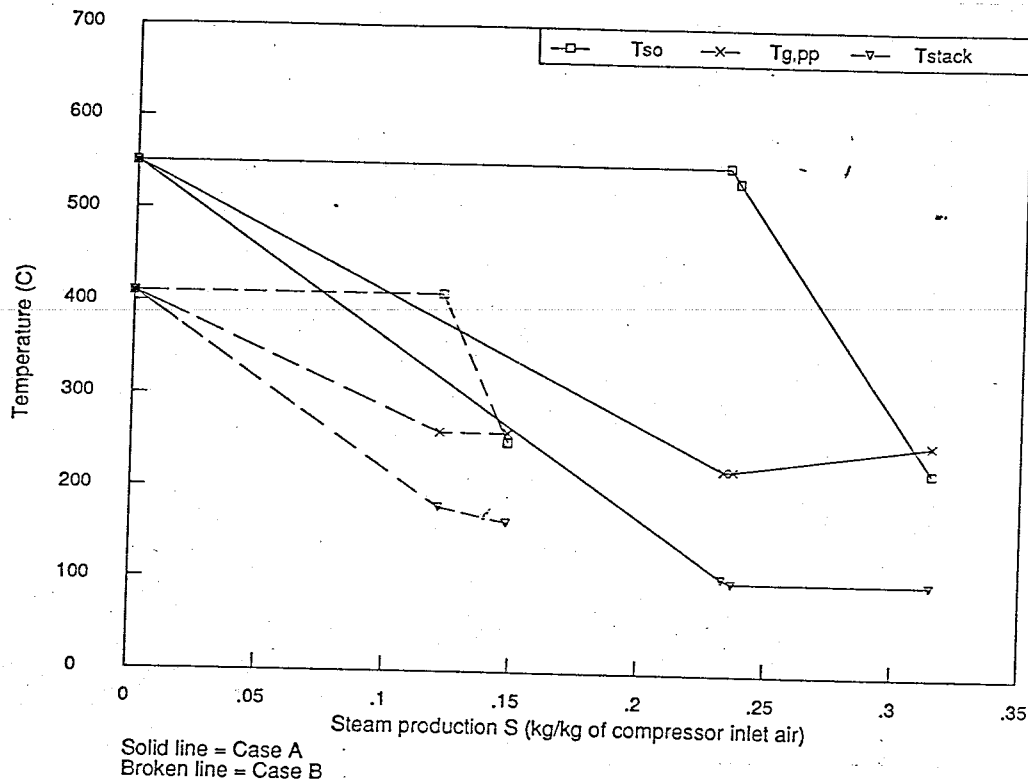


Figure 2.4: "Back-of-the-Envelope" HRSG Calculations

These calculations use the following typical values to gain insight into the limits affecting HRSG operation:

- Maximum steam temperature = 550C
- Minimum stack gas temperature = 100C
- Minimum hot-end approach = 20C
- Minimum pinch-point temperature difference = 10C
- Feedwater entry temperature = 15C
- Specific heat capacity of exhaust gases = 1.3kJ/kgK
- Specific heat capacity of water = 4.2kJ/kgK
- Specific heat capacity of steam = 2.1kJ/kgK

Tso = steam temperature at superheater outlet

Tpp,g = gas-side temperature at pinch-point

Tstack = exhaust gas stack temperature

Case A represents a HRSG used in a STIG cycle based on a heavy-duty gas turbine. It assumes a gas turbine exhaust temperature of 600C and an evaporation pressure of 20bar. At values of S between zero and 0.233, steam is produced at the maximum permissible temperature (this is region (a) of Figure 2.3). At S between 0.233 and 0.237 the pinch-point temperature difference is at its minimum limit, and so Tg,pp is constant (region (c)). At higher S, the stack temperature is at its lower limit (region (d)). The maximum possible steam production, when steam exits the HRSG saturated, is at S equal to 0.315.

Case B assumes a gas turbine exhaust temperature of 430C and a 40bar evaporation pressure, values representative of an aeroderivative STIG. The low exhaust temperature leads to low steam temperature at low S and a low maximum steam production (at S equal to 0.148). At this point the pinch-point limit is still in operation - the stack limit is never encountered.

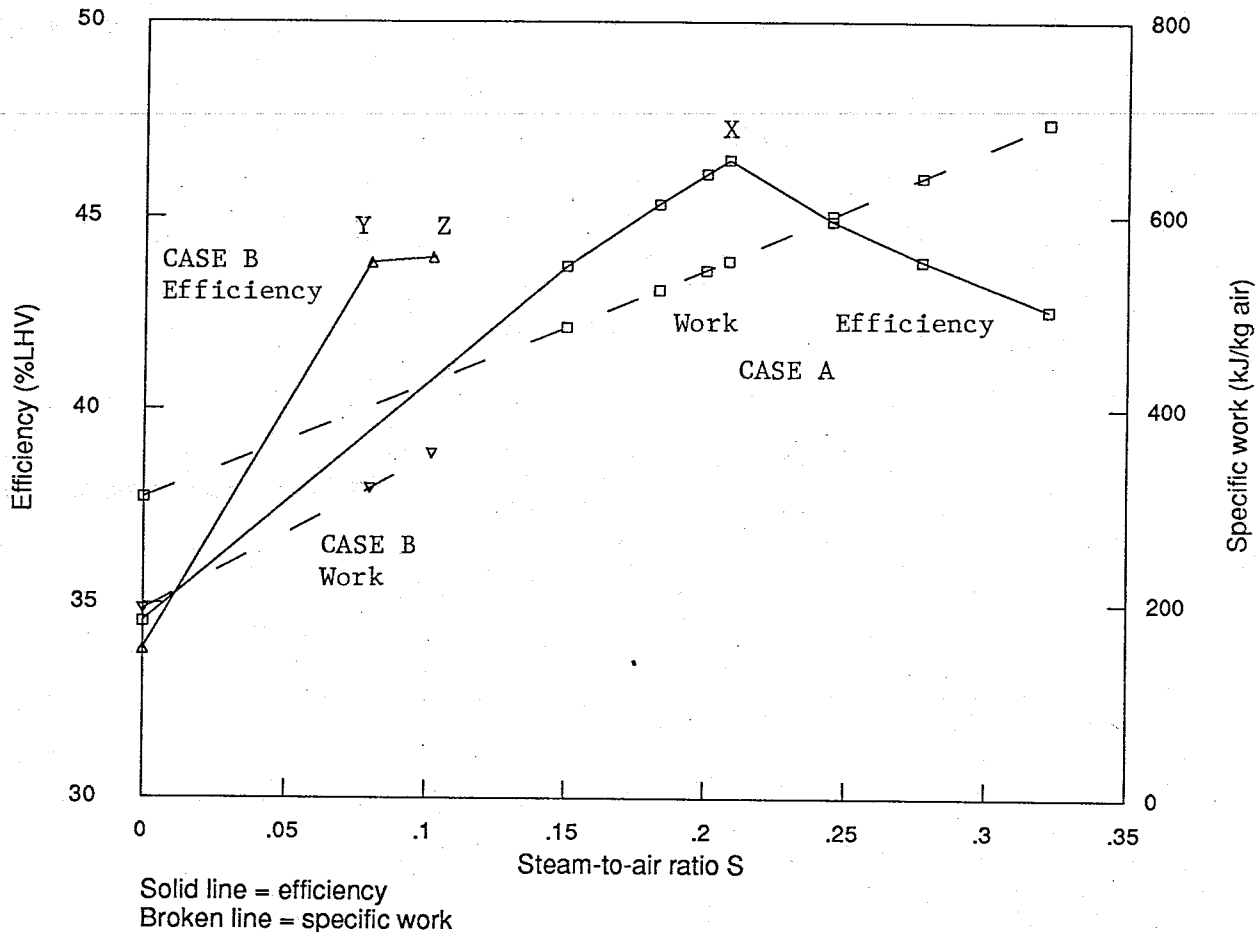


Figure 2.5: Variation of STIG Cycle Performance with Steam Flow

The plot shows the results of STIG cycle calculations carried out using the Consonni computer program (described in Chapter Five). As these are intended for pedagogic purposes only, a number of simplifying assumptions are made. These include no pressure or thermal losses, no turbine cooling, and compressor and turbine polytropic efficiencies of 85%. Consequently the numerical values for efficiency and specific work are somewhat artificial. It is the variation of these with S that is of interest here.

Case A is for a turbine inlet temperature of 1100C and a pressure ratio of 12. Efficiency is greatest at $S=0.208$ (point X). At this point steam is produced at maximum superheat, while the stack temperature is at its lower limit.

Case B is for a TIT of 1100C and a pressure ratio of 35. At $S=0.080$ (point Y) steam is at maximum superheat, and the pinch-point temperature difference is at its minimum possible value. At $S=0.102$, steam is saturated and the pinch-point limit is still in operation. The stack limit is never encountered.

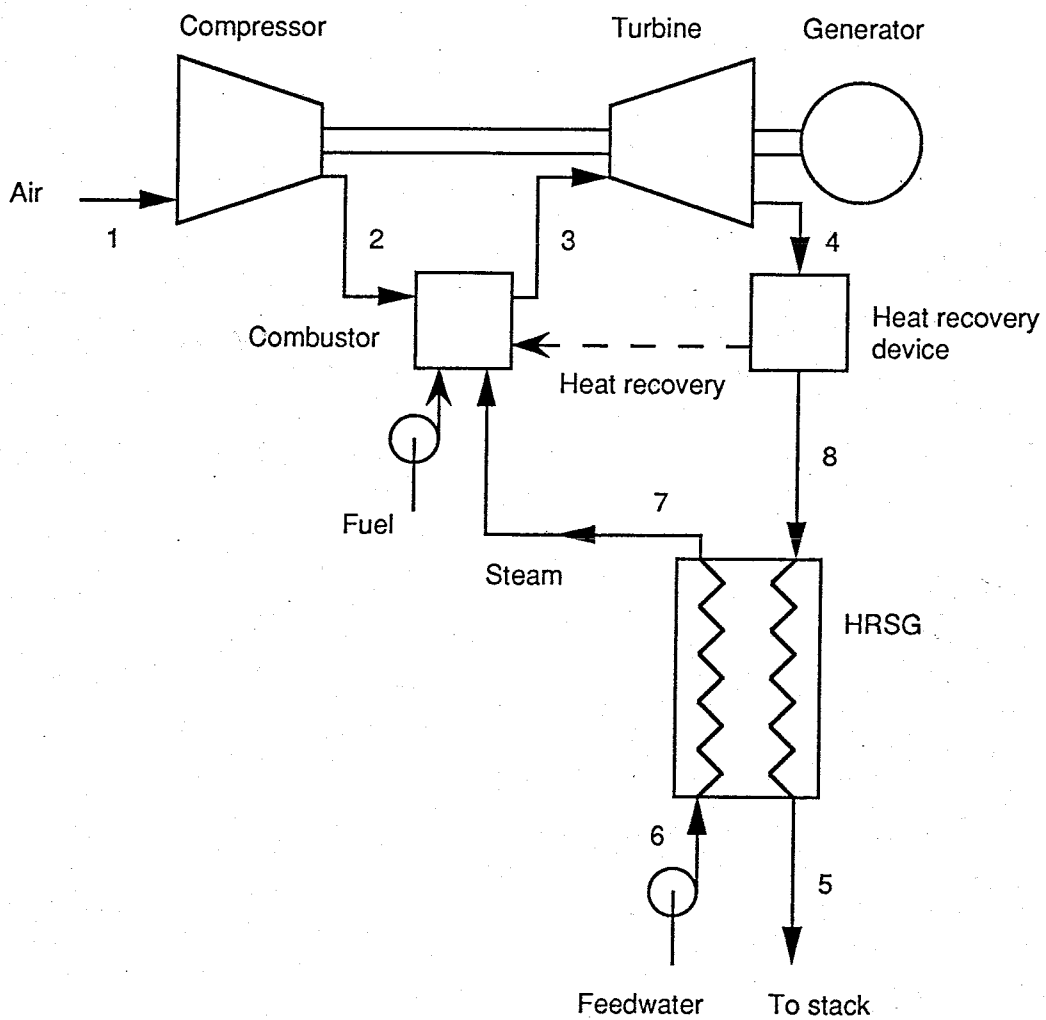


Figure 2.6: Modified STIG Cycle

An amount of heat q_r is somehow recovered from the exhaust and returned to the combustor. The exhaust flow then generates steam in a HRSG as in a conventional STIG cycle.

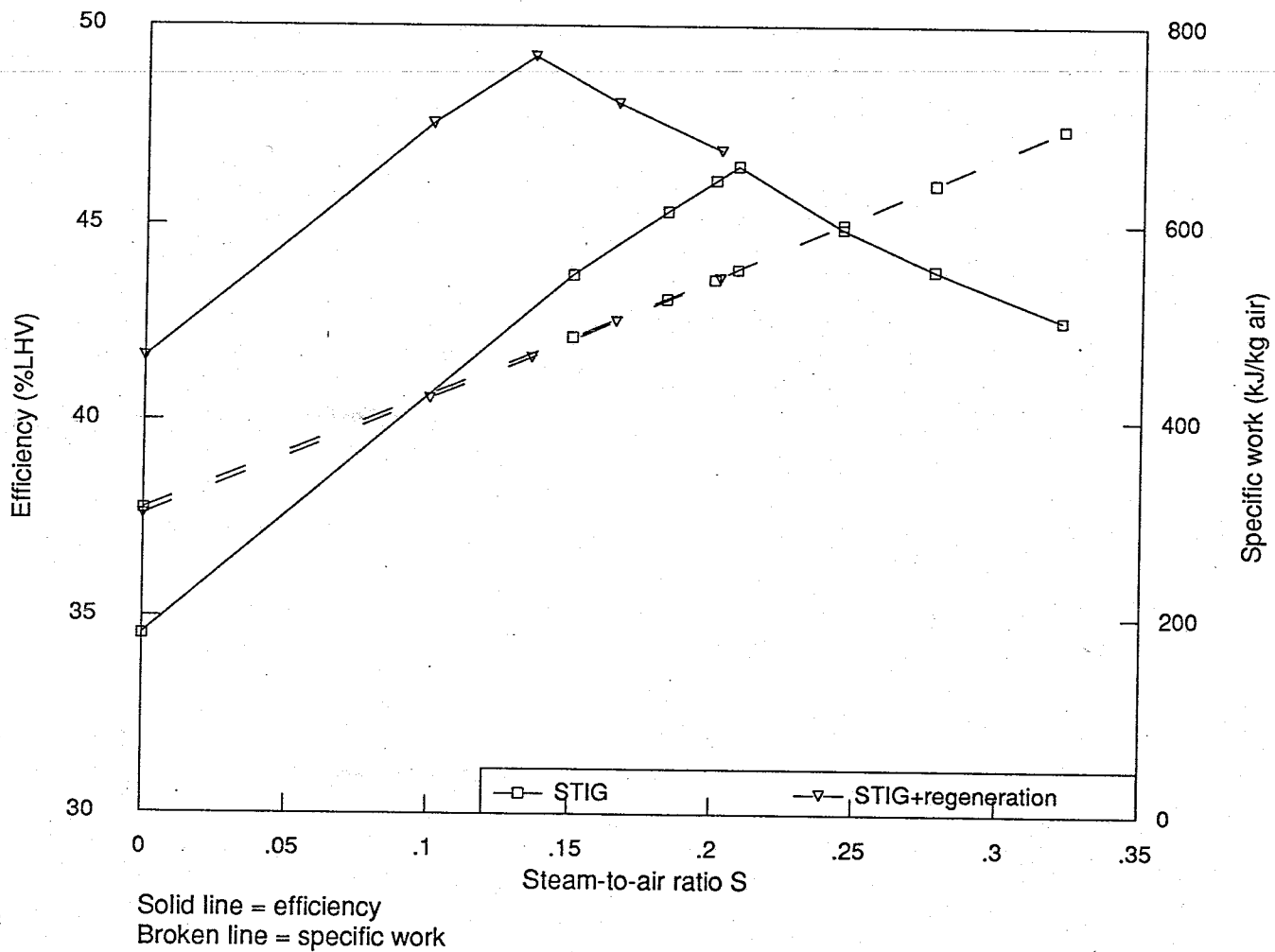


Figure 2.7: Variation of Modified STIG Cycle Performance with Steam Flow

Calculations are carried out in the same manner as in Figure 2.5. In the modified cycle, heat is transferred from the exhaust flow to the compressor discharge air in a 90% effective heat exchanger. Both cycles have a turbine inlet temperature of 1100C and a pressure ratio of 12.

The modified STIG cycle has the greater optimal efficiency. This occurs at a lower steam flow than for the STIG cycle.

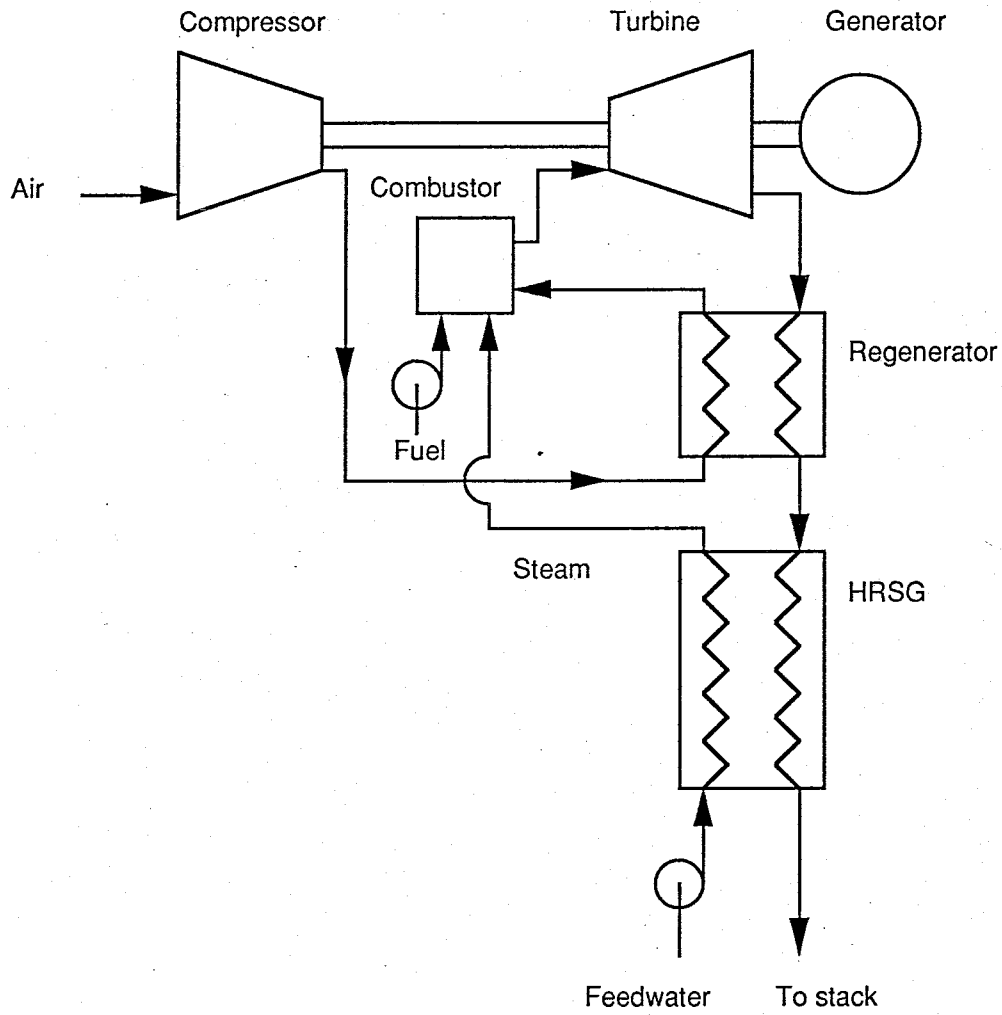


Figure 2.8: STIG Cycle with Regeneration

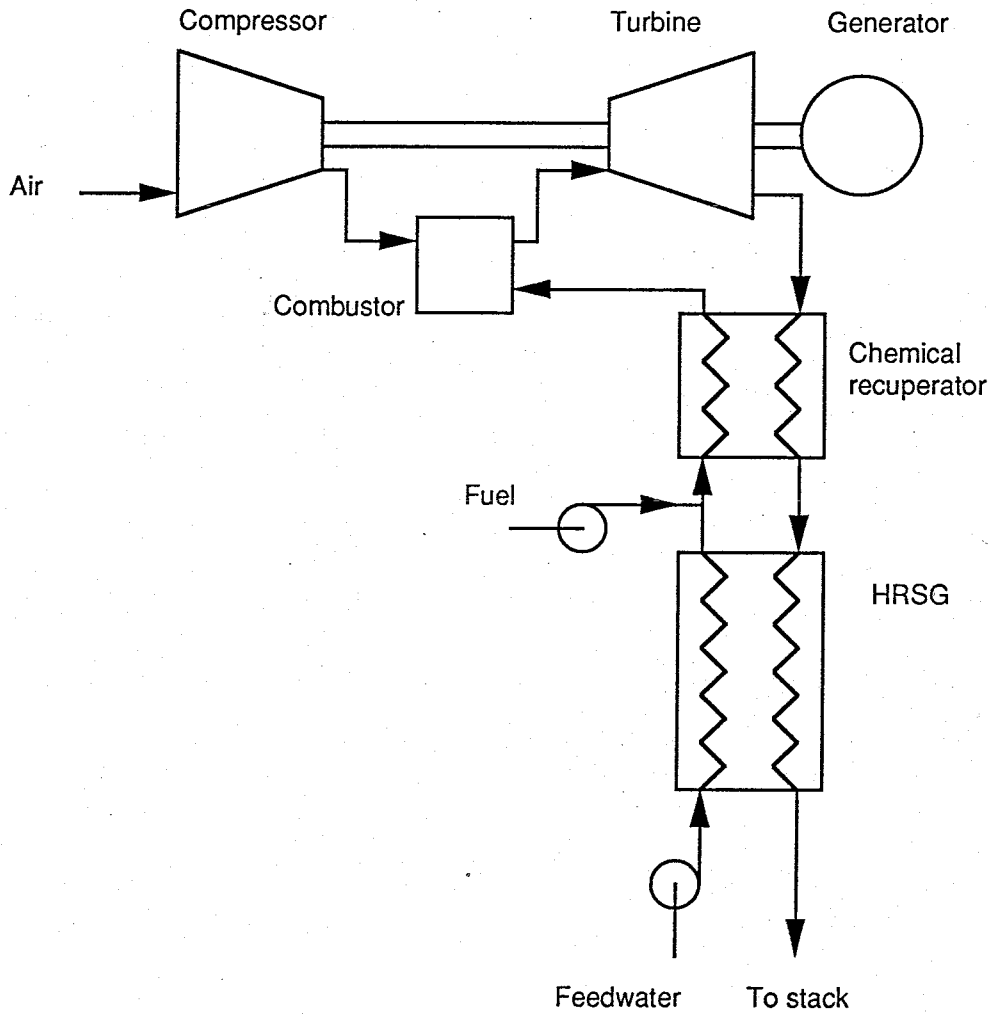


Figure 2.9: Chemically Recuperated Gas Turbine Cycle

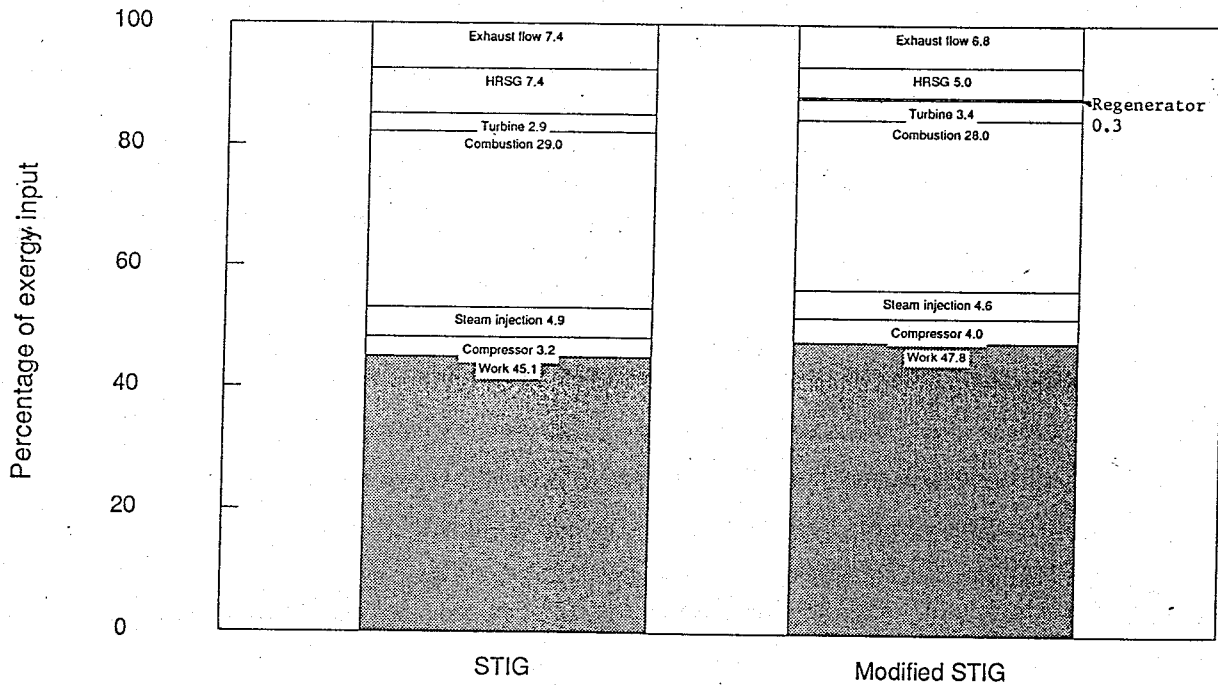


Figure 2.10: Breakdown of Exergy Losses for STIG and Modified STIG Cycles

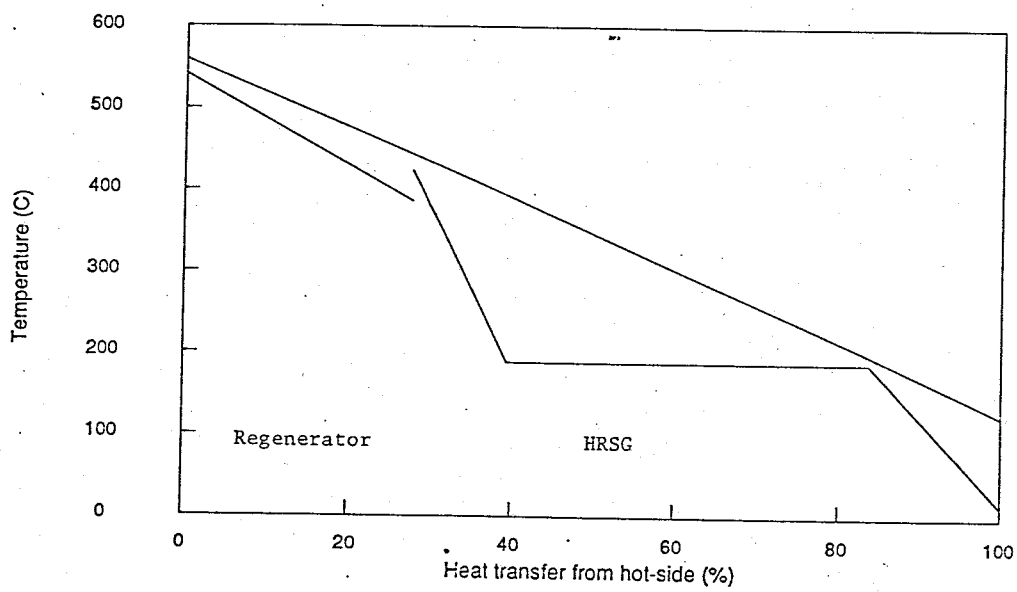
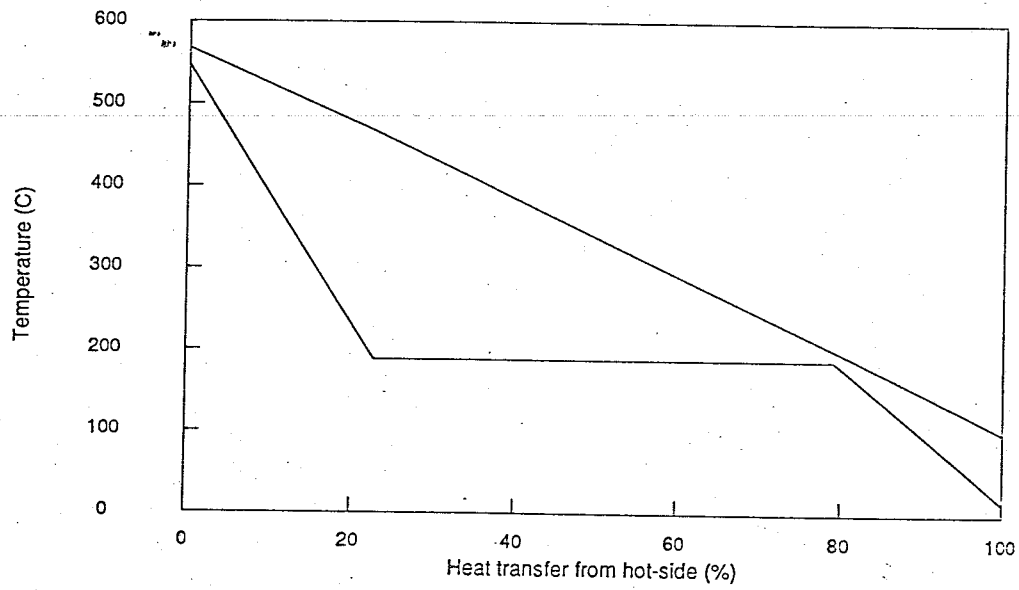


Figure 2.11: Heat Recovery Temperature Profiles for STIG and Modified STIG Cycles

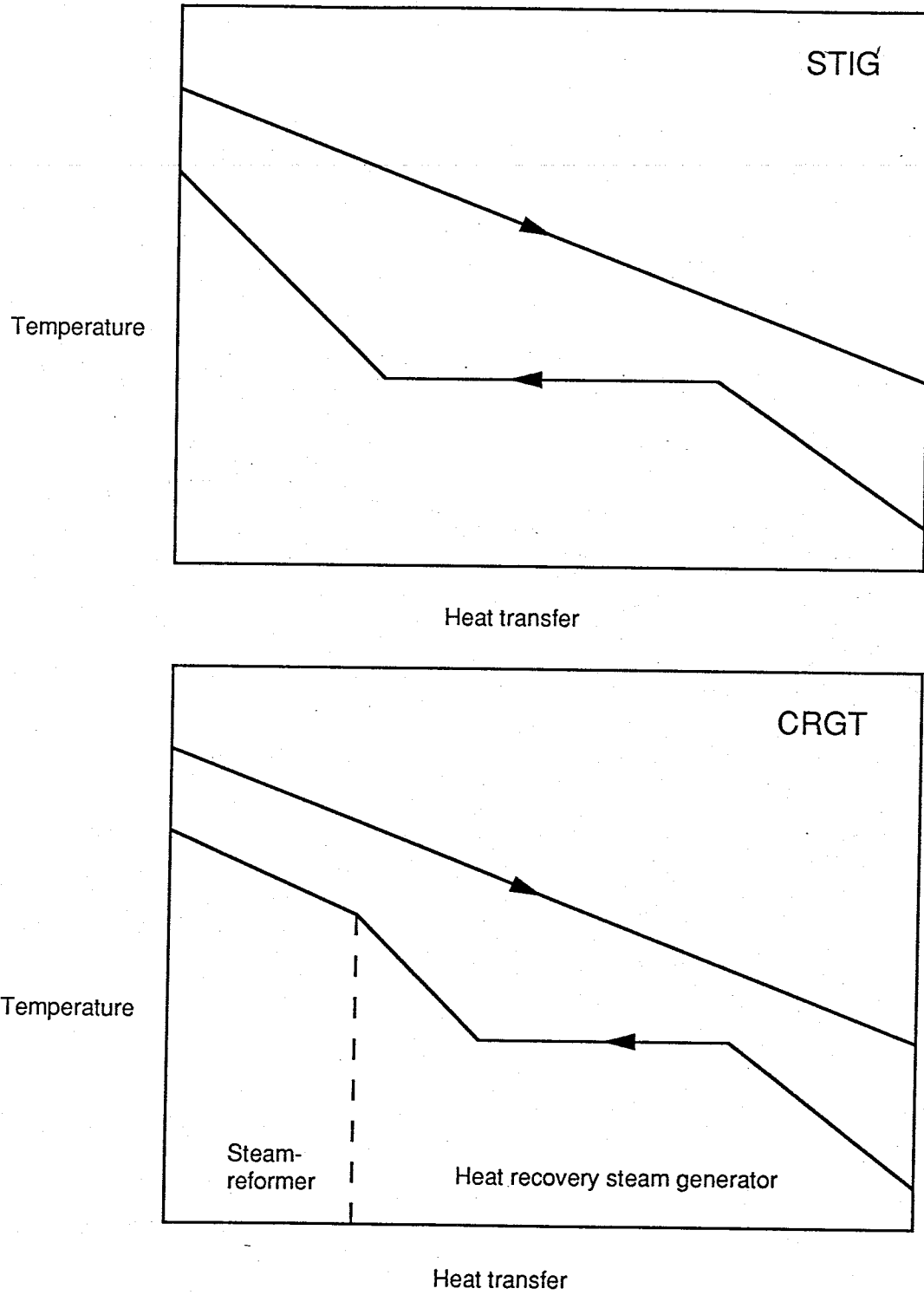


Figure 2.12: Heat Recovery Temperature Profiles for STIG and CRGT Cycles

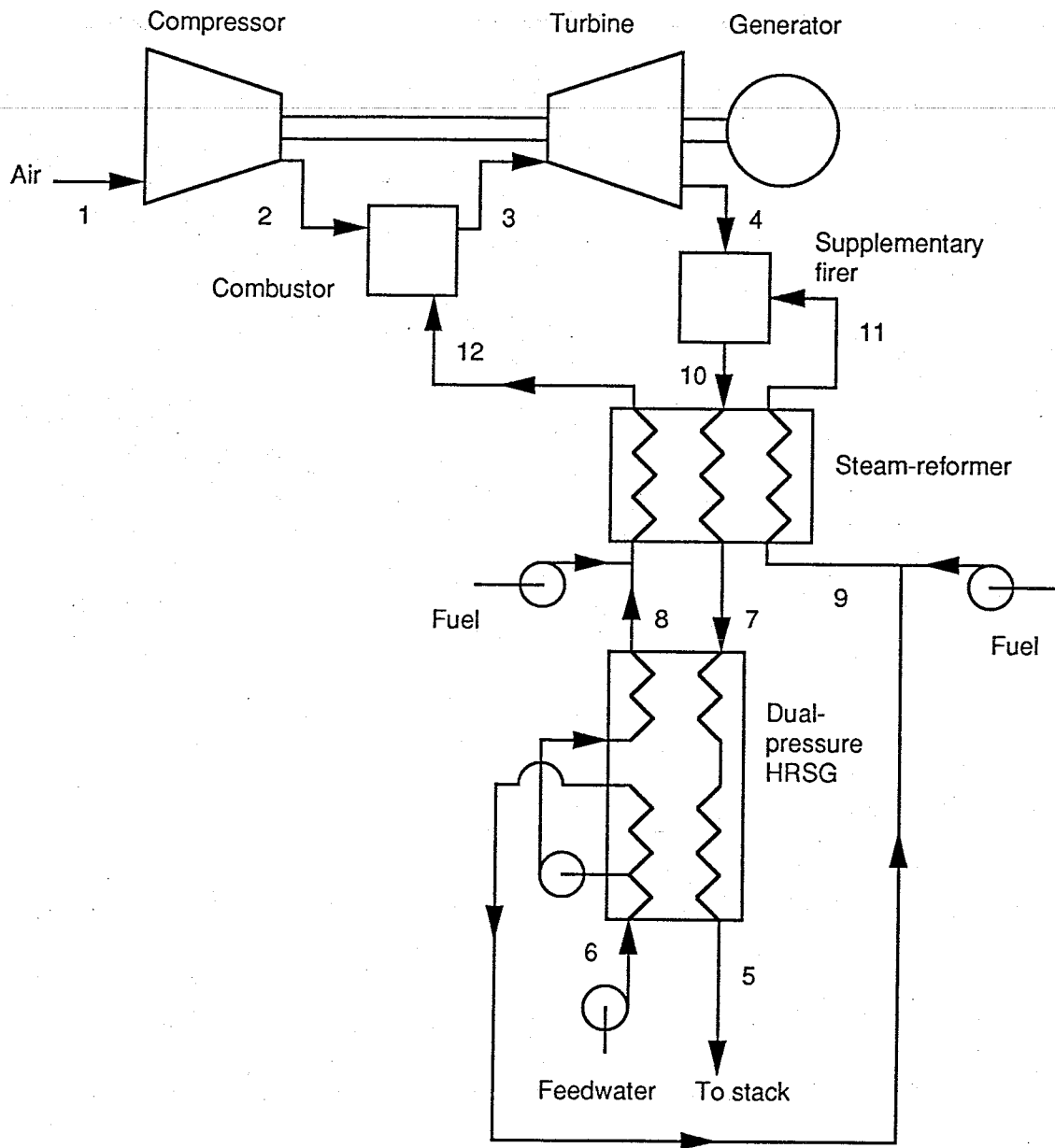


Figure 2.13: CRGT Cycle with Supplementary Firing

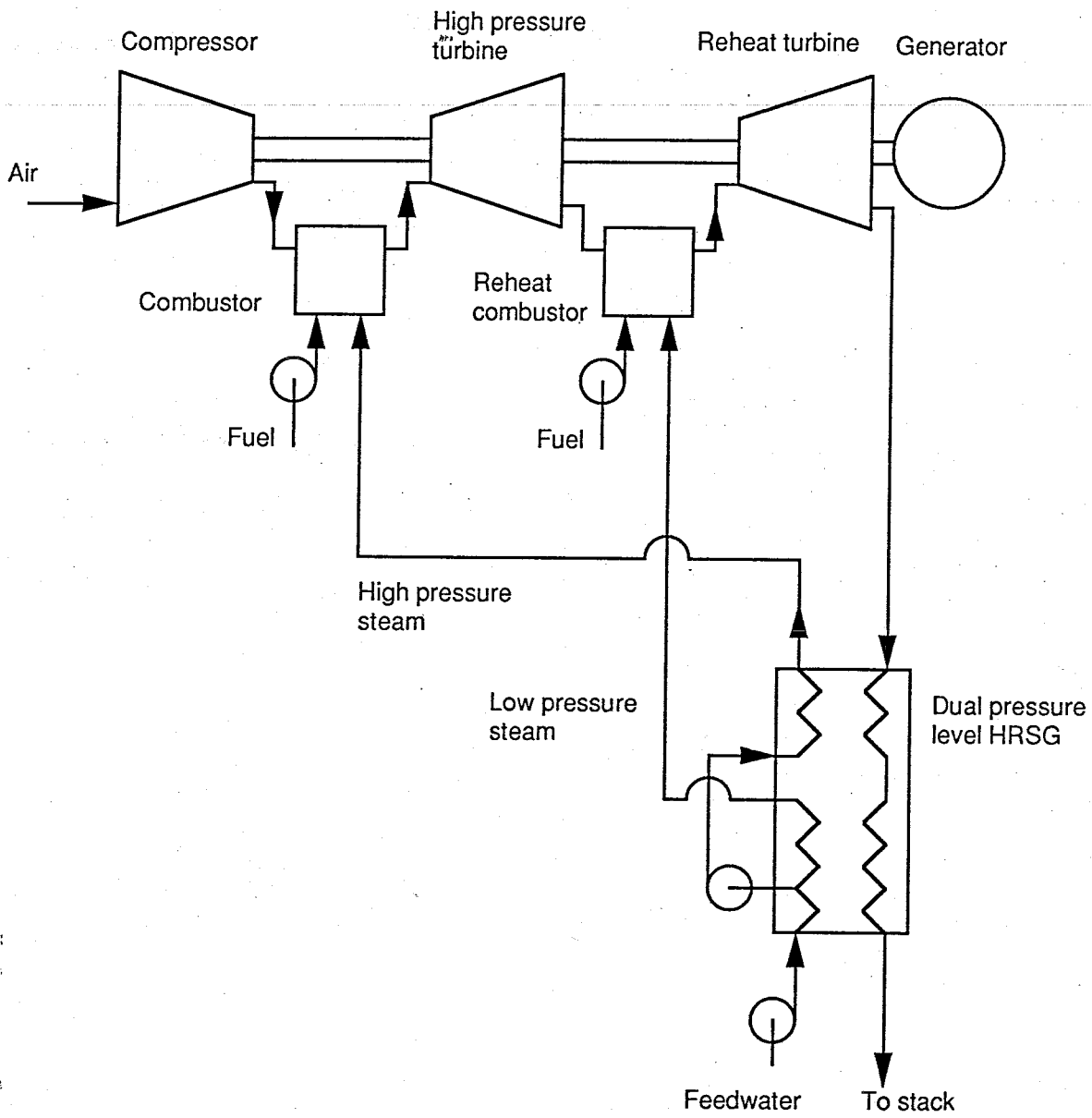


Figure 2.14: Reheat STIG Cycle

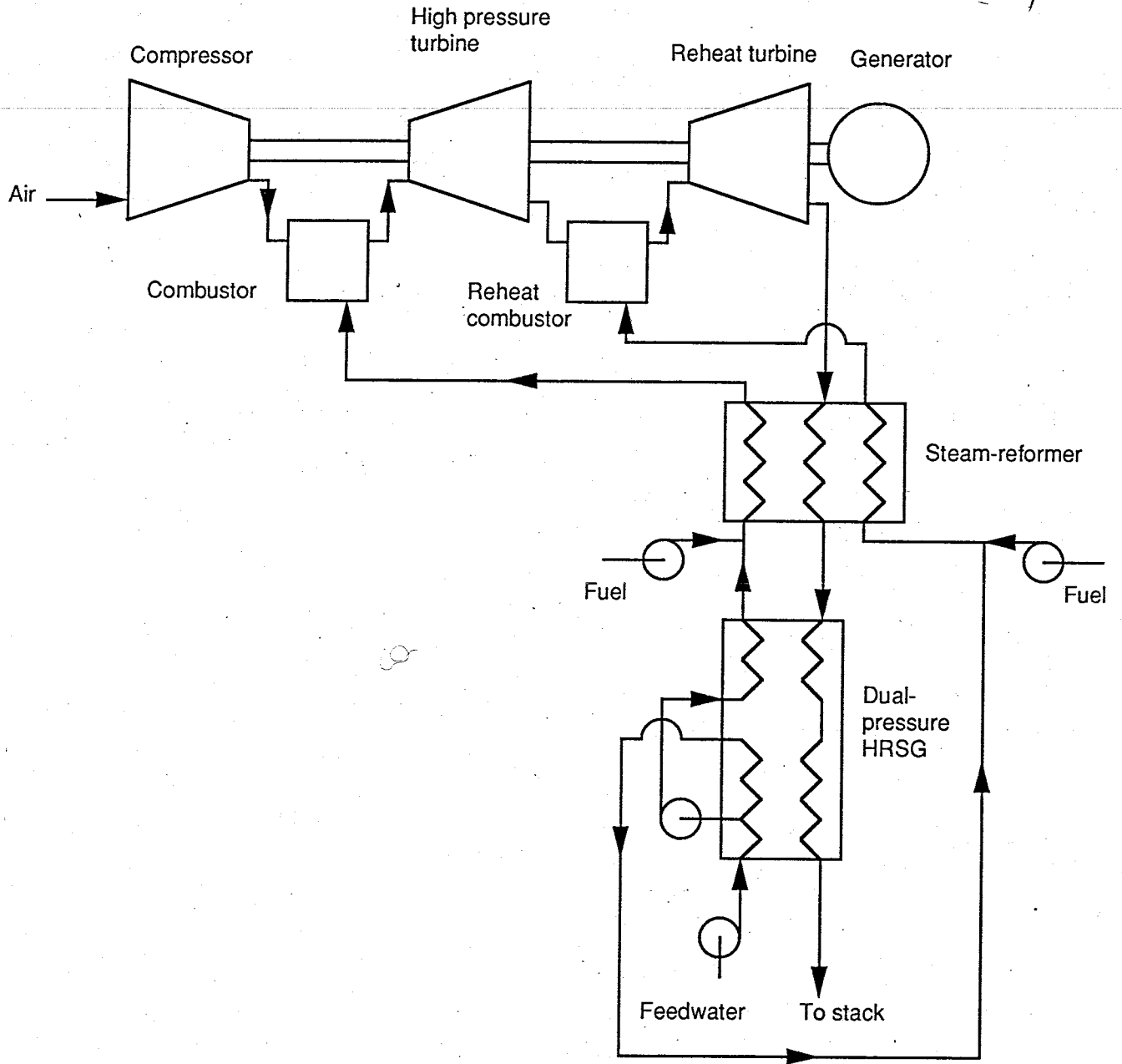


Figure 2.15: Reheat CRGT Cycle

CHAPTER THREE: CHEMICAL FUNDAMENTALS

3.1 Introduction

3.2 Steam Reforming of Methane

3.3 Steam Reforming of Methanol

References

Figures

3.1 INTRODUCTION

Chapter Two showed that the efficiency of a steam-injected gas turbine cycle can be improved by using exhaust heat to drive an endothermic chemical reaction involving the fuel. The energy recovered from the exhaust returns to the combustor in the form of added chemical energy in the fuel. In the combustor this chemical energy is converted wholly to sensible energy in the resulting gas mixture.

The recuperation reaction should be sufficiently endothermic at conditions (temperature and pressure) compatible with a gas turbine cycle to obtain worthwhile chemical heat recovery. The reactants should be cheap and readily available. Two reactions which meet these goals to a large extent are the reactions between steam and natural gas or methanol. In both cases one of the reactants is steam, which can be produced by using some of the gas turbine exhaust heat to boil water.

Natural gas is the obvious first choice fuel for a CRGT cycle. The detailed cycle calculations of Chapters Six and Seven use methane rather than natural gas for convenience. Natural gas typically consists of around 90% methane, 5% higher hydrocarbons, and 5% nitrogen and other inert gases. Hence the trends observed for pure methane will be applicable to natural gas. Section 3.2 investigates the chemistry of the reaction between steam and methane.

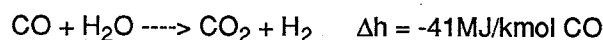
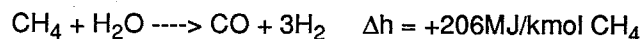
While this thesis focuses primarily on natural gas-fired CRGT cycles, methanol is a promising alternative fuel. Section 3.3 briefly considers steam reforming of methanol.

3.2 STEAM REFORMING OF METHANE

Natural gas is a widely available fuel. It is cheap, currently costing in the range 2.0-3.0\$/GJ¹. An extensive distribution infrastructure is already in place. The main drawback of this reaction is that equilibrium constraints typically prevent complete consumption of the reactants at temperatures typical of a gas turbine exhaust. This restricts the amount of chemical heat recovery possible. Nevertheless this reaction is the obvious first choice to be the recuperation reaction.

The reaction between steam and natural gas, often termed "steam reforming", is widely used in the chemical process industry for hydrogen production for ammonia or methanol synthesis. Around 70% of world ammonia production is based on hydrogen obtained from natural gas reforming (Czuppon and Buividas, 1980). Typical reactor conditions are 700-900C and up to 35bar. The steam-to-methane ratio is in the range 3-5 to prevent carbon formation which can reduce the effectiveness of the nickel-based catalyst².

Methane reacts with steam via two independent reactions:



The first reaction is highly endothermic, while the second, often known as the water gas shift reaction, is exothermic. This reaction is undesirable as far as it reduces the net endothermicity, but unavoidable. The reactions are equilibria, so the product is a mixture of methane, carbon monoxide, carbon dioxide, hydrogen, and water³. Thus the reaction may be written more generally as follows:



¹ This is the average price for electric utilities (Department of Energy, June 1990).

² For details of the methane steam reforming process for hydrogen production, see Kent (1983), Minet and Olesen (1980). See also Section 4.6.

³ Another possible equilibrium product is solid carbon. This is a significant product only at low steam-to-fuel ratio (around 1) and low reforming pressure (below about 7bar). Carbon formation is undesirable as it reduces catalyst effectiveness and impedes reformer performance. In chemically recuperated gas turbines (running on natural gas fuel), carbon formation is negligible provided the steam-to-fuel ratio is sufficiently high.

where n is the molar steam-to-fuel ratio and v_i is the amount of species i in the product. The endothermicity may be expressed as a heat of reaction per unit mass of methane, Δh_{cr} . This is the quantity of most interest in a CRGT cycle, as it is a measure of the chemical heat recovery. Alternatively Δh_{cr} can be thought of as the amount by which the heating value of the fuel (per unit mass of methane entering the reformer) is enhanced.

The heat of reaction Δh_{cr} is a function of three independent parameters - temperature T , pressure p , and steam-to-fuel ratio n . Figure 3.1 shows how Δh_{cr} varies with these parameters assuming equilibrium is always reached⁴. The ranges of T , p , and n are chosen to encompass expected typical values for CRGT cycles. Δh_{cr} is generally small compared to the heating value of methane. For example, for a cycle with a reforming temperature of 900K, a pressure of 20atm, and steam-to-fuel ratio of 5, then Δh_{cr} is around 11% of methane's lower heating value of 50010kJ/kg. A high Δh_{cr} is favored by high temperature, low pressure, and high steam-to-fuel ratio. There is an upper limit to Δh_{cr} of around 13000kJ/kg or 26% of the lower heating value of methane. In this situation all of the initial methane is consumed and the reaction goes to completion⁵.

This suggests that another performance measure for the reaction is the fraction of methane converted to products (Figure 3.2). A high methane conversion corresponds to a high endothermicity. The concept of methane conversion is used in later chapters to indicate the amount of heat recovered from the gas turbine exhaust by chemical recuperation. Figure 3.3 shows how the equilibrium composition varies with temperature. As temperature increases, a greater proportion of the methane and steam is converted to hydrogen and carbon monoxide. The temperature dependence of the equilibrium composition is strongest in the range 750-1000K.

⁴ In practice, use of a nickel-based catalyst enables a close approach to equilibrium. Chapter Four addresses this point in more detail.

⁵ The upper limit to endothermicity varies slightly with steam-to-fuel ratio. For n equal to one, the maximum value of Δh_{cr} is 12,900kJ/kg. This corresponds to when the reaction

$$\text{CH}_4 + \text{H}_2\text{O} \rightleftharpoons \text{CO} + 3\text{H}_2$$
 goes to completion. For n greater than one, the presence of carbon dioxide among the products leads to a slightly lower value because of the exothermicity of the water gas shift reaction

$$\text{CO} + \text{H}_2\text{O} \rightleftharpoons \text{H}_2 + \text{CO}_2$$

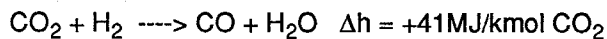
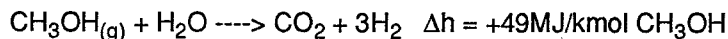
Gas turbine outlet temperature typically lies in this range, and is therefore likely to be an important factor influencing CRGT performance.

Figure 3.4 shows the lower heating value of the product mixture (per unit mass of mixture) as a fraction of the lower heating value of methane. Because of the diluting effect of the reactant steam, the resulting mixture has a heating value less than that of methane, despite the "enhancement" effect of the recuperation reaction. The value obtained is strongly dependent on the steam-to-fuel ratio, but only weakly dependent on the reforming temperature. The gas turbine combustor must be suitably designed to burn this low heating value fuel gas⁶.

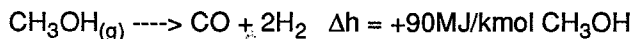
3.3 STEAM REFORMING OF METHANOL

Consideration of methanol-fueled CRGT cycles is beyond the scope of this thesis. This section mentions two possible recuperation reactions involving methanol, but makes no attempt to investigate them in detail⁷.

Methanol reacts with steam more readily than does natural gas, and is completely consumed at temperatures typical for a gas turbine exhaust. The resulting fuel gas is a mixture of hydrogen, carbon monoxide, carbon dioxide, and steam. Equilibrium calculations predict methane and carbon as significant products, but the reaction kinetics are such that their formation can be neglected⁸. The steam reforming reactions are as follows:



A second possible recuperation reaction involving methanol is simple decomposition:



⁶ See Chapter Four for a discussion of combustor design.

⁷ For previous studies of methanol-fueled CRGT cycles see Janes (1979), Davies et al (1983), Klaeyle et al (1987), Tsuruno and Fujimoto (1987), and Granquist et al (1990).

⁸ Methane is an undesirable product, because its formation renders the methanol reforming reaction less endothermic or even exothermic. Given a suitable catalyst, methane formation is so slow that the product mixture is essentially free of methane (Kurpit, 1975; Davies et al, 1983). It is assumed that carbon formation can be neglected in a similar manner.

Given a suitable catalyst, the reaction will occur readily at temperatures typical of a gas turbine exhaust. Again formation of methane and carbon is negligible (Davies et al, 1983).

It appears that methanol is chemically an attractive fuel for chemically recuperated gas turbines. While methanol is not a naturally available fuel, it can be manufactured from natural gas, oil, coal, or biomass. From a practical viewpoint its use is sensible only if a methanol infrastructure is in place. A hydrogen/carbon monoxide fuel gas is an intermediate in the manufacture of methanol from coal or natural gas. It is globally more efficient to burn this gas directly in a gas turbine rather than go completely to methanol only for this reaction to be reversed during chemical recuperation. A reason for going to methanol might be its ease of transport if a methanol infrastructure exists. Because methanol is being considered as a substitute for gasoline, there is a possibility such an infrastructure will develop. Under these circumstances, methanol would be a candidate to fuel CRGTs.

REFERENCES

- T A Czuppon and L J Buividas, "Hydrogen for Ammonia Production and the Economics of Alternative Feedstocks", in W N Smith and J G Santangelo, editors, Hydrogen: Production and Marketing, American Chemical Society, 1980
- D G Davies, N H Woodley, R W Foster-Pegg, and M E Karpuk, Improved Combustion Turbine Efficiency with Reformed Alcohol Fuels, ASME 83-GT-60
- Department of Energy, Monthly Energy Review, April 1990
- A Granquist, I Grunden, F Houllis, T Schmidt, and C Tarnstrom, Foradlad Metanol Som Bransle For Gasturbin, Department of Heat Technology, Kungl Tekniska Hogskolan (Royal Institute of Technology), Stockholm Sweden, March 1990
- J Janes, "Increasing Gas Turbine Efficiency through the use of a Waste Heat Methanol Reactor", Proceedings of the 14th Intersocietal Energy Conversion Engineering Conference, 1979
- J A Kent, editor, Riegel's Handbook of Industrial Chemistry, Van Nostrand Reinhold, 1983
- S Klaeyle, R Laurent, and F Nandjee, New Cycles for Methanol-Fuelled Gas Turbines, ASME 87-GT-175
- S S Kurpit, "1.5 and 3kW Indirect Methanol-Air Fuel Cell Power Plants", Proceedings of the 10th Intersocietal Energy Conversion Engineering Conference, 1975
- R G Minet and O Olesen, "Technical and Economic Advances in Steam Reforming of Hydrocarbons", in W N Smith and J G Santangelo, editors, Hydrogen: Production and Marketing, American Chemical Society, 1980
- S Tsuruno and S Fujimoto, Gas Turbine Cycle with Steam Reforming of Methanol, presented at 1987 Tokyo International Gas Turbine Congress

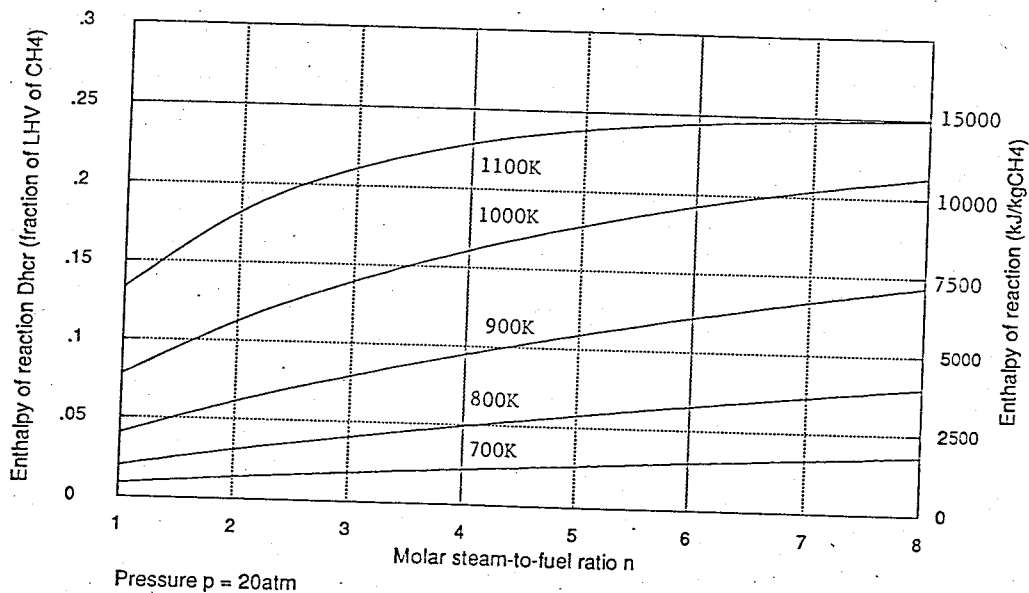
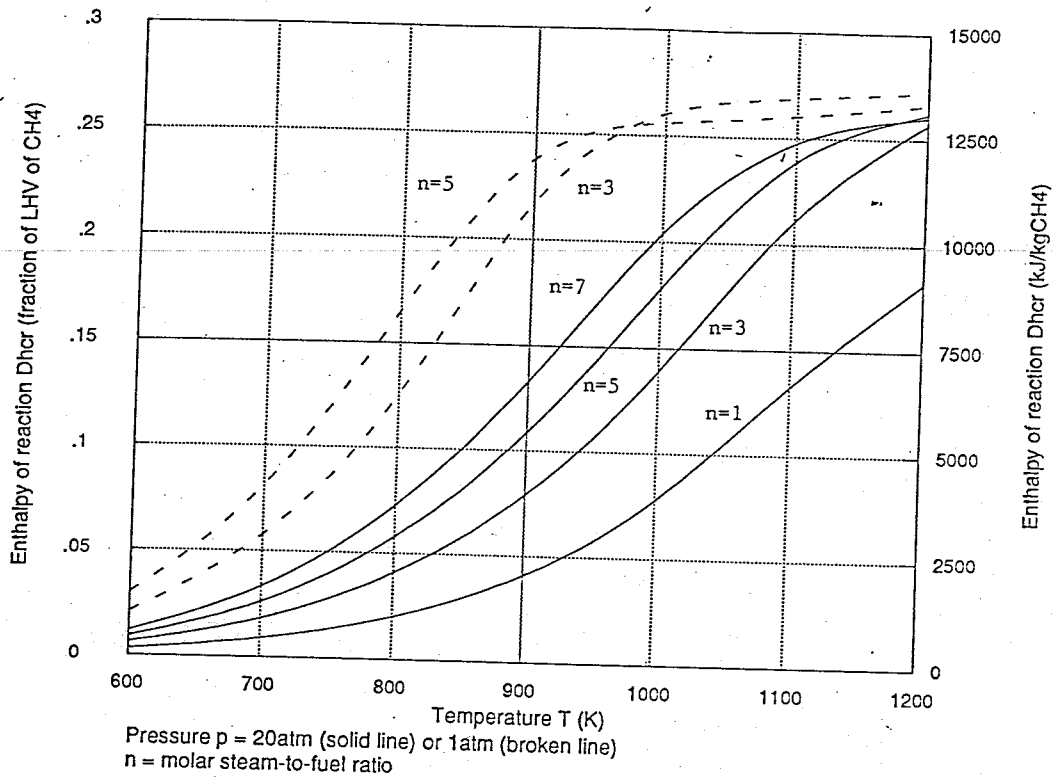


Figure 3.1: Variation of Endothermicity of Methane Steam Reforming with Reaction Conditions

The enthalpy change for the endothermic steam reforming reaction, Δh_{cr} , is expressed in kJ per kg of methane and as a fraction of the lower heating value of methane (which is 50010kJ/kg).

Note that the curves approach different high temperature asymptotes because the enthalpy of the complete reaction varies slightly with steam-to-fuel ratio n (see Footnote 5 in text).

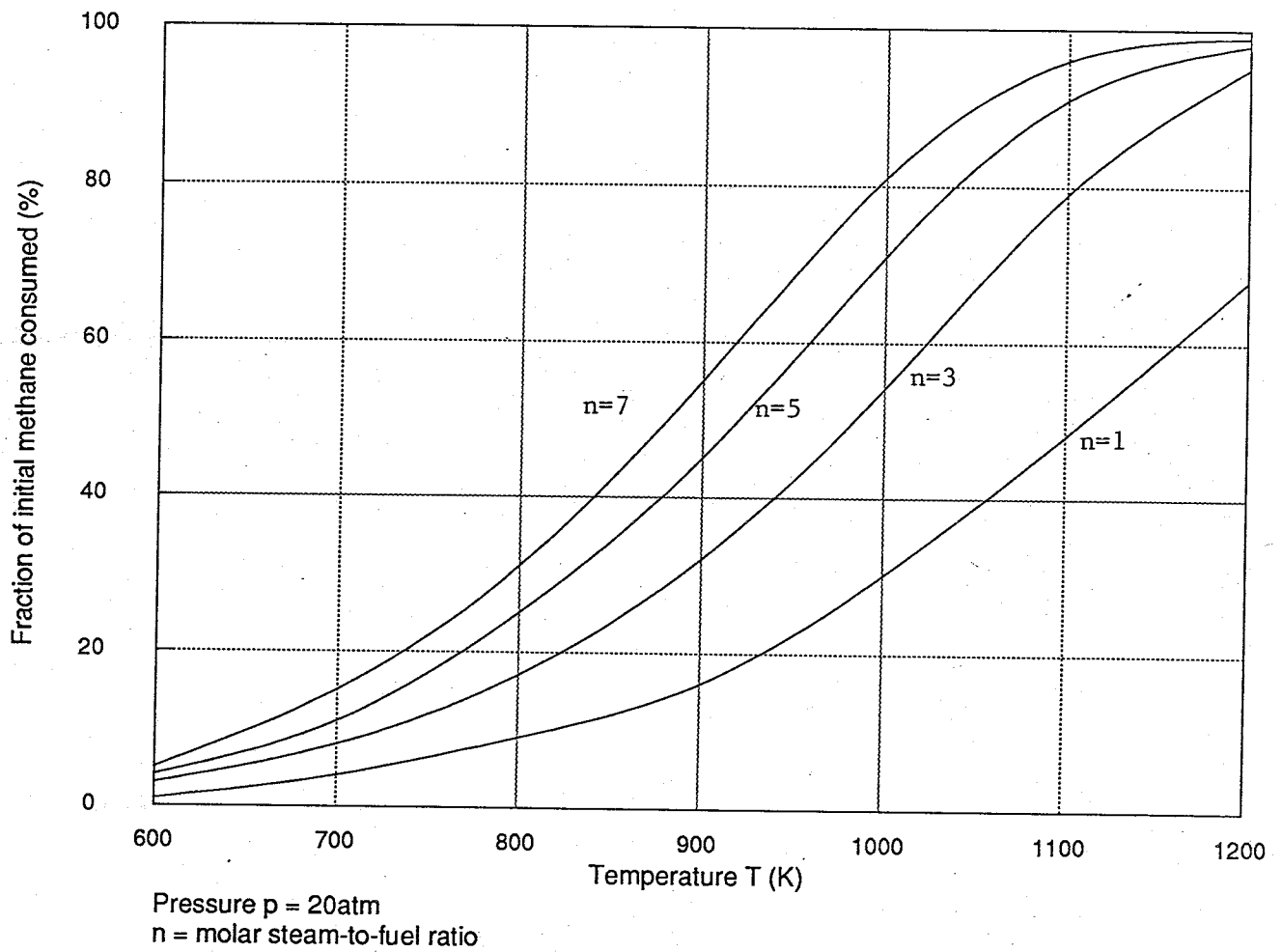


Figure 3.2: Methane Conversion in Steam Reforming Reaction

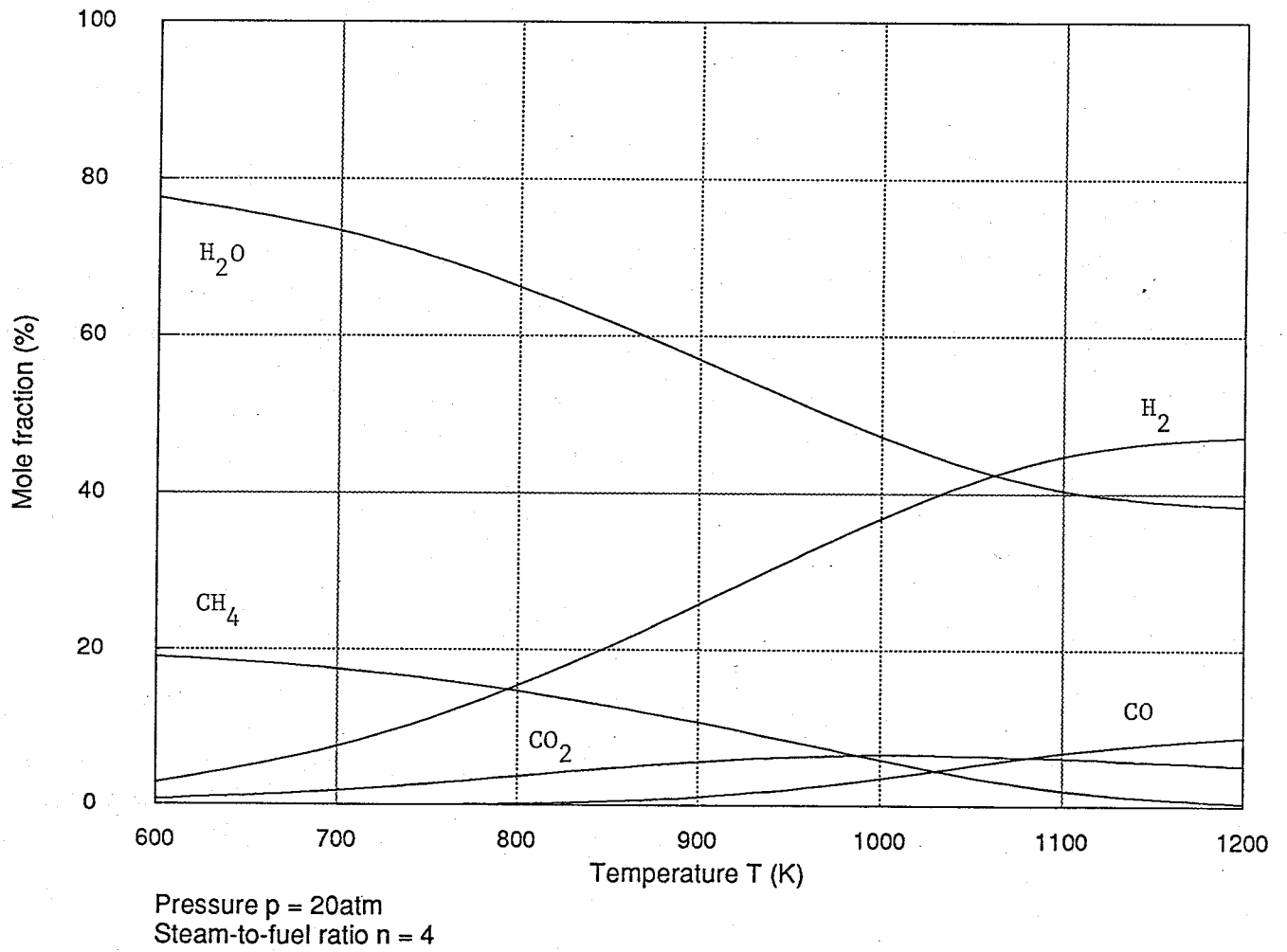


Figure 3.3: Equilibrium Composition for Methane Steam Reforming Reaction

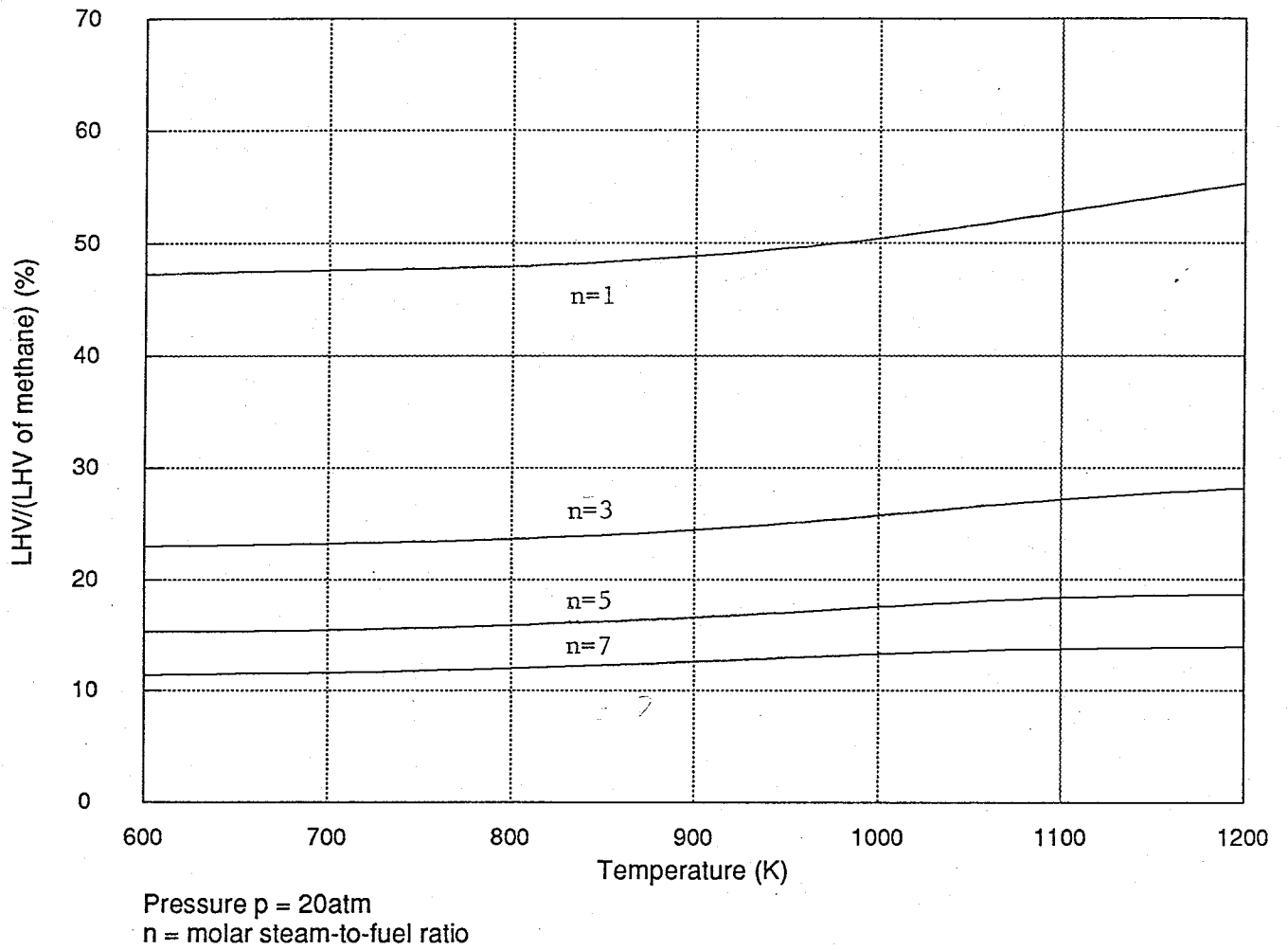


Figure 3.4: Heating Value of Fuel Gas Resulting from Methane Steam Reforming

CHAPTER FOUR: PRACTICAL CONSIDERATIONS

- 4.1 Introduction
- 4.2 Existing Gas Turbine Emissions Control Technologies
- 4.3 Chemically Recuperated Gas Turbine Emissions
- 4.4 Combustion of Low Heating Value Fuels
- 4.5 Gas Turbine Design Issues
- 4.6 Heat Recovery Steam Reformer
- 4.7 Operational Issues
- 4.8 Economics
- References
- Figures

4.1 INTRODUCTION

This study is primarily concerned with understanding the thermodynamics of CRGT cycles. However a number of practical issues must be addressed to achieve the theoretical thermodynamic performance with a real machine. This chapter highlights some of these practical problems, but makes no attempt to explore them in detail¹. The major areas of concern are the combustibility of the low heating value fuel gas, the resulting emissions, and the uncertainties surrounding undeveloped components such as the heat recovery steam reformer.

4.2 EXISTING GAS TURBINE EMISSIONS CONTROL TECHNOLOGIES

The formation of oxides of nitrogen (NO_x) during combustion is the main pollutant problem associated with gas turbines. NO_x plays a role in both acid rain formation and local air pollution². Increasingly strict environmental regulation has led to rapid development of NO_x control technologies in recent years. This section describes both currently available technologies and

¹ Janes (1990) addresses many of the issues raised here in more detail in Janes (1990).

² NO_x is a precursor in ozone formation. Tropospheric ozone is a health hazard.

those still undergoing development³. Section 4.3 explains that a major factor promoting interest in chemically recuperated gas turbines is the expectation of very low NO_x emissions.

Gas turbines typically have uncontrolled NO_x levels of 250 parts per million (ppm) by volume when running on natural gas and 400ppm with distillate fuel oil⁴. NO_x forms during combustion by three different chemical mechanisms, and is referred to according to its origin: thermal NO_x, prompt NO_x, or fuel NO_x. The vast majority (for natural gas fuel) is thermal NO_x, formed by the reaction of nitrogen and oxygen in the combustion air at the elevated flame temperatures. Thermal NO_x production increases exponentially with peak combustion temperature. Prompt NO_x forms from a reaction between atmospheric nitrogen and CH and C₂ radicals originating primarily from hydrocarbons in the fuel⁵. Fuel NO_x evolves from chemically bound nitrogen in the fuel, and is negligible for natural gas which contains essentially no fuel-bound nitrogen.

NO_x control technologies fall into three categories: exhaust gas clean-up systems such as selective catalytic reduction (SCR), steam or water injection, and dry low NO_x combustor designs. Combustion strategies which reduce thermal NO_x often lead to increased carbon monoxide emissions, and so the solution adopted must be a compromise achieving acceptable levels of both. Regulatory limits in some areas are as low as 9ppm for NO_x and 50ppm for carbon monoxide. These levels can at present be met by combining SCR with water or steam injection or dry low NO_x combustors. Current rapid improvement in dry low NO_x technology suggests that designs capable of 9ppm without SCR will be commercialized in the next two or three years.

³ More detailed discussions of NO_x control options can be found in Sidebotham and Williams (1989), Hilt and Waslo (1984), Touchton (1985), Lefebvre (1983), Smith (1987), and Aoyama and Mandai (1984).

⁴ These values are representative of aeroderivative gas turbines. Heavy-duty machines generally have lower flame temperatures and hence lower uncontrolled NO_x levels. Throughout this thesis, all NO_x levels are corrected to a 15% oxygen concentration in the exhaust gases. This common convention corrects for the fact that primary zone NO_x levels are diluted by different amounts in combustors of different overall equivalence ratio. This allows comparison of NO_x emissions on a per unit of fuel basis. (A still better measure would be to express NO_x per unit of power output.)

⁵ C₂ radicals are almost entirely absent during the combustion of methane (or methanol), but will be present during the combustion of fuels containing higher hydrocarbons.

4.2.1 Selective Catalytic Reduction

Selective catalytic reduction (SCR) is currently the only commercially available exhaust gas clean-up system. In many areas, it is considered the "best available control technology" (see for example SCAQMD, 1989). In this process, ammonia added to the exhaust stream reduces NO_x to nitrogen in the presence of a catalyst such as titanium dioxide. SCR can achieve NO_x reductions typically of 80%. The reaction must occur within a temperature range of around 350-400C - high enough to promote NO_x reduction, but low enough to prevent catalyst degradation. This is achieved by placing the catalyst beds part way along the heat recovery steam generator.

As well as the extra cost involved, SCR has a number of operating drawbacks. A sophisticated control system is required to allow enough ammonia injection to maximize NO_x removal without having excess ammonia escape through the stack. The need for the exhaust gas temperature to be within a narrow window at the catalyst beds imposes problems for part-load operation or supplementary firing, and precludes the option of by-passing the HRSG. Fears of catalyst poisoning by sulfur contained in distillate oil might prevent dual fuel operation⁶. Ammonia is costly to handle safely, and the possibility of accidents poses potential health risks. The catalyst elements, which must be replaced periodically, are toxic and hence create a disposal problem. Current uncertainty surrounding potential nitrous oxide (N_2O) formation requires clarification - nitrous oxide is a powerful and long-lived greenhouse gas, so successful penetration of this technology could conceivably contribute significantly to global warming.

Despite these drawbacks, SCR operating experience is accumulating rapidly. At least 30 units are operating in the US, mostly in California. Performance so far has been better than anticipated (Stambler, 1990).

4.2.2 Steam or Water Injection

Both steam or water injection and dry low NO_x combustors work on the principle of reducing peak flame temperatures. Peak flame temperature is the key factor influencing NO_x formation in a gas

⁶ Natural gas is essentially sulfur-free. However many gas turbines have dual fuel capability, enabling them to switch to distillate fuel if the natural gas supply is interrupted.

turbine combustor, because thermal NO_x production increases exponentially with this parameter. Before considering steam or water injection, it is first necessary to understand the operation of a "conventional" combustor, that is without NO_x control.

A gas turbine combustor (Figure 4.1) operates at a very lean overall fuel-to-air ratio because metallurgical constraints limit the maximum turbine inlet temperature, typically to less than 1300C. This lean ratio is much less than the lean limit of flammability. The combustor is designed to distribute the air flow to different regions in such a way that the local fuel-to-air ratio around the fuel nozzle is close to stoichiometric, and thus able to support combustion. This region, known as the primary zone, is where the peak temperatures occur, and hence where NO_x and carbon monoxide formation are greatest. Further air added in the intermediate zone encourages oxidation of carbon monoxide to carbon dioxide. The remaining air is added in the dilution zone to bring the temperature down to that acceptable by the turbine. Further conversion of carbon monoxide might occur even at the low temperatures in the dilution zone. Hence acceptable carbon monoxide emissions depend on good design (sufficient length for example) of the intermediate and dilution zones.

NO_x levels depend primarily on the peak temperatures in the primary zone. Since fuel and air are not premixed before injection into the primary zone, diffusion controls the rate of combustion. The reaction rate is greatest where the fuel and air come together in stoichiometric proportions, and it is here that the highest temperatures and most NO_x formation occurs. Consequently the stoichiometric adiabatic flame temperature is a good indicator of NO_x levels (Sidebotham and Williams, 1989).

Steam or water injection leads to reduced NO_x levels because the diluting effect of the water or steam lowers the stoichiometric adiabatic flame temperature. Figure 4.2 shows the results of steam injection experiments carried out on a General Electric LM5000 gas turbine. On a per unit mass basis, water is a more effective NO_x suppressant than steam because it lowers the flame temperature more. Figure 4.3 shows a correlation between NO_x reduction and flame temperature which can be used to estimate NO_x levels for different gas turbine cycles and fuels.

A theoretical upper bound to the amount of H₂O injection is set by the occurrence of flameout below a certain flame temperature⁷. In practice the limiting factor is likely to be the need for acceptably low carbon monoxide levels, since slower combustion at lower flame temperature leads to an increase in emissions of partially burned products such as unburned hydrocarbons and carbon monoxide (Figures 4.2 and 4.4). NO_x levels at this point are typically around 25ppm⁸.

If carbon monoxide levels do limit the amount of steam or water injection, then an alternative to combining steam or water injection with SCR to achieve low levels of both NO_x and carbon monoxide might be to use relatively more injection with exhaust gas clean-up of carbon monoxide rather than NO_x. Carbon monoxide levels in the exhaust could be reduced using a catalytic oxidation unit similar to the catalytic converter used in automobiles. This process involves no added reagent, and avoids many of the operating problems of SCR.

Both steam and water injection can significantly affect overall cycle performance (see Sidebotham and Williams, 1989). Power output increases owing to the extra mass flow through the turbine. Steam injection increases the efficiency of a simple cycle (as described in Section 1.2.5), but generally reduces combined cycle efficiency because the NO_x control steam could otherwise be used to produce work in the steam turbine. Water injection always penalizes efficiency. Other disadvantages of steam or water injection are the need for water treatment to prevent damage to turbine blades⁹, and increased pressure pulsations in the combustor leading to reduced parts life.

⁷ A flame cannot be supported below a certain temperature - this is called the flameout limit. For natural gas (and most other hydrocarbons), flameout occurs at around 1800K-2000K in a practical combustor (lower flame temperatures might be achieved under laboratory conditions).

⁸ The ability of existing dry gas turbine designs to accommodate increased mass flow imposes another limit on the amount of steam or water injection. For aeroderivatives, this limit can be relaxed using suitable design modifications, but such modifications are harder to do for heavy-duties. In steam-injected gas turbines, steam above that which can be delivered to the primary zone for NO_x control is injected with into the air flow leaving the compressor for power augmentation.

⁹ The need for high water quality is not a major drawback because the cost of water treatment is small compared the cost of the gas turbine. See for example, Soroka and Kamali (1987).

4.2.3 Dry Low NO_x Combustors

The drawbacks of steam or water injection, particularly reduced combined cycled efficiency, have led to rapid progress in dry low NO_x combustor design in recent years. Many gas turbine manufacturers have developed dry combustors capable of 25ppm NO_x with acceptable carbon monoxide levels (for natural gas fuel), while one has recently offered a dry NO_x guarantee of 9ppm (Gas Turbine World, July-August 1990). This guarantee was offered after an existing turbine installation consistently achieved emissions levels as low as this (Gas Turbine World, March-April 1990)¹⁰.

Dry low NO_x combustors operate off-stoichiometric in the primary zone to reduce flame temperature. Different dry low NO_x techniques include lean/lean staged combustion, rich/lean staged combustion, and lean premixed combustion, of which the last is the most promising. A potential problem is high carbon monoxide production at part-load owing to incomplete combustion. This is overcome by using staged combustion (a pilot flame preceding the main flame) or variable geometry. These enable the variation of combustor operating characteristics in order to minimize emissions over the whole load range. As in the case of steam or water injection, a catalytic oxidation unit could reduce carbon monoxide levels in the exhaust gases.

4.2.4 Catalytic Combustion

Another promising technology is catalytic combustion, which uses a catalyst to enable combustion at very lean fuel-to-air ratios and hence relatively low temperatures. Thermal NO_x production would be practically zero at these temperatures, while the catalyst would promote complete conversion of carbon monoxide to carbon dioxide. The main developmental problem is finding catalysts and substrates with sufficient high temperature durability. Kimura (1990) suggested 10 years as the time to commercialization, but stressed that this is only a rough estimate and depends on the resources channelled to catalytic combustion development¹¹.

¹⁰ The 9ppm NO_x guarantee was offered for a gas turbine with external ("silo") combustors. It is generally easier to design for low emissions with this type of combustor than with annular or can-annular combustors because there is no constraint on combustor size.

¹¹ General Electric regards catalytic combustion as a "back-up" technology, in case they cannot meet NO_x targets with lean premixed combustion (Kimura, 1990).

4.3 CHEMICALLY RECUPERATED GAS TURBINE EMISSIONS

4.3.1 NO_x and Carbon Monoxide

This section investigates the likely emissions characteristics of chemically recuperated gas turbines. Simple combustion theory is invoked to project that CRGTs will achieve "ultra-low" NO_x levels (i.e. an order of magnitude lower than is currently possible). Experiments are required to confidently predict NO_x levels for the reformed fuel gas, because of scientific uncertainty regarding prompt NO_x. Moreover, only "hard data" from combustion tests will convince potential buyers of the emissions capability of CRGTs. Since the prospect of ultra-low NO_x is a major reason for interest in CRGT, it is important that these tests are carried out as soon as possible. General Electric plans to perform such tests in 1991 with funding from the Gas Research Institute (Puzson, 1990).

Section 4.2 explained how both steam or water injection and dry low NO_x combustors seek to control NO_x emissions by reducing peak flame temperatures. This process is limited by increased carbon monoxide levels at lower temperatures and by flameout, the inability to support a flame below a certain temperature. With steam injection, the carbon monoxide constraint typically limits the steam-to-fuel mass ratio to between 2 and 3, corresponding to a stoichiometric adiabatic flame temperature of approximately 2200-2300K¹². The correlation of Figure 4.3 indicates NO_x levels of 10-25ppm, assuming 250ppm uncontrolled NO_x. Manufacturers typically guarantee 25ppm NO_x with steam injection.

Table 4.1 shows the fuel gas compositions resulting from methane steam reforming at four sets of reaction conditions, along with the corresponding flame temperatures. Providing the steam-to-fuel ratio n is large enough, the reformed fuel gas has a flame temperature lower than the 2200-2300K obtainable with steam injection. On Figure 4.3, 2160K corresponds to about 4ppm NO_x,

¹² In this section all flame temperatures are stoichiometric adiabatic flame temperatures assuming compressor discharge air at 800K and 15atm. This enables comparison between fuels and the use of the correlation of Figure 4.3. Because of the various simplifying assumptions used, the absolute values of flame temperatures and NO_x levels might not be highly accurate. It is the comparative values of these quantities which are of interest here.

and 2050K to about 1ppm. These low temperatures are not achievable with steam injection because of flameout or high carbon monoxide emissions. With CRGT, it is believed that the presence of a significant quantity of hydrogen in the fuel gas enables these low temperatures to be reached (Janes, 1990). Hydrogen has a much lower flameout temperature than methane (around 1300K compared to 1800-2000K for methane), so one would expect the flameout temperature of the reformed fuel gas also to be lower than that of methane. It is also projected that the presence of hydrogen will reduce carbon monoxide emissions at a given flame temperature.

Table 4.1: Stoichiometric Adiabatic Flame Temperature for Typical Reformed Fuel Gas Compositions

	A	B	C	D
Reforming Conditions:				
Temperature (K)	1000	1000	800	800
Pressure (atm)	20	20	20	20
Steam-to-methane ratio	2	6	2	6
Fuel gas composition (vol%):				
CH ₄	15	3	27	10
CO	5	3	0	0
CO ₂	6	6	4	3
H ₂	40	33	16	15
H ₂ O	34	55	53	72
Stoichiometric adiabatic flame temperature (K):	2440	2160	2350	2050

Calculations performed using *STANJAN* computer program (Reynolds, 1986), assuming compressor discharge air at 800K and 15atm.

Extrapolating down to ultra-low NO_x levels like this might be inappropriate. The main pitfall is the probable existence of a residual level of prompt NO_x unaffected by flame temperature. Prompt NO_x levels cannot be accurately predicted at present, but Lefebvre (1983) suggests a range of 0-30ppm with the higher values occurring at low flame temperature. The experimental emissions data shown in Figure 4.2 show NO_x suppression by steam injection (and hence flame temperature reduction) to as low as 6ppm, suggesting a prompt NO_x level at least below 6ppm. Prompt NO_x is formed by a mechanism involving CH radicals originating from hydrocarbons in the fuel. Hence prompt NO_x formation will be lower for the reformed gas than for unreformed methane.

It seems likely that chemical recuperation can lead to ultra-low NO_x emissions, maybe as low as 1ppm, although this is yet to be verified by experiment. It is also important to quantify the expected levels to enable comparison with other NO_x control strategies. While the prospect of very low emissions is a strong motivating factor for research into chemically recuperated gas turbines, it should be remembered that dry low NO_x combustors are improving rapidly and will soon be capable of achieving below 10ppm NO_x . Nevertheless, it appears likely that chemically recuperated cycles have a fundamental advantage over natural gas-fired cycles with NO_x control because they have a lower flameout temperature, and hence a lower "best possible" level of NO_x emissions.

4.3.2 Sulfur Dioxide

Sulfur dioxide derives from the combustion of sulfur in fuels, and is the major cause of acid rain. The sulfur content of natural gas is negligible compared to that for coal, and emissions of sulfur dioxide are not generally a cause for environmental concern at natural gas-fired gas turbine power plants.

The nickel-based catalyst used for the chemical recuperation reaction would be poisoned by even trace quantities of sulfur in the incoming natural gas, so this must undergo a sulfur removal step beforehand. Sulfur can be removed by passing the natural gas through a bed of zinc oxide pellets at room temperature (Janes, 1990).

4.4 COMBUSTION OF LOW HEATING VALUE FUELS

The use of low heating value fuel presents several problems for the combustor designer, for example low flame temperature and high fuel flow rate. Medium heating value fuels might be able to utilize existing natural gas combustors with little or no modification - a common minor modification is an increased fuel nozzle area to accommodate the greater fuel flow. As the heating value decreases more substantial redesign becomes necessary.

The problems of flameout and high carbon monoxide emissions associated with low flame temperature have been detailed above. These set a lower limit (yet to be determined) to the flame

temperature of the reformed fuel. Both the flame temperature and the heating value of the reformed fuel depend on its composition. Hence heating value is a crude indicator of flame temperature (for given inlet air conditions), and the flameout limit translates to a lower limit to the heating value of the reformed fuel. This Section surveys the literature on combustion of low heating value fuels, and this generally quotes a limiting heating value. However it is emphasized that it is the flame temperature that directly influences combustability.

The heating value of the fuel gas produced by steam reforming of methane or natural gas depends strongly on the steam-to-fuel ratio and weakly on the recuperation temperature and pressure (see Chapter Three). The steam-to-fuel ratio is typically in the range 3-6, and the resulting fuel gas heating value ranges from around 6MJ/kg to 14MJ/kg¹³. For combustor design purposes, heating value is more conveniently expressed on a volumetric basis. The corresponding range for the reformed fuel gas is then 4.7-7.4MJ/nm³ (120-190Btu/scf)¹⁴. For comparison, methane has a heating value of 50MJ/kg and 36MJ/nm³ (900Btu/scf).

Commercially available gas turbines can be equipped for operation on fuels of heating value down to 300-350Btu/scf with relatively minor combustor modifications (Meier et al, 1986; Keller, 1990). Tests at General Electric have demonstrated the successful operation of a modified LM2500 gas turbine combustor with a 150btu/scf fuel (Sabla and Kutzko, 1985). The fuel contained carbon monoxide, hydrogen, and nitrogen, and was meant to be representative of fuels derived from gasification of coal or biomass. A GE coal gasification study reports tests achieving stable combustion with a 104Btu/scf fuel (Corman, 1986)¹⁵. Lefebvre (1983) reports that while combustion below 6MJ/nm³ (150Btu/scf) is problematical, 4.1MJ/nm³ (104Btu/scf) has been achieved.

Section 4.3 suggested that the presence of hydrogen in a fuel lowers leads to a low flameout limit, because hydrogen itself has a low flameout temperature¹⁶. The fuel gas resulting from

¹³ Unless stated otherwise, heating values quoted in this chapter are lower heating values.

¹⁴ A normal cubic meter (nm³) is defined at 273.15K and 101.325kPa. A standard cubic foot (scf) is defined at 60F and 14.696psia. Molecular mass of the fuel gas is typically in the range 12-18, depending on the composition.

¹⁵ Note that these tests were concerned with flame stability only, and did not address the question of carbon monoxide levels.

steam reforming of natural gas typically contains upwards of 20% hydrogen by volume, whereas for a coal-derived fuel the proportion would be nearer 10%. Hence the steam-reformed fuel should show stable combustion at heating values at least as low as can be achieved by coal-derived fuel, that is around 100Btu/scf.

Another potential problem associated with low heating value fuels relates to combustor cooling. With a low heating value fuel, a relatively large fraction of combustion air enters the primary zone, leaving less air available for cooling of the combustor liner (Boyce, 1982). On the other hand the lower flame temperature leads to less heat radiation from the flame to the liner, and this lightens the cooling load. Combustor cooling is an important constraint which must be fully addressed by the designer.

Another issue is the fuel gas temperature. The fuel enters the combustor via a fuel control valve, and on current gas turbines this is designed for a maximum fuel temperature of around 550C. In CRGTs the fuel gas typically exits the heat recovery steam reformer at 700-800C, and this necessitates a redesign of the fuel valve incorporating high temperature materials¹⁷.

4.5 GAS TURBINE DESIGN ISSUES

4.5.1 Intercooling

Intercooled gas turbines are not yet commercially available. General Electric has designed an intercooled version of the LM6000 STIG machine (known as LM8000 ISTIG), but has not received any orders. Corman (1986) estimates the cost of developing ISTIG to be around \$100m.

Adding intercooling to existing non-intercooled gas turbines presents certain design problems, but these are not insurmountable¹⁸. In a direct-contact (evaporative) intercooler water is sprayed into

¹⁶ Sabla and Kutzko (1985) report that while stable combustion was achieved for a 150Btu/scf fuel containing hydrogen, the limit for methane-based fuels without hydrogen was 300Btu/scf.

¹⁷ An alternative is to cool the fuel gas down to 550C, but this represents a thermodynamic loss.

¹⁸ Intercooling could be incorporated into new designs more easily, but completely new gas turbine designs are infrequent because of the substantial cost.

the hot stream, which gives up heat to evaporate it. To prevent damage to the downstream compressor blades, water quality must be very high and the intercooler design must ensure that all droplets evaporate before reaching the first blade row. An indirect intercooler avoids this problem by keeping the air and cooling water flows separated in a conventional counter-current heat exchanger. However, the difficulty of diverting the air flow out of and back into the compressor might be considerable, particularly with an existing design. This can be achieved only at the expense of a considerable pressure loss¹⁹.

Besides design of the intercooler itself, addition of intercooling to an existing gas turbine necessitates modifications to the gas turbine. If evaporative intercooling is used, the high pressure compressor and turbine must be able to accommodate the increased mass flow. Addition of intercooling enables a higher turbine inlet temperature, because the compressor bleed-air is cooler and hence a more effective coolant. However a very high firing temperature might present problems of combustor cooling.

There are no major technological barriers to the realization of intercooling, and to that extent its development should be "straightforward".

4.5.2 Reheat Combustor

Compared to gas in the main gas turbine combustor, the gas entering a reheat combustor is at a higher temperature and has a lower oxygen content. These factors pose problems for the reheat combustor design. While there is enough oxygen available in the gas flow for complete combustion, it must be demonstrated that stable combustion can be maintained.

One problem faced by combustor designers is keeping the combustor liner below its maximum allowable temperature. The combustor liner receives heat mainly as radiation from the flame. Convective cooling is achieved by directing some of the incoming air in a thin film along the liner surface. The temperature of this air is important in determining the effectiveness of combustor cooling. In a main combustor the incoming combustion air is typically at around 400C, but in a

¹⁹ The GE ISTIG design assumes a 3% pressure drop (PG&E, 1984).

reheat combustor the incoming gases will be hotter than this - for example around 800C. This will make combustor cooling much more difficult. One option is to use high temperature ceramic materials for the combustor liner. It might be necessary to introduce another cooling medium such as water or steam or pre-cooled air.

NO_x formation during reheat combustion must be considered. As with the main combustor, stoichiometric adiabatic flame temperature is the primary factor influencing NO_x levels. The higher inlet temperature (compared to the main combustor) indicates a higher flame temperature, but the reduced oxygen concentration makes for a lower flame temperature. Which of these factors dominates, and hence the effect on NO_x levels, will depend on the specific cycle in question.

As an example, consider fuel B of Table 4.1. The flame temperature in the main combustor, assuming combustion air at 800K and 15atm, is 2160K. Suppose the combustion gases entering a reheat combustor are at 1100K and 5atm and comprise 60% nitrogen (by volume), 10% oxygen, 27% steam, and 3% carbon dioxide (this composition is typical of the reheat CRGT cycles considered in Chapter Seven). The corresponding flame temperature of fuel B is then 1930K, over 200K lower than in the main combustor. Consequently the amount of NO_x formation in the reheat combustor would be small compared to that in the main combustor.

While this temperature would suggest very low NO_x levels, it might lead to high carbon monoxide emissions or flameout. As for the main combustor, reheat combustor design involves a compromise between low NO_x and acceptable carbon monoxide formation. It is believed that the presence of hydrogen in the reformed fuel of a CRGT cycle enables a lower flame temperature before carbon monoxide or flameout problems are encountered than for natural gas fuel (see Section 4.3). This facilitates the design of a low NO_x reheat combustor.

Reheat combustor research was carried out in the 1980s for the Japanese Moonlight Project, which involved the successful construction of an experimental reheat gas turbine, the AGTJ-100A²⁰. This was designed to operate at a turbine inlet temperature of 1300C, a reheat

²⁰ See for example Hori and Takeya (1981), Arai et al (1987), Yagamishi (1987).

temperature of 1170C, and an overall pressure ratio of 55. The prototype did not quite meet these targets, but nevertheless a combined cycle efficiency of 52.3% was obtained (Yamagishi, 1987). Reheat combustor development was a major component of the Moonlight Project. The reheat combustor of the AGTJ-100A was designed to operate at a reheat firing temperature around 1170C, an inlet gas temperature of 700-800C, and an inlet oxygen concentration of around 12% (by volume). Mori et al (1982) found that for these conditions the flame temperature in the reheat combustor is lower than in the main combustor, leading to lower NO_x formation. Their combustion tests also indicated high combustion efficiency over a wide operating range. An additional benefit of the low flame temperature is a reduced radiative heat transfer to the combustor liner, and this partially alleviates the problem of liner cooling. Takeya and Yasui (1988) report tests achieving stable combustion with natural gas fuel and 9% inlet oxygen concentration.

The Japanese work has proved that there are no fundamental technological barriers impeding development of reheat combustors²¹. Nevertheless designing a completely new combustor is a considerable undertaking, and a reheat combustor presents extra difficulties because of the high temperature and low oxygen concentration of the inlet gas.

4.5.3 Reheat Turbine and Steam Cooling

A reheat turbine must be cooled because the entering gas temperature will be much higher than the maximum allowable metal temperature (typically around 800C in current gas turbines). The low density of the high temperature, low pressure, inlet flow requires that the reheat turbine have large physical size. The combination of these two features presents a considerable, but not insurmountable, challenge to the turbine designer. Blade creep limitations of the larger blades might restrict the reheat turbine inlet temperature to a lower value than the high pressure turbine inlet temperature. Alternatively this temperature might be restricted by reheat combustor design limitations (see Section 4.5.2 above). The AGTJ-100A built during the Japanese Moonlight project is the only reheat gas turbine to be built in recent years²². The reheat firing temperature for this turbine is 1170C.

²¹ This is not surprising as the reheat combustor is similar in function to the afterburner of an aircraft engine. The design and use of afterburners is a well-established practice.

²² A few reheat gas turbines were built in the early years of gas turbine development, mostly in Switzerland and the USSR (Rice 1982). These were not successful partly because the

Coolant is required for the high pressure turbine and the reheat turbine. As seen above, the reheat combustor also might require some other coolant besides the incoming combustion gas. Meeting this demand with compressor bleed-air has a considerable negative effect on performance, as the bleed flow represents a significant fraction of the total air flow²³. Some manufacturers pre-cool the cooling air to reduce the amount required.

An alternative to air-cooling is to use steam from the HRSG to meet part or all of the cooling load. Little research work has been carried out to date on steam cooling, and no steam-cooled gas turbine has yet been built. Steam is a more effective coolant than bleed-air because it has a higher specific heat capacity (by a factor of about two) and is often available at a lower temperature. Another advantage is that steam requires negligible compression work compared to bleed-air. A disadvantage is that steam used for cooling cannot be used for steam injection, chemical recuperation, or a combined cycle²⁴. The amount of steam required to cool the various components must be known in order to determine the effects on the cycle thermodynamic performance.

Rice (1982) proposes a combined cycle with a fully steam-cooled reheat gas turbine. The reheat combustor is cooled by steam from the steam cycle, and so doubles as a reheater for the steam cycle.

4.6 HEAT RECOVERY STEAM REFORMER

4.6.1 General Design Considerations

The heat recovery steam reformer (HRSR) is another as-yet-undeveloped component of a chemically recuperated gas turbine cycle. It is likely to resemble a conventional heat recovery

low pressure ratios and turbine inlet temperatures of that time are far from optimal for reheat cycles.

²³ The bleed air for the high pressure turbine alone may be as much as 25% of the total air flow.

²⁴ However steam used for cooling eventually enters the main flow and performs useful work in downstream turbine stages. Hence steam cooling is thermodynamically similar to steam injection for power augmentation.

steam generator, with a chemical reactor section (the steam reformer) added on to the hot end. At a recent workshop, representatives of the chemical process industry expressed confidence that HRSR development presented no major technical problems and should be "routine"²⁵.

This confidence derives from extensive experience of designing methane steam reformers for hydrogen production for methanol or ammonia synthesis, where the operating conditions of 700-1000C and up to 40bar are at least as severe if not more so than will be the case for CRGTs²⁶. An industrial steam reformer is a large furnace containing rows of vertically-arranged tubes containing the catalyst. The methane/steam mixture flows through the tubes, which absorb heat from flames located between rows. The dominant mode of heat transfer is by radiation. To withstand the high temperatures involved, the tubes are made of nickel-chromium-iron superalloys and are manufactured by an advanced technique known as continuous centrifugal casting. Tube life is in the range 6-12 years (Kent, 1983). Catalyst life is typically 3 years but can be longer for less severe operating conditions (Short, 1989).

Recuperator designers will be able to benefit to some extent from methane steam reforming experience in the chemical process industry, but there are important differences between an industrial steam reformer and a gas turbine chemical recuperator. The major difference is that heat transfer occurs by radiation in most industrial steam reformers but will be convective in a recuperator. However, a proprietary new ammonia production process developed by ICI appears to have a convective reformer in place of the conventional radiative steam reformer (Short, 1989), suggesting that a convective recuperator is feasible.

The reformer of a CRGT cycle will be similar to the superheater of a HRSG except that the tubes will contain a catalyst. Methane is added to the steam leaving the evaporator, and the reaction proceeds as the mixture progresses towards the hot end. The catalyst ensures fast reaction times, so the reaction rate is controlled by the heat transfer rate from the hot exhaust gas to the tubes and the reformed fuel gas leaves the reformer close to equilibrium. As for a HRSG, the

²⁵ Chemically Recuperated Gas Turbines Workshop organized by the California Energy Commission in Los Angeles, 1 February 1990.

²⁶ For descriptions of methane steam reforming in the chemical process industry, see Chenier (1986), Kent (1983), Minet and Olesen (1980).

optimum design results from a trade-off in selecting the minimum temperature difference between the hot and cold streams. This approach temperature is an important design parameter as it influences the heat transfer rate, which in turn affects the heat transfer area, number of tubes, reformer pressure drops, and volume of catalyst. Small approaches are thermodynamically preferable, but the large heat transfer area needed to achieve these increases the cost.

Metallurgical constraints of the superheater tubes in a HRSG limit the exit steam temperature to around 550C. The material used is typically an iron-nickel-chromium alloy such as alloy 800 (Babione, 1988)²⁷. A steam reformer must operate at up to 800C to obtain a reasonable degree of reaction, and so superior materials are needed for the hotter sections. Such materials exist (for example the nickel superalloys used for industrial steam reformers), but are expensive. Another difference is that reaction temperature and pressure might be lower in a recuperator than in an industrial steam reformer. Milder conditions will prolong tube life and catalyst life.

Another important design consideration is the pressure drop experienced by the reacting mixture. The pressure drop in a reformer tube will be greater than in a HRSG superheater tube of the same length because the reformer tube is filled with catalyst pellets. The overall pressure drop depends on the number of passes required, which in turn depends on heat transfer rates.

4.6.2 Catalyst Performance

Nickel-based catalysts suitable for the steam reformer are available (Richardson, 1990). These would be low temperature versions of well-proven catalysts used in the chemical process industry for steam reforming of hydrocarbons. The lower operating temperature is expected to lead to a longer operating life. As described in Section 4.3.2, the natural gas must be free of sulfur to prevent catalyst poisoning. Carbon deposition in the reformer can reduce catalyst effectiveness, and so the steam-to-methane ratio should be sufficiently high to avoid carbon formation. (This ratio is usually in the range 3-5 in industrial steam reformers.)

²⁷ This alloy is used also for the superheater and reheater tubes of conventional steam-electric power plants.

4.6.3 Two-Phase Evaporation

In the configuration described above, the methane or natural gas fuel is added to the feedwater stream only after the feedwater has been evaporated to become steam. This is the most practical approach as it enables design of the economizer and evaporator sections to benefit from established HRSG practice. This approach is adopted both in the calculations of this study and in the Pacific Gas and Electric Company evaluation of CRGT (De Candia, 1989).

An alternative is to premix the fuel and feedwater prior to entering the HRSG. In a conventional HRSG, water boils at constant temperature, and this entails a high average temperature difference between the hot gas flow and the water. This represents a Second Law loss. The thermodynamic advantage of premixing water and fuel is that a two-component mixture boils at a varying temperature, and this allows the cold-side temperature profile to follow the hot-side profile more closely, thereby reducing the overall log mean temperature difference of the heat exchanger²⁸. This study makes no attempt to evaluate the advantage of this approach, but this should be the subject of a future investigation²⁹.

While thermodynamically preferable, this configuration would be difficult to engineer. The Janes cycle (Janes, 1990) proposes two-phase boiling in a conventional drum-type design. Feedwater and natural gas mix prior to entering the economizer. However drum-type boilers are designed for constant temperature evaporation, so it is unclear how variable temperature evaporation could be achieved. The presence of a two-phase mixture in the economizer would reduce heat transfer coefficients and might require an increased heat transfer area.

A second option for achieving two-phase boiling is to use a once-through boiler rather than the usual drum-type boiler. Once-through boilers have been developed but are uncommon. Proponents of once-through boilers cite a number of operating advantages over drum-type boilers (see for example Babione, 1988 and Soroka and Kamali, 1987).

²⁸ This principle is exploited in the Kalina cycle, a variation of the Rankine cycle which uses a mixture of water and ammonia as the working fluid (see for example Kalina, 1984).

²⁹ As seen in Chapter Two, the main thermodynamic advantage of a chemically recuperated gas turbine cycle is that the reduced steam flow compared to a STIG enables better matching of heat recovery profiles while maintaining a low stack temperature. Further research is recommended to determine the additional benefit from two-phase boiling.

4.6.4 Dew-Point Limit

The temperature of the gas turbine exhaust flow on leaving an HRSG is designed to be above at least 100C. Below this temperature there is a danger that water vapor will condense and combine with sulfur compounds to form a corrosive acid. HRSGs can be designed to recover heat at low exhaust gas temperatures by employing corrosion-resistant materials. However the extra expense involved is justifiable only if the low grade heat recovered has some value (it might be used in a district heating network, for example).

In a CRGT there is no sulfur in the exhaust as it is removed from the incoming natural gas to prevent poisoning of the reformer catalyst. This opens up the possibility of heat recovery down to a lower stack temperature in a HRSG of conventional materials, for example by preheating the natural gas or feedwater. However a draft fan might be required to compensate for the diminished buoyancy of the flue gas.

4.7 OPERATIONAL ISSUES

As well as the design issues considered so far in this chapter, there are many operational issues to be addressed before the chemically recuperated gas turbine concept can be implemented. This section briefly mentions some of these, but makes no attempt to investigate them in detail.

Part-load operation of gas turbines is usually achieved by reducing fuel flow while keeping air flow approximately constant. This leads to a lower turbine inlet temperature and lower peak flame temperatures in the combustor. As a CRGT will operate at low flame temperature even at full-load, achieving stable combustion and acceptable carbon monoxide emissions at part-load might be difficult. If the CRGT is to be operated at full-load most of the time, then high emissions levels at part-load for brief periods during startup and shutdown might be acceptable.

Another means of obtaining reduced power output might be to reduce the steam injected into the gas turbine, either by direct injection or indirectly via the reformer. This might occur in cogeneration applications when a reduction in electrical output can be tolerated to meet an

increased steam demand. However reducing the steam-to-fuel ratio in the reformer would lead to increased NO_x emissions. Further investigation is required to determine if a CRGT cycle can generate enough steam for both process applications and sufficient NO_x control.

Power plants often operate in cycling mode, where they run for a few hours once or twice a day to meet daily peaks in electricity usage. Gas turbines are well-suited to this application because of their relatively short startup time. With a CRGT there would be a time lag between gas turbine startup and full steam production and reformer operation. During this time the gas turbine could run on unreformed natural gas fuel, assuming higher NO_x emissions are tolerable for this period. Another issue surrounding cycling concerns the reforming catalyst. In the chemical process industry, steam reforming is a continuous process. It must be determined that cycling does not adversely affect catalyst performance or lifetime.

Operators place much emphasis on the reliability, availability, and ease of maintenance of a power plant. These qualities must be demonstrated for a CRGT plant.

4.8 ECONOMICS

It is too early to make an accurate estimate of the cost of a CRGT at this stage. Firm efficiency and power output numbers are needed to estimate capital and running costs. Then there are the additional costs of developing new components such as the HRSR or reheat combustor and turbine. This section aims merely to highlight some of the cost issues surrounding gas turbine power plants.

The cost of electricity produced by a power plant depends on its initial capital cost and its operating and maintenance costs, including fuel costs. Fuel costs account for a relatively large fraction of total lifetime costs for base-load plants, while capital costs assume more importance for peaking plants.

Gas turbines offer lower capital costs than traditional steam-electric power plants. Simple cycle turbine-generator sets are typically around \$200/kW for large heavy-duty gas turbines and twice

that for aeroderivatives (Gas Turbine World 1990 Handbook)³¹. Williams and Larson (1989) estimate total plant costs to be approximately \$560/kW for a combined cycle plant, \$440/kW for a STIG, and \$430\$/kW for an ISTIG. These costs compared to \$820/kW for a natural gas-fired steam-electric plant and \$1440/kW for a coal-fired steam-electric plant with flue gas desulfurization (Williams and Larson derive the values for steam-electric plants from EPRI, 1986). The steam-injected plants are cheaper than combined cycles because they avoid the expense of a steam turbine and condenser, even though they utilize expensive aeroderivative gas turbines. However another study (Cohn, 1988) estimated \$550kW for a large combined cycle plant versus \$840/kW for a large STIG plant³².

The CRGT proposed by Janes (1990) is based around an aeroderivative gas turbine with intercooling and reheat. The California Energy Commission has made a preliminary estimate of capital cost for such a plant of \$465/kW (Bemis, 1989). Its estimates for STIG and ISTIG plants are \$840/kW and \$474/kW respectively. Table 4.2 shows these estimates. The increase in capacity resulting from intercooling and reheating more than offsets the cost of these modifications. The HRSG of a STIG is replaced in a CRGT by a heat recovery steam reformer (HRSR), which will be similar in size to a HRSG but will contain high temperature tubing in the reformer section. Hence a HRSR will have the added expense of high quality materials for the reformer tubes, and also of the catalyst inside them³³. It is not clear from Table 4.2 whether the CEC has allowed for the extra material costs.

If NO_x emissions turn out to be as low as expected, a CRGT might be chosen in situations where other gas turbine plants would require SCR. The cost of an SCR system is around \$150/kW (Smock, 1989).

³⁰ Prices are in 1989 dollars. Where sources quote values in the nominal dollars of other years, conversions are made using the US GNP deflator.

³¹ The General Electric LM6000 aeroderivative gas turbine, available in 1992, is projected to cost \$230-\$250/kW (de Biasi, 1990).

³² The study concluded that STIGs are competitive with combined cycles only for small plant sizes (50MW or less), where the STIGs do not suffer from the poor economies of scale associated with the steam turbine and condenser of combined cycles. However utilities are generally not interested in plants of this size.

³³ Because it is likely that the catalyst must be replaced every few years, its cost should maybe be included as an operating cost rather than in the capital cost.

Table 4.2: Capital Cost Estimate for CRGT

Reproduced from Bemis (1989). Refer to this for more details.

Costs are given in millions of dollars.

<u>Cost component</u>	<u>3 STIGs</u> (3x44MW)	<u>ISTIG</u> (112MW)	<u>CRGT</u> (160MW)
Gas turbine & accessories	45.0	15.8	31.6 ^a
HRSG & accessories	32.0	11.2	13.2 ^b
Contingency	12.0	4.2	6.0 ^c
Fuel equipment	0.5	0.5	0.5 ^d
Site work	4.9	4.9	4.9 ^d
Demineralized water system	4.6	4.6	4.6 ^d
Switchyard	1.8	1.8	2.5 ^e
Contingency	1.8	1.8	2.5 ^e
Utility management	3.1	3.1	3.0
A/E license & preliminary engineering	1.5	1.5	1.5
Licensing	0.5	0.5	0.5
Administration & general expenses	2.1	2.1	2.0
Contingency	1.1	1.1	1.6 ^e
Total cost	110.9	53.1	74.4
\$/kW	840	474	465

Notes:

- (a) Assume turbine cost is 2xISTIG cost, to cover development.
- (b) Add \$2.0m to ISTIG for catalyst
- (c) Estimated at 1.5xISTIG contingency due to increased complexity
- (d) Assumed equal to ISTIG cost
- (e) Pro-rated from ISTIG swithyard cost

Fuel costs depend both on the fuel used and on the efficiency with which that fuel is converted to electricity. While natural gas is more expensive than coal³⁴, the high efficiency of combined cycle plants offsets this³⁵. Similarly the projected high efficiency of a CRGT plant will justify the use of natural gas as fuel. A "back-of-the-envelope" calculation suggests that for a 50% efficient power plant running on natural gas, then a further improvement in efficiency of one percentage point leads to lifetime fuel savings of around \$30/kW for a constant gas price. If gas prices increase at an average annual rate of 4.3%, leading to a factor of 3.5 increase in price in 30 years, this value

³⁴ The price of natural gas for utilities is currently around \$2.50/GJ, compared to \$1.40/GJ for coal (Department of Energy, 1990).

³⁵ Gas turbines running on gasified coal are on the verge of commercialization. An important factor influencing recent utility orders for combined cycles has been the knowledge that coal gasification technology will be available to allow conversion to coal as fuel if gas prices increase sharply. (However efficiency is lower with coal than with natural gas.)

increases to approximately \$50/kW³⁶. This price projection is consistent with US Department of Energy projections (Department of Energy, 1990).

Other operating costs for a CRGT will include labor costs, water treatment, and catalyst renewal. A CRGT is at an advantage if alternatives would require an SCR system to meet NO_x regulations, as SCR adds about 25% to a plant operating cost (Smock, 1989).

REFERENCES

- M Arai, T Imai, K Teshima, and A Koga, Research and Development on the HPT of the AGTJ-100B, ASME 87-GT-263
- K Aoyama and S Mandai, "Development of a Dry Low NO_x Combustor for a 120MW Gas Turbine", ASME Journal of Engineering for Gas Turbines and Power, October 1984
- R A Babione, Evaluation of a Once-Through Heat Recovery Steam Generator Concept, EPRI AP-5772, April 1988
- G R Bemis (principal author), Technology Characterizations, State of California Energy Resources Conservation and Development Commission, October 1989
- V de Biasi, "LM6000 dubbed the 40/40 machine due for full-load tests in late 1991", Gas Turbine World, May-June 1990
- M P Boyce, Gas Turbine Engineering Handbook, Gulf Publishing, 1982
- J B Burnham, M H Giuliani, and D J Moeller, "Development, Installation, and Operating Results of a Steam Injection System (STIG) in a General Electric LM5000 Gas Generator", ASME Journal of Engineering for Gas Turbines and Power, July 1987
- F De Candia, ISTIG Enhancement Evaluation, Volume I, Pacific Gas and Electric Company report 007.4-89.1, September 1989
- P J Chenier, Survey of Industrial Chemistry, Wiley, 1986
- A Cohn, "Steam-Injected Gas Turbines Versus Combined Cycles", EPRI Journal, October/November 1988
- J C Corman, System Analysis of Simplified IGCC Plants, General Electric Corporate Research and Development, Schenectady NY, September 1986
- Department of Energy, Monthly Energy Review, May 1990
- Department of Energy, Annual Outlook for US Electric Power 1990: Projections Through 2010, DOE/EIA-047(90), June 1990
- EPRI: Technical Assessment Guide Volume 1: Electricity Supply - 1986, Electric Power Research Institute, EPRI P-4463-SR, December 1986

³⁶ This calculation assumes a current gas price of \$2.50/GJ, a 6.1% real discount rate (as recommended by the Electric Power Research Institute), a 30 year lifetime, and a 70% capacity factor. For plants of lower efficiency, then a percentage point increase in efficiency is more valuable because the amount of fuel saved per unit of electricity is greater.

Gas Turbine World, pp12, March-April 1990

Gas Turbine World, pp23, July-August 1990

Gas Turbine World 1990 Handbook, Pequot Publishing, Southport CT, February 1990

M B Hilt and J Waslo, "Evolution of NO_x Abatement Techniques Through Combustor Design for Heavy-Duty Gas Turbines", ASME Journal of Engineering for Gas Turbines and Power, October 1984

A Hori and K Takeya, "Outline of Plan for Advanced Reheat Gas Turbine", ASME Journal of Engineering for Gas Turbines and Power, October 1981

J Janes, Chemically Recuperated Gas Turbine, California Energy Commission Draft Staff Report, January 1990

A I Kalina, "Combined-Cycle System with Novel Bottoming Cycle", ASME Journal of Engineering for Gas Turbines and Power, October 1984

S Keller of General Electric Marine and Industrial Engine Service Division, Evendale OH, personal communication, 10 April 1990

J A Kent, editor, Riegel's Handbook of Industrial Chemistry, Van Nostrand Reinhold, 1983

G Kimura of General Electric Corporate Research and Development, Schenectady NY, personal communication, December 1990

A W Lefebvre, Gas Turbine Combustion, McGraw-Hill, 1983

J G Meier, W S Y Hung, and V M Sood, "Development and Application of Industrial Gas Turbines for Medium-Btu Gaseous Fuels", ASME Journal of Engineering for Gas Turbines and Power, January 1986

R G Minet and O Olesen, "Technical and Economic Advances in Steam Reforming of Hydrocarbons", in W N Smith and J G Santangelo, editors, Hydrogen: Production and Marketing, American Chemical Society, 1980

K Mori, J Kitajima, T Kimura, and S Miki, "Preliminary Study on Reheat Combustors for Advanced Gas Turbines", ASME Journal of Engineering for Gas Turbines and Power, January 1982

PG&E: Scoping Study: LM5000 Steam-Injected Gas Turbine, Pacific Gas and Electric Company, San Francisco, July 1984

J Puzson of the Gas Research Institute, Chicago IL, personal communication, November 1990

W C Reynolds, The Element Potential Method for Chemical Equilibrium Analysis: Implementation in the Interactive Program STANJAN. Version 3, Stanford University Department of Mechanical Engineering, January 1986

I G Rice, "The Reheat-Gas-Turbine Combined Cycle", Mechanical Engineering, April 1982

J Richardson of United Catalysts Corporation, Louisville KY, personal communication, May 1990

P E Sabla and G G Kutzko, Combustion Characteristics of the GE LM2500 Combustor with Hydrogen-Carbon Monoxide-Based Low Btu Fuels, ASME 85-GT-179

SCAQMD, Air Quality Management Plan, South Coast Air Quality Management District, 1989 Revision, March 1989

H Short, "NH₃ Breakthrough: Small Plants", Chemical Engineering, July 1989

G W Sidebotham and R H Williams, Technology of NO_x Control for Stationary Gas Turbines, Princeton University Center for Energy and Environmental Studies Draft Report, January 1989, (Final report as yet unpublished).

K O Smith, NO_x Reduction for Small Gas Turbine Power Plants, EPRI AP-5347, September 1987

R Smock, "Gas Turbines Dominate New Capacity Ordering", Power Engineering, August 1989

G Soroka and K Kamali, "Modular Remotely Operated, Fully Steam-Injected Plant for Utility Application", Proceedings of the 1987 ASME Cogen-Turbo Conference, Montreux Switzerland, September 1987

I Stambler, "Trends in Low-NO_x Combustion Design and Operating Experience", Gas Turbine World, March-April 1990

K Takeya and H Yasui, "Performance of the Integrated Gas and Steam Cycle (IGSC) for Reheat Gas Turbines", ASME Journal of Engineering for Gas Turbines and Power, April 1988

G L Touchton, "Influence of Gas Turbine Combustor Design and Operating Parameters on Effectiveness of NO_x Suppression by Injected Steam or Water", ASME Journal of Engineering for Gas Turbines and Power, July 1985

R H Williams and E D Larson, "Expanding Roles for Gas Turbines in Power Generation", in T B Johansson, B Bodlund, and R H Williams, editors, Electricity: Efficient End-Use and New Generation Technologies, and Their Planning Implications, Lund University Press, 1989

K Yagamishi, Development of Advanced Gas Turbines in Japan, presented at International Gas Turbine Congress, Tokyo, October 1987.

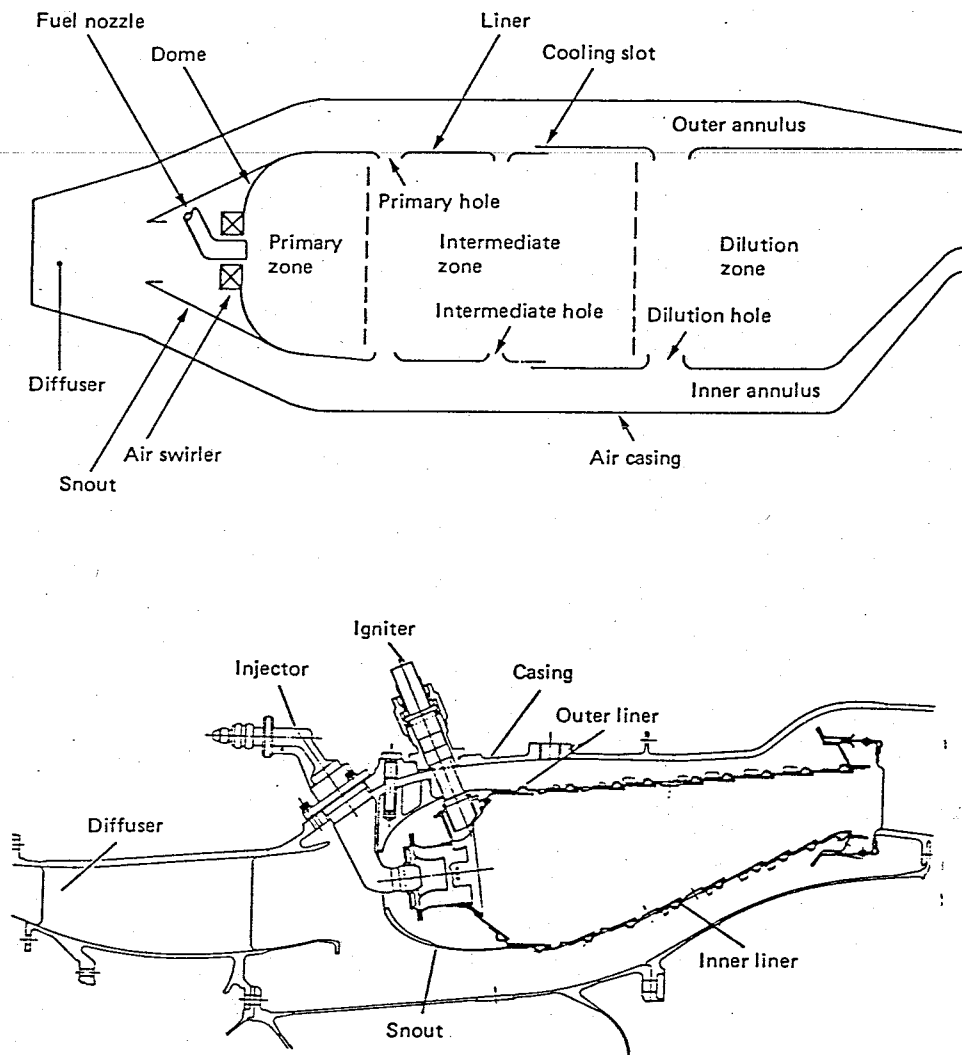


Figure 4.1: Schematic of "Conventional" Combustors

The top diagram is a general schematic showing the various zones. The lower diagram is a sectional view of the combustor used in a General Electric CF6-50 gas turbine.

Combustion occurs in the primary zone at a near-stoichiometric fuel-to-air ratio. More air is added in the intermediate zone to dilute the flow and help convert carbon monoxide to carbon dioxide. The remaining air is added in the dilution zone to bring the gas temperature down to a level acceptable by the turbine.

NO_x levels are determined primarily by peak temperatures in the primary zone, while carbon monoxide levels are influenced by the design of all three zones.

Source: Lefebvre (1983)

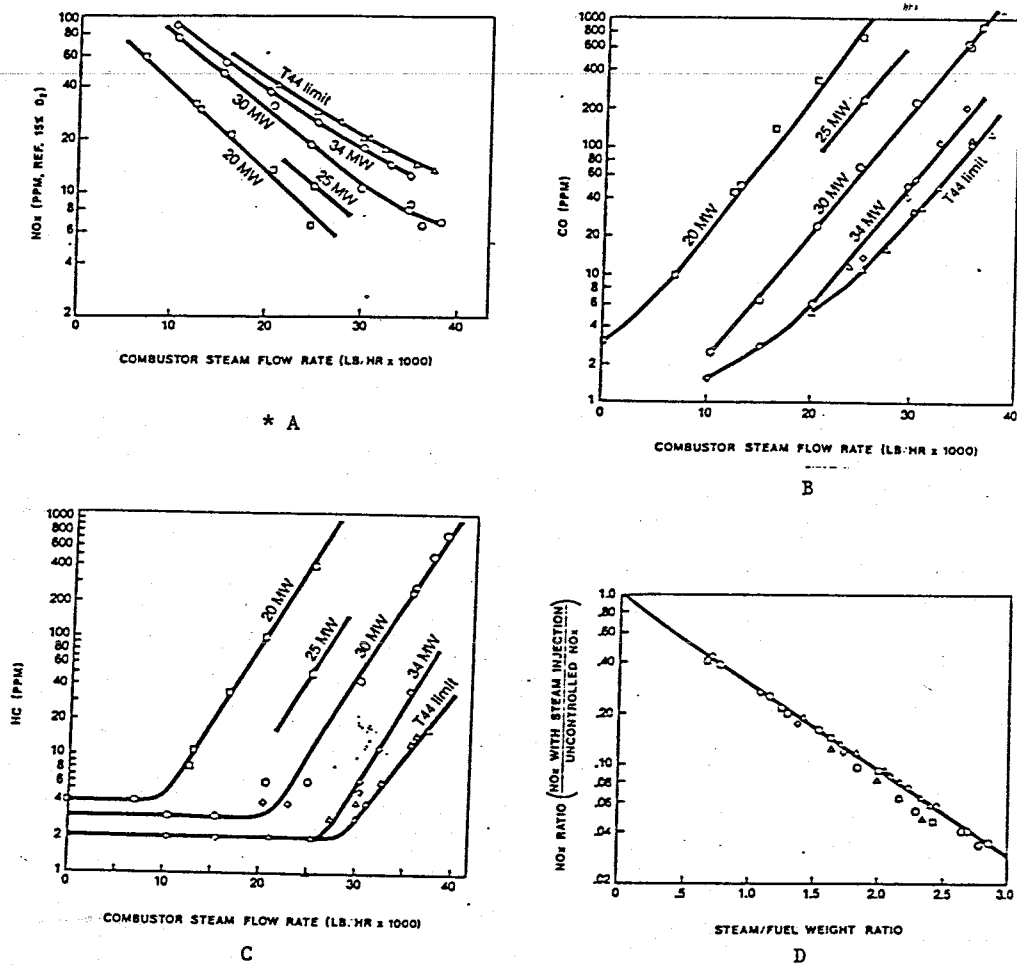


Figure 4.2: Effect of Steam Injection on Emissions

Results shown are for a General Electric LM5000 gas turbine. The T44 limit is the maximum power limit.

Figure A shows how NO_x formation decreases with increasing amounts of steam injection. However this trend is accompanied by increasing levels of carbon monoxide (B) and unburned hydrocarbons (C). Figure D shows NO_x emissions non-dimensionalized as a fraction of uncontrolled levels. Power output is reduced by reducing fuel flow to the combustor. As this lowers combustor temperatures, NO_x levels are low and carbon monoxide levels are high at part-load.

Source: Burnham et al (1987)

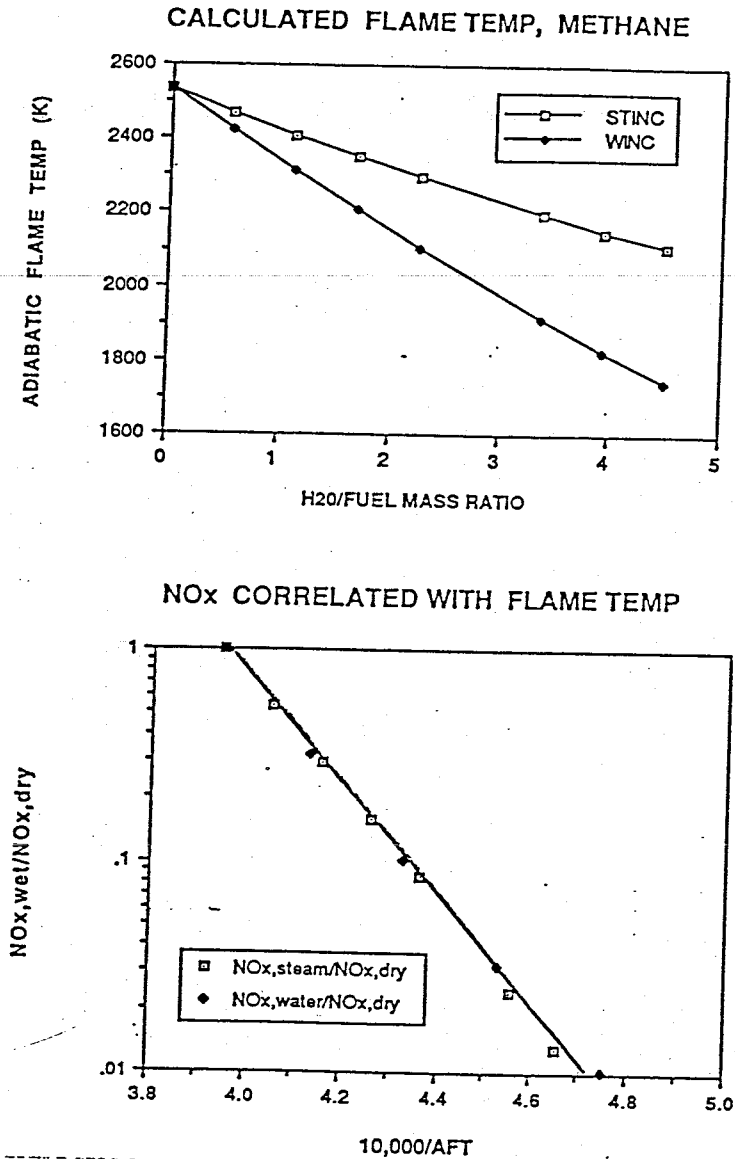


Figure 4.3: Correlation of NO_x Emissions with Flame Temperature

The top figure shows how steam or water injection lowers the stoichiometric adiabatic flame temperature (AFT) of the fuel. This temperature corresponds approximately to peak temperatures in the combustor, and is the main factor determining NO_x levels. Water is a more effective NO_x suppressant than steam on a unit mass basis because it lowers the flame temperature more. (Methane is used to represent natural gas, which typically contains 95% methane.)

The lower figure plots flame temperature against a manufacturer's NO_x estimates for different levels of steam and water injection. The resulting single straight-line confirms that water and steam injection achieve NO_x suppression by reduction of peak combustion temperatures. This curve can be used to obtain approximate estimates of NO_x emissions for any combustor whose peak flame temperature is known.

Source: Sidebotham and Williams (1989)

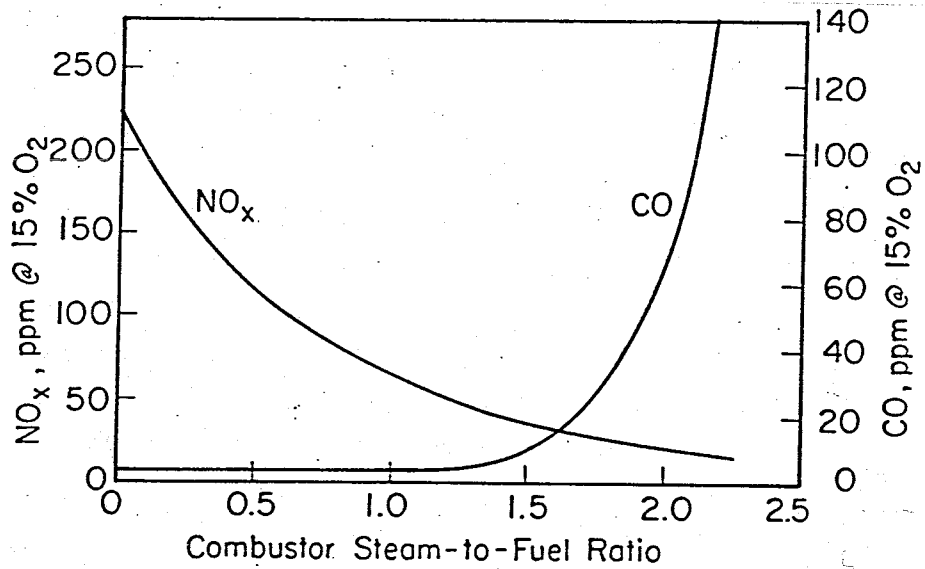
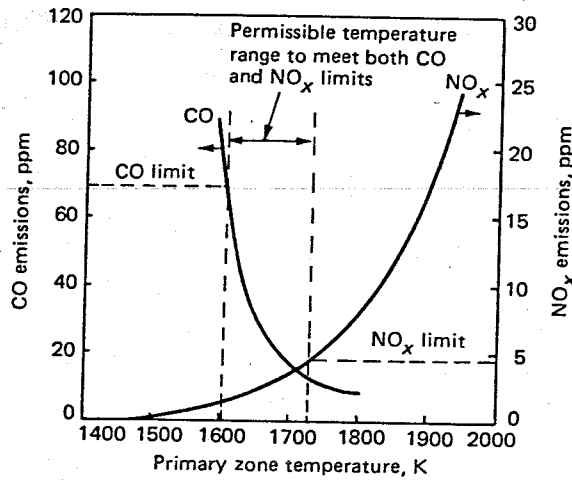


Figure 4.4: Trade-Off Between NO_x and Carbon Monoxide Emissions

The upper figure plots emissions against primary zone temperature for a hypothetical combustor. It shows that only a narrow temperature band is acceptable to meet NO_x and carbon monoxide limits of 5ppm and 70ppm respectively. (The averaged primary zone temperature is lower than the peak flame temperature.)

The lower figure plots emissions against steam-to-fuel ratio for a gas turbine with steam injection for NO_x control. Steam-to-fuel ratio is related to flame temperature as shown in Figure 4.3.

Sources: *Lefebvre (1983) (upper figure)*
Williams and Larson (1989) (lower figure)

CHAPTER FIVE: CHEMICALLY RECUPERATED GAS TURBINE COMPUTER MODEL

5.1 Introduction

5.2 The Consonni Gas Turbine Model

5.3 Modelling Chemical Recuperation

5.4 General Approach for Cycle Calculations

References

Appendix 5A

Notation

Figures

5.1 INTRODUCTION

This chapter describes the computer model used to calculate chemically recuperated gas turbine cycles (CRGTs). The model was developed by adding the capability to handle chemical recuperation to an existing gas turbine program developed by Stefano Consonni of Princeton University's Center for Energy and Environmental Studies¹. Section 5.2 briefly describes the Consonni model, and Section 5.3 relates how it has been modified to incorporate chemical recuperation. Section 5.4 describes the general methodology used for the cycle calculations presented in Chapters Six and Seven.

5.2 THE CONSONNI GAS TURBINE MODEL

This section briefly describes the Consonni gas turbine model. For a fuller description see Consonni (1991).

The Consonni model is designed to predict the performance of power cycles which use both gas and steam as working fluids, for example steam-injected cycles or combined cycles. The model is not intended to mimic specific gas turbines, but rather to have the flexibility to represent generic gas turbines of different size and type. The model uses a number of input parameters to describe

¹ Now at Politecnico di Milano, Italy.

turbomachinery efficiency, cooling sophistication, and so on. Values for these representing today's "state-of-the-art" were found by averaging technological inputs of gas turbines currently on the market². The model is intended for calculation of design-point performance only - it cannot predict off-design operation.

The model allows the user to construct a cycle by choosing components from the following list: compressor, combustor, turbine, heat exchanger, mixer, splitter, and heat recovery steam generator (HRSG). These are connected by appropriately numbering the input and output streams. A subroutine for each component calculates unknown properties of these flows, given component data such as compressor efficiency or heat exchanger pressure drop. The model calculates each component in turn, and then re-iterates until specified flow-point properties reach convergence. Finally overall power output and efficiency are calculated, and an exergy analysis is performed if desired.

The working fluid at each point is described by its thermodynamic properties, mass flow, and composition. Any mixture of a list of twenty common species is allowed. A subroutine *CNSJ* calculates thermodynamic properties of the mixture given its composition and any two independent properties (Consonni, 1987).

The turbine subroutine incorporates a detailed cooling scheme which calculates the coolant flow necessary to keep all metal temperatures below a specified limit. The coolant may be compressor bleed-air or steam. Two parameters represent the sophistication of the cooling technology, one for convection cooling and one for film cooling. Values for these typical of modern gas turbines have been derived from existing performance data (Consonni, 1991).

The HRSG subroutine allows evaporation at up to four pressure levels. The user specifies the desired steam conditions and all approach temperatures and pinch-points, and the routine then maximizes steam production at each level. It calculates the feed pump work, and also the performance of the steam turbine and condenser for combined cycles.

² The model can also predict the result of future innovations on gas turbine performance. However this requires an estimate of how the input parameters will change as a result of innovations.

Verification of Consonni Model

Consonni has derived sets of input parameters to represent four generic gas turbines: current heavy-duty, current aeroderivative, advanced heavy-duty, and advanced aeroderivative (Consonni, 1990b). The "current" data was obtained by calibrating the model against performance data for gas turbines currently in production. The advanced data are derived from performance data for the latest generation of gas turbines. These turbines, for example the General Electric 7F and LM6000, have only recently been introduced or will be introduced in the next two years. Table 5.1 shows the four data sets.

Table 5.1: Input Parameters for Gas Turbine Model

	Heavy-duty		Aeroderivative	
	Current	Advanced	Current	Advanced
Compressor efficiency (%)	89.5	89.75	89.5	91.0
Turbine efficiency (%)	93.0	94.0	93.0	94.0
Compressor efficiency slope	.0432	.0432	.0354	.0354
Turbine efficiency slope	.0414	.0414	.0245	.0245
Convection cooling parameter	75	90	75	90
Film cooling parameter	-.36	-.38	.36	.45
Maximum metal temperature in nozzle (C)	820	850	820	850
Maximum metal temperature in turbine (C)	790	800	790	800

Notes:

- (a) Turbomachinery efficiencies shown are the asymptote to which efficiency approaches as machine size increases. The Consonni model has an in-built function to account for the size of the engine (smaller turbines are less efficient). The "efficiency slopes" determine the severity of the size effect.
- (b) Negative film cooling parameters signify that film cooling is used in the first turbine stator row (the "nozzle") only. Positive values indicate that all cooled stages use film cooling in addition to convection cooling.
- (c) All four cases use the following input values:
 Heat losses = 1% of heat added to combustor by fuel
 Combustor pressure drop = 3%
 Leakage flow = 1% of total air flow
 "Organic" efficiency (measures bearing losses etc) = 99.6% (see Consonni 1991 for definition)

Given these data, it should be possible to reproduce approximately the performance of actual gas turbines by running the Consonni model with the same pressure ratio, turbine inlet temperature, and mass flow rate of air. This was tested by comparing the predictions of the Consonni model against the published performance of one gas turbine in each of the four categories. The most

commonly available performance data are the cycle efficiency, power output, and turbine outlet temperature. Table 5.2 shows the test results. Agreement is good for all four cases, but not exact because of the averaging process involved in deriving the input parameters. Nevertheless, it can be concluded that the four data sets can confidently be used to represent the four generic turbine types. Consonni (1991) presents a more detailed evaluation of the accuracy of the model.

Table 5.2: Results of Gas Turbine Verification Tests

Gas turbine		Efficiency (% LHV)	Power (MW)	TOT (C)
ABB GT13E (current heavy-duty)	Actual	35.2	150	516
	Model	34.3	145	514
GE Frame 7F (advanced heavy-duty)	Actual	35.0	152	583
	Model	35.0	149	595
GE LM5000 (current aeroderivative)	Actual	37.3	34.5	445
	Model	38.0	36.1	445
GE LM6000 (advanced aeroderivative)	Actual	41.5	42.4	452
	Model	41.3	42.2	450

Notes:

- (a) Actual performance data for GT13E, 7F, and LM5000 from Gas Turbine World 1990 Handbook. LM6000 from de Biasi (1990).
- (b) TOT = turbine outlet temperature
- (c) Efficiency and power output are shaft values. If actual data gave electrical output and efficiency, then these were converted to shaft values assuming a generator efficiency of 98.5%.

5.3 MODELLING CHEMICAL RECUPERATION

The Consonni model was modified for chemical recuperation by the addition of a subroutine to model the steam reformer³. Figure 5.1 shows the model diagrammatically. There may be just one steam-fuel reaction, or two in parallel at different pressures⁴.

³ A few minor changes were made to existing subroutines also. The HRSG routine was modified to allow the user to specify that the mass of steam at a given pressure level and a given degree of superheat be some value other than the maximum possible.

⁴ If the cycle has reheat or supplementary firing there will be two fuel gas flows. Because low pressures favor the recuperation reaction, it is beneficial to keep the flows separate and at the lowest possible pressures rather than to reform all the fuel at high pressure.

In reality steam will be generated and will react with the fuel in a single component - the heat recovery steam reformer. This is essentially a heat recovery steam generator with a chemical reactor (referred to here as the steam reformer or chemical recuperator) added onto the hot-end. The recuperator subroutine models only the steam reformer, as the existing HRSG subroutine can be used for the steam generation section. The model always assumes the fuel is introduced after the evaporation stage⁵.

The model derives the composition of the product fuel gas by using an "equilibrium approach temperature" to describe how nearly the reaction reaches equilibrium. This concept is widely used in the chemical process industry as a measure of catalyst performance. A zero equilibrium approach indicates that the reaction achieves equilibrium. If the reaction temperature is 600C, for example, then an equilibrium approach of 10C signifies that the product composition is the equilibrium composition at 590C. Note that this implicitly assumes that the reaction proceeds towards equilibrium, and that an equilibrium composition is the "ideal" outcome of the reaction given a "perfect" catalyst. Chapter Three showed how steam reforming of methanol results in a mixture from which methane is absent, even though equilibrium calculations indicate methane formation. For this reason the recuperator model cannot be used for methanol-fueled cycles.

Appendix 5A describes the recuperator model in detail.

5.4 GENERAL APPROACH FOR CYCLE CALCULATIONS

This section describes the objectives of the detailed cycle calculations presented in Chapters Six and Seven, and the general methodology used to achieve these objectives.

The coupling of a gas turbine with methane steam reforming is a new concept on which little attention has been focused to date. A large number of issues must be addressed before making the decision to develop such a new technology. These range from the basic thermodynamic performance through hardware design and off-design operation to economic attractiveness. The

⁵ The steam may be superheated before introduction of the fuel.

necessary first step on this journey is a thorough understanding of the thermodynamic principles underlying CRGT. For example, how does the heat recovery steam reformer interact with the rest of the cycle? What are the thermodynamic pluses and minuses of chemical recuperation? Are some gas turbine cycle configurations more suited to chemical recuperation than others? This thesis aims to answer such questions. Chapter Two made a start, predicting that addition of chemical recuperation to a steam-injected gas turbine generally increases efficiency at the expense of power output. Chapters Six and Seven continue by using the computer model to investigate CRGT cycles in more detail.

Chapter Six considers a very simple cycle consisting of a gas turbine and a heat recovery steam reformer with single pressure evaporation. The simplicity of this cycle enables observation of the effect of the chemical heat recovery by comparison with a conventional steam-injected gas turbine. With this simple cycle fully understood, Chapter Seven progresses to more advanced cycles. While the number of potential cycle configurations is enormous, only the most promising are selected for analysis. These calculations give a more realistic estimate of the performance that can be expected from real machines. Comparisons are made with the leading competitors among non-chemically recuperated cycles. Both aeroderivative and heavy-duty gas turbines are considered. For each class of machine, the analysis uses input component data representing the current "state-of-the-art", that is the latest generation of machines. All calculations use pure methane as fuel.

A design-point analysis is used. That is to say, components such as compressors, turbines, and boilers are assumed to be designed optimally for the particular working fluid properties and flow-rates of the cycle in question. Off-design issues, while important in the design of an actual machine, are beyond the scope of this investigation (and beyond the capabilities of the model). CRGTs might be well-suited to cogeneration applications, just as STIGs are, because of good part-load performance. However the range of possible steam conditions is so vast that for reasons of simplicity only power-only cycles are considered. Of course, these may be thought of as the power-only mode of cogeneration machines, but then it will be the power-only mode which is designed optimally.

In Chapter Six, the cycle is fully optimized, and a parametric investigation of different turbine inlet temperatures and pressure ratios is carried out. Doing the same for the complex cycles of Chapter Seven is impractical, as there are many more variables to be optimized. Instead only a few cases are presented.

REFERENCES

V de Biasi, "LM6000 dubbed the 40/40 machine due for full-load tests in late 1991", Gas Turbine World, May-June 1990

S Consonni, A Computer Program to Calculate Working Fluid Thermodynamic Properties of Steam-Injected Gas Turbine Cycles, Princeton University Center for Energy and Environmental Studies Working Paper No 89, July 1987

S Consonni, 1990a, Entropy Analysis of Mixed Gas/Steam Cycles, Politecnico di Milano, July 1990

S Consonni, 1990b, personal communication, September 1990

S Consonni, Performance Prediction of Gas-Steam Cycles for Power Generation, PhD thesis, Princeton University Department of Mechanical and Aerospace Engineering (Center for Energy and Environmental Studies), due June 1991

S Consonni and A Lloyd, Chemically Recuperated Gas Turbine Cycles, to be submitted for the ASME COGEN-TURBO V conference to be held in Budapest, Hungary, September 1991

Gas Turbine World 1990 Handbook, Pequot Publishing, Southport CT, February 1990

J Richardson of United Catalysts Corporation, Louisville KY, personal communication, May 1990

APPENDIX 5A

Input and Output Data

This section lists the known and unknown quantities for the recuperator subroutine calculation.

The details of this calculation are described in the following section.

The recuperator routine takes the following quantities as known inputs:

- Mass flow of high (and low) pressure fuel as required by the combustor (and reheat combustor or supplementary firer).
- Composition and properties of the incoming fuel and steam flows.
- Properties, composition and mass flow of the gas turbine exhaust.
- Gas-side and reaction-side pressure drops.

- Overall heat loss (as a fraction of the total heat given up by the gas turbine exhaust).
- Hot end approach temperature for high (and low) pressure reactions
- Molar steam-to-fuel ratio for high (and low) pressure reactions.

The model uses this input information to calculate the following:

- Properties, composition, and higher and lower heating value of high (and low) pressure fuel gas.
- Required mass flows of incoming steam and fuel.
- Properties of the gas-side flow exiting the recuperator.

Calculation Method

Figure 5.2 shows the calculation method in flow-chart form. The various steps are described below. The term "gas-side" refers to the gas turbine exhaust flow, while "fuel-side" refers to the reacting steam/fuel flow. Equations are given for one fuel-side flow only. If there are two flows then identical calculations are carried out for the second flow as for the first. A list of notation appears at the end of the chapter.

First the gas-side entry and fuel-side exit pressures are calculated given the pressure drop as a fraction of entry pressure⁶⁷.

$$p_{g,i} = p_{g,o} / (1 - \Delta p_g)$$

$$p_{fg} = (1 - \Delta p_f) p_s$$

The required mass flow of fuel gas is calculated by the combustor subroutine, and depends on the fuel gas heating value obtained in the previous iteration. Conservation of mass dictates that this is equal to the combined mass flow of incoming fuel and steam. The individual mass flows can be determined using the molar steam-to-fuel ratio.

⁶ The gas-side entry pressure is treated as unknown and the exit pressure as known. The gas turbine exit pressure is found by adding the HRSG and recuperator (and any other component in the exhaust stream) pressure drops to the stack pressure, which is assumed to be atmospheric pressure.

The fuel is assumed to be at a higher pressure than the steam.

⁷ Chapter Six discusses the choice of suitable values for input parameters such as pressure drops.

$$m_s = n \cdot m_{fg} / (n + M_f / M_s)$$

$$m_f = m_{fg} - m_s$$

The fuel gas temperature on exiting the recuperator is set by the incoming gas-side temperature and the approach temperature.

$$T_{fg} = T_g - \Delta T_{app}$$

Now that T_{fg} , p_{fg} , and n are all known, the steam-fuel reaction can be calculated. The approach to equilibrium indicates how nearly the reaction reaches equilibrium, and is a measure of catalyst performance. For example, an approach to equilibrium of 10C signifies that the composition is the equilibrium composition at $(T_{fg} - 10)C$. Its value depends upon the catalyst operating temperature. The equilibrium approach is assumed to be zero above 650C and to decrease linearly below 650C so that at 500C it is 10C:

$$\Delta T_{eq} = 0 \quad T_{fg} > 650C$$

$$\Delta T_{eq} = 43.33(1 - T_{fg}/650) \quad T_{fg} < 650C$$

These values are representative of currently available catalysts for methane steam reforming (Richardson, 1990).

The CNSJ subroutine calculates the fuel gas composition and properties (including higher and lower heating values) in two steps.

$$\text{Fuel gas composition} = f [n, p_{fg}, (T_{fg} - \Delta T_{eq})]$$

$$\text{Fuel gas properties} = f [T_{fg}, p_{fg}, \text{composition}]$$

The fuel-side calculations are now complete, and are repeated for the second pressure level if there is one. The gas-side exit enthalpy follows from an energy balance for the complete recuperator.

$$m_g (1 - \Delta h) (h_{g,i} - h_{g,o}) = (m_{fg} h_{fg} - m_s h_s - m_f h_f)$$

Other gas-side exit properties follow from the pressure and enthalpy (the composition and mass flow are the same as at entry). Finally, a check is carried out to ensure that the gas-side exit

temperature is hotter than the incoming steam/fuel mixture by at least the specified approach temperature⁸.

Exergy Analysis

The Consonni program includes an exergy analysis option⁹. When convergence is reached, exergy losses around the cycle are analyzed. For each component, the entropy change due to various loss sources, such as frictional pressure drop, is calculated. The associated irreversibility or exergy loss is the product of that entropy change and the ambient temperature. The sum of these irreversibilities, the exergy of all flows exiting the cycle, and the work obtained should be equal to the exergy input to the cycle.

The Consonni program performs two exergy analyses. The first assumes that the exergy of a fuel is the reversible work obtainable by bringing the system to thermo-mechanical equilibrium with the environment, while the second imposes chemical equilibrium also. The difference between the two arises because the exhaust stream has a different composition from the environment, and so work could be obtained by a reversible mixing process. If this work is considered irrecoverable by any practical device, then it makes sense to exclude it from the analysis. This term is typically very small, and so the two analyses produce very similar results.

Irreversibilities in the recuperator are attributed to pressure drop, thermal losses, mixing, chemical reaction, and heat transfer. The distinction between reaction losses, heat transfer losses, and mixing losses is somewhat artificial because the three processes are interdependent.

The entropy change due to pressure drops is given by

$$\Delta S_{p\text{-loss}} = (m_g R/M_g) \ln(p_{g,i}/p_{g,o}) + (m_f R/M_f) \ln(p_f/p_{fg}) + (m_s R/M_s) \ln(p_s/p_{fg})$$

⁸ The model assumes that in the recuperator section the closest approach between the gas- and fuel-side temperatures always occurs at the hot-end. If the check for this fails, then the program notifies the user. In reality it is possible for the minimum approach to be at the cold-end if the flow rates of steam and fuel are high enough. The model does not have the capability to handle this situation. The cycles calculated in this study are such that the minimum approach is always at the hot-end.

⁹ See Consonni (1990a) for a detailed description.

The entropy change due to thermal losses is

$$\Delta S_{q\text{-loss}} = m_g[(s_{g,o} - s') + q_{\text{lost}}/T_0]$$

where q_{lost} is the heat loss defined by

$$q_{\text{lost}} = \Delta h(h_{g,i} - h_{g,o})$$

and s' is the entropy which the exiting gas-side flow would have in the absence of thermal losses.

Note that this ΔS term includes the entropy change of the environment as well as the entropy change of the gas-side flow.

Mixing losses are further subdivided into two categories. The first arises from the change of composition of the fuel-side flow, and represents the work that could be obtained by performing this change using an ideal mixing process. The entropy change due to change of composition is given by

$$\Delta S_{\text{comp}} = (m_{fg}R/M_{fg})\sum[x_i \ln(1/x_i)]_{fg} - (m_f R/M_f)\sum[x_i \ln(1/x_i)]_f - (m_s R/M_s)\sum[x_i \ln(1/x_i)]_s$$

This term is not included in the first exergy analysis, which assumes that this loss is irrecoverable in practice, but is included in the second exergy analysis.

Other mixing losses arise from heat transfer between the steam and fuel as they mix, and from real gas effects associated with steam. The difficult thermodynamic concepts used in evaluating these losses are best understood by consulting Consonni (1990a). Let the entropy change associated with these losses be ΔS_{mix} .

Heat transfer irreversibilities arise from heat transfer across finite temperature differences between the gas- and fuel-side flows. The entropy loss is evaluated by integrating the temperature difference along the recuperator:

$$\Delta S_{h/t} = \int (1/T_{\text{fuel-side}} - 1/T_{\text{gas-side}})dh$$

The dependence of the gas- and fuel-side temperatures on the amount of heat transferred is not known. Linear temperature profiles are assumed as an approximation. The inlet fuel-side temperature is taken to be the temperature resulting upon mixing the incoming fuel and steam flows.

Finally the entropy change due to chemical reaction is found by subtracting all of the above entropy changes from the total change for the recuperator (and the environment).

$$\Delta S_{\text{chem}} = m_g(s_{g,o} - s_{g,i}) + (m_{fg}s_{fg} - m_s s_s - m_f s_f) + m_g q_{\text{lost}}/T_0 - [\Delta S_{p\text{-loss}} + \Delta S_{q\text{-loss}} + \Delta S_{\text{comp}} + \Delta S_{\text{mix}} + \Delta S_{h/t}]$$

Note that ΔS_{comp} was described as the entropy change arising from the change of composition associated with mixing. However composition can also change as a result of chemical reaction. This can lead to the situations where ΔS_{comp} or ΔS_{chem} is negative. This appears to violate the Second Law of Thermodynamics. The explanation is that it is not physically possible to separate the reaction process from the change of composition. The entropy change for the combined process, $(\Delta S_{\text{comp}} + \Delta S_{\text{chem}})$ should always be positive.¹⁰

NOTATION

Note that quantities such as mass flow rate, heat, and entropy change are expressed per unit mass of air entering the compressor.

h - enthalpy (kJ/kg)

m - mass flow rate (kg/kg_{air})

M - molecular mass (kg/kmol)

n - molar steam-to-fuel ratio

p - pressure (kPa)

q_{lost} - thermal loss from recuperator (kJ/kg_{air})

s - entropy (kJ/kgK)

R - universal gas constant (=8.314kJ/kmolK)

T - temperature (K)

x_i - mole fraction of mixture component i

Δh - heat loss (as fraction of total heat transfer from hot-side)

Δp_f - fuel-side pressure loss (as fraction of entry pressure)

Δp_g - gas-side pressure loss (as fraction of entry pressure)

ΔS_{xxx} - entropy change due to loss source xxx (kJ/kg_{air}K)

ΔT_{app} - hot-end approach temperature difference (K)

¹⁰ A future paper (Consonni and Lloyd, 1991) will address this point in greater detail.

ΔT_{eq} - equilibrium approach temperature (K)

Subscripts:

f - fuel entering recuperator

fg - fuel gas exiting recuperator

g,i - gas-side incoming flow

g,o - gas-side outgoing flow

s - steam entering recuperator

0 - ambient conditions

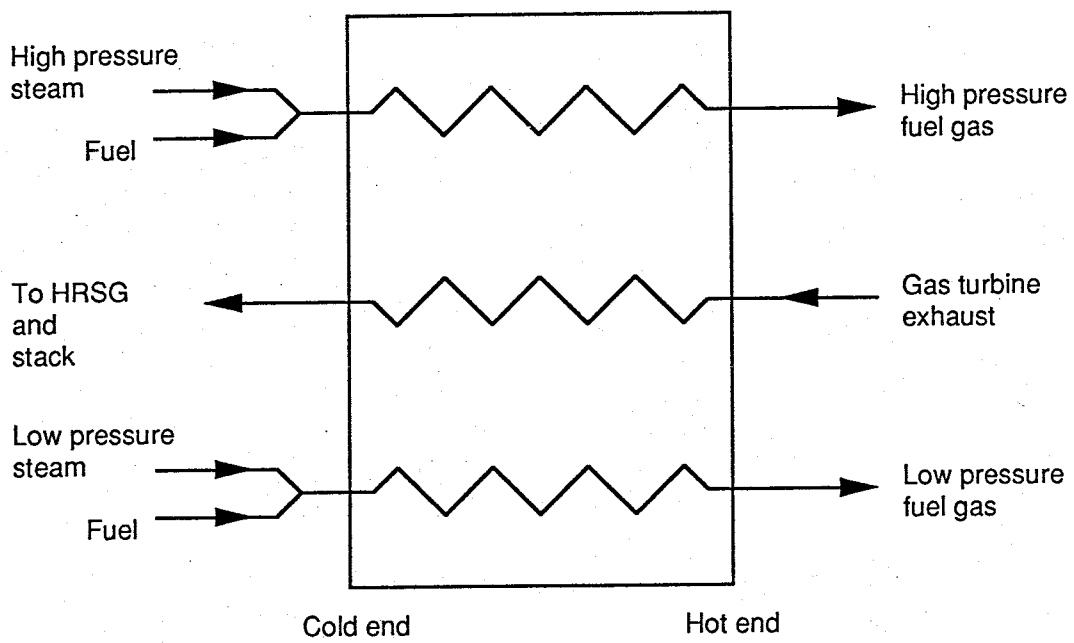


Figure 5.1: Schematic Diagram of Recuperator Model

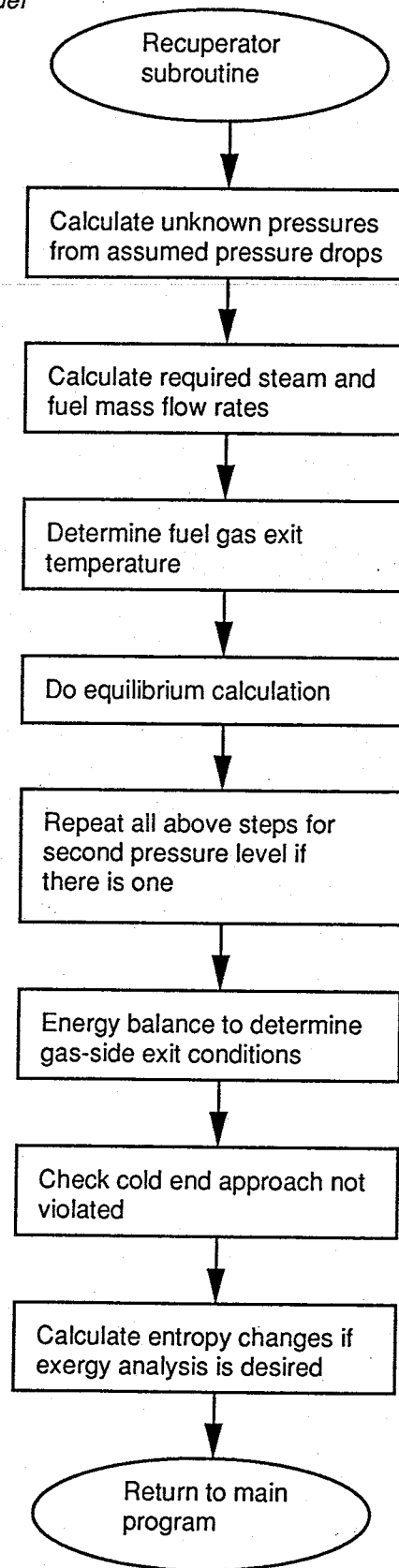


Figure 5.2: Flow Chart Showing Recuperator Subroutine Calculation

CHAPTER SIX: SIMPLE CRGT CYCLE

6.1 Cycle Description

6.2 Example Comparison of CRGT with STIG and Combined Cycles

6.3 Parametric Analysis

6.4 Discussion

References

Appendix 6A

Figures

6.1 CYCLE DESCRIPTION

This chapter investigates the most simple chemically recuperated gas turbine (CRGT) cycle configuration in order to gain a clear understanding of how chemical recuperation affects the cycle performance. With this goal in mind, Section 6.2 presents a detailed comparison of a CRGT with steam-injected gas turbine (STIG) and combined cycles operating at the same turbine inlet temperature (TIT) and pressure ratio. The conditions chosen are a heavy-duty gas turbine at a TIT of 1250C and a pressure ratio of 15. Section 6.3 extends the comparison of CRGT and STIG to other TITs and pressure ratios, and also to aeroderivative gas turbines. Section 6.4 reviews the findings of Sections 6.2 and 6.3 and discusses their implications for practical CRGT cycles. Appendix 6A tests some of the assumptions made in carrying out the calculations of this chapter.

The cycle, shown in Figure 6.1, consists of a gas turbine and a heat recovery steam reformer. The reformer consists of a conventional heat recovery steam generator (HRSG) with a chemical recuperator (reformer) section placed at the hot-end. Some or all of the steam produced in the HRSG may be routed through the reformer, while the remainder is injected directly into the gas turbine combustor.

Table 6.1: Input Data for Cycle Calculations

GAS TURBINE	Heavy-duty	Aeroderivative
Inlet air flow (kg/s)	400	120
Compressor efficiency (%)	89.75	91.0
Turbine efficiency (%)	94.0	94.0
Compressor efficiency slope	.0432	.0354
Turbine efficiency slope	.0414	.0245
Convection cooling parameter	90	90
Film cooling parameter	-.38	.45
Maximum metal temperature in nozzle (C)	850	850
Maximum metal temperature in turbine (C)	800	800

Notes:

- (a) Turbomachinery efficiencies shown are the asymptote to which efficiency approaches as machine size increases. The Consonni model has an in-built function to account for the size of the engine (smaller turbines are less efficient). The "efficiency slopes" determine the severity of the size effect.
- (b) Negative film cooling parameters signify that film cooling is used in the first turbine stator row (the "nozzle") only. Positive values indicate that all cooled stages use film cooling in addition to convection cooling.
- (c) All four cases use the following input values:
 Inlet pressure drop = 1%
 Heat losses = 1% of heat added to combustor by fuel
 Combustor pressure drop = 3%
 Leakage flow = 1% of total air flow
 "Organic" efficiency (measures bearing losses etc) = 99.6% (see Consonni 1991 for definition)
 Fuel pump compresses methane from 5bar supply pressure to 1.5 times cycle pressure ratio
- (d) Data supplied by Consonni (1990b)

STEAM REFORMER

Gas-side pressure drop = 2%
 Fuel-side pressure drop = 10%
 Heat losses = 2% of total heat transfer from hot-side
 Hot-end approach temperature = 20C
 Equilibrium approach temperature: see Appendix 5A

HEAT RECOVERY STEAM GENERATOR

Gas-side pressure drop = 2.5%
 Superheater pressure drop = 5%
 Heat losses = 2% of total heat transfer
 Hot-end approach temperature = 20C
 Minimum pinch point temperature difference = 10C
 Minimum stack temperature = 100C
 Maximum steam temperature = 550C
 Evaporation pressure (in bar) = 1.5 times the cycle pressure ratio

The component input data used, listed in Table 6.1, are typical of modern "state-of-the-art" machines. The gas turbine performance parameters used are those representing "advanced" aeroderivative and heavy-duty machines, as described and verified in Section 5.2. The HRSG

data are typical of modern designs. Data for the steam reformer are not available as none have been built yet, so estimates must be made. The hot-end approach is set at 20C, the same as for the HRSG. The equilibrium approach temperature is zero for reforming temperatures above 650C, and increases linearly for temperatures below this (see Appendix 5A). The fuel-side pressure drop is set at 10%, which is similar to that for an industrial steam reformer (Minet and Olesen, 1980)¹.

The turbine is assumed to consist of a cooled section followed by an uncooled section. The cooled section ends when no cooling is required to keep the blade metal temperature below the specified limit. The convection cooling parameter indicates the sophistication of the blade cooling passages, while the film cooling parameter indicates the amount of film cooling. In both cases, a higher value corresponds to better cooling. Both heavy-duty and aeroderivative gas turbines are assumed to be single-shaft machines².

To avoid added complexity, the HRSG has only one pressure level. In practice two or three are likely, with the lower pressure steam being injected further down the turbine, sent to process, or used in a combined cycle. The use of multi-pressure evaporation generally increases efficiency by achieving a better match of HRSG temperature profiles and hence reducing irreversible heat transfer losses. All calculations and comparisons made in Sections 6.2 and 6.3 are for cycles with single pressure evaporation. Section 6.4 discusses the implications of multi-pressure evaporation for the relative merits of STIG and CRGT cycles (see also Chapter Seven).

For STIG and CRGT cycles the boiler evaporation pressure is assumed to be 50% greater than the overall pressure ratio, to allow for pressure losses in the superheater and reformer and for the required pressure drop at the fuel nozzle³. Similarly, the fuel pump compresses the fuel from

¹ See Lloyd (1990) for a more detailed discussion of selection of input data for the steam reformer.

² For the calculations of this chapter, just one compressor and turbine are specified, regardless of whether the gas turbine is a heavy-duty or an aeroderivative machine. This is to avoid the added complexity of having to balance shafts and optimize intermediate pressures for multi-shaft machines. In the aeroderivative case, the higher turbine and compressor efficiencies typical of two-shaft machines are used. These and other input parameters were derived in a calibration process which assumed single-shaft aeroderivatives, and so representing two-shaft machines as single-shaft in this manner will not lead to a misrepresentation of aeroderivative performance.

the supply pressure (assumed to be 5bar) up to a pressure 50% greater than the overall pressure ratio. Appendix 6A test the sensitivity of cycle performance to evaporation pressure.

The calculations of this chapter assume that cycle components are optimally designed for the particular cycle conditions under consideration. For example, it is assumed that the gas turbine of a STIG is designed to accommodate all injection steam available from the HRSG. In practice this might not be the case if an existing "dry" turbine is to be modified for steam injection⁴. The assumption of optimal design is appropriate in evaluating the fundamental merits of different cycles, as this chapter aims to do. Section 6.4 considers how chemical recuperation might be applied with existing gas turbines.

6.2 EXAMPLE COMPARISON OF CRGT WITH STIG AND COMBINED CYCLES

6.2.1 Assumptions

This section presents a detailed comparison of STIG, CRGT and combined cycles based on a heavy-duty turbine with a TIT of 1250C and pressure ratio of 15. Sections 6.2.2 and 6.2.3 compare STIG and CRGT cycles, while Section 6.2.4 is concerned with how CRGT compares to combined cycles. The aim is to provide a detailed understanding of how chemical recuperation affects the cycle performance. While this example makes the comparison at only one set of operating conditions, many of the resulting qualitative observations can be generalized to other conditions.

A heavy-duty gas turbine was chosen because the high turbine outlet temperature (TOT) and low pressure ratio associated with such machines are favorable for a high degree of chemical recuperation (see Chapter Three). Hence one might expect that addition of chemical recuperation to a STIG cycle would affect heavy-duty machines more than aeroderivatives⁵. The TIT of 1250C and pressure ratio of 15 are typical of the latest generation of heavy-duty gas turbines. As this

³ This figure is representative of currently available STIG cycles. For example, at one LM5000 STIG plant in California, high pressure steam is produced at 765psi (approximately 50bar) for injection into the combustor at around 33bar (Kolp and Moeller, 1989).

⁴ Because of the expense of developing new gas turbines, manufacturers typically try to improve performance or meet new market opportunities by adapting existing models.

⁵ The calculations of Section 6.3 evaluate this intuitive claim.

thesis is concerned with chemically recuperated gas turbines for central power generation, the chosen air flow rate, at 400kg/s, is typical of the large heavy-duty gas turbines used by electric utilities.

Note that comparing different cycles at the same pressure ratio might not be strictly "fair" because different cycles generally optimize at different pressure ratios for a given TIT. The parametric analysis of Section 6.3 accounts for this by calculating a range of pressure ratios. For simplicity the example of this section uses the same pressure ratio of 15 for all three cycles.

In both the STIG and CRGT cycles, steam is produced with the maximum allowable degree of superheat. Appendix 6A shows that this maximizes efficiency, but that a lower degree of superheat can achieve a greater power output⁶. In the CRGT cycle, all steam from the HRSG is sent to the reformer. This leads to a large amount of chemical heat recovery and hence maximizes efficiency (see Appendix 6A).

6.2.2 Discussion of Results

Figure 6.2 shows the results of the STIG cycle calculation. A specific work of 596kJ/kg is obtained at 45.6% efficiency⁷. This compares to a simple cycle performance of 344kJ/kg at 35.2% for the same gas turbine operating at the same cycle parameters.

The CRGT cycle has a specific work of 507kJ/kg at 47.6% efficiency (Figure 6.3). The efficiency improvement over the STIG cycle of approximately two percentage points is accompanied by a decrease in power output of around 15%. The result that adding chemical recuperation increases efficiency but reduces power output was predicted in Chapter Two.

⁶ Because CRGT is a candidate for base-load power generation, it is assumed for this example that high efficiency is more important than higher power output. Section 6.3 discusses the trade-off between power and efficiency in more detail.

⁷ Throughout this analysis power output is quantified in terms of specific work. The specific work is equal to the power output divided by the mass flow rate of air entering the compressor. Use of specific work enables comparison between machines of different size. Unless stated otherwise, performances quoted are shaft values and do not account for generator losses.

Chapter Two discovered that the mass flow rate of steam in the cycle is an important factor determining performance. In this example the steam flow is $0.143\text{kg/kg}_{\text{air}}$ for the CRGT cycle compared to $0.217\text{kg/kg}_{\text{air}}$ for the STIG. It is the lower steam flow of the CRGT cycle that is responsible for the lower power output. The reduced steam flow is also related to the higher efficiency, since it is more efficient to recover heat chemically rather than by steam generation.

Note that the CRGT cycle has a higher stack temperature (140C) than the STIG cycle (108C). Both are higher than the stack temperature limit of 100C, indicating that in each case steam production is limited by the minimum allowable pinch-point temperature difference rather than by the minimum allowable stack temperature. In both cases the gas-side temperature at the economizer/evaporator interface in the HRSG is 228C, 10C greater than the evaporation temperature of 218C. Because the STIG cycle has a greater feedwater flow than the CRGT, it requires more exhaust heat for economizer heating, and so the stack temperature is lower. The CRGT cycle is more efficient than the STIG despite its higher stack temperature because the reduction in heat recovery losses resulting from the lower steam flow outweighs the effect of the increased stack temperature⁸.

In the CRGT cycle, the molar steam-to-fuel ratio in the reformer is around 6.0. The resulting fuel gas has the following composition (by volume): 8.1% methane, 0.4% carbon monoxide, 4.5% carbon dioxide, 19.0% hydrogen, and 68.0% steam. The lower heating value is 7.0MJ/kg (compared to 50MJ/kg for methane). This fuel gas has a stoichiometric adiabatic flame temperature of approximately 1950K⁹. The flame temperature of the STIG cycle depends on what

⁸ This is not believed to be a general result. Chapter Two suggested that for certain cycle conditions (for example very high pressure ratio), the penalty of increased exhaust losses associated with a higher stack temperature might outweigh the gain from improved heat recovery profiles. In this case the CRGT cycle would be less efficient than the STIG.

⁹ The problems associated with burning a low heating value gas are discussed in Chapter Four. The need to maintain stable combustion with acceptable carbon monoxide emissions will set a lower limit to the heating value of the fuel gas. This limit will depend on both the flame temperature and the composition of the fuel. Current understanding is not sufficient to enable prediction of the value of this limit. This analysis assumes that the fuel gas can always be burned in a suitably designed combustor.

The program calculates the stoichiometric adiabatic flame temperature of the fuel assuming complete combustion to carbon dioxide and steam without dissociation. The lowest flame temperature calculated for cycles analyzed in this Chapter is 1955K. Allowing for dissociation of the products of combustion, this corresponds to an actual flame temperature around 1900K. It is reasonable to assume that a fuel gas with this flame temperature can be burned in a suitably designed combustor.

proportion of the injection steam is injected into the primary zone of the combustor for NO_x control. Chapter Four observed that the maximum steam-to-fuel ratio (by weight), before flame-out or unacceptable carbon monoxide levels, is in the range 2-3, corresponding to flame temperatures of approximately 2150-2250K in this case. Assuming the presence of hydrogen in the CRGT fuel gas allows stable combustion (with acceptable carbon monoxide emissions) at 1950K, then the CRGT cycle will have lower NO_x emissions than the STIG cycle.

The required flow of compressor bleed-air is around 18% less in the CRGT cycle than in the STIG. This is related to the fact that the CRGT cycle has a lower mass flow in the turbine, leading to a smaller turbine and so less metal to be cooled.

6.2.3 Exergy Analysis

Table 6.2 shows a detailed entropy breakdown for the CRGT cycle as generated by the cycle calculation program. Two exergy analyses are performed. One (labelled "Wrev" in Table 6.2) assumes that the exergy of a fuel is the reversible work obtainable by bringing the system to thermo-mechanical equilibrium with the environment, while the other imposes chemical equilibrium also. The difference between the two arises because the exhaust stream has a different composition from the environment, and so work can be obtained by a reversible mixing process. If this work is considered irrecoverable by any practical device, then it makes sense to exclude it from the analysis¹⁰. This term is typically very small, and so the two analyses produce very similar results.

The exergy input to the cycle must equal the sum of the exergy loss in each component, the exergy of the exhaust stream, and the work obtained. The exergy loss of each component is further subdivided according to their source, such as pressure loss or irreversible heat transfer. Consonni (1990a and 1991) gives details of these terms for components other than the reformer.

¹⁰ Perfect gas mixing losses can be eliminated only by using ideal membranes which are transparent to one species and opaque to all others. However the mixing loss of a condensable vapor can be reduced by means of thermo-mechanical processes, and the reversible work of these is included in the thermo-mechanical exergy analysis. Hence the thermo-mechanical analysis identifies steam mixing losses, for example in steam-injected cycles.

See Consonni (1990a) for further details.

Table 6.2: Exergy Analysis for CRGT Cycle

The exergy analysis is for the example CRGT cycle based on a heavy-duty gas turbine at a TIT of 1250C and a pressure ratio of 15. Two analyses are presented: the thermo-mechanical analysis (labelled "Wrev") does not consider irreversible mixing as a loss, while the full analysis ("Exergy") does include this.

	Wrev (%)	Total	Exergy (%)	Total
TOTAL INPUT (kJ/kg₁)		1093.977		1122.226
Input flows				
Point 1 (inlet air)	.000	.000	.000	.000
Point 14 (feedwater)	.001	.001	.826	.826
Point 18 (fuel)	99.999	100.000	99.174	100.000
Inlet filter				
Pressure losses	.076	.076	.074	.074
Compressor				
Compression	2.156	2.233	2.102	2.176
Organic losses	.127	2.359	.124	2.300
Steam injector				
Pressure losses	.003	2.362	.003	2.303
H ₂ O mixing	.034	2.396	.033	2.336
Mixing	00.000	2.396	.003	2.339
Combustor				
Thermal losses	1.206	3.602	1.176	3.515
Pressure losses	.796	4.398	.776	4.291
Combustion	28.252	32.650	27.541	31.832
Mixing	00.000	32.650	-.622	31.210
Turbine				
Coolant compression	.194	32.844	.189	31.399
Throttling	.821	33.665	.801	32.199
Nozzle & cooled expansion	1.251	34.916	1.220	33.419
Heat transfer	.741	35.657	.722	34.141
Coolant discharge	1.962	37.618	1.912	36.053
Mixing	00.000	37.618	.112	36.165
Uncooled expansion	.501	38.119	.488	36.653
Diffuser	.755	38.874	.736	37.389
Organic losses	.326	39.200	.318	37.707
Fuel pump				
Compression	.109	39.310	.107	37.813
Organic losses	.003	39.312	.003	37.816
Reformer				
Pressure losses	.421	39.733	.410	38.226
Chemical reaction	-.490	39.243	-.478	37.749
Thermal losses	.187	39.430	.183	37.931
Mixing heat transfer	.160	39.590	.156	38.087
H ₂ O mixing	.827	40.417	.806	38.893
Mixing	00.000	40.417	.700	39.593
Real gas effects	-.031	40.387	-.030	39.563
Heat transfer	.382	40.768	.372	39.935
HRSG				
Gas-side pressure losses	.242	41.010	.236	40.171
Thermal losses	.439	41.449	.428	40.599
Pumps and water-side	Δp .005	41.454	.005	40.604
Deaerator heat transfer	1.046	42.587	1.020	41.709
1st level heat transfer	3.580	46.167	3.490	45.198
Output flows				
Point 10 (stack)	7.121	53.288	9.265	54.464
Point 12 (leakage air)	.339	53.627	.330	54.794
NET WORK	46.362	99.989	45.195	99.989

Appendix 5A explains how the reformer loss terms are calculated. The pressure loss term derives from frictional pressure drops, while the heat loss term reflects thermal losses to the environment. The heat transfer term measures exergy losses associated with irreversible heat transfer between the gas- and fuel-side flows. The losses labelled "mixing heat transfer", "H₂O mixing", and "real gas effects" arise when steam and methane mix at the reformer inlet, and reflect the fact that steam is a real rather ideal gas (for more details see Consonni, 1990a). The term labelled "mixing" shows the exergy loss owing to irreversible mixing of ideal gases. This is set to zero in the thermo-mechanical exergy analysis, which does not consider this to be a loss. The exergy loss due to chemical reaction is found by subtracting all the other loss terms from the total reformer loss¹¹.

Table 6.3 compares the exergy accounts for the STIG and CRGT cycles¹². Here, the exergy input is about 23% greater for the STIG than for the CRGT. This follows from the 23% greater fuel flow of the STIG. The table shows exergy values in kJ/kg of compressor inlet air, and as a percentage of the total exergy input. Expressing exergies as percentages of the input exergy allows comparison of cycles with different fuel-to-air ratios. For example, while the compressor exergy loss in kJ/kg of air is about the same for the two cycles, the loss as a fraction of input exergy is greater for the CRGT.

The largest exergy loss in each cycle occurs in the combustor. For the STIG cycle, the loss associated with steam injection is shown separately from the combustion loss. There is no separate steam injection in the CRGT, but losses associated with the injection of the large mass flow of fuel gas are embedded in the combustion loss. The sum of steam injection and combustion losses is 32.0% for the STIG and 30.3% for the CRGT. Both cycles involve mixing of

¹¹ Note that the chemical reaction loss is negative here, and this seems to violate the Second Law of Thermodynamics. Appendix 5A identified this possibility, which arises because chemical reaction losses are not physically separable from mixing losses. The mixing loss term is actually the loss owing to change of composition. It is calculated from the compositions (in terms of mole fractions of component gases) of the fuel-side flows entering and leaving the reformer, and thus reflects change of composition owing to the chemical reaction as well as to mixing. One way of interpreting the negative chemical reaction loss is to imagine that the reaction only proceeds if the entropy increase associated with the change of composition outweighs the entropy decreases of the chemical reaction.

A future paper (Consonni and Lloyd, 1991) will address this point in greater detail.

¹² From hereon, only the thermo-mechanical exergy analysis is presented. For clarity, only the total loss is shown for each component.

and chemical reaction between methane, steam, and air. In the STIG these processes occur wholly in the combustor, but in the CRGT some mixing and chemical change occurs in the recuperator and so the combustor loss is reduced.

Table 6.3: Exergy Analysis Comparing STIG, CRGT, and Combined Cycles

All cycles for a heavy-duty gas turbine, turbine inlet temperature = 1250C, pressure ratio = 15.
All exergies in kJ/kg of inlet air.

	(kJ/kg)	STIG (%)	(kJ/kg)	CRGT (%)	Combined cycle (kJ/kg)	(%)
TOTAL EXERGY INPUT	1343	100.0	1094	100.0	1002	100.0
EXERGY LOSSES						
Inlet filter	1	0.1	1	0.1	1	0.1
Compressor	24	1.8	25	2.3	26	2.6
Fuel pump	1	0.1	1	0.1	1	0.1
Steam injector	64	4.8				
Combustor	366	27.2	331	30.3	293	29.3
Turbine	87	6.4	70	6.4	54	5.4
Reformer			16	1.5		
HRSG	101	7.5	59	5.4	50	5.0
Steam turbine					24	2.4
Condenser					33	3.2
Output flows	104	7.7	82	7.5	37	3.7
WORK	596	44.4	507	46.4	484	48.2
WORK+LOSSES	1344	100.0	1092	100.0	1003	100.0

This must be set against a 1.5% exergy loss in the recuperator of the CRGT. Of this, chemical reaction and mixing losses account for approximately 0.5%, irreversible heat transfer from the exhaust gases to the fuel-side flow for 0.4%, pressure loss for 0.4%, and heat loss to the environment for 0.2%.

The HRSG loss, due mainly to irreversible heat transfer, is 5.4% for the CRGT cycle. The 6.9% total of recuperator and HRSG loss is less than the 7.5% HRSG loss of the STIG cycle, even though the CRGT value includes some chemical losses as well as heat transfer and other losses. This is because addition of chemical recuperation to the cycle allows a better match of exhaust-side and cold-side temperature profiles, as discussed in Chapter Two. Figure 6.4 shows these profiles for the two cycles. Exergy loss due to irreversible heat transfer alone in the HRSG and reformer is 5.0% for the CRGT compared to 6.6% for the STIG.

The exergy lost up the stack is slightly greater for the STIG than for the CRGT. The effect of the lower steam content of the CRGT exhaust is offset to a large extent by the higher air-to-fuel ratio and higher stack temperature.

When all losses are summed, 44.4% of the exergy input to the STIG cycle remains as useful work. For the CRGT, this exergetic efficiency is 46.4%. The difference between the two is in line with the difference between the LHV efficiencies of 45.6% for the STIG and 47.6% for the CRGT¹³. Notice that this difference, at about 2.0%, is similar to the difference in HRSG/reformer heat transfer losses of the two cycles. Hence a simple (but incomplete) explanation for the greater efficiency of the CRGT is that addition of chemical recuperation reduces the irreversibilities associated with heat recovery from the gas turbine exhaust.

6.2.4 Comparison of CRGT and Combined Cycles

It is instructive to extend the example to a combined cycle at the same turbine inlet temperature and pressure ratio. Figure 6.5 shows the cycle. A single evaporation boiler produces steam which drives a separate steam turbine before condensing and returning to the boiler as feedwater. The evaporation pressure is 60 bar, which is around the optimum value at the gas turbine outlet temperature of about 570C. The condensing temperature is 42C, typical of an installation using wet cooling towers¹⁴. The steam turbine is assumed to have a polytropic efficiency of 80%¹⁵.

The calculated performance is 484kg/kg_{air} at 49.6% efficiency. This compares to 507kJ/kg_{air} at 47.6% efficiency for the CRGT cycle. The combined cycle is more efficient than the CRGT despite a 16C higher stack temperature. Once again an exergy analysis provides insight into the relative merits of the two cycles (Table 6.3). The combined cycle's major advantage is that there are none of the mixing losses associated with adding steam to the gas cycle (either directly in a

¹³ The LHV and "exergetic" efficiencies are not the same only because they are defined differently. The LHV efficiency is the work divided by the fuel lower heating value, while the exergetic efficiency is the work divided by the fuel exergy.

¹⁴ A lower condensing temperature can be used if the power plant is sited next to the sea or a river. In this example, reducing the condensing temperature from 42C to 30C leads to an efficiency increase of almost one percentage point.

¹⁵ Steam turbine efficiency is strongly size-dependent. Steam turbines used in large combined cycle plants for base-load power generation typically have power ratings of the order of 50MW. 80% is a suitable polytropic efficiency for turbines of this size.

STIG or indirectly in a CRGT). Other pluses are a reduced stack loss (despite a higher stack temperature) owing to the absence of large quantities of steam in the exhaust, and a reduced turbine loss because of the lower total and coolant flows. The loss due to heat transfer irreversibilities during heat recovery is 4.2% for the combined cycle compared to 5.0% for the CRGT. These advantages of the combined cycle must be set against the losses associated with the steam turbine and condenser.

When all of these factors are combined, the combined cycle turns out to be more efficient than the CRGT in this example. While it is dangerous to claim this as a general result, insights from the exergy analysis indicate that the combined cycle is likely to be generally the more efficient. Combined cycles are more efficient than STIG cycles because they do not suffer from the mixing loss associated with injecting steam into the gas cycle. Addition of chemical recuperation to a STIG cycle to form a CRGT cycle leads to an efficiency improvement owing to reduced heat recovery irreversibilities, but the mixing loss is still present. In this example the CRGT heat recovery losses are still greater than those of the combined cycle. This is because in a combined cycle the steam cycle is uncoupled from the gas cycle, and so the evaporation pressure can be chosen to achieve a good heat recovery profile. The heat recovery profiles of both CRGT and combined cycles can generally be manipulated to reduce heat transfer irreversibilities by adjustment of pressure levels and degree of steam superheat and reheat¹⁶. When both cycles have good heat recovery profiles, the CRGT cycle will still have the mixing loss from steam injection. Hence the combined cycle is likely to be the more efficient.

6.3 PARAMETRIC ANALYSIS

This section presents a parametric analysis in which turbine inlet temperature (TIT) and overall pressure ratio are varied for heavy-duty and aeroderivative gas turbines. The aim is investigate how the overall cycle performance changes with these parameters and with the type of gas turbine. By finding the optimal pressure ratio at a given TIT, fair comparison can be made between CRGT and STIG cycles.

¹⁶ For example, combined cycles with two or three pressure levels and steam reheat can be over 50% efficient. Chapter Seven compares multi-evaporation CRGT cycles are compared to multi-evaporation combined cycles.

In selecting cycle parameters for a gas turbine, the TIT is usually set as high as possible without leading to cooling flows so high as to penalize performance. The TIT chosen depends on the current state-of-the-art in blade metallurgy and cooling technology. Once the TIT is selected, the cycle pressure ratio is chosen to achieve the desired combination of high power output and high efficiency. Because power output and efficiency generally optimize at different pressure ratios, the value chosen is a compromise depending on whether the machine is intended primarily for peaking or base-load applications. As seen in Section 4.8, low capital cost and therefore high power output are relatively important for peaking plants, while low fuel costs and therefore high efficiency assume a greater importance for base-load plants.

6.3.1 Heavy-duty Gas Turbine

Figure 6.6 shows the variation of specific work and efficiency with pressure ratio for STIG and CRGT cycles at various TITs. As for a simple cycle, specific work generally optimizes at a lower pressure ratio for a given TIT than does efficiency.

These optima result from changing thermodynamic trade-offs as pressure ratio changes. A high pressure ratio leads to a high turbine work output but at the expense of increased compressor work. At the same time the cooling-air bled from the compressor is hot, and so a large quantity is needed, tending to reduce the turbine work. At low pressure ratio the turbine outlet temperature is high, leading to a large amount of total steam production and, in a CRGT cycle, chemical heat recovery. A high steam production favors a high power output, but efficiency is penalized owing to high HRSG losses. As described in Chapter Two, addition of chemical recuperation redresses this by sacrificing some power for an improvement in efficiency.

Figure 6.7 shows how various cycle variables change with pressure ratio for the heavy-duty CRGT cycle at a TIT of 1250C. The amount of chemical heat recovery can be gauged by the fraction of the initial methane flow that is converted to products in the reformer. As pressure ratio increases, the turbine outlet temperature and hence the reforming temperature decrease. A higher reforming pressure is required as the combustor pressure is higher. The lower TOT and higher evaporation pressure act to reduce total steam production and hence the steam-to-fuel

ratio in the reformer. These three factors all act to reduce the extent of the steam reforming reaction, and the result is that the methane conversion declines rapidly with increasing pressure ratio. At a TIT of 1250C, methane conversion falls from 69% at a pressure ratio of 10 to 9% at a pressure ratio of 30.

A high TIT leads to high TOT, methane conversion, and total steam production, and hence a high efficiency and specific work. The maximum efficiency at a TIT of 1250C is 48%, two percentage points greater than the maximum efficiency at a TIT of 1100C. However at very high temperatures, the cooling air demand becomes prohibitive. As described above, the optimal turbine inlet temperature is determined by the current state-of-the-art of cooling technology and blade metallurgy. The curves of Figure 6.6 suggest that the optimum is currently in the region of 1250C, and that there are no real gains in going to 1400C¹⁷. Of course improved blade materials or cooling methods will raise the optimum TIT.

As well as CRGT cycle performances, Figure 6.6 also shows performance for STIG cycles at TITs of 1100C and 1250C¹⁸. STIG and CRGT cycles have significantly different performances at low pressure ratio, but these performances converge with increasing pressure ratio. This is because the amount of chemical heat recovery possible decreases as the TOT decreases. The CRGT cycle produces less work at a given pressure ratio than the STIG cycle but generally at greater efficiency, in line with the predictions of Chapter Two. At very high pressure ratios the efficiency advantage of CRGT over STIG is small and might even be negative (for example compare the 1100C curves at a pressure ratio of 30). Chapter Two identified this outcome also.

Efficiency optimizes at a lower pressure ratio (around 17) for the CRGT than for the STIG (around 22), because chemical recuperation is favored by a high TOT and low reforming pressure. The latest generation of heavy-duty gas turbines has TITs close to 1250C. At this temperature, the optimized efficiency for the CRGT cycle is around 47.9%, while that for the STIG is about 47.3%. This gain of around half a percentage point is achieved at the expense of a specific work penalty

¹⁷ This result is in line with the latest generation of gas turbines. For example, the General Electric Frame 7F has a TIT of 1260C.

¹⁸ At 1400C, STIG cycle steam production is very high, particularly at low pressure ratios. Below a pressure ratio of around 20, if all available steam is injected into the combustor then the oxygen concentration falls below the stoichiometric quantity required for a TIT of 1400C.

of approximately 5%. The difference between optimized CRGT cycle efficiency and optimized STIG cycle efficiency increases with TIT.

6.3.2 Aeroderivative Gas Turbine

The parametric trends for a typical aeroderivative gas turbine (Figure 6.8) are very similar to those for a heavy-duty turbine. This is unsurprising as both types share many of the same input parameters. The major differences between the two are that the aeroderivative case assumes a higher large-size compressor efficiency than the heavy-duty¹⁹, a smaller air flow, and a higher film cooling parameter (with film cooling of all cooled stages rather than just the first stage nozzle). The first two differences tend to offset each other. The improved cooling becomes important at high TITs, so at 1400C the aeroderivative cycles out-perform the heavy-duty cycles.

As for the heavy-duty gas turbine, the optimized CRGT efficiency at a TIT of 1250C is around 48%, about half a percentage point greater than the STIG efficiency.

6.4 DISCUSSION

6.4.1 Review of Results

This chapter is primarily concerned with comparing the simplest CRGT and STIG configurations to develop a detailed understanding of the effect of chemical recuperation on performance. In the example of Section 6.2, a heavy-duty CRGT cycle at a TIT of 1250C and a pressure ratio of 15 was found to be two percentage points more efficient than a STIG cycle at the same conditions. This efficiency gain is obtained at the expense of a reduction in specific work. The parametric analysis of Section 6.3 found that the superior efficiency but reduced work of a CRGT cycle compared to a STIG is a general result, except that the STIG cycle might be the more efficient at very high pressure ratios. These findings are as predicted by the analysis of Chapter Two. At turbine inlet temperatures typical of modern gas turbines (around 1250C), the CRGT cycle has a

¹⁹ The "large-size" efficiency is the asymptotic value to which turbomachinery efficiency approaches as machine size increases. Compressor and turbine efficiencies decrease with decreasing machine size because wall losses in the blade passages become relatively more important.

maximum efficiency (at the optimal pressure ratio) of approximately 48%, around half a percentage point greater than the maximum STIG cycle efficiency.

The CRGT cycle in the example of Section 6.2 was found to be less efficient than a single-evaporation combined cycle based on the same gas turbine.

6.4.2 Practical Considerations

The analysis of this chapter assumes "rubber turbines", that is turbines optimally designed for the cycle in question. This is appropriate for evaluation of the potential of thermodynamic cycles. In practice CRGT cycles are likely to be realized by modifying existing gas turbines in order to avoid excessive development costs. This section considers how this restriction affects the attractiveness of chemical recuperation.

The latest generation of heavy-duty gas turbines operates at TITs around 1250C and pressure ratios of about 14. Figure 6.6 suggests that at these conditions, a CRGT cycle will be about 47% efficient, compared to 45% for a STIG. However, both of these values assume the gas turbine can accommodate the increased mass flow in the turbine of a STIG or CRGT cycle compared to a simple cycle. In practice there is a limit to the extra mass flow, above which there is a danger of unstable compressor operation such as surge or stall. This limit can be relaxed to some extent by modifications such as increasing the flow area of the first stage turbine nozzle, but a point will be reached at which further modification is not economically justifiable.

The effect of a turbine mass flow restriction on STIG and CRGT cycle performance can be observed by returning to the example of Section 6.2 and limiting steam injection to $0.05\text{kg}/\text{kg}_{\text{air}}$ ²⁰. In the STIG cycle, this amount of steam is injected directly into the combustor, while in the CRGT cycle it goes to the reformer and enters the combustor indirectly in the form of fuel gas.

²⁰ This value is broadly representative of current gas turbines. The absolute value is not important in the analysis that follows. What is important is the fact that not all of the steam available from the HRSG can be injected into the gas turbine.

Table 6.4 compares the performance of these restricted cycles to the unrestricted cycles of Section 6.2. The former are far less efficient than the latter because only a small fraction of exhaust heat is recovered when steam production is limited. The limit on mass flow in the gas turbine leads to a reduced power output also.

Table 6.4: Comparison of Restricted and Unrestricted STIG and CRGT Cycles

	Unrestricted		Restricted	
	STIG	CRGT	STIG	CRGT
Specific work (kJ/kg _{air})	596	507	399	393
LHV efficiency (%)	45.6	47.6	37.9	40.2
Steam production (kg/kg _{air})	.217	.143	.050	.050
Stack temperature (°C)	108	140	439	384
Methane conversion (%)	n/a	37.3	n/a	18.0

All cycles are based on a heavy-duty gas turbine at a turbine inlet temperature of 1250°C and a pressure ratio of 15. In the restricted cases, a limit on the acceptable mass flow in the turbine constrains steam production to .05kg/kg of inlet air.

The restricted CRGT cycle is 2.3 percentage points more efficient than the restricted STIG, while the power outputs are approximately the same. This is in contrast to the unrestricted comparison where adding chemical recuperation improved efficiency by two percentage points at the expense of a 5% reduction in power output. The power outputs are the same for the two restricted cycles because they have the same mass flow in the gas turbine. Addition of chemical recuperation does not change steam production but simply enables additional steam recovery above that achieved by steam production. Hence the restricted CRGT has a lower stack temperature than the restricted STIG, and the efficiency advantage is greater than in the unrestricted comparison. This is despite the fact that the low steam production leads to a low steam-to-fuel ratio in the reformer, resulting in a methane conversion of only 18%.

Similar arguments apply to aeroderivative gas turbines. Currently available large aeroderivatives have pressure ratios in the range 25-30 and TITs around 1200°C. Figure 6.8 suggests that at these conditions an unrestricted CRGT cycle will be barely (if at all) more efficient than an unrestricted STIG and will have an inferior power output. However if turbine mass flow is restricted, then the efficiency advantage of CRGT will be larger and there will be no reduced power penalty.

Hence it appears that the advantages of adding chemical recuperation to a STIG cycle are more favorable with existing gas turbines than with "rubber turbines". However the above analysis is misleading in that it neglects other opportunities for heat recovery. Further exhaust heat recovery could be achieved by production of additional steam for injection further down the gas turbine or for use in a separate steam turbine. Addition of chemical recuperation would then reduce the opportunity for this extra steam production, and so the advantage of the restricted CRGT cycle over the restricted STIG will not be as large as indicated in Table 6.4.

6.4.3 Technological Improvement

The analysis so far has been based around the latest generation of gas turbines, currently being commercialized. This section considers whether future technological improvements to gas turbines are likely to make CRGT cycles more or less attractive.

The major trend in gas turbine history has been a steady increase in turbine inlet temperature (TIT), brought about by advances in high-temperature materials and in cooling technology. This trend is likely to continue with the introduction of single-crystal blades and eventually ceramic blades. Cycle pressure ratios also will continue to increase, as the optimal pressure ratio is higher at higher TIT.

Turbine outlet temperature (TOT) has been shown to be an important factor influencing the performance of CRGT cycles. TOT determines both the reforming temperature and the amount of steam available for reforming. A high TOT leads to a high methane conversion, and hence a large efficiency advantage of a CRGT cycle over a STIG cycle. While the trend of increasing TIT points towards higher TOT, this will be offset by the parallel trend of increasing pressure ratio which tends to reduce TOT. A higher pressure ratio also necessitates a higher reforming pressure, whereas chemical recuperation is favored by low pressure. Because these effects act in opposite directions, the net result is that continued technological improvement of gas turbines is unlikely to affect greatly the attractiveness of CRGT cycles compared to other cycles²¹.

²¹ This argument does not address the possibility of step changes in gas turbine technology such as the introduction of reheat gas turbines or steam cooling. Chapter Seven considers major cycle modifications such as these.

6.4.4 Prospects for CRGT Cycles

The analysis of this chapter has shown that the simplest CRGT cycle configuration is generally more efficient than a STIG cycle at the same TIT, but has a lower power output. If the cycle is intended for base-load electricity generation, then high efficiency is important and the CRGT cycle would probably be economically more attractive than the STIG. This is particularly true for the large heavy-duty gas turbines used by electricity utilities, because the high TOTs of these machines encourage a large amount of chemical heat recovery.

The main competitor of CRGT for base-load applications is not the STIG cycle but the combined cycle. Currently available combined cycles have achieved efficiencies as high as 52%. Compared to this, a 48% efficient CRGT cycle does not appear so attractive. However such comparisons should be made on a fair basis. The 52% efficient combined cycle uses multi-pressure evaporation and/or steam reheat to minimize heat transfers losses in the HRSG, but the 48% efficient CRGT cycle has only a single-pressure HRSG. In the example of Section 6.2, which compared single-evaporation CRGT and combined cycles, the combined cycle came out ahead in efficiency by approximately two percentage points.

The comparison of most use in evaluating CRGT is between the most efficient combined cycles and the best possible CRGT cycles. This is the comparison which utilities will make. The most efficient combined cycles use multi-pressure evaporation and/or steam reheat as described above. The possibility of using such modifications to improve CRGT efficiency also is explored in Chapter Seven.

REFERENCES

S Consonni, 1990a, Entropy Analysis of Mixed Gas/Steam Cycles, Politecnico di Milano, July 1990

S Consonni, 1990b, personal communication, September 1990

S Consonni, Performance Prediction of Gas-Steam Cycles for Power Generation, PhD thesis, Princeton University Department of Mechanical and Aerospace Engineering (Center for Energy and Environmental Studies), due June 1991

S Consonni and A Lloyd, Chemically Recuperated Gas Turbine Cycles, to be submitted for the ASME COGEN-TURBO V conference to be held in Budapest, Hungary, September 1991

D A Kolp and D J Moeller, "World's First Full STIG LM5000 Installed at Simpson Paper Company", ASME Journal of Engineering for Gas Turbines and Power, April 1989

A J Lloyd, User's Manual for CRGT Computer Program for Calculation of Chemically Recuperated Gas Turbine Cycles, CEES Working Paper No 116, Princeton University Center for Energy and Environmental Studies, November 1990

R G Minet and O Olesen, "Technical and Economic Advances in Steam Reforming of Hydrocarbons", in W N Smith and J G Santangelo, editors, Hydrogen: Production and Marketing, American Chemical Society, 1980

APPENDIX 6A

This Appendix investigates the validity of some of the assumptions made for the calculations of this chapter.

6A.1 Optimization of Steam Flows

The parametric analysis of Section 6.3 compares the performances of STIG and CRGT cycles for different generic gas turbine types at various TITs and pressure ratios. For fair comparison with other cycles, each case must be optimized at those conditions. In STIG cycles the variable to be optimized is the mass flow rate of steam. In CRGT cycles an additional variable requiring optimization is the fraction of total steam used in the reformer. This section investigates how these steam flows optimize for two particular cases, and discusses whether the results are general. The examples chosen are a heavy-duty gas turbine with a pressure ratio of 15 and an aeroderivative with a pressure ratio of 35. Both have a turbine inlet temperature of 1250C.

In this chapter an "optimal" cycle performance is considered to be one where efficiency is maximized. As explained in Section 6.3, the optimal performance of practical cycles will depend on economic trade-offs between power output and efficiency.

STIG Cycle

The variable determining the total steam production is the degree of superheat chosen. It is assumed that for a given degree of superheat as much steam is generated as is possible using

the gas turbine exhaust heat. Generally, increasing the superheat decreases the available mass flow of steam. The total steam production is usually limited by the condition that the pinch-point temperature difference is above a specified minimum, but in some cases the limiting factor might be the condition that the stack temperature is above a specified value. The degree of superheat is limited either by the condition that the steam in the HRSG should not exceed a certain temperature, set by metallurgical considerations, or by the constraint that the exiting steam temperature must be below the incoming gas temperature by a specified margin (the hot-end approach). The values of these limits used in this analysis were a 10C pinch-point, a 100C stack temperature, a 550C maximum steam temperature, and a 20C hot-end approach.

Figure 6.9 shows the effect of degree of superheat on specific work and efficiency of a STIG cycle. Efficiency increases while specific work decreases as the amount of superheat increases from zero to the point at which steam leaves the superheater at its upper temperature limit.

For the heavy-duty turbine, STIG cycle efficiency increases from 42.0% with saturated steam to over 45.6% with steam superheated by 332C. At this point the steam temperature is at the limiting value of 550C. Specific work diminishes over the same range by about a quarter as a result of a reduced steam flow in the turbine. The mass of steam which can be produced using the gas turbine exhaust decreases from 0.35kg/kg_{air} at zero superheat to 0.22kg/kg_{air} at maximum superheat.

This trend is in line with the argument of Chapter Two that for a given stack temperature a lower steam production results in a higher cycle efficiency, because alternative methods of heat recovery generally have lower losses associated with them. Here, the "alternative" method of heat recovery is to superheat further existing steam rather than produce more saturated steam.

Stack temperature is constant at its lower limit of 100C for low superheat. Beyond around 200C superheat, the pinch point is the factor limiting steam production, and stack temperature rises slightly to 108C at maximum superheat. In this regime, a lower feedwater mass flow at the same evaporation pressure and temperature results in a lower economizer heating load and hence a higher stack gas temperature. In this example, the reduced steam flow effect outweighs this, and so the efficiency continues to rise.

The 35-pressure-ratio aeroderivative case shows similar trends. The higher pressure ratio leads to a low turbine outlet temperature (around 450C, compared to around 600C for a pressure ratio of 15). The amount of steam available is reduced, so the specific work is lower. Steam production is 0.15kg/kg_{air} at zero superheat and 0.10kg/kg_{air} at maximum superheat. Steam temperature at maximum superheat is restricted to 426C by the turbine outlet temperature of 446C. This and the fact that a high evaporation pressure is needed to enable steam injection into the combustor lead to a maximum superheat of only 210C.

Notice that a change in degree of superheat from zero to 100C results in a lower efficiency increase for the aeroderivative STIG than for the heavy-duty STIG (Figure 6.9). This is related to the high stack temperature associated with the aeroderivative cycle (stack temperature is 162C at zero superheat and 190C at maximum superheat). The high stack temperature results from the high evaporation pressure and the low steam production, which is limited by the pinch-point. At this high stack temperature, the efficiency penalty associated with increasing degree of superheat and hence raising stack temperature further is significant, and acts to offset the gain from reduced HRSG losses. In certain rare circumstances, for example at very high pressure ratios, this effect could lead to maximum efficiency at zero superheat. Chapter Two identified this possibility, pointing out that such cycles are likely to be far from optimal anyway and of little practical interest. Hence the assumption that STIG cycle efficiency is always greatest at maximum superheat will not distort the conclusions drawn from this chapter.

In summary, the message from this analysis is that STIG cycle efficiency is generally maximized when the steam is superheated as much as possible. This is consistent with the desire to recover heat from the exhaust using as little steam as possible. However, this is achieved only at the expense of a power output significantly lower than that obtainable with saturated steam. Maximum superheat is always used in the calculations of this chapter.

CRGT Cycle

The amount of steam sent to the reformer is varied by varying the molar steam-to-fuel ratio, n . Chapter Three introduced this variable, showing to be an important factor influencing the extent of

the recuperation reaction. Figure 6.9 shows the effect of varying n on CRGT cycle performance for the two sample cases. The steam-to-methane ratio increases from one to the point where all the steam goes to the reformer - this occurs at n equal to 5.9 for the heavy-duty gas turbine and 4.4 for the aeroderivative²².

The key trend is that efficiency increases with steam-to-fuel ratio while specific work decreases. In the heavy-duty case, efficiency improves by approximately 1.3 percentage points from n equal to one to maximum n , while specific work falls by approximately 10% over this range. The reason for this is that as n increases, so too does the amount of heat recovered chemically, as was shown in Chapter Three. As chemical heat recovery increases, total steam production decreases while maintaining approximately the same stack temperature. Steam production and stack temperature are 0.184kg/kg_{air} and 122C respectively at n equal to one, and 0.143kg/kg_{air} and 140C at maximum n . As predicted in Chapter Two, the result is a gain in efficiency but a loss in power output.

The amount of chemical heat recovery depends on the equilibrium position of the steam reforming reaction. This is strongly influenced by the steam-to-fuel ratio, ranging from a methane conversion of 12% at n equal one to 37% at maximum n . Less than half of the methane reacts even when all available steam is sent to the reformer, owing to the relatively low reforming temperature of around 570C. At the maximum value of n , the lower heating value of the resulting fuel gas is 7MJ/kg, less than a seventh of the heating value of methane.

A striking feature of the aeroderivative CRGT curve is that performance hardly changes with steam-to-fuel ratio. The low TOT associated with the high pressure ratio aeroderivative also leads to a low reformer temperature of around 430C. The extent of the reforming reaction is strongly dependent on temperature, and at this low temperature only a small fraction of the methane is converted (7% at maximum n). Consequently the gain in efficiency from recuperating is small for the aeroderivative. Compared to the STIG cycle there is no gain at all - the efficiency gain from recuperating is outweighed by the efficiency penalty associated with the higher stack temperature resulting from a lower total steam production. At maximum n , steam production is 0.088kg/kg_{air}

²² n must be at least one to avoid soot formation in the reformer.

and stack temperature is 202C. The possibility that CRGT cycles might be less efficient than STIG cycles was identified in Chapter Two.

In optimizing the steam-to-fuel ratio, it has been assumed that, because the STIG cycle optimizes when the steam is fully superheated (and hence total steam production is low), then a CRGT cycle optimizes in the same way. In fact, for an optimal steam-to-fuel ratio, where all the steam from the HRSG goes through the reformer, the degree of superheat is virtually irrelevant. In these circumstances all of the steam is being further heated in the reformer. Specifying the degree of superheat is merely equivalent to specifying the location in the heat recovery steam reformer where the fuel is added and the reaction begins. Exploratory calculations suggest that because the fuel gas conditions at the reformer outlet are unaffected by this, the effect on the overall cycle performance is negligible.

The conclusion from this analysis is that at a given pressure level, the efficiency of a CRGT cycle is maximized when all steam produced in the boiler is used in the reformer. However, a CRGT cycle might be less efficient than a STIG cycle at high pressure ratios, in which case the optimal cycle is one in which no steam (or fuel) is sent to the reformer - namely the STIG cycle. In the calculations of this chapter, it is assumed that the optimal steam-to-fuel ratio for a CRGT cycle is that which results in all steam being routed through the reformer. Section 6.3 compares the performance of CRGT and STIG cycles over a range of cycle parameters.

6A.2 Sensitivity to Evaporation Pressure

For the calculations of this chapter, the boiler evaporation pressure is assumed to be 50% greater than the overall pressure ratio, to allow for pressure losses in the superheater and reformer and for the required pressure drop at the fuel nozzle. Similarly, the fuel pump compresses the fuel from the supply pressure up to a pressure 50% greater than the overall pressure ratio.

The sensitivity of CRGT cycle performance to evaporation pressure was investigated by running one particular case at evaporation pressures of 30%, 50%, and 70% greater than the cycle pressure ratio. The case chosen was a heavy-duty gas turbine CRGT cycle at a TIT of 1250C and pressure ratio of 15. Efficiency varied by approximately half a percentage point from 47.4% at

30% to 47.9% at 70%, while the change in specific work over this range was negligible. The efficiency gain at lower evaporation pressure follows mainly from increased chemical heat recovery at the resulting lower reforming pressure.

It might be possible to use a lower evaporation pressure than 50% greater than the combustor pressure, particularly if suitable design improvements are made to the superheater and combustor. This would lead to a small but not insignificant efficiency gain. The 50% assumption reflects typical current practice and is applied to all calculations in this chapter.

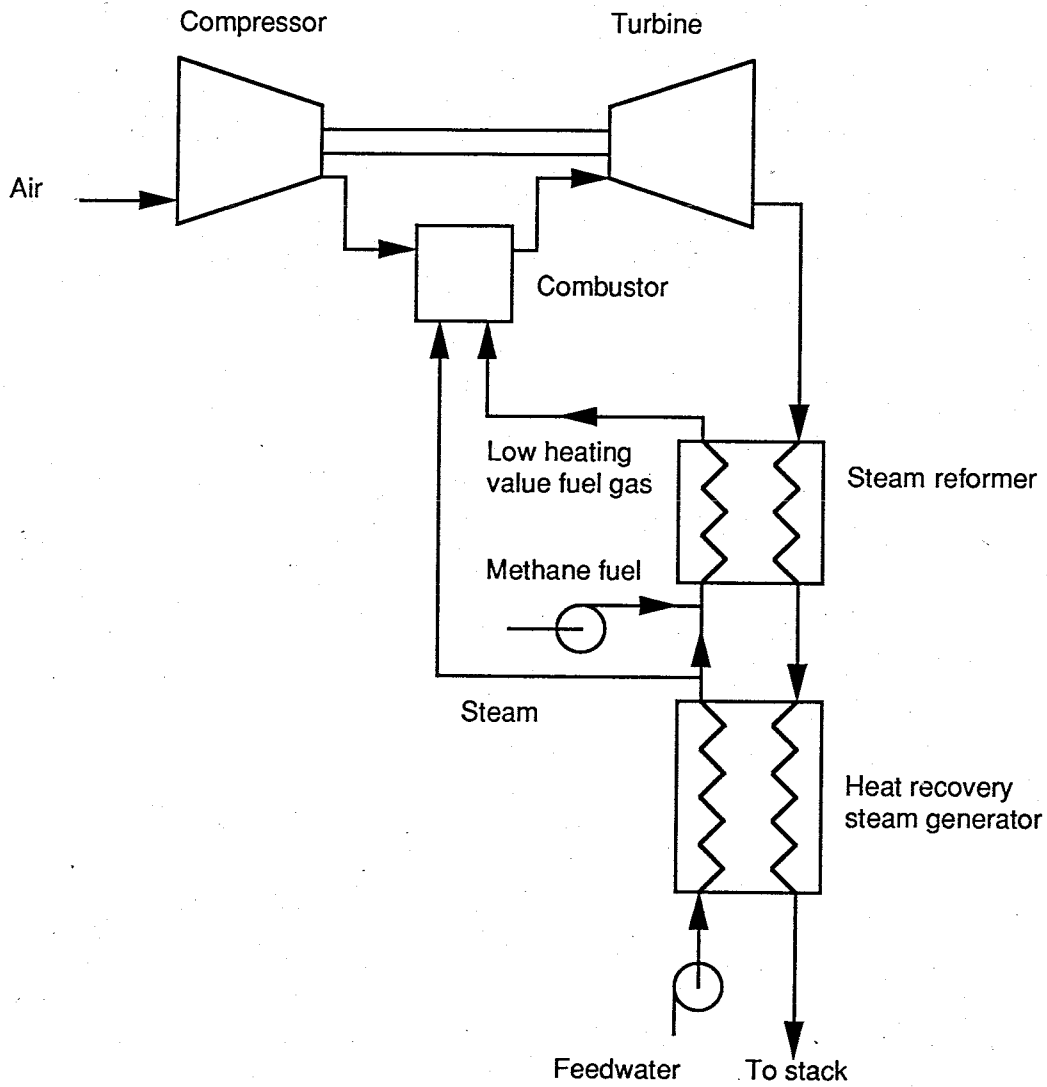


Figure 6.1: Chemically Recuperated Gas Turbine Cycle

Some or all of the superheated steam exiting the HRSG mixes with methane fuel and sent to the reformer, while the rest is injected directly into the gas turbine combustor. The reformer contains a catalyst which facilitates a reaction between steam and methane resulting in a low heating value fuel gas containing methane, carbon monoxide, carbon dioxide, hydrogen, and steam.

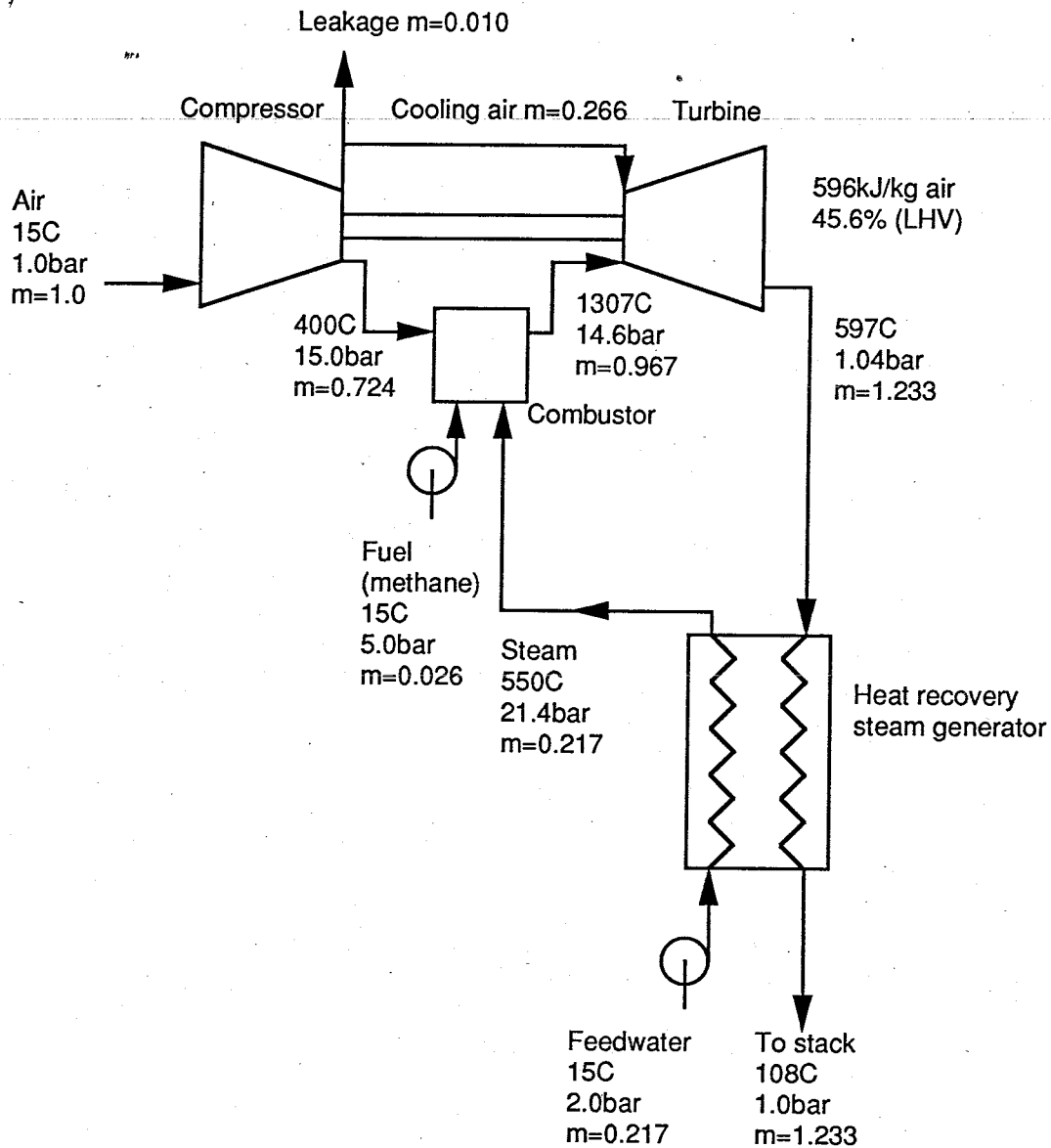


Figure 6.2: Flow Diagram for STIG Cycle Calculation

The cycle is based on a heavy-duty gas turbine operating at a turbine inlet temperature of 1250°C and a pressure ratio of 15. Efficiency and specific work are shaft values.

Note that TIT is the temperature entering the first stage rotor of the turbine. Because there is a temperature drop across the first stage stator, the combustor exit temperature is higher than the TIT.

For simplicity, the diagram shows all bleed-air extracted at the compressor exit. In fact, it is extracted at various points along the compressor, as described in Consonni (1991).

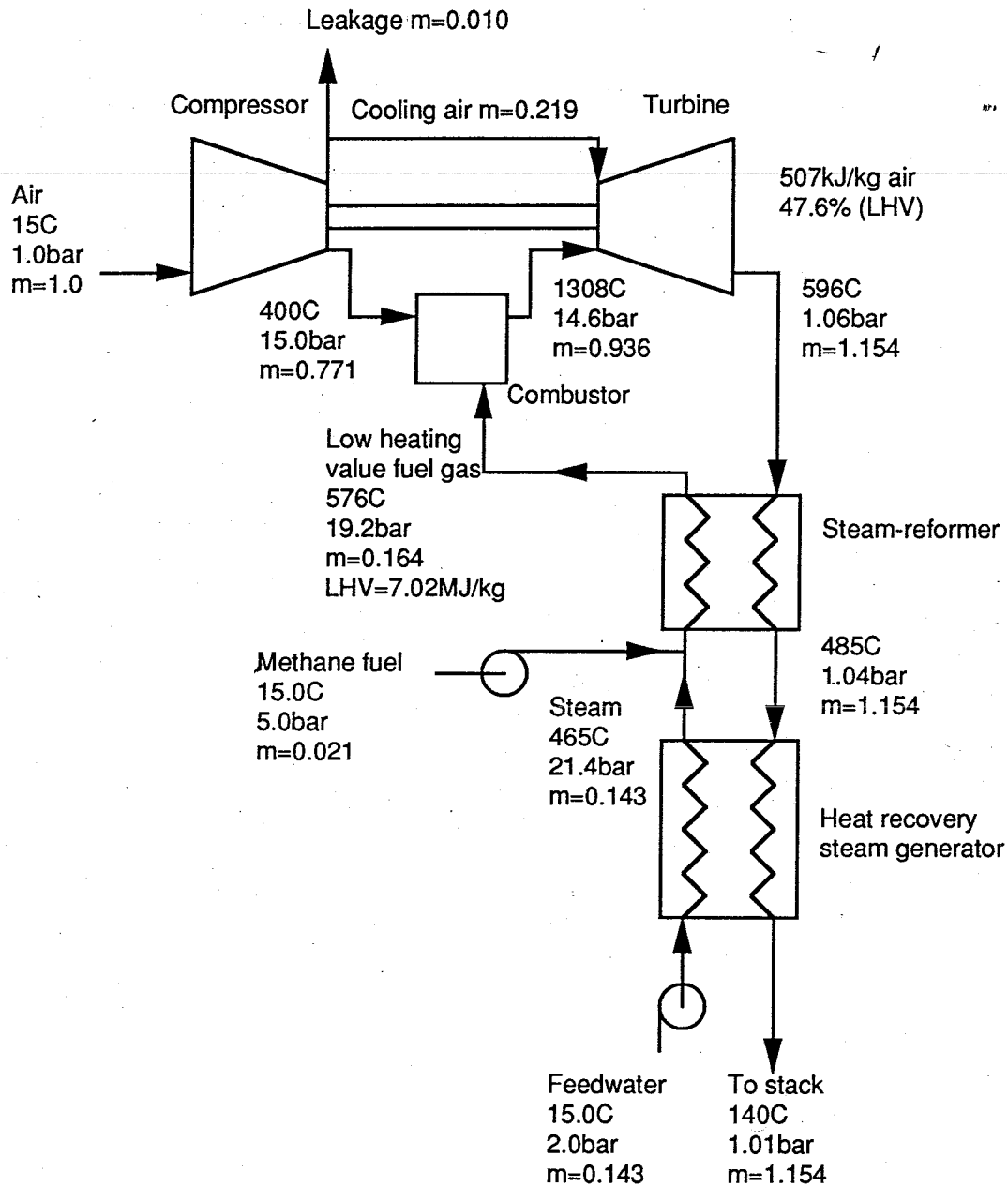


Figure 6.3: Flow Diagram for CRGT Cycle Calculation

The cycle is based on a heavy-duty gas turbine operating at a turbine inlet temperature of 1250°C and a pressure ratio of 15. Efficiency and specific work are shaft values.

The molar steam-to-methane ratio entering the reformer is 6.0. The resulting fuel gas has the following composition (by volume): 8.1% methane, 0.4% carbon monoxide, 4.5% carbon dioxide, 19.0% hydrogen, and 68.0% steam.

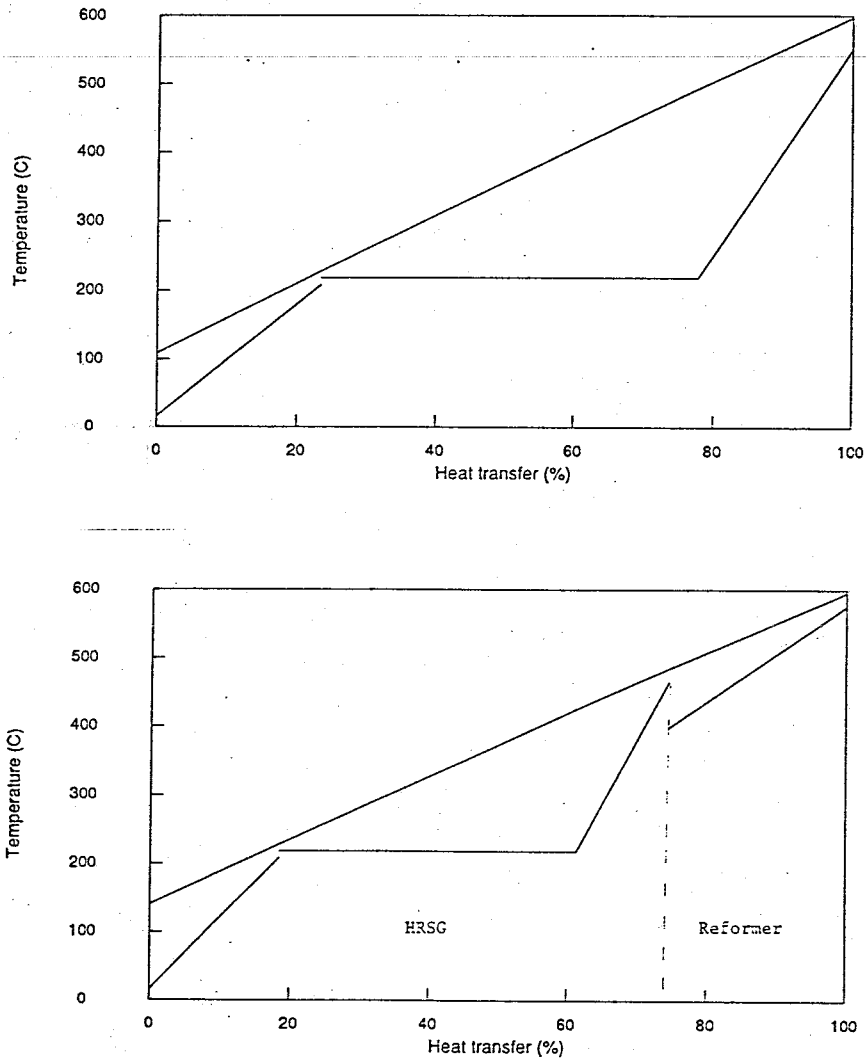


Figure 6.4: Heat Recovery Profiles for STIG and CRGT Cycles

Both cycles are based on a heavy-duty gas turbine operating at a turbine inlet temperature of 1250C and a pressure ratio of 15.

The area between the two profiles is a measure of the exergy loss owing to irreversible heat transfer. This area is large for the STIG cycle (top) because evaporation occurs at constant temperature. In the CRGT cycle (bottom), part of the exhaust heat is recovered chemically in the reformer, so the HRSG generates less steam and heat transfer irreversibilities are reduced.

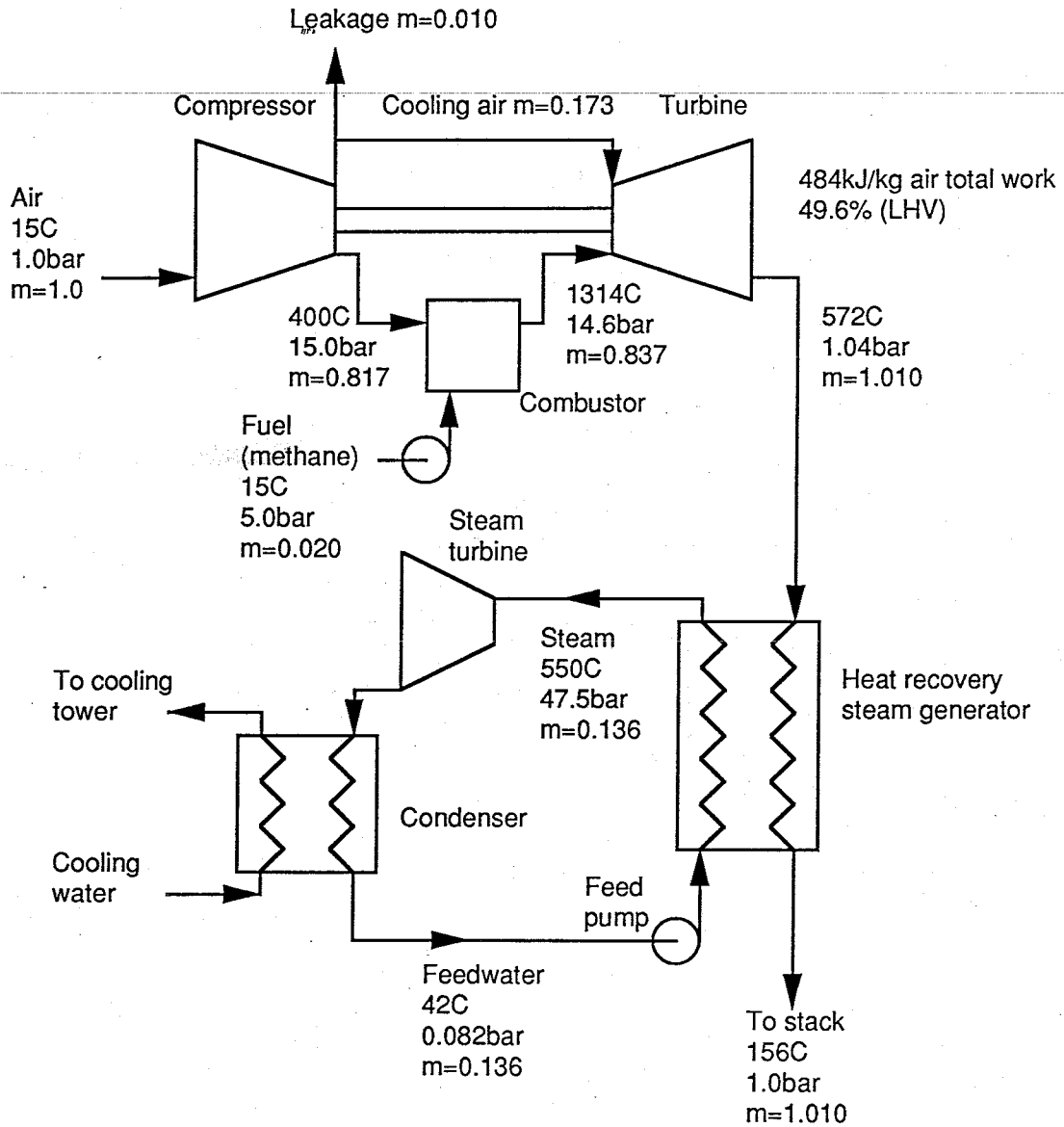


Figure 6.5: Flow Diagram for Combined Cycle Calculation

The cycle is based on a heavy-duty gas turbine operating at a turbine inlet temperature of 1250°C and a pressure ratio of 15. HRSG evaporation pressure is 60 bar and condenser pressure is 0.082 bar, corresponding to a 42°C condensing temperature. Efficiency and specific work are shaft values.

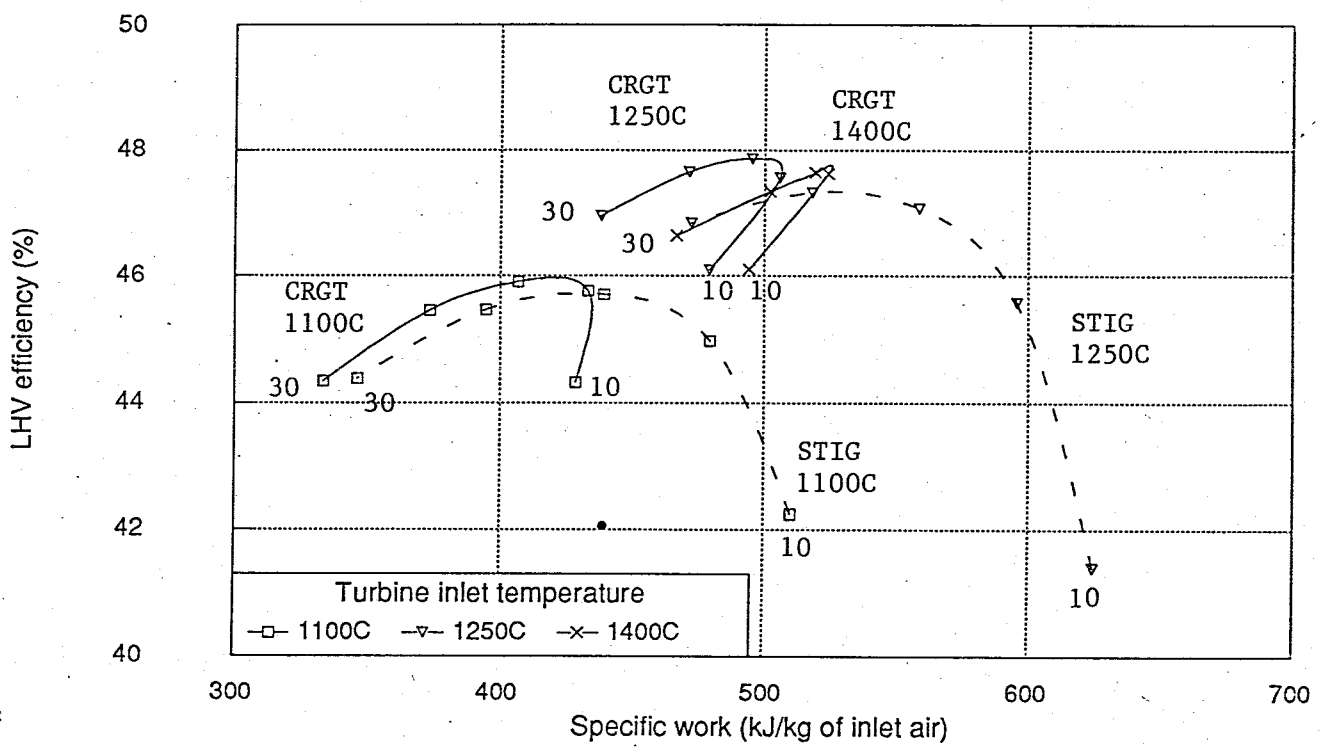


Figure 6.6: Heavy-Duty Gas Turbine CRGT and STIG Cycles

The solid lines are CRGT cycles, while the dotted lines are STIG cycles. Data points are shown at pressure ratios of 10, 15, 20, 25, and 30.

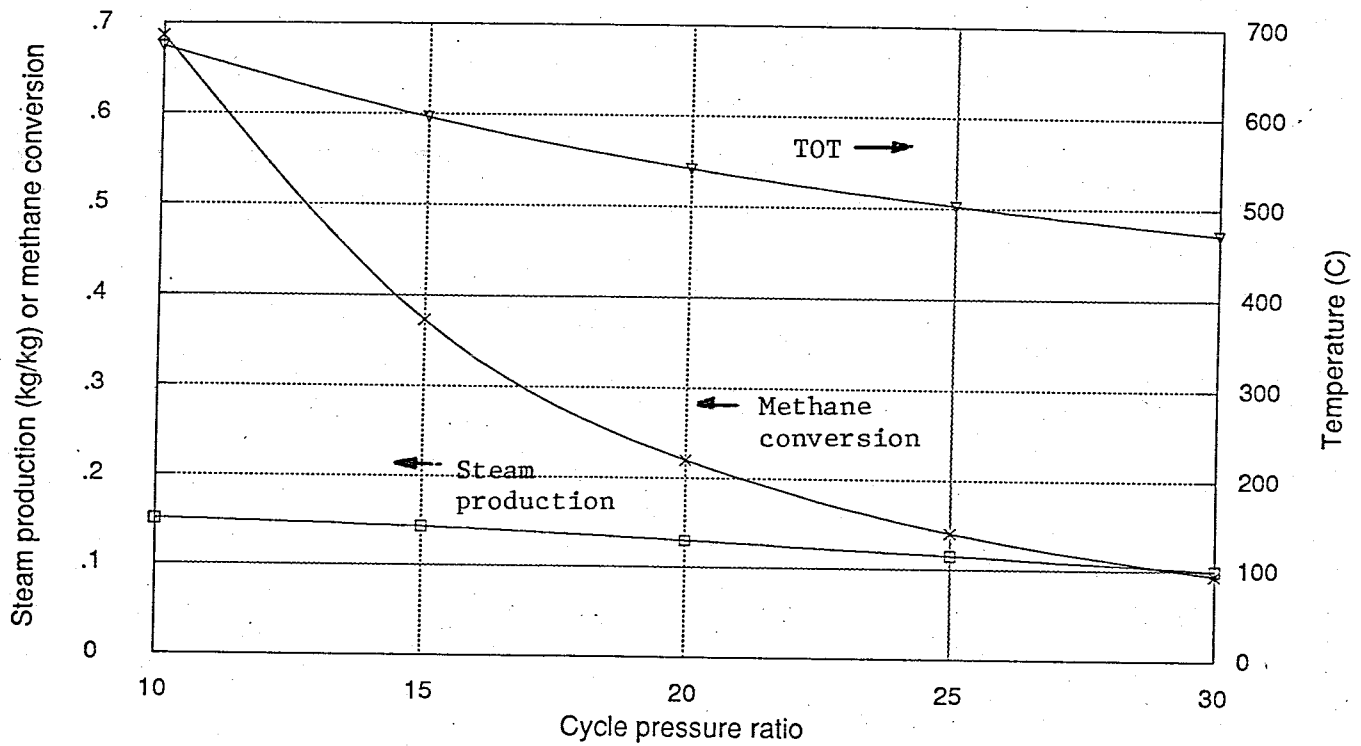


Figure 6.7: Variation of Selected CRGT Cycle Properties

Data are for a heavy-duty CRGT cycle at a TIT of 1250C. The left-hand axis measures both steam productions (in kg per kg of compressor inlet air) and methane conversion in the steam reforming reaction (as a fraction of the methane entering the reformer). TOT is the turbine outlet temperature.

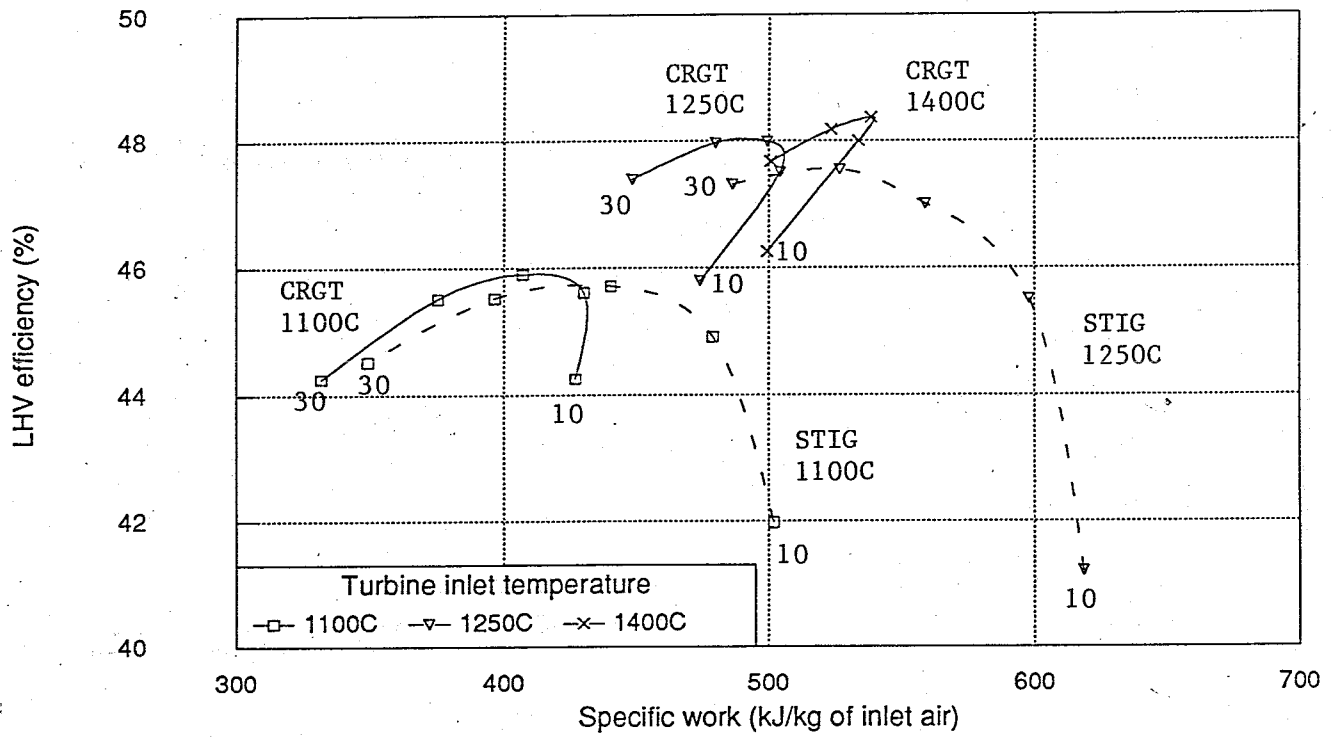


Figure 6.8: Aeroderivative Gas Turbine CRGT and STIG Cycles

The solid lines are CRGT cycles, while the dotted lines are STIG cycles. Data points are shown at pressure ratios of 10, 15, 20, 25, and 30.

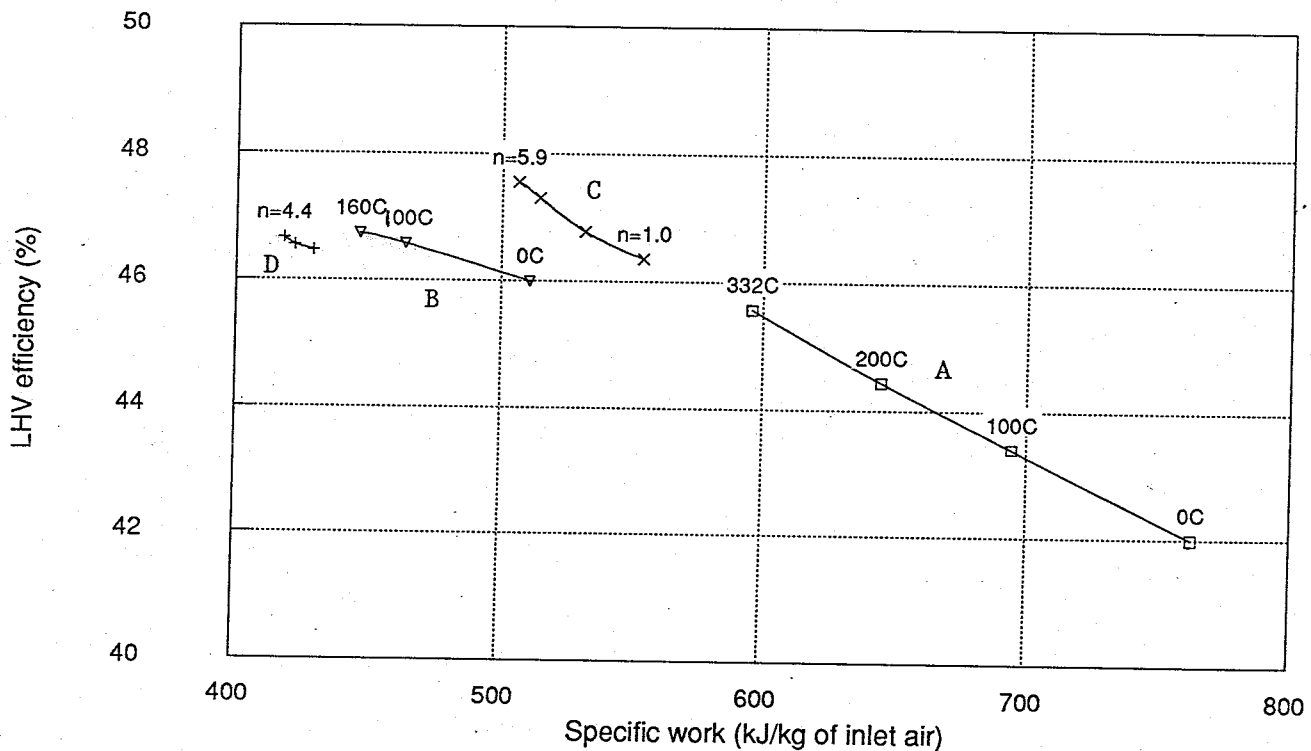


Figure 6.9: Optimization of Steam Flows in STIG and CRGT Cycles

Curve A shows the effect of degree of superheat on a heavy-duty STIG cycle at a TIT of 1250C and a pressure ratio of 15. Efficiency is maximized when the degree of superheat is as much as possible. In this case the maximum superheat is 332C, corresponding to the 550C maximum steam temperature. Steam production is 0.35kg per kg of compressor inlet air for saturated steam and 0.22kg/kg at maximum superheat.

Curve B is the same curve for an aeroderivative STIG cycle at 1250C TIT and a pressure ratio of 35. Steam production is 0.15kg/kg for saturated steam and 0.10kg/kg at maximum superheat.

Curves C and D show the effect of steam-to-fuel ratio on CRGT cycle performance. C assumes the same cycle conditions as A above, while D corresponds to B. The molar steam-to-methane ratio (n) in the reformer varies from 1.0 to the maximum possible, at which point all steam available from the HRSG travels to the reformer. At lower n , steam not used in the reformer is injected directly into the gas turbine combustor.

CHAPTER SEVEN: ADVANCED CRGT CYCLES

7.1 Introduction

7.2 CRGT with Back Pressure Steam Turbine

7.3 CRGT with Supplementary Firing

7.4 CRGT with Intercooling and Reheat

7.5 Review

References

Figures

7.1 INTRODUCTION

The simple CRGT configuration of Chapter Six can be modified in many ways. This chapter investigates three modifications which aim to improve performance in some way. Section 7.2 considers whether the use of a multi-pressure level HRSG and back pressure steam turbine can make the CRGT cycle competitive with a multi-evaporation combined cycle, Section 7.3 explores supplementary firing, and Section 7.4 evaluates a CRGT cycle with intercooling and reheat.

The complexity of these cycles means that a rigorous optimization procedure and parametric analysis are not practical. Instead each cycle is analyzed at just one turbine inlet temperature (TIT) and pressure ratio. A heavy-duty gas turbine at a TIT of 1250C and a pressure ratio of 15 was chosen for Sections 7.2 and 7.3. 1250C is typical of the latest generation of gas turbines, and at this TIT both CRGT cycles and combined cycles optimize at a pressure ratio close to 15.

The intercooled reheat CRGT cycle considered in Section 7.4 is very similar to that proposed by Jack Janes of the California Energy Commission. The Janes concept involves the addition of reheat to the intercooled LM8000 General Electric aeroderivative gas turbine. The calculations presented here use the same cycle parameters as the Janes cycle, and results are compared with published estimates for that cycle.

7.2 CRGT WITH BACK PRESSURE STEAM TURBINE

If chemically recuperated gas turbines are to be used for base-load power generation they must be able to compete with combined cycles, the current utility choice. Section 6.2 compared a single-evaporation CRGT cycle with a single-evaporation combined cycle. Both cycles were based on a heavy-duty gas turbine at a TIT of 1250C and a pressure ratio of 15. The combined cycle was 49.6% efficient, compared to 47.6% for the CRGT cycle¹. Practical combined cycles use multi-pressure evaporation and steam reheat to reduce heat transfer irreversibilities in the HRSG and hence boost efficiency to over 50%. This section explores whether similar techniques can be applied to a CRGT cycle, and whether such an improved cycle will be more efficient than a multi-evaporation combined cycle. This is the comparison of most interest to utilities. Again the example case chosen is the heavy-duty gas turbine at a TIT of 1250C and a pressure ratio of 15.

7.2.1 Multi-Evaporation Combined Cycle

Figure 7.1 shows a combined cycle with two evaporation pressure levels and one level of steam reheat. This configuration is typical of the most efficient combined cycles available today. Extra efficiency could be obtained by adding another evaporation or reheat level, but the efficiency increment is not usually large enough to justify the extra cost. High pressure (HP) steam at 150bar and 550C expands through a steam turbine to 10bar, whereupon it returns to the HRSG for reheating. Steam produced in the 10bar drum is added, and the resulting low pressure (LP) steam flow is heated to 550C and returned to the steam turbine. The HP evaporation pressure of 150bar is typical of modern combined cycles. The efficiency gain of going to a higher pressure rarely justifies the extra cost of improved drum materials required at the higher evaporation temperature. The LP evaporation pressure of 10bar is around the optimal value for maximum efficiency². The HRSG economizer, evaporator, and superheater sections are arranged in order of decreasing temperature from the hot-end to minimize heat transfer losses.

¹ The combined cycle assumed a condensing temperature of 42C, appropriate for a plant equipped with wet cooling tower. A lower condensing temperature can be used if the power plant is sited next to the sea or a river. In this example, reducing the condensing temperature from 42C to 30C leads to an efficiency increase of approximately one percentage point.

² The value of 10bar was arrived at by "trial and error" calculations rather than by a rigorous optimization procedure. However, it is believed that the error in cycle efficiency resulting from using a not-quite-optimal figure is less than 0.1 percentage points.

The condensing temperature is 42C, typical of a plant equipped with wet cooling towers. The steam turbine is assumed to have a polytropic efficiency of 80%³. The gas turbine and HRSG input parameters are the same as assumed in Chapter Six for a heavy-duty gas turbine (see Table 6.1).

The calculated performance is 507kJ/kg_{air} at 52.0% efficiency. The gas turbine generates approximately two thirds of the total power output, and the steam turbine one third. Exergy loss due to irreversible heat transfer in the HRSG is 2.8% of total exergy input compared to 4.2% for the single-evaporation cycle of Section 6.2. Stack temperature is 123C for the multi-evaporation cycle compared to 156C for the single-evaporation case. The improved efficiency of the multi-evaporation cycle is a consequence both of a better match of HRSG temperature profiles and of heat recovery down to a lower stack temperature.

7.2.2 CRGT with Back Pressure Steam Turbine

Figure 7.2 shows a CRGT cycle in which high pressure steam produces work in a steam turbine before proceeding to the reformer for fuel reforming. Besides producing extra work, addition of the steam turbine allows a better match of heat recovery profiles in the HRSG. HP steam is produced at 150bar and superheated to 550C, and expands to 22.5bar in the steam turbine. It then mixes with LP steam from the 22.5bar drum and is reheated to 550C before entering the reformer. The LP evaporation pressure of 22.5bar is set by the requirement to be 50% greater than the gas turbine combustor pressure. Other input parameters are the same as for the combined cycle, except that the steam turbine polytropic efficiency is assumed to be only 70% because of its small size (around 10MW).

The calculated performance is 516kJ/kg at 49.1% efficiency. This efficiency is better than the 47.6% of the single-evaporation CRGT cycle of Section 6.2, but is significantly inferior to the 52.0% of the multi-evaporation combined cycle. One reason for this is that the CRGT cycle has a

³ Steam turbine efficiency is strongly size-dependent. Steam turbines used in large combined cycle plants for base-load power generation typically have power ratings of the order of 50MW. 80% is a suitable polytropic efficiency for turbines of this size.

higher LP evaporation pressure than the combined cycle and consequently is unable to recover heat down to as low a temperature. The CRGT cycle has a stack temperature of 146C compared to 123C for the combined cycle. One solution to this problem would be to add another evaporation level at 5bar and use this low pressure steam in a separate steam cycle. However the resulting efficiency is still only 50.2%, and there is also the extra cost of adding an extra boiler level, a low pressure steam turbine, and a condenser. A cheaper alternative is to inject the 5bar steam into the gas turbine, but then the efficiency is even lower at 49.7%.

Once again exergy analysis provides valuable insights. First consider the heat recovery profiles of the two cycles (Figure 7.3). Both cycles have well matched hot- and cold-side temperature profiles compared to the single evaporation cycles of Section 6.2 (see Figure 6.4). This is reflected in low heat recovery heat transfer losses of 2.8% for the combined cycle and 3.1% for the CRGT cycle⁴. Addition of more pressure levels could further reduce these losses if economically justifiable. The essential point is that for both cycles the heat recovery profiles can be suitably designed to achieve low heat transfer losses, and that the CRGT cycle has no inherent advantage.

Table 7.1 shows the exergy loss breakdowns for the multi-evaporation CRGT and combined cycles. The combined cycle has a very low stack loss compared to the CRGT, arising both from the absence of large amounts of steam in the exhaust⁵ and from the low stack temperature⁶. However the extra exergy losses associated with the condenser and steam turbine tend to cancel this advantage. The combined cycle has a lower combustor loss than the CRGT and avoids the loss associated with mixing and chemical reaction in the reformer. This loss source, associated with injecting steam into the gas cycle, is that which accounts for a combined cycle's superior

⁴ Neither cycle has the best theoretically possible heat recovery profile, in which the cold-side temperature always increases towards the hot-end. In the CRGT cycle, addition of cold methane to superheated LP steam causes a drop in temperature. In both cases all LP superheater tubes are placed at the cold-end side of all HP economizer tubes. Such arrangements are more convenient in practice than inter-dispersing the various heating sections to achieve the best possible profile.

⁵ There will of course be some steam originating from humidity of the inlet air and as a product of combustion.

⁶ It was seen above that adding a third evaporation level to the CRGT to match the stack temperature of the combined cycle closes the efficiency gap by only around one percentage point.

efficiency compared to a STIG cycle. Adding chemical recuperation to a STIG cycle to form a CRGT cycle merely transfers some of this loss to the reformer. Hence a combined cycle has a superior efficiency to a CRGT cycle also.

Table 7.1: Exergy Analysis Comparing Multi-Evaporation CRGT and Combined Cycles

Both cycles for a heavy-duty gas turbine, turbine inlet temperature = 1250C, pressure ratio = 15. Both have two pressure level HRSGs with steam reheat. The CRGT cycle incorporates a back pressure steam turbine.
All exergies in kJ/kg of inlet air

	(kJ/kg)	CRGT (%)	Combined cycle (kJ/kg)	Combined cycle (%)
TOTAL INPUT EXERGY	1080	100.0	1002	100.0
EXERGY LOSSES				
Inlet filter	1	0.1	1	0.1
Compressor	25	2.3	26	2.6
Fuel pump	1	0.1	1	0.1
Combustor	326	30.2	293	29.3
Turbine	71	6.6	54	5.4
Reformer	15	1.4		
HRSG	39	3.6	37	3.7
Steam turbine	6	0.5	23	2.2
Condenser			34	3.4
Output flows	79	7.3	26	2.6
WORK	516	47.8	507	50.6
WORK+LOSSES	1079	99.9	1002	100.0

The net result is that the combined cycle is about three percentage points more efficient than the CRGT cycle with a back pressure steam turbine. This is a large difference in base-load power generation applications, where small changes in efficiency can have a big impact on the cost of electricity. Addition of a third evaporation level could improve the CRGT efficiency, but the combined cycle could also be improved in this way. Remember also that the combined cycle calculation assumed a conservative condensing temperature of 42C, and that a lower temperature (and hence higher efficiency) would be possible if the plant were situated next to a river or the sea. While neither cycle in this example was rigorously optimized for maximum efficiency, it is believed that both are close to optimum. The size of the difference in efficiency is such that optimizing the two cycles will have little effect on the overall conclusion.

This conclusion is that a multi-evaporation CRGT cycle is not as efficient as a multi-evaporation combined cycle, as the CRGT is always burdened with the mixing loss associated with injecting steam into the gas cycle.

7.3 CRGT WITH SUPPLEMENTARY FIRING

Chapter Three showed that the extent of the chemical recuperation reaction is strongly influenced by the temperature at which it occurs. In a CRGT cycle this temperature is determined by the temperature of the exhaust gas flow entering the steam reformer. Modern heavy-duty gas turbines typically have a turbine outlet temperature (TOT) in the range 500-600C, and this leads to a methane conversion of less than 40% in a CRGT cycle. For aeroderivatives this figure is even lower, as the higher pressure ratio of aeroderivatives leads to a lower TOT. One way of improving the methane conversion, and hence the amount of chemical heat recovery, is to add supplementary firing (duct burning) between the turbine outlet and the reformer inlet in order to raise the temperature of the exhaust gases. This section investigates how supplementary firing affects cycle performance, particularly whether it increases or reduces efficiency.

Again the example case chosen is a heavy-duty gas turbine at a TIT of 1250C and a pressure ratio of 15. The supplementary firing temperature is initially set to 800C. This temperature was chosen because methane conversion is almost complete (close to 100%) at this temperature, so going to a higher temperature will not increase the amount of chemical heat recovery. The cycle calculation is then repeated for a supplementary firing temperature of 700C.

Figure 7.4 shows the cycle. In this configuration only the fuel for the main combustor is reformed, while the supplementary firer uses unreformed methane (a cycle in which both fuel flows undergo steam reforming is presented below). In order to minimize heat transfer losses the HRSG has two pressure levels with reheat as in the previous section. High pressure steam at 150bar expands to 22.5bar in a steam turbine and is reheated along with additional steam produced in the 22.5bar steam drum before proceeding to the reformer. A polytropic efficiency of 70% is assumed for the steam turbine.

The calculated cycle performance is a specific work of $580\text{kJ/kg}_{\text{air}}$ at 47.3% efficiency. This compares with $516\text{kJ/kg}_{\text{air}}$ at 49.1% for the cycle without supplementary firing (the "unfired cycle") calculated in the previous section. Addition of supplementary firing has resulted in a 12% work increase but at the expense of an efficiency reduction of 1.8 percentage points. Methane conversion is 95.8%, indicating a large amount of chemical heat recovery. This is a consequence of supplementary firing of the exhaust flow, both directly via the increased reforming temperature, and also indirectly because the higher HRSG gas-side inlet temperature enables a greater steam production and hence a higher steam-to-fuel ratio in the reformer⁷. Total steam production at $0.180\text{kg/kg}_{\text{air}}$ is higher than the $0.132\text{kg/kg}_{\text{air}}$ of the unfired cycle.

Table 7.2 shows the exergy breakdown for the cycle and compares this to that of the unfired cycle. The most noticeable feature of the analysis for the supplementary fired cycle is that the combustor losses are divided between the main combustor and supplementary firer. However the total combustor loss is about the same in the two cases. When comparing the two cycles it is helpful to note that the supplementary fired cycle has a lower air-to-fuel ratio but a higher steam-to-fuel ratio than the unfired cycle. Hence compressor and turbine losses are lower (as a percentage of input fuel exergy) for the supplementary fired case, but steam turbine losses are higher. The HRSG and recuperator losses are higher with supplementary firing as more heat must be recovered from the exhaust to reach a low stack temperature. These extra heat recovery losses include direct losses associated with irreversible heat exchange and indirect losses such as increased loss due to superheater pressure drops because of the increased steam flow. When all these various pluses and minuses are added, the supplementary fired cycle comes out 1.8 percentage points less efficient than the unfired cycle. A simplified explanation for the inferior efficiency is that supplementary firing leads to increased heat recovery losses because a greater total heat recovery from the exhaust flow is required.

⁷ The stoichiometric adiabatic flame temperature for the fuel gas is approximately 1900K. This is only slightly lower than the 1950K or so for the unfired case because the dilution effect of the higher steam-to-fuel ratio (9.0 here compared to 5.6 in the unfired cycle) is offset by the higher hydrogen concentration in the resulting fuel gas (pure hydrogen has a relatively high flame temperature).

Table 7.2: Exergy Analysis Comparing CRGT Cycles With and Without Supplementary Firing

Both cycles for a heavy-duty gas turbine, turbine inlet temperature = 1250C, pressure ratio = 15. Both have a two pressure level HRSG with steam reheat and a back pressure steam turbine.

All exergies in kJ/kg of inlet air

Totals might not add to exactly 100% because of rounding errors.

	(kJ/kg)	Unfired (%)	(kJ/kg)	Supp fired (%)
TOTAL INPUT EXERGY	1080	100.0	1259	100.0
EXERGY LOSSES				
Inlet filter	1	0.1	1	0.1
Compressor	25	2.3	25	2.0
Fuel pump	1	0.1	1	0.1
Combustor	326	30.2	278	22.1
Turbine	71	6.6	76	6.1
Supplementary firer			114	9.1
Reformer	15	1.4	27	2.1
HRSG	39	3.6	55	4.4
Steam turbine	6	0.5	9	0.7
Output flows	79	7.3	89	7.1
WORK	516	47.8	580	46.0
WORK+LOSSES	1079	99.9	1255	99.8

To test the generality of this result, the calculation was repeated for a different supplementary firing temperature. The temperature chosen was 700C, which is intermediate between the 800C used above and the 600C of an unfired cycle. The predicted performance is 535kJ/kg_{air} at 48.1% efficiency, and this is also intermediate between the other two cases. This suggests that efficiency decreases monotonically with supplementary firing temperature and that the most efficient cycle will always be the unfired one. This is consistent with the observation that there is no gain from going to higher and higher supplementary firing temperatures because there is an upper limit (of 100% methane conversion) to the amount of chemical heat recovery.

The calculations presented so far are for a cycle in which only the fuel for the main combustor is steam-reformed, while unreformed methane fuels the supplementary firer. This configuration was chosen for simplicity, but the possibility of reforming the supplementary fuel also should be considered as a means of further increasing chemical heat recovery⁸. Figure 7.5 shows a cycle

⁸ If one of the motivations for choosing a CRGT cycle is its low NO_x emissions, then it might be necessary to reform the supplementary fuel to prevent high levels of NO_x formation in the supplementary firer. However the flame temperature in the supplementary firer for unreformed methane might be lower than that in the main combustor even if reformed fuel is used in the main combustor. This follows from the lower firing temperature in the supplementary

which does this. The reformer comprises two fuel-side flows in parallel. A third steam drum provides 2bar steam for the low pressure reformer. The optimal distribution of steam flows is to produce as much as possible high pressure (HP) steam rather than restrict HP steam production to enable more LP steam production. While more LP steam would allow a higher methane conversion in the LP reformer, a reduction in HP steam leads to not only a lower conversion in the HP reformer but also a reduction in power output of both the steam and gas turbines.

The calculated performance for this cycle at a supplementary firing temperature of 800C is 531kJ/kg_{air} at 47.7% efficiency. The efficiency improvement of 0.4 percentage points resulting from adding reforming of the supplementary fuel must be set against the added cost of the two-pressure reformer and the extra pressure level in the HRSG. This efficiency is still below the 49.1% of the unfired cycle.

The fact that addition of supplementary firing reduces efficiency is a well-known result for STIG and combined cycles, so it is not surprising that the same is true of CRGT cycles. While the elevated TOT of a CRGT cycle with supplementary firing does lead to a large amount of chemical heat recovery, this must be set against the extra heat added to the exhaust gases in the supplementary firer. Chapter Two argued that supplementary firing will lead to an efficiency gain only if the increase in chemical heat recovery outweighs the heat added by the supplementary fuel and so allows lower steam production while maintaining the same stack temperature. In the example calculations presented here this was not the case. The fact that there is an upper limit to the amount of methane conversion suggests that this is a general result.

Supplementary firing is a means of improving power output of a cycle because the extra steam produced can perform work either in the gas turbine or in a separate steam turbine. Alternatively supplementary firing might be used in a cogeneration application to boost process heat output. However supplementary firing makes little sense in a base-load power generation application where the objective is to maximize efficiency. A CRGT cycle is more efficient (but has a lower specific work) than a STIG cycle because the addition of chemical recuperation allows a reduced

firer, and from the depleted oxygen content of the incoming gas flow. In the cycle of Figure 7.4, the flame temperature is almost identical in the main combustor and in the supplementary firer at around 1900K. (It is assumed here that combustors can be designed to operate at this low temperature.)

steam flow, but adding supplementary firing simply reverses this effect. Hence if high power output is the object then an unfired or supplementary fired STIG cycle is preferable to a CRGT with supplementary firing. The only situation where a CRGT cycle with supplementary firing might be considered is one requiring both high power output and very low NO_x emissions.

7.4 CRGT WITH INTERCOOLING AND REHEAT

An alternative method of attaining a high turbine outlet temperature (TOT) is to use reheat. Reheat is the addition of heat to the working fluid part-way down its expansion rather than at the end, as is the case with supplementary firing. This allows the conversion of some of the supplementary fuel exergy to work in the gas turbine, and so reheat does not suffer from the same efficiency penalty as does supplementary firing. Providing a low stack temperature can be maintained, then a reheat cycle should theoretically be more efficient than one without reheat because it has a higher mean temperature of heat addition. However this simplistic argument is complicated by the need to provide additional cooling with reheat. Cooling considerations have a major effect on reheat gas turbine performance.

The high TOT associated with reheat is favorable for the steam reforming reaction, so that the efficiency gain from adding recuperation to a reheat STIG cycle should be relatively large. This section investigates a CRGT with both intercooling and reheat. Intercooling is added to reduce the compressor work and hence increase power output. At the same time, the cooling air bled from the compressor is colder, and so less is required to cool the turbine. For convenience the intercooled reheat CRGT cycle is hereafter referred to as the IR-CRGT cycle.

In order to separate the effect of chemical recuperation from the effects of intercooling and reheat, the IR-CRGT cycle is compared with equivalent ISTIG, reheat ISTIG and reheat combined cycles. Once again the complexity of these cycles means that a rigorous optimization procedure and parametric analysis are not practical. Instead the calculations are performed for just one case - an aeroderivative gas turbine resembling the General Electric (GE) LM8000⁹. This

⁹ The GE LM8000 has been designed but not yet developed. It is based on the same aircraft engine (the CF6-80C2) as is the LM6000, which will be commercially available in 1992. The LM8000 is similar to the LM6000 but incorporates more gas generator modifications and intercooling.

turbine was chosen as it is featured in the CRGT cycle proposed by Janes (1990). Janes argues that a CRGT cycle based on the LM8000 can be developed at relatively low cost, and so such a cycle is of considerable practical interest.

Published performance estimates for the Janes cycle are discussed below. This section presents calculations carried out to validate further these findings. The aim is not to reproduce the LM8000-based cycle exactly, as the Consonni model is not designed to reproduce specific machines. Moreover, the data required to do this is commercially sensitive and therefore unavailable. Rather, the objective is to ascertain that a cycle with the same operating parameters as the Janes cycle has approximately the same performance, and thus provide independent confirmation of the previous estimates.

Important cycle operating parameters used in the calculations are matched to the LM8000 cycle. These parameters are turbine inlet temperature, reheat firing temperature, overall pressure ratio, reheat pressure, intercooling pressure, and compressor inlet mass flow rate. Component input data, such as pressure drops, are matched to the Janes cycle (as reported in De Candia, 1989) where available. Otherwise they are set at the values of Table 6.1, with the "aeroderivative" data set used for the gas turbine. This data set was tested in Chapter Five and was found to reproduce accurately the simple cycle performance of the LM6000, which is derived from the same aircraft engine as is the LM8000.

7.4.1 Published Performance Estimates

The first performance estimate for an advanced CRGT cycle was made by Jack Janes of the California Energy Commission (CEC), with the help of General Electric. The cycle is based on the GE LM8000 gas turbine, and incorporates intercooling and reheat. The gas turbine is mainly air-cooled, but also uses a small amount of steam for cooling.

The gas turbine section of the cycle was calculated by General Electric (GE, 1989). As the reheat turbine is as yet undesignated, GE assumed three levels of cooling air demand, leading to a range of performance estimates. The three reheat turbine cooling levels chosen were 0%, 4.5%, and 9% of the compressor inlet air flow. A steam flow of around 1.2% of compressor air flow is used

in addition to bleed-air to cool the high pressure turbine. However "no attempt was made to vary steam cooling flows to control to a bulk metal temperature" (GE, 1989, pp2), so it is unclear whether sufficient cooling flows were assumed. The GE report does not specify the flow rate of bleed-air assumed for cooling of the high pressure turbine. GE identified in their follow-up recommendations the need for clarification of the uncertainty surrounding cooling flows.

The CEC used the results of the GE gas turbine analysis to calculate the heat recovery steam reformer, and returned their results to GE for the next iteration. A drawback of the GE/CEC analysis is that this calculation process was stopped after two iterations, and before convergence was reached. The Pacific Gas & Electric Company (PG&E) carried out independent calculations to confirm the GE/CEC results, though still using gas turbine data supplied by GE. The reheat turbine cooling flow was assumed to be 4-5% of the compressor inlet flow. Both studies compared the CRGT cycle to corresponding ISTIG and reheat ISTIG cycles. The PG&E study also included a reheat combined cycle.

Table 7.3 shows the estimated performances for both studies. The PG&E figures are likely to be more accurate because the calculations were completed to convergence. Both studies found that adding reheat to the LM8000 ISTIG improves power output by 50-60% and increases efficiency by over one percentage point. Adding chemical recuperation leads to a further efficiency improvement of up to 3 percentage points, but at the expense of a decrease in power output of around 20%. The IR-CRGT cycle has a higher efficiency than the reheat combined cycle.

Table 7.3: Previous Performance Estimates for IR-CRGT Cycle

	GE/CEC		PG&E	
	Power (MW)	Efficiency (%LHV)	Power (MW)	Efficiency (%LHV)
ISTIG	121	52.0	117	52.0
Reheat ISTIG	184	53.3	185	53.6
IR-CRGT	142 to 150	54.7 to 56.4	152	56.1
Reheat combined cycle			160	54.1

Notes:

(a) GE/CEC numbers derived from GE (1989).
 (b) PG&E numbers from De Candia (1989).
 (c) Both based on GE LM8000 engine, pressure ratio=34, TIT=1370C, reheat temperature=1260C.
 (d) Power output and efficiency are net plant values.

7.4.2 ISTIG

Figure 7.6 shows an intercooled steam-injected gas turbine (ISTIG) cycle. Compressor air is cooled part-way through compression in an indirect contact, counter-flow heat exchanger. Some of the heat given up by the air preheats the HRSG feedwater. The HRSG produces steam at three pressures. High pressure (HP) steam is injected into the combustor, while intermediate (IP) and low pressure (LP) steam is injected further down the turbine. Evaporation pressure and degree of superheat at each level are as in the PG&E study. As much steam as possible is produced at each pressure.

Figure 7.6 shows conditions at various points around the cycle, while Table 7.4 compares calculated values of some important cycle characteristics with those obtained in the PG&E study. The calculated shaft output and efficiency are 115MW and 51.5%. Assuming a generator efficiency of 98.4% (as in the PG&E study), the electrical power output is 113MW_e at 50.7% efficiency. The PG&E estimate is 117MW_e at 52.0% efficiency. Agreement with the PG&E numbers is generally good except for the 1.3% difference in efficiency. The discrepancy is likely to originate from different assumptions about turbine cooling, but the cooling flow information required to investigate this is proprietary and thus not available for this analysis.

Table 7.4: Comparison of Cycle Performance Predictions

	Present study	PG&E
ISTIG		
Compressor discharge temperature (C)	394	386
Turbine outlet temperature (C)	472	472
Stack temperature (C)	123	143
Stack mass flow (kJ/kg _{air})	1.20	1.19
Power output (MW _e)	113	117
Electrical efficiency (%LHV)	50.7	52.0
REHEAT ISTIG		
Compressor discharge temperature (C)	390	382
Turbine outlet temperature (C)	602	660
Stack temperature (C)	122	125
Stack mass flow (kJ/kg _{air})	1.32	1.32
Power output (MW _e)	171	185
Electrical efficiency (%LHV)	51.3	53.6
INTERCOOLED REHEAT CRGT		
Compressor discharge temperature (C)	390	383
Turbine outlet temperature (C)	632	694
Stack temperature (C)	123	141
Stack mass flow (kJ/kg _{air})	1.24	1.19
Power output (MW _e)	149	152
Electrical efficiency (%LHV)	52.7	56.1
REHEAT COMBINED CYCLE		
Compressor discharge temperature (C)	390	382
Turbine outlet temperature (C)	677	734
Stack temperature (C)	164	141
Stack mass flow (kJ/kg _{air})	1.07	1.08
Power output (MW _e)	141	160
Electrical efficiency (%LHV)	53.6	54.1
Notes:		
(a) PG&E numbers from De Candia (1989)		

7.4.3 Reheat ISTIG

Figure 7.7 shows an ISTIG cycle with reheat. On exiting the high pressure turbine, the gas flow is reheated to 1260C in the reheat combustor and then expands through the reheat turbine. The reheat pressure is 12.8bar¹⁰.

The reheat turbine must be cooled because of the elevated gas temperature. Since very high flow rates of compressor bleed-air tend to penalize performance it might be preferable to use steam to meet some of the cooling load. In the configuration studied here, steam cools the first-stage

¹⁰ Neither the reheat firing temperature nor the reheat pressure is optimized. Both are set at the values used in the PG&E study. Rough exploratory calculations reveal that the optimal reheat pressure is around 8bar.

nozzles of the high pressure turbine, while compressor bleed-air cools the rest of the high pressure turbine and the reheat turbine¹¹.

The HRSG has three pressure levels. Superheated HP steam is injected into the main combustor. The HP steam used for cooling is not superheated, as more effective cooling is achieved at low steam temperature. Superheated IP steam is injected into the reheat combustor, while saturated LP steam is injected part-way down the reheat turbine. As before, as much steam as possible is produced at each pressure level.

The calculated performance is 173MW (shaft) at 52.0% efficiency. Power output is 50% greater than for the ISTIG cycle, while efficiency has improved by half a percentage point. The increased power results both from the extra expansion work in the reheat turbine and from the fact that the elevated turbine outlet temperature (TOT) leads to a greater steam production. Despite the large power increase, the efficiency improvement is modest because of the reheat turbine's large demand for cooling air.

The required mass flow of bleed-air to the reheat turbine is around 20% of the inlet air flow. This is substantially greater than the 4-5% assumed in the PG&E study. The reheat temperature and pressure in this cycle are similar to the temperature and pressure in the main combustor of today's heavy-duty gas turbines, which have bleed-air flow rates typically around 20%. Even allowing for the fact that aeroderivatives generally have more sophisticated cooling technology than heavy-duties, the calculated reheat turbine cooling flow of 20% seems reasonable, while the PG&E figure appears to be rather optimistic¹². This discrepancy has a major effect on the overall cycle performance. The PG&E study obtains an electrical efficiency of 53.6% compared to 51.3% here, while the power outputs are 185MW_e and 171MW_e respectively¹³. The high cooling flow in

¹¹ The PG&E study also assumes partial steam cooling, but uses both air and steam to cool all sections of the high pressure turbine. The arrangement used here is chosen both for convenience of implementation and because it is believed to be near optimal. It is generally preferable to use steam to cool higher pressure sections of the turbine rather than lower pressure sections, as the cooling steam proceeds to perform work once it joins the main turbine flow. Steam used for cooling the first-stage nozzles does not lose any of its potential to do work as no work is performed in stationary blade rows.

¹² Note also that both analyses assume that the reheat combustor does not require external cooling. As discussed in Chapter Four, designing such a combustor represents a considerable challenge.

¹³ Presumably a fraction of this difference in efficiency has the same source as the efficiency difference observed for the ISTIG cycle.

the present calculation leads to a TOT substantially lower than the PG&E value (see Table 7.4). This restricts available steam production, and will have implications for chemical recuperation.

7.4.4 Intercooled Reheat CRGT

Figure 7.8 shows a reheat ISTIG cycle with chemical recuperation. The reheat firing temperature is 1260C and the reheat pressure is 10.0bar¹⁴. The steam reformer has two fuel-side flows in parallel but at different pressures. High pressure (HP) fuel gas goes to the main combustor and low pressure (LP) fuel gas supplies the reheat combustor. The HRSG produces steam at three pressures. Saturated HP steam is used to cool the first-stage nozzles of the high pressure turbine, while all remaining HP steam is superheated and sent to the HP steam reformer. All IP steam is superheated and used in the LP steam reformer. Low pressure (2bar) steam is injected into the reheat turbine as before.

The calculated performance is 151MW (shaft) at 53.4% efficiency. The efficiency improvement over the reheat ISTIG of 1.4 percentage points is obtained at the expense of a power reduction of around 14%. Note that even with reheat the turbine outlet temperature is only 638C, so methane conversion is relatively low at 29% in the HP reformer and 28% in the LP reformer. The TOT could be increased by raising the reheat firing temperature or lowering the reheat pressure, and this would lead to more chemical heat recovery. However the required cooling flow rates would also increase, so the effect on efficiency is unlikely to be large.

The flow of bleed-air required for cooling of the reheat turbine is calculated to be 18% of the compressor inlet flow. As for the reheat ISTIG, this far exceeds the value of 4-5% assumed in the PG&E study, and so the predicted performance is significantly inferior to the PG&E estimate. Assuming the same generator efficiency of 98.7%, the electrical efficiencies are 56.1% in the PG&E study and 52.7% here. The difference in cooling air flows leads to a 56C higher TOT for the PG&E calculation (Table 7.4). As TOT is an important factor influencing the amount of both

¹⁴ Again neither the reheat firing temperature nor the reheat pressure is optimized. Both are set at the values used in the PG&E study. However, rough exploratory calculations reveal that the reheat pressure chosen is close to the optimal value.

chemical recuperation and steam production, this discrepancy leads to a significant difference in overall performance, particularly in efficiency.

7.4.5 Reheat Combined Cycle

Figure 7.9 shows a reheat combined cycle with intercooling. Once again the gas turbine operating conditions are matched to the PG&E values. Reheat pressure is 8.3bar and the gas turbine is fully air-cooled¹⁵. The HRSG has two pressure levels. High pressure steam at 100bar drives the steam turbine with steam reheat at 35bar. The condensing temperature is 38C, and the steam turbine is assumed to have a polytropic efficiency of 80%. 0.045kg/kg_{air} of 35bar steam produced in the LP steam drum is injected into the main combustor for NO_x control, while any remaining available LP steam is used in the steam cycle¹⁶.

The calculated performance is 144MW (shaft) at 54.5% efficiency. This translates to an electrical output of 141MW_e at 53.6% efficiency. The turbine mass flow is lower than in the reheat ISTIG and IR-CRGT cycles, because most steam is sent to the steam turbine rather than injected into the gas turbine. As a result a smaller reheat turbine is required, and so the reheat turbine cooling flow is lower at around 13% of inlet air flow. However this value is still much greater than the 4-5% used by PG&E, and this accounts for the superior performance estimates of 160MW_e at 54.1% for the PG&E study.

Note that in the present calculation the reheat combined cycle is more efficient than the IR-CRGT, but that the PG&E study obtained the opposite result (Table 7.4). This derives from the fact that in the PG&E study the reheat turbine cooling flow is assumed to be the same for the reheat combined cycle as for the IR-CRGT cycle, and so the reheat combined cycle does not gain from a reduced load resulting from a lower total mass flow in the reheat turbine. Another factor is that the two analyses assume different steam turbine efficiencies. The current calculation assumes a polytropic efficiency of 80%, which is appropriate for a well-designed steam turbine of

¹⁵ The cooling load is lower than in the reheat ISTIG and advanced CRGT cycles because the mass flow in the turbine is lower. Hence bleed-air alone can meet the cooling load.

¹⁶ The flame temperature in the reheat combustor is typically 200-300K lower in the reheat combustor than in the main combustor, and so NO_x formation will be less of a problem.

this size (De Candia, 1990)¹⁷. This translates into adiabatic efficiencies of 80% for the high pressure steam turbine and 87% for the low pressure steam turbine. De Candia (1989) implies a conservative adiabatic efficiency of 70% for the high pressure turbine, while the low pressure turbine efficiency is not available. In both cases addition of another pressure level could improve the steam cycle performance.

7.4.6 Summary and Discussion

Both the present calculations and the PG&E study found the IR-CRGT cycle to be more efficient than the reheat ISTIG, which in turn is more efficient than the ISTIG. However the absolute values of these efficiencies differed substantially between the two analyses, primarily because the calculated value for the required flow of compressor bleed-air for cooling of the reheat turbine is much greater than the 4-5% assumed by PG&E. Consequently the PG&E estimate for the electrical efficiency of the IR-CRGT cycle, at 56.1%, is higher than the 52.7% predicted here. The dilution effect of the extra cooling air leads to lower turbine outlet temperatures than in the PG&E study, resulting in a reduced capability for steam production and/or chemical recuperation. Hence the predicted power outputs for all cycles with reheat are lower than in the PG&E study, while the efficiency benefit of adding recuperation is smaller.

The IR-CRGT cycle is less efficient than the reheat combined cycle in the present study, whereas the opposite is the case in the PG&E study. This stems partly from different assumptions about cooling of the reheat turbine. Other possible reasons for the relatively poor performance of the PG&E reheat combined cycle are a conservative estimate for steam turbine cycle efficiency and a poorly optimized steam cycle. In fact the steam cycles of both studies could be improved by adding another pressure level or adjusting evaporation pressures of existing levels.

The issue of what parameters should be optimized and which should be fixed is a complex one, and depends on the extent of design freedom for the cycle components. The cycles studied here are based on an existing gas turbine with the aim of achieving a highly efficient cycle at low development cost, and so the most important parameters such as turbine inlet temperature,

¹⁷ The cycle performance assuming a 70% polytropic efficiency for the steam turbine is 141MW (shaft) at 53.4% efficiency, a reduction of about one percentage point.

pressure ratio, and reheat pressure must be taken as given. This still allows some freedom in HRSG design, specification of steam injection locations, and, in a combined cycle, steam cycle design. While a rigorous optimization procedure for these elements was not attempted, it is believed that the configurations chosen are near optimal and that the resulting errors in efficiency estimates are of the order of tenths of a percentage point. Hence the lack of optimization will not affect the overall ranking of cycles.

From a fundamental thermodynamic perspective, it would be more interesting to compare cycles based on "rubber turbines" rather than existing turbines. In this case the turbine inlet temperature and reheat temperatures would be determined by metallurgical and cooling constraints, while the overall pressure ratio, reheat pressure, and intercooling pressure would all be optimized. Turbine cooling is of major importance in cycles with reheat, and particular attention should be paid to minimizing cooling flows. One issue which has so far received little attention is the optimal mix of steam and compressor bleed-air for cooling. Pre-cooling of bleed-air to reduce the amount required is another promising avenue worthy of exploration.

One of the motivations for looking at a CRGT cycle with reheat was that the elevated turbine outlet temperature (TOT) of a reheat cycle promises a large amount of chemical heat recovery. The high pressure ratio of the aeroderivative gas turbine used in the example calculation leads to a TOT of 677C, which is not a great deal higher than the 600C TOT of a low pressure ratio heavy-duty gas turbine without reheat. This and the high pressure required in the HP fuel reformer result in a methane conversion of under 30%, which is less than for the heavy-duty gas turbine. Remember however that this finding was obtained for an existing gas turbine. An optimally designed cycle is likely to employ a lower overall pressure ratio and/or reheat pressure, leading to a higher TOT and hence a higher methane conversion.

In the absence of a detailed comparison of rigorously optimized IR-CRGT, reheat ISTIG, and reheat combined cycles, exergy arguments can be employed to make inferences as to their relative merits. No cycle will have a major advantage in exhaust heat recovery irreversibilities, since all three can achieve well-matched heat recovery temperature profiles by suitable selection of evaporation pressures. The reheat ISTIG and IR-CRGT cycle will still suffer from large mixing losses associated with injecting steam directly or indirectly into the gas turbine and from relatively

high stack losses owing to the discharge of steam up the stack¹⁸. The IR-CRGT will be more efficient than the reheat ISTIG because the use of chemical heat recovery enables a reduced steam production while maintaining a low stack temperature and a well-matched heat recovery profile. The combined cycle does not have from these mixing losses, but instead has losses associated with the steam turbine and condenser of the steam cycle. In cycles without reheat the efficiency cost of the steam cycle losses is more than offset by the benefits following from the lack of steam injection, and so the combined cycle is significantly more efficient than either the STIG or the CRGT cycle. There is no reason why the addition of reheat should change this result. Hence, while improving the efficiency of all three cycles, it is unlikely that reheat will affect their relative rankings.

7.5 SUMMARY

The aim of this chapter was to investigate whether the basic CRGT could be modified to obtain an efficiency competitive with that of a combined cycle. This is an important factor influencing the attractiveness of CRGT cycles for base-load power generation¹⁹. The short answer to this question is "no", because the CRGT cycle will always suffer from the mixing loss associated with mixing steam into the gas cycle.

Currently available combined cycles use multi-pressure HRSGs to obtain efficiencies around 52%, but a multi-evaporation CRGT cycle remains below 50% efficient. Supplementary firing was introduced to elevate the temperature at which steam reforming occurs and so increase the extent of methane conversion. However overall efficiency declines because the extra chemical heat recovery is insufficient to offset the additional heat input associated with the supplementary fuel. Reheat is a better way to raise the reforming temperature, as the reheat turbine extracts work directly from the heat added in the reheat combustor. The efficiency of an intercooled reheat CRGT cycle based on the General Electric LM8000 machine was calculated to be about 52.7%. This compares with a reheat combined cycle, estimated to be 53.6% efficient.

¹⁸ The exergy loss associated with the steam content of the stack gases arises from rejecting heat at above-ambient temperature. The latent heat of the steam does not represent an exergy loss if transferred at ambient temperature because you cannot obtain work in a condensation process.

¹⁹ Chapter Eight considers other factors such as NO_x emissions.

The cycles studied in this chapter were not rigorously optimized, but rather used cycle parameters typical of today's state-of-the-art gas turbines. This approach is justified in that practical CRGT cycles are likely to be built around existing gas turbines in order to avoid the high cost of designing completely new gas turbines. However from a theoretical thermodynamic perspective there is a danger of making "unfair" comparisons between sub-optimal cycles. The multi-evaporation and supplementary fired cycles of Sections 7.2 and 7.3 used a turbine inlet temperature and pressure ratio typical of modern heavy-duty gas turbines, which are designed for optimal combined cycle efficiency. The parametric analysis of Chapter Six found that simple CRGT cycles optimize at similar conditions, so the comparisons in these Sections 7.2 and 7.3 are likely to be "fair" assuming addition of extra HRSG pressure levels and/or supplementary firing does not significantly change the optimal conditions. The task of verifying this is left as future follow-on work.

Similar arguments apply to reheat cycles. The cycle calculations of this chapter were based on an aeroderivative gas turbine resembling the General Electric LM8000 because this could be converted into a reheat CRGT machine at relatively low cost (at least compared to the cost of developing a completely new gas turbine). Again, a detailed optimization of theoretical reheat cycles was not attempted here but could be the subject of another investigation. The subject of cooling of reheat cycles needs further attention too. The reheat cycle performance estimates obtained in the current study differed significantly from those presented by PG&E because different assumptions were made about the cooling flows required.

The result that CRGT cycles are not as efficient as combined cycles does not mean that there is no role for CRGT cycles either specifically for base-load power generation or in gas turbine applications generally. There might well be situations when the inherent low NO_x emissions of CRGT cycles render their use particularly attractive. A detailed discussion of possible niches for CRGT cycles is included in Chapter Eight.

REFERENCES

F De Candia, ISTIG Enhancement Evaluation, Volume I, Pacific Gas and Electric Company report 007.4-89.1, September 1989

D De Candia of Pacific Gas and Electric Company, San Francisco CA, personal communication, December 1990.

GE: Advanced Chemically Recuperated Gas Turbine Cycle Evaluation Project, Preliminary Assessment of the System Concept, Program Final Report, by R. Hines of General Electric Marine and Industrial Engines Division, Evendale OH, 1989

J Janes, Chemically Recuperated Gas Turbine, California Energy Commission Draft Staff Report, January 1990

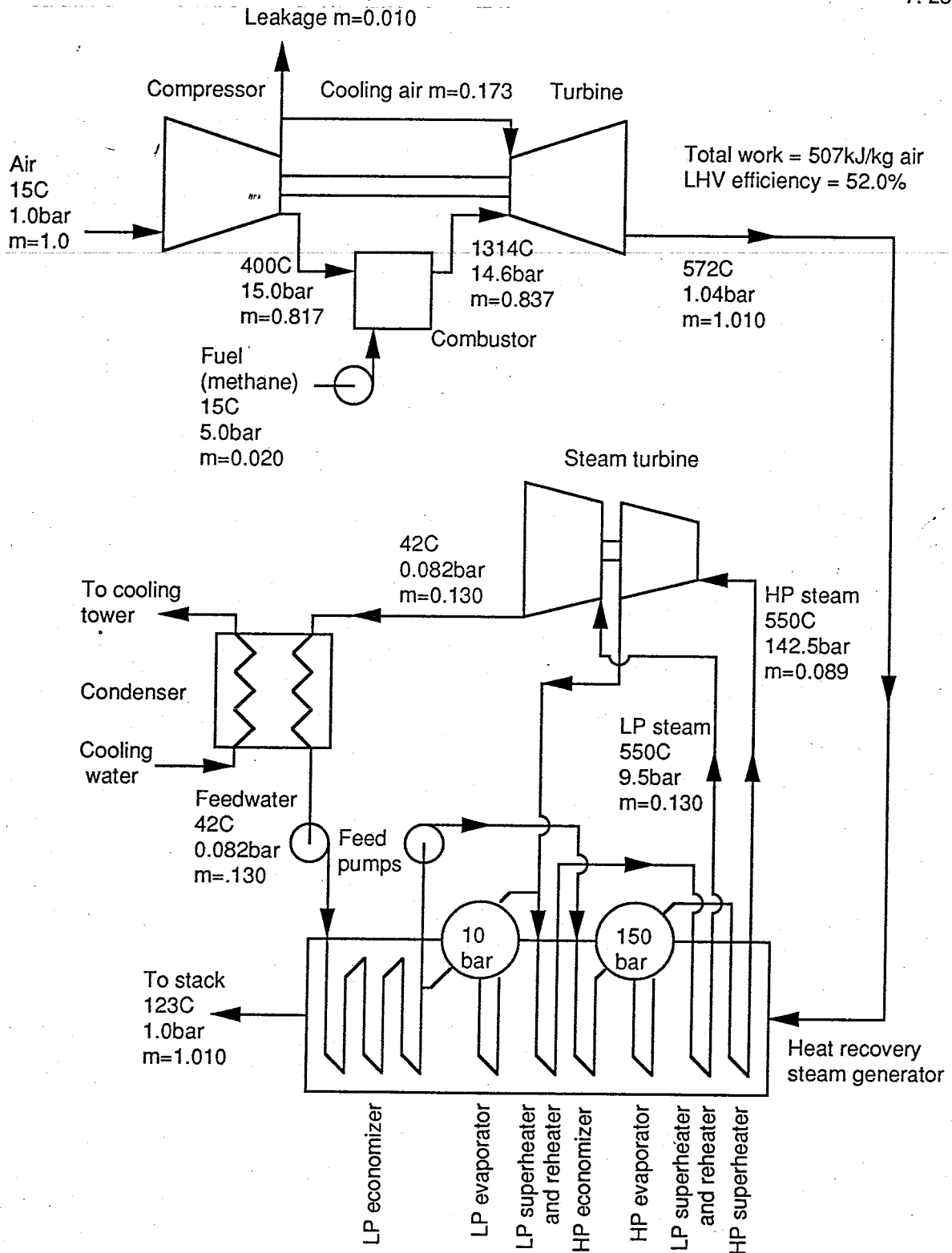


Figure 7.1: Multi-Evaporation Combined Cycle

The HRSG incorporates two pressure levels with steam reheat. High pressure steam expands in a steam turbine to 10bar and then returns to the HRSG for reheat. The reheat steam mixes with expansion down to the condensing pressure.

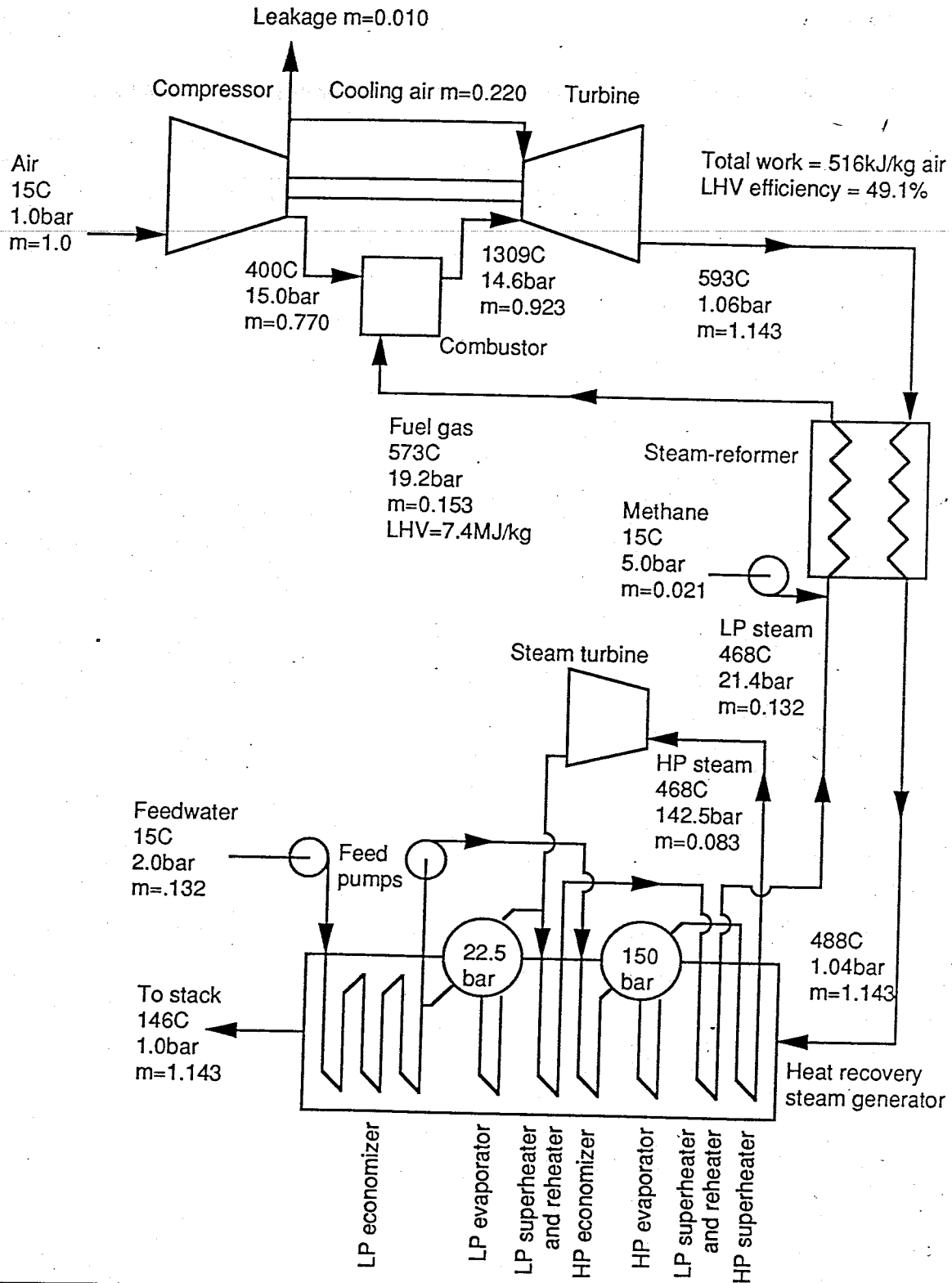


Figure 7.2: CRGT Cycle with Topping Steam Turbine

The HRSG incorporates two pressure levels with steam reheat. High pressure steam expands in a steam turbine to 22.5bar and then returns to the HRSG for reheat. The reheat steam is mixed with additional steam generated in the LP drum, and the resulting LP steam flow is sent to the reformer to participate in the chemical recuperation reaction.

Methane conversion is 35.2%, resulting in a fuel gas of lower heating value 7.4MJ/kg and composition (by volume) 8.9% CH₄, 0.4% CO, 4.4% CO₂, 18.9% H₂, and 67.4% H₂O.

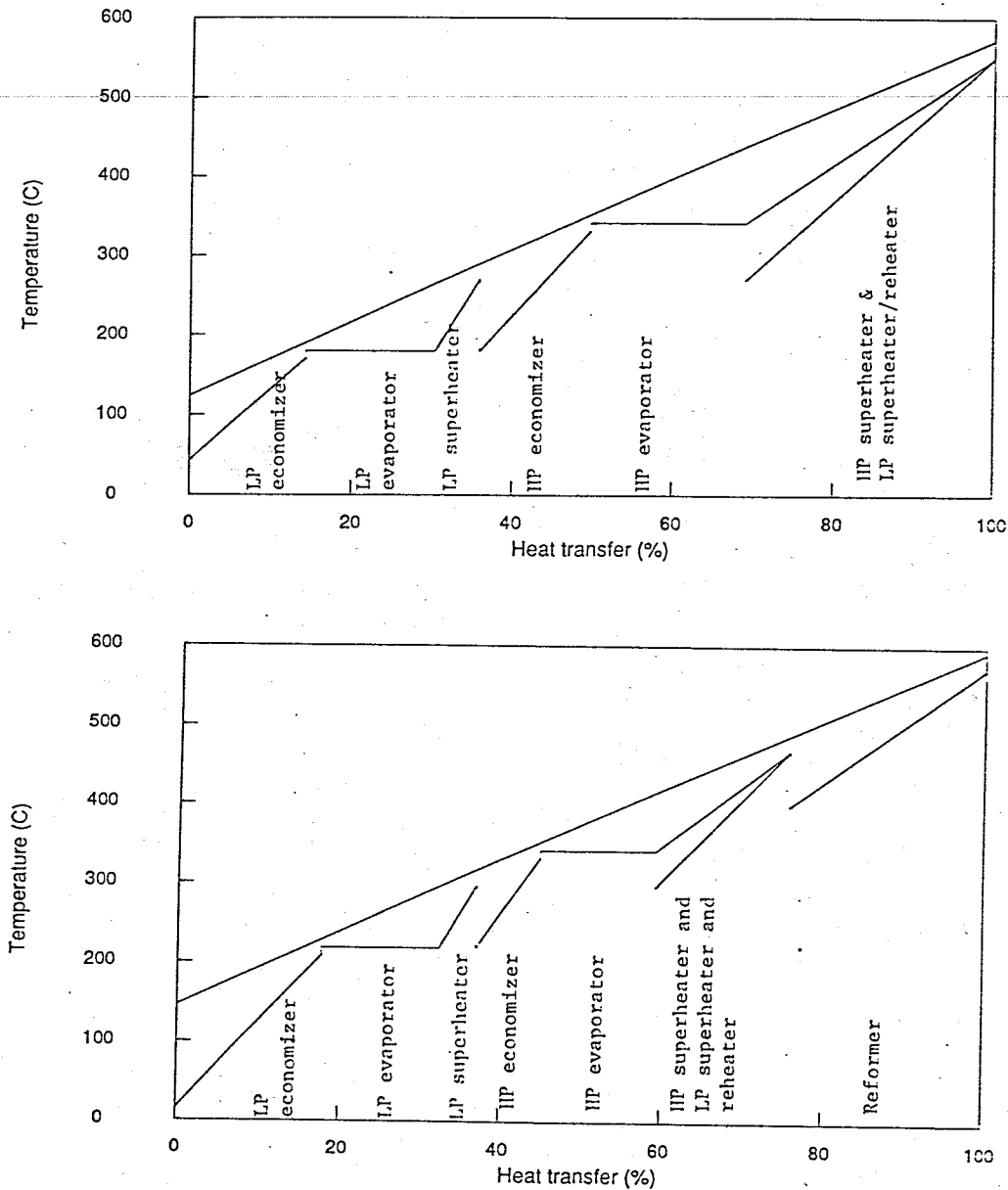


Figure 7.3: Heat Recovery Profiles for Advanced Combined and CRGT Cycles

Both cycles feature HRSGs with two pressure levels and steam reheat. The reheat steam is added to steam from the LP evaporator on entering the LP superheater, which therefore also serves as the reheater. The HP and LP superheaters are placed in parallel at the hot-end to enable both steam flows to attain the maximum possible exit temperature. In the CRGT cycle, methane is added to the LP steam flow on entering the reformer.

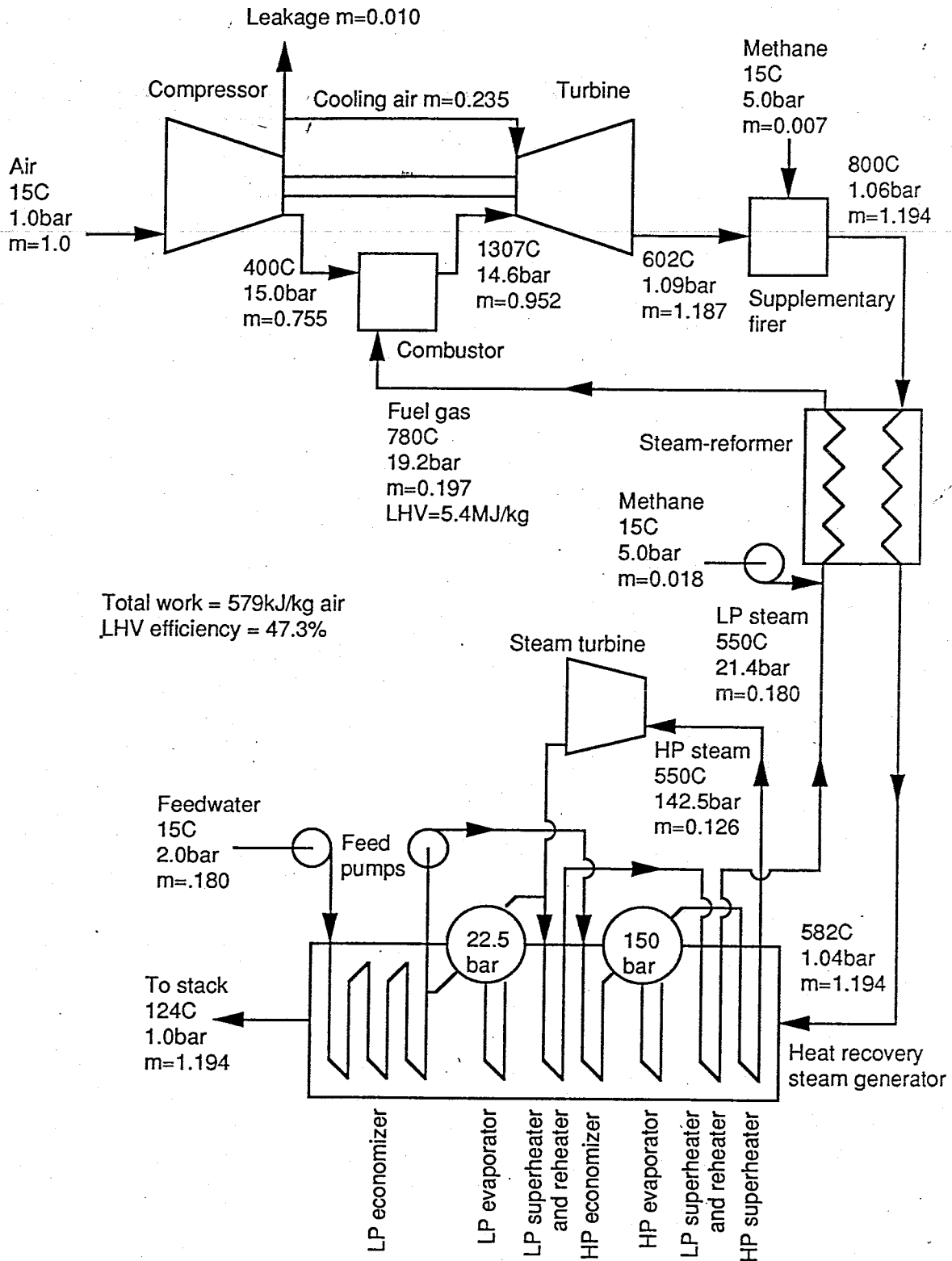


Figure 7.4: CRGT Cycle with Supplementary Firing

The cycle is based on an industrial gas turbine at a turbine inlet temperature of 1250C and a pressure ratio of 15, and incorporates a two-pressure HRSG with reheat and a topping steam turbine.

Methane conversion is 95.8%, resulting in a fuel gas of lower heating value 5.4MJ/kg and composition (by volume) 0.3% CH₄, 2.3% CO, 5.7% CO₂, 29.7% H₂, and 62.0% H₂O.

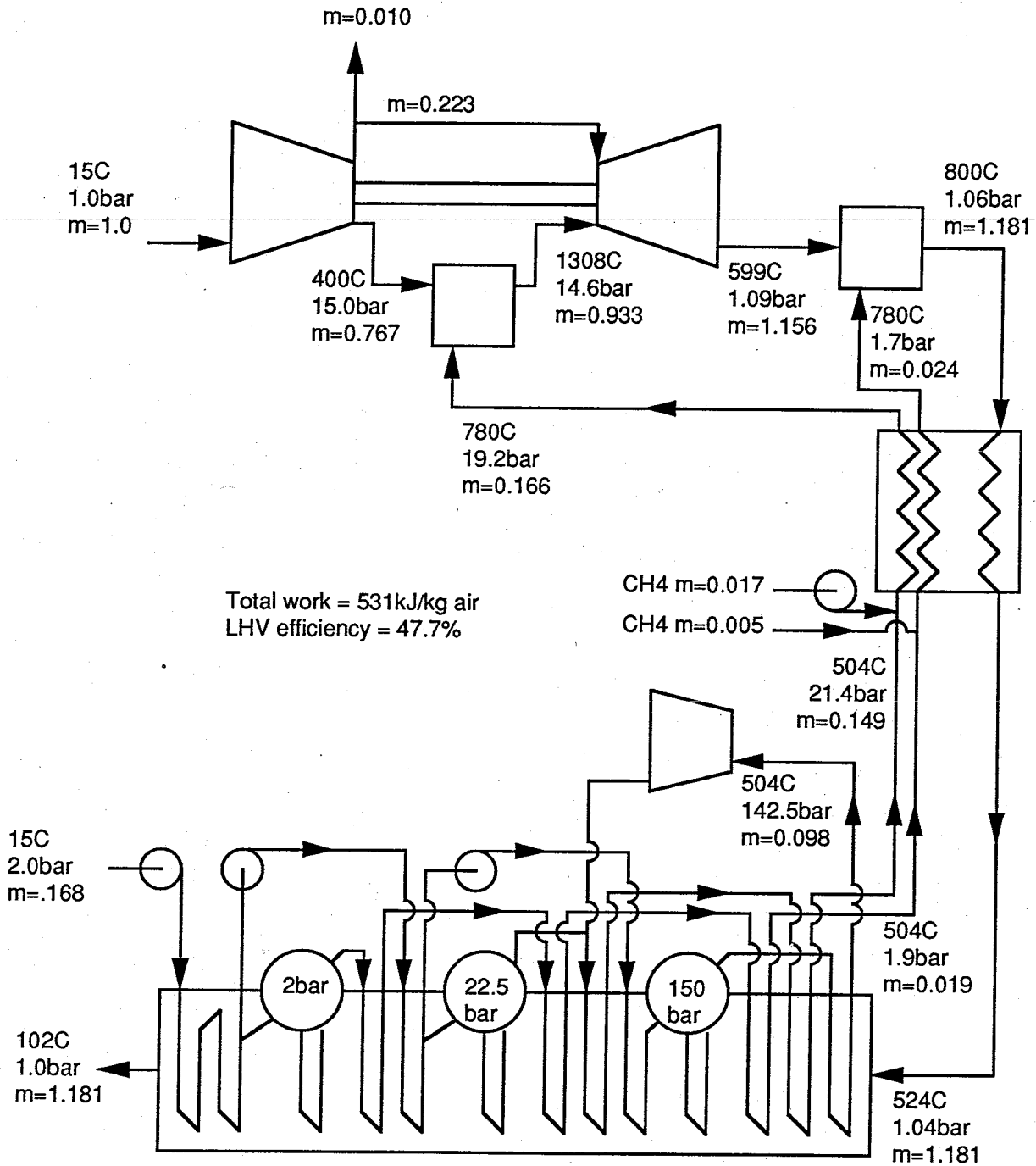


Figure 7.5: CRGT Cycle with Supplementary Firing and Reforming of Supplementary Fuel

The cycle is based on a heavy-duty gas turbine at a turbine inlet temperature of 1250C and a pressure ratio of 15, and incorporates a three-pressure HRSG with reheat and a back pressure steam turbine. The reformer consists of two fuel-side flows in parallel and at different pressure, one producing fuel gas for the main combustor and the other for the supplementary firer.

Methane conversion is 93.6% in the HP reformer and 99.2% in the LP reformer, leading to fuel gas lower heating values of 6.3MJ/kg and 12.8MJ/kg respectively.

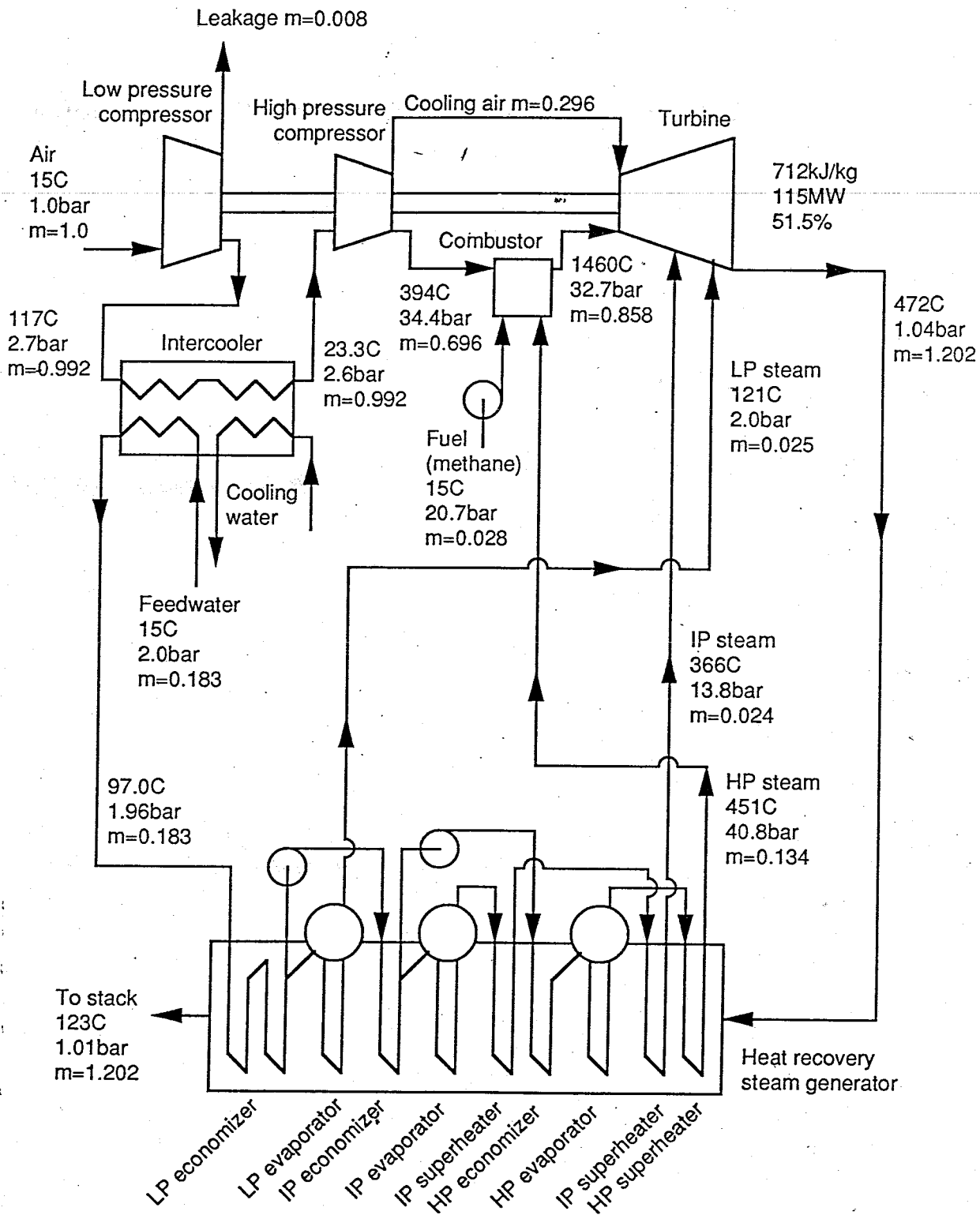


Figure 7.6: Flow Diagram for ISTIG Cycle Calculation

The cycle is based on an aeroderivative gas turbine with a turbine inlet temperature of 1370C and a pressure ratio of 34. The three-pressure level HRSG produces steam for injection into the combustor and at two locations along the turbine. Specific work, power output, and efficiency are shaft values.

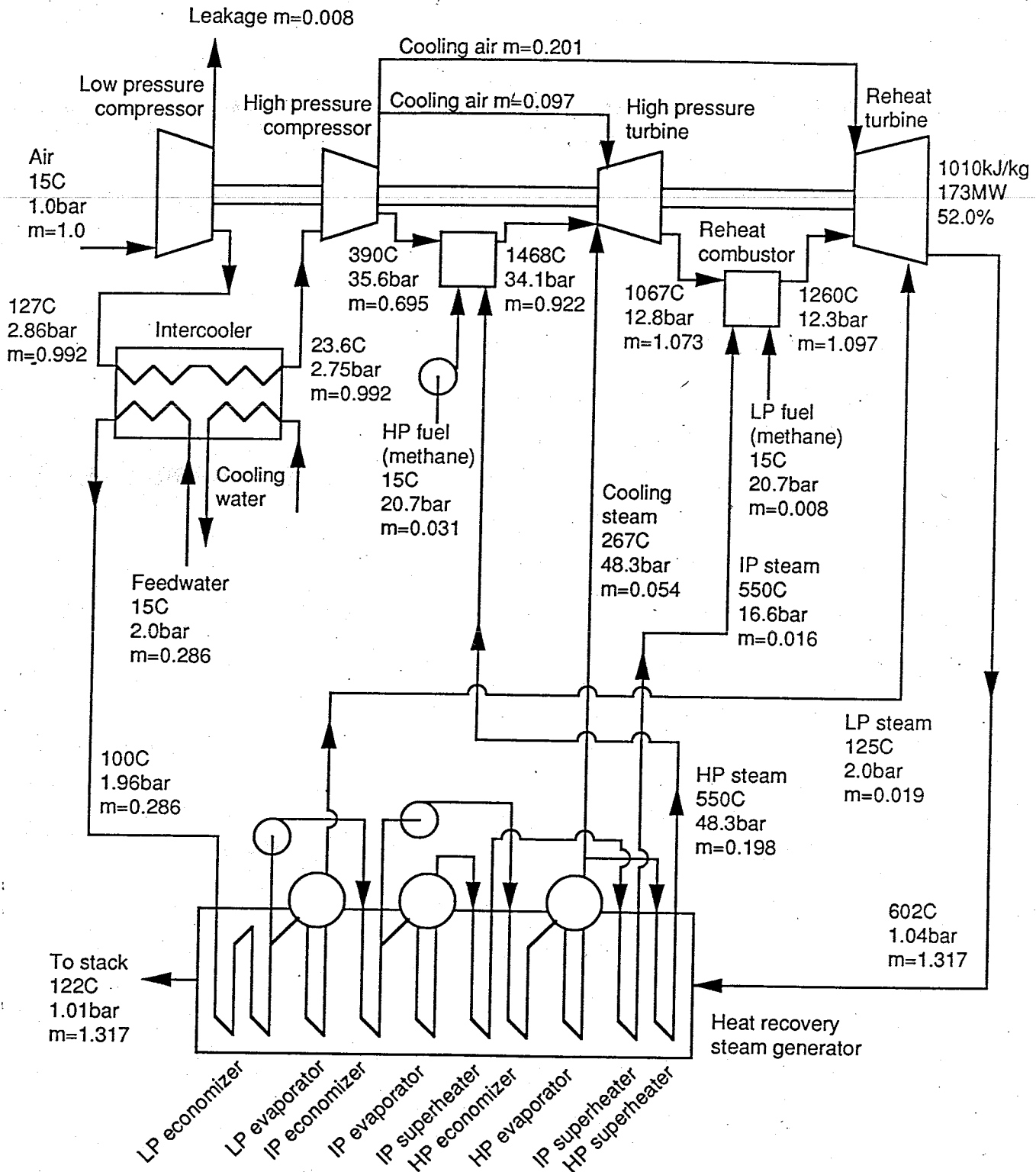


Figure 7.7: Flow Diagram for Reheat ISTIG Cycle Calculation

The cycle is based on an aeroderivative gas turbine with a turbine inlet temperature of 1370C and a pressure ratio of 35. Reheat to 1260C occurs at 12.8bar. The 3-pressure level HRSG produces steam for injection into the main and reheat combustors and part-way along the reheat turbine. Saturated high pressure steam cools the first-stage nozzles of the high pressure turbine. Specific work, power output, and efficiency are shaft values.

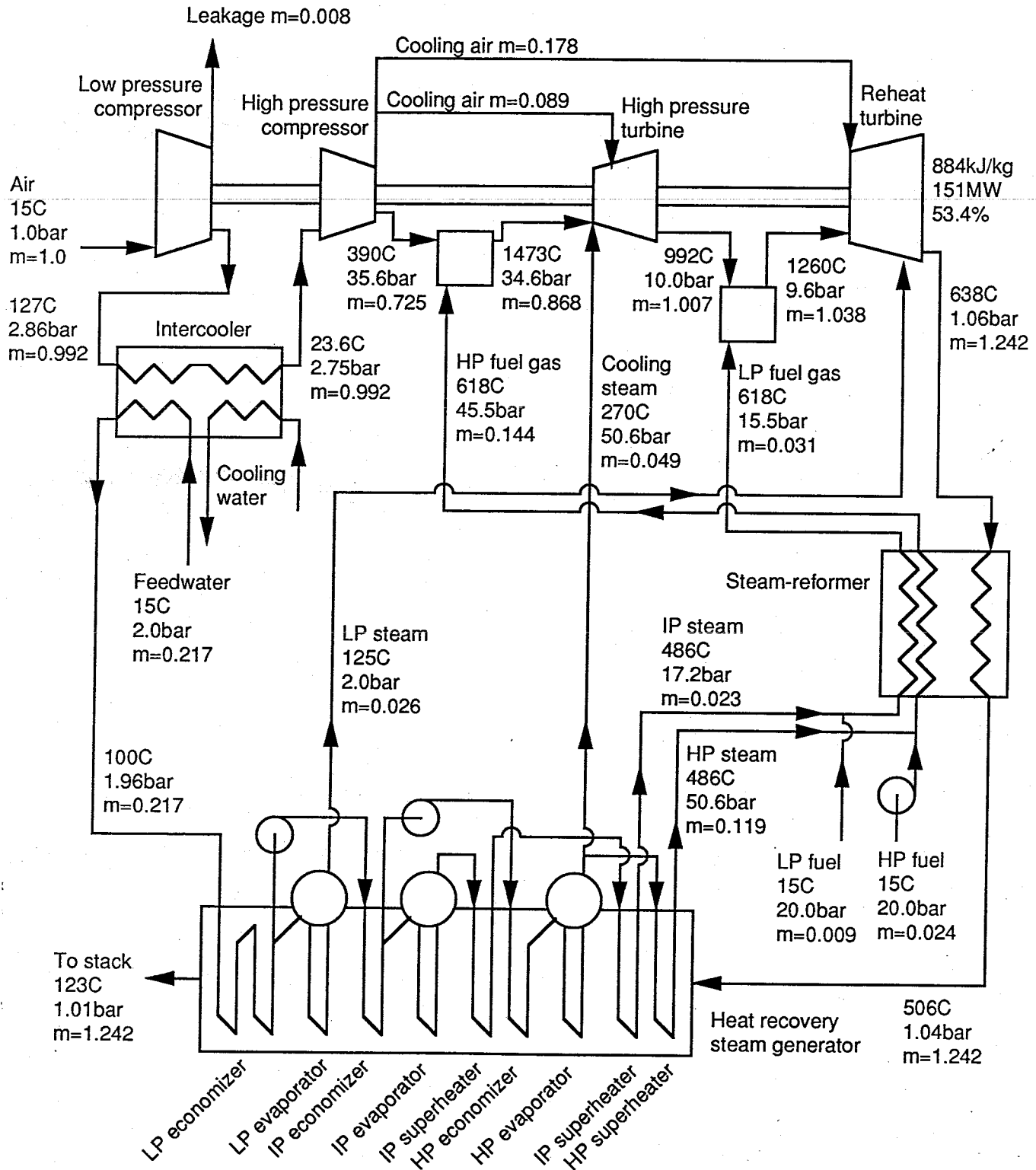


Figure 7.8: Flow Diagram for Intercooled Reheat CRGT Cycle Calculation

The cycle is based on an aeroderivative gas turbine with a turbine inlet temperature of 1370C and a pressure ratio of 35. Specific work, power output, and efficiency are shaft values.

The high pressure fuel gas for the main combustor has the following composition (by volume): 12.0% CH₄, 0.5% CO, 4.3% CO₂, 18.7% H₂, 64.5% H₂O. The low pressure fuel gas, used in the reheat combustor, is 19.0% CH₄, 1.5% CO, 5.9% CO₂, 28.0% H₂, 45.6% H₂O.

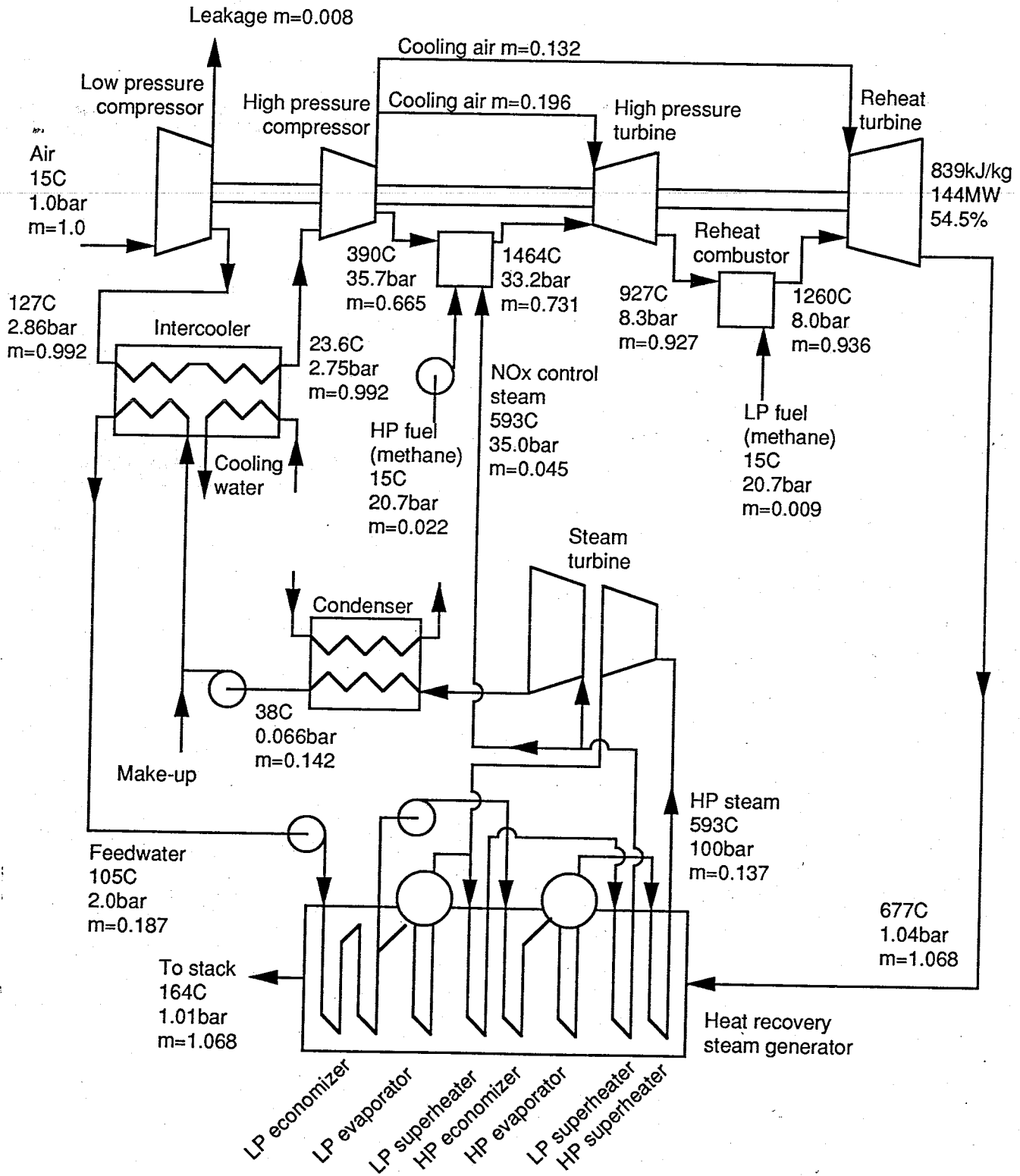


Figure 7.9: Flow Diagram for Reheat Combined Cycle Calculation

The cycle is based on an aeroderivative gas turbine with a turbine inlet temperature of 1370°C and a pressure ratio of 35. Specific work, power output, and efficiency are shaft values.

The steam cycle features two-pressure levels with reheat. Most of the LP steam is injected into the gas turbine combustor for NO_x control.

CHAPTER EIGHT: CONCLUSIONS

8.1 Review

8.2 Prospects for Chemically Recuperated Gas Turbines

8.3 Suggestions for Future Work

References

8.1 REVIEW

Gas turbines are assuming an expanding role in power generation and cogeneration¹. This is a result both of continuing improvements to gas turbine engines themselves and of the development of new cycle configurations. Chapter One introduced the chemically recuperated gas turbine (CRGT) cycle as a proposed development of the steam-injected gas turbine (STIG) cycle promising high efficiency and low capital cost with low NO_x emissions. The objective of this thesis was to gain a better understanding of the thermodynamics of CRGT cycles and of how they compare with other cycles as a first step in their overall evaluation. The thermodynamic performance can then be linked with economic and environmental considerations to try to identify practical roles for CRGTs. While this thesis does not attempt detailed analyses of the economic and environmental aspects, possible roles for CRGTs are explored in Section 8.2.

Chapter Two presented a simplified thermodynamic analysis comparing the CRGT cycle to the STIG cycle from which it is derived (and which it resembles thermodynamically). This approach afforded a clear understanding of the role of heat recovery in overall cycle performance, and of how chemical recuperation affects heat recovery. It indicated that a CRGT cycle is generally (but not always) more efficient than a STIG cycle operating at the same turbine inlet temperature and pressure ratio². Chemical heat recovery allows a reduction in steam production while maintaining a low stack temperature, enabling a better match of heat recovery temperature profiles and

¹ 60% of electricity generation capacity added in the US in the 1990s is expected to be based on gas turbines, with 40,000MW to be ordered by 1995 (Smock, 1989). A similar revolution is under way in Europe. Moreover the recent expansion of gas turbine use in cogeneration applications is expected to continue. US gas turbine cogeneration capacity grew from less than 1,000MW in 1980 to 20,000MW in 1987 (Williams and Larson, 1989).

² The exceptions are cycles with very high pressure ratios and/or low turbine inlet temperatures.

hence low heat transfer irreversibilities. The efficiency gain is achieved only at the expense of a loss of work output resulting from the reduced steam flow.

Steam reforming of natural gas is a chemical recuperation reaction well suited for natural gas-fired CRGTs. Chapter Three investigated the characteristics of steam reforming relevant to CRGT cycles. Steam and methane react to form a low heating value fuel gas which is a mixture of methane, carbon monoxide, carbon dioxide, hydrogen, and water. Use of a nickel-based catalyst ensures that this mixture has a near-equilibrium composition. The fraction of methane converted, a measure of the heat absorbed by the reaction (per unit of methane fuel), is greater at high temperature, low pressure, and high steam-to-fuel ratio.

Chapter Four discussed pollutant emissions and other practical considerations relevant to CRGTs. The reformed fuel gas is projected to burn in the gas turbine combustor with very low NO_x formation. NO_x emissions are the major pollution concern associated with gas turbines. Stricter environmental regulations have led to the development of NO_x control technologies such as selective catalytic reduction (SCR), steam or water injection, and dry low NO_x combustors. SCR, often regarded as the "best available control technology", is costly and restricts operational flexibility. Steam or water injection and dry low NO_x combustion reduce NO_x formation by lowering peak flame temperatures in the combustor, but these can be lowered only so far before carbon monoxide emissions become unacceptable. The presence of hydrogen in the reformed fuel gas reduces this limiting temperature, and so CRGTs should be able to achieve "ultra-low" NO_x levels without SCR. Uncertainty about prompt NO_x formation means that tests are required to determine the exact level of NO_x emissions.

While "ultra-low" NO_x emissions may be achievable in theory, there remains the problem of designing a combustor which can realize this in practice. This is just one of a number of CRGT development issues highlighted in Chapter Four. Another is the development of the heat recovery steam reformer, a task which involves adapting reformer designs used in the chemical process industry for gas turbine applications. These development efforts should be "straightforward" in that they require no major technological breakthroughs, but rather involve adaptation of existing technologies to new applications and operating conditions. Realization of CRGT cycles with reheat requires the more considerable undertaking of developing a reheat combustor and reheat

turbine, but many gas turbine experts argue that the considerable performance gains from going to reheat will justify such an undertaking, regardless of whether or not CRGT technology is developed.

Chapter Five described a computer model specially developed to calculate the thermodynamic performance of CRGT cycles. The model was constructed by developing a model of the steam reformer and adding it to an existing gas turbine cycle program. The model was used in Chapters Six and Seven to compare the performances of various CRGT cycle configurations with those of other gas turbine cycles.

Chapter Six presented calculations for the simplest CRGT cycle to illuminate the role played by chemical recuperation in the overall cycle thermodynamic performance. A detailed example comparing CRGT, STIG, and combined cycles at one set of operating conditions was presented primarily for pedagogic purposes. This was followed by a parametric analysis comparing CRGT and STIG cycles over a range of turbine inlet temperatures (TITs) and pressure ratios. The analysis considered both aeroderivative and heavy-duty gas turbines, with performances representative of the generation of machines currently being commercialized.

The parametric analysis confirmed the prediction of Chapter Two that a CRGT cycle is generally more efficient than a STIG cycle operating at the same TIT and pressure ratio (except at low TIT and/or very high pressure ratio). For a given TIT, the maximum efficiency of the CRGT is approximately half a percentage point greater than that of a STIG for both heavy-duty and aeroderivative gas turbines³, and occurs at a lower pressure ratio. The efficiency advantage is obtained only at the expense of a reduction in specific work.

The attractiveness of the CRGT compared to other cycles changes if the pressure ratio is fixed by the desire to build the cycle around an existing gas turbine. Conditions representative of the latest generation of heavy-duty gas turbines were chosen for the detailed example. At these conditions (1250C TIT and pressure ratio of 15), the CRGT cycle was found to be around two percentage

³ An interesting discovery of Chapter Six was that, at a given TIT and pressure ratio, the distinction between "rubber turbines" of aeroderivative and heavy-duty type has little effect on overall cycle performance. In practice these two classes of machine perform differently because aeroderivatives typically operate at higher pressure ratio than heavy-duties.

points more efficient than the STIG, but less efficient than the combined cycle by the same margin. At the high pressure ratios typical of modern aeroderivative gas turbines, the efficiency advantage of CRGT over STIG is negligibly small or even negative. The performance advantage of CRGT relative to STIG is larger in situations where the amount of steam injection is limited by a constraint on gas turbine mass flow.

Chapter Seven focused on more advanced CRGT cycles. The cycle modifications investigated were a multi-pressure HRSG, supplementary firing, and reheat and intercooling. Because of the complexity of these, just a few example cases were presented rather than a full parametric analysis. The cases presented were for cycle conditions typical of modern gas turbines. Cycle operating parameters for the multi-evaporation and supplementary-fired cases are near-optimal, while the cycles with reheat are based on a previous study, for which conditions such as reheat pressure and temperature may not be optimal.

A CRGT based on a heavy-duty gas turbine with a TIT of 1250C and a pressure ratio of 15, and with a dual-pressure HRSG with steam reheat and a topping steam turbine, was calculated to be 49.1% efficient. This is significantly less than the 52.0% obtained for a combined cycle based on the same gas turbine and a similar HRSG (and a 42C condensing temperature). The use of multi-level evaporation enables both cycles to achieve well matched heat recovery profiles and hence low heat transfer irreversibilities. However the CRGT cycle suffers from exergy loss associated with mixing steam into the gas cycle, and so the combined cycle is the more efficient.

Addition of supplementary firing to a CRGT cycle reduces efficiency while improving work output. Methane conversion increases at the elevated reforming temperature, but the extra chemical heat recovery is less than the heat added to the exhaust gases in the supplementary firer. Consequently a higher steam production is necessary to achieve the heat recovery required to maintain a low stack temperature, exergy losses associated with heat recovery are increased, and efficiency is reduced.

A CRGT cycle with intercooling and reheat (IR-CRGT) based on a General Electric LM8000 aeroderivative gas turbine was calculated to be 52.7% efficient (electrical efficiency), compared to 50.7% for an intercooled steam-injected gas turbine (ISTIG) and 51.3% for a reheat ISTIG. The

IR-CRGT cycle was found to be less efficient than a reheat combined cycle (53.6%). The IR-CRGT cycle is very similar to that proposed by Jack Janes of the California Energy Commission, but a Pacific Gas & Electric Company study of that cycle obtained an estimated efficiency of 56.1%. The discrepancy is caused primarily by a big difference in the estimate of the cooling flow required for the reheat turbine.

8.2 PROSPECTS FOR CHEMICALLY RECUPERATED GAS TURBINES

This section explores appropriate roles for CRGTs in practice. The discussion is necessarily speculative because cost estimates are available only for the intercooled, reheat CRGT (IR-CRGT) cycle proposed by Janes (Janes, 1989).

8.2.1 Applications for CRGTs

The choice of thermodynamic cycle for a given gas turbine application depends on many factors. The most important are costs, both capital cost and lifetime cost, but these in turn depend on many other aspects. The thermodynamic performance affects the cost calculation in that a high specific work encourages a low capital cost (in \$/kW), while a high efficiency leads to low fuel costs. The weighting attached to power output and efficiency in the economic analysis is determined by the proposed application - low fuel costs are relatively important in base-load plants, while low capital cost is preferable for peaking plants. The environmental characteristics of a gas turbine are becoming increasingly important as stricter emissions regulations increase the cost of compliance. Other factors determining the choice of cycle include ease of operation and maintenance, reliability, fuel availability, and site-specific factors such as water consumption for plants to be located in arid areas. For new technologies, the cost of development and commercialization must also be taken into account.

While this thesis made no attempt at an economic analysis for a CRGT, it is still possible to offer a few predictions concerning cost. A CRGT has virtually identical components to a STIG except that the HRSG is replaced by a heat recovery steam reformer, which resembles a HRSG but has a reactor section at the hot-end. Setting aside development costs, the extra capital cost of a CRGT compared to a STIG will be the cost of this reactor. If this operates at temperatures above

around 550C, then materials superior to those traditionally used in HRSGs will be required. There is also the cost of the catalyst, which may need renewal every few years. Note also that because a CRGT cycle has a lower power output for a given gas turbine size than does a STIG, the cost per kW of the gas turbine and auxiliaries will be higher. Hence a CRGT will have a higher capital cost than a STIG. The CRGT will have lower fuel costs owing to its higher efficiency, although the magnitude of its efficiency advantage varies considerably with cycle conditions (see Chapter Six).

The fuel costs of a CRGT will be higher than those of a combined cycle, which has a still higher efficiency. The CRGT will probably have the lower capital cost, as the expense of the chemical recuperator will be more than offset by the avoidance of the steam turbine, condenser, and possible cooling tower of the combined cycle. However for base-load power generation, where high efficiency is important, a combined cycle is likely to be the preferred option (unless NO_x restrictions are especially tight - see Section 8.2.2).

The arguments of the preceding two paragraphs suggest that the capital cost of a CRGT cycle (without reheat or intercooling) lies between those of STIG and combined cycles. Williams and Larson (1989) estimate total plant costs to be approximately \$560/kW for a combined cycle plant and \$440/kW for a STIG, and so \$500/kW might be an appropriate "off-the-cuff" estimate for the cost of a CRGT plant. Obviously there is a need for better cost estimates.

The California Energy Commission has made a preliminary cost estimate for the intercooled, reheat CRGT (IR-CRGT) cycle (Bemis, 1989). The estimated total plant cost was \$465/kW, compared to \$840/kW for a three-unit STIG plant, and \$474/kW for an ISTIG. These figures illustrate that reheat cycles need not be more expensive (in \$/kW) than non-reheat cycles, because the extra power output offsets the added cost of the reheat components. The unit cost of a reheat ISTIG cycle was not estimated. It would be lower than that of the IR-CRGT because of the greater power output and the absence of a reformer.

Desirable attributes for peaking plants are high power output, low capital cost, fast startup time, and simplicity of operation. CRGT cycles, like STIG and ISTIG cycles, provide high output at relatively low capital cost, but all of these cycles have higher capital costs, longer startup times, and are more complex than simple cycles. The presence of the catalyst means that particular

care is necessary when operating CRGT cycles. Hence the CRGT cycle is not a strong candidate for peaking plants, and the simple cycle is likely to remain the preferred solution⁴.

Another possible application of CRGTs is in cogeneration. Gas turbine technologies currently used in this area include STIG cycles and combined cycles with condensing-extraction steam turbines (CEST) or back pressure steam turbines. STIGs and CEST combined cycles are well suited to applications with variable process steam loads, because steam not required for process can be injected into the gas turbine or further expanded in the steam turbine to produce extra electricity for sale to the local grid (provided the regulatory structure enables this). For CRGT cycles some steam will always be required for the reformer, and this may limit the availability of process steam. However, the steam required by the reformer need not be large unless very low NO_x emissions are required⁵. Moreover, extra steam can always be made available, albeit at the expense of efficiency, by supplementary firing of the gas turbine exhaust. A CRGT cycle could respond to varying process steam loads either by injecting excess steam directly into the combustor, as for a STIG, or by increasing the steam-to-fuel ratio in the reformer (assuming the combustor can handle a fuel gas of variable heating value). Hence there appears to be no reason why CRGTs are not suitable for cogeneration, but their attractiveness will depend on the exact nature of the process load and of course on economic factors.

Gas turbines used in cogeneration applications are generally smaller than those chosen by utilities. This raises the question of whether CRGT cycles are appropriate for small gas turbines. One issue to be resolved is whether the chemical recuperation technology will be robust enough for operation by a large number of organizations with little experience of chemical process control. Similar concerns surrounded the introduction of selective catalytic reduction (SCR) for NO_x control, which, like chemical recuperation, involves incorporating a catalyzed chemical reaction into a gas turbine cycle. There were fears that this would lead to poor reliability because gas turbine operators are traditionally not familiar with this kind of technology. However, the SCR

⁴ For example the General Electric LM6000, available in 1992, will have a power output of 42MW and a simple cycle efficiency of 41.5%. This will be the first gas turbine to achieve a simple cycle efficiency greater than 40%. Projected capital cost is \$230-250/kW (de Biasi, 1990).

⁵ Chapter Three showed that the steam-to-fuel ratio in the reformer is an important factor determining the heating value of the reformed fuel gas, and hence its flame temperature in the combustor. A high steam-to-fuel ratio translates into a low flame temperature and hence low NO_x emissions.

experience in the US has passed expectations (Stambler, 1990). Also, this concern would not apply to the chemical industry, which constitutes a large fraction of the gas turbine cogeneration market in the US.

8.2.2 NO_x Control Considerations

The discussion so far has made little mention of the NO_x issue. In a situation of static technology, the need to control NO_x emissions adds both capital costs and operation costs of a gas turbine, and can considerably affect the economic attractiveness of various cycle options. Technological innovations such as the CRGT can reduce the cost of NO_x control - the commonly held notion that improved environmental controls always pose additional costs ignores the possibility of innovation. Specifically, the inherently low NO_x levels of CRGTs make them attractive when NO_x is a concern. CRGTs appear especially promising in situations which would otherwise necessitate the use of SCR. An SCR unit costs around \$150/kW (Smock, 1989) and has operational drawbacks and costs (see Chapter Four).

Of course the degree of NO_x control demanded by the local regulations is important. There has been a continued reduction in allowed NO_x emissions, with levels as low as 9ppm recently proposed for Southern California. Until recently such low levels have required the use of SCR plus steam or water injection or a dry low NO_x combustor. However one manufacturer has recently guaranteed 9ppm without SCR for a large heavy-duty gas turbine installation (with a dry low NO_x combustor), and other manufacturers plan to follow suit in the next two or three years (*Gas Turbine World*, July-August, 1990). Hence there appears to be no NO_x control incentive for developing a CRGT if NO_x regulations stay at around 10ppm.

This argument is misleading in that until now dry low NO_x combustors have been developed only for large heavy-duty gas turbines, while aeroderivatives and smaller heavy-duties continue to rely on steam or water injection (*Gas Turbine World*, March-April, 1990). As described in Chapter Four, there is a lower limit of around 25ppm to the degree of NO_x control achievable without unacceptable carbon monoxide emissions. Achievement of lower levels without SCR requires the development of dry low NO_x combustors for these turbines. In these circumstances, the cost of developing a CRGT may not far exceed what would have to be spent anyway.

Of course NO_x regulations might become even stricter as time progresses. The exact NO_x level attainable with CRGT is still unknown but is thought to be well below 10ppm and possibly as low as 1ppm (see Chapter Four), so CRGT becomes more attractive with tougher regulations. While there will be continued progress in dry low NO_x technology, Chapter Four explained that the hydrogen-rich fuel gas of CRGT has a fundamental advantage over natural gas in that it can burn at a lower limiting flame temperature and so the theoretically achievable minimum NO_x level is lower. Catalytic combustion could achieve emissions levels at least as low as CRGT, but this technology is several years away from commercialization because of the problem of finding catalysts and substrate materials to withstand high temperatures⁶.

In summary, the inherently good NO_x characteristics of the CRGT make it attractive in areas of strict NO_x regulations, especially in situations where SCR would otherwise be necessary. While continued progress in dry low NO_x combustor technology is likely, the CRGT has a fundamental advantage. The CRGT will become progressively more attractive as regulations become stricter. The long-term potential of catalytic combustion tends to reduce the incentive to develop CRGT, and a more accurate assessment of this potential is required.

8.2.3 Future Trends and Developments

The preceding discussion has hinted that future developments will also play a role in determining the commercial competitiveness of CRGTs. This makes assessment of CRGT even more difficult because of the uncertainty surrounding these developments. This dynamic situation results from continuing innovation in gas turbine technologies and from external changes such as increases in fuel prices or new environmental legislation. Examples of this have already been mentioned in relation to the NO_x issue. It was observed that tougher NO_x regulations make CRGT more attractive, while the prospect of catalytic combustion reduces the motivation to develop CRGT. There are many other examples relating to gas turbines cycles more generally.

⁶ Kimura (1990) gave a very rough estimate of 10 years as the time-scale for introduction of catalytic combustors.

The main technological development for gas turbines themselves is likely to be a continuation of the historical trend towards higher turbine inlet temperature (TIT) and pressure ratio. Section 6.3.4 argued that it is the effect of these trends on turbine outlet temperature (TOT) that will determine the change in the relative performances of the CRGT cycle and its competitors, because TOT is the primary determinant of the amount of chemical recuperation. Because increased TIT and increased pressure ratio tend to pull the TOT in opposite directions, the net result is that continued progress in gas turbine technology is unlikely to affect greatly the attractiveness of the CRGT.

The development of reheat gas turbines is a major step which will have a big impact for the gas turbine industry. Some commentators believe that this is inevitable, and point to the now standard use of reheat with large steam turbines (Rice, 1980). Realization of the reheat gas turbine will involve development efforts for the reheat combustor, the reheat turbine, and probably steam cooling. Nevertheless, reheat promises big improvements in both power output and efficiency for all gas turbine cycles. If use of gas turbines for power generation and cogeneration becomes as widespread as predicted, development costs would be shared among many customers. It is then not hard to imagine the development of reheat gas turbines.

A back-of-the envelope calculation can illustrate this point. Suppose the development cost for a reheat gas turbine is one billion dollars, and that a reheat cycle is on average two percentage points more efficient than one without reheat⁷. A rough calculation in Chapter Four discovered that, for projected future gas prices, the fuel savings from an efficiency improvement of one percentage point are worth approximately \$50/kW. The number of 100MW gas turbines for which fuel savings alone will pay back the \$1 billion development cost is then only 100.⁸

⁷ These numbers are chosen arbitrarily. The efficiency gain from reheat depends on the cycle operating conditions, but two percentage points is a reasonable estimate. The development cost for a reheat gas turbine is not known. The cost of development of intercooling has been estimated at \$100m (Corman, 1986), so an estimate of \$1 billion for reheat, a much more complex cycle modification, is not unreasonable given the added complexity.

⁸ This calculation assumes reheat and non-reheat turbines have the same capital cost in \$/kW excluding the development surcharge for the former. This is based on the fact that the additional cost of the reheat combustor and turbine is offset by the large increase in power output. Indeed, it was found earlier that the reheat cycle might even be cheaper.

While addition of reheat will improve performance of all gas turbine cycles, it is likely to be particularly beneficial for the CRGT cycle because the high TOT associated with reheat favors a large chemical heat recovery. The calculations of Chapter Seven found that a non-reheat CRGT cycle is two to three percentage points less efficient than a non-reheat combined cycle, but for reheat cycles this margin was around one percentage point⁹. The PG&E study found the reheat CRGT to be more efficient than the reheat combined cycle.

The Janes proposal is for a CRGT with reheat based on the General Electric LM8000 gas turbine, which in turn features a currently available gas generator. This is attractive in that it avoids the cost of developing a completely new gas turbine. Instead all that is required is the development of a reheat turbine to replace the power turbine of the non-reheat engine and a reheat combustor. This can be achieved at lower cost and in a shorter time than introduction of a completely new gas turbine. The down-side is that the restriction to an existing gas generator may lead to a reheat cycle at sub-optimal operating conditions. This option is only available with aeroderivative gas turbines, where the power turbine is physically separate from the gas generator. No such distinction exists for heavy-duty gas turbines, for which introduction of reheat would require a major redesign of the whole engine. Note that this "short-cut" to reheat with aeroderivatives results in a reheat gas turbine which could be used in a STIG, ISTIG, CRGT, or combined cycle.

An as yet undeveloped cycle which is thermodynamically a strong competitor to CRGT is the evaporative regenerative cycle (discussed in Chapter One). This promises efficiency close to that of a combined cycle but at low capital cost (similar to that of a STIG cycle). However this cycle does not have the good emissions characteristics of the CRGT.

Natural gas-fired combined cycles are now being chosen for base-load electricity generation, despite the higher price of natural gas compared to coal, because of the superior efficiency and much lower capital cost of the combined cycle compared to a conventional steam cycle (and because of the environmental advantages of natural gas over coal). An important factor influencing the trend towards combined cycles is the knowledge that coal gasification technology

⁹ Note that the reheat and non-reheat cycles of Chapter Seven were at different TIT and pressure ratio, so this might not be a fair comparison. Particularly, the reheat combined cycle studied might not be very close to optimal. Further calculations are required to obtain a fair comparison.

is on the verge of commercialization, so that gas turbines can be converted to run on gasified coal if gas prices rise sharply. A CRGT could be converted to coal by replacing the reformed fuel gas with coal gas, and injecting steam directly into the combustor rather than sending it to the reformer. The reformer would be removed, and the cycle would no longer be a CRGT but rather a coal-fired STIG. Note that the combustor of a CRGT is designed to burn a low heating value fuel, and so could accommodate the fuel gas resulting from coal gasification with little or no modification.

Concerns about global warming may lead to attempts to reduce carbon dioxide emissions from burning of fossil fuels. An interesting new proposal is the use of the chemical recuperation reaction as part of a carbon dioxide recovery process for natural gas-fired gas turbines (Blok, 1990)¹⁰. The basic idea is that the relatively high concentration of carbon-containing species in the reformed fuel gas makes for relatively easy removal, certainly when compared to recovery of carbon dioxide from a power plant's stack gases. After leaving the reformer, the fuel gas enters a reactor where steam and carbon monoxide react to form hydrogen and carbon dioxide (this is the "water gas shift reaction"). Conversion of carbon monoxide to carbon dioxide makes for its easy removal, while the chemical energy contained in the carbon monoxide is exploited to increase the hydrogen content of the fuel. The carbon dioxide is removed in a chemical absorption process and disposed of (for example in a disused gas well). The remaining fuel gas, comprising hydrogen, steam, and methane, is sent to the gas turbine combustor. A high methane conversion in the reformer is desirable because unreacted methane is not removed from the fuel gas, and for this reason the process will use a gas turbine with reheat or supplementary firing.

8.2.4 Summary

The major "selling point" of CRGT is its excellent emissions characteristics. Hence CRGTs are attractive in areas of strict NO_x regulations, particularly if SCR would otherwise be needed. The performance and economics of CRGTs will change with continued technological innovation. For example, a CRGT with intercooling and reheat will offer the triple benefit of high efficiency, low emissions, and low capital cost.

¹⁰ This idea follows previous research on carbon dioxide recovery from coal gasification power plants. See, for example, Hendriks et al (1989).

8.3 SUGGESTIONS FOR FUTURE WORK

This investigation has uncovered many opportunities for further research. Indeed, more information about the performance and costs of CRGTs is essential to enable an evaluation more rigorous than the preliminary assessment presented here. The following is a list of suggestions for further work, roughly ordered according to priority as perceived by the author:

- 1) The advanced cycles with reheat studied in Chapter Seven require further attention, particularly to resolve uncertainty concerning the required cooling flow for the reheat turbine. If the cooling estimates of the present study are correct, then cooling air requirements in reheat cycles constitute a large fraction of the total air flow. Further studies could investigate methods to reduce the cooling flow - for example steam cooling or pre-cooling of cooling air. These should aim to identify the optimal cycle conditions and cooling arrangements.
- 2) A more detailed assessment of the prospects for catalytic combustion is required. An estimate of the likely time-scale of development and commercialization will help in determining whether there is a role for CRGT in the meantime.
- 3) Experiments are required to predict confidently emissions for the reformed fuel gas, because of scientific uncertainty regarding prompt NO_x and carbon monoxide levels. Moreover, only "hard data" from combustion tests will convince potential buyers of the emissions capability of CRGTs. General Electric plans to perform such tests in 1991 with funding from the Gas Research Institute (Puzson, 1990).
- 4) A "first-cut" economic analysis of the CRGT would enable a far better assessment of its practical promise. Capital cost and development cost estimates are required for the heat recovery steam generator, and, for reheat cycles, for the reheat combustor and reheat turbine.
- 5) Chapter Four identified a number of practical issues which would need to be addressed before a CRGT could be realized. These include the design of the heat recovery steam reformer, the design of a combustor for the low heating value fuel gas, and part-load operation. The California

Energy Commission is currently sponsoring a detailed design study and cost estimate for a heat recovery steam reformer suitable for the conditions of the Janes cycle (Janes, 1990). Preliminary reformer designs and cost estimates could also be attempted for other CRGT cycles.

6) The current study focussed on the use of CRGTs in power-only applications, particularly base-load power generation, but there may be roles for CRGTs in other applications such as cogeneration. One possible role for chemical recuperation is in carbon dioxide recovery from natural gas-fired power plants.

7) Chapter Four raised the possibility of using two-phase evaporation of a water-methane mixture to further improve the cycle thermodynamic performance. Both the thermodynamic and practical aspects of this configuration require clarification.

REFERENCES

G R Bemis (principal author), Technology Characterizations, State of California Energy Resources Conservation and Development Commission, October 1989

V de Biasi, "LM6000 dubbed the 40/40 machine due for full-load tests in late 1991", Gas Turbine World, May-June 1990

K Blok, Department of Science, Technology, and Society, University of Utrecht, personal communication, October 1990

J C Corman, System Analysis of Simplified IGCC Plants, General Electric Corporate Research and Development, Schenectady NY, September 1986

Gas Turbine World, "Trends in Low-NO_x Combustion Design and Operating Experience", pp12, March-April 1990

Gas Turbine World, pp23, July-August 1990

C A Hendriks, K Blok, and W C Turkenburg, "The Recovery of Carbon Dioxide from Power Plants", proceedings of the Symposium Climate and Energy held in Utrecht, September 1989

J Janes, Chemically Recuperated Gas Turbine, California Energy Commission Draft Staff Report, January 1990

J Janes of the California Energy Commission, personal communication, August 1990

G Kimura of General Electric Corporate Research and Development, Schenectady NY, personal communication, December 1990

J Puzson of the Gas Research Institute, Chicago IL, personal communication, November 1990

I G Rice, "The Combined Reheat Gas Turbine/Steam Turbine Cycle", ASME Journal of Engineering for Gas Turbines and Power, January 1980

R Smock, "Gas Turbines Dominate New Capacity Ordering", Power Engineering, August 1989

I Stambler, "SCR Experience in US Showing Better than Expected Performance", Gas Turbine World, March-April 1990

R H Williams and E D Larson, "Expanding Roles for Gas Turbines in Power Generation", in T B Johansson, B Bodlund, and R H Williams, editors, Electricity: Efficient End-Use and New Generation Technologies, and Their Planning Implications, Lund University Press, 1989

